US011043660B2

(12) **United States Patent**
Ochiai et al.

(10) **Patent No.: US 11,043,660 B2**
(45) **Date of Patent: Jun. 22, 2021**

(54) **POSITIVE ELECTRODE ACTIVE MATERIAL INCLUDING LITHIUM COBALTATE COATED WITH LITHIUM TITANATE AND MAGNESIUM OXIDE**

(71) Applicant: **SEMICONDUCTOR ENERGY LABORATORY CO., LTD.**, Kanagawa-Ken (JP)

(72) Inventors: **Teruaki Ochiai**, Kanagawa (JP); **Takahiro Kawakami**, Kanagawa (JP); **Mayumi Mikami**, Kanagawa (JP); **Yohei Momma**, Kanagawa (JP); **Masahiro Takahashi**, Kanagawa (JP); **Ayae Tsuruta**, Kanagawa (JP)

(73) Assignee: **Semiconductor Energy Laboratory Co., Ltd.**, Atsugi (JP)

(*) Notice: Subject to any disclaimer, the term of this patent is extended or adjusted under 35 U.S.C. 154(b) by 0 days.

(21) Appl. No.: **16/923,494**

(22) Filed: **Jul. 8, 2020**

(65) **Prior Publication Data**

US 2020/0343530 A1 Oct. 29, 2020

Related U.S. Application Data

(63) Continuation of application No. 15/638,449, filed on Jun. 30, 2017, now Pat. No. 10,741,828.

(30) **Foreign Application Priority Data**

Jul. 5, 2016 (JP) 2016-133143
Jul. 6, 2016 (JP) 2016-133997
(Continued)

(51) **Int. Cl.**
H01M 4/131 (2010.01)
H01M 4/1315 (2010.01)
(Continued)

(52) **U.S. Cl.**
CPC ***H01M 4/131*** (2013.01); ***H01M 4/134*** (2013.01); ***H01M 4/1315*** (2013.01);
(Continued)

(58) **Field of Classification Search**
CPC .. H01M 4/131; H01M 4/1315; H01M 4/1391; H01M 4/13915; H01M 4/625; H01M 4/8657
(Continued)

(56) **References Cited**

U.S. PATENT DOCUMENTS

4,302,518 A 11/1981 Goodenough et al.
4,668,595 A 5/1987 Yoshino et al.
(Continued)

FOREIGN PATENT DOCUMENTS

CN 001715193 A 1/2006
CN 101148263 A 3/2008
(Continued)

OTHER PUBLICATIONS

Katsuno.H et al., "Growth modes in two-dimensional heteroepitaxy on an elasticsubstrate", J. Cryst. Growth (Journal of Crystal Growth), Feb. 15, 2005, vol. 275, No. 1-2, pp. e283-e288, Elsevier.
(Continued)

Primary Examiner — Sean P Cullen
(74) *Attorney, Agent, or Firm* — Fish & Richardson P.C.

(57) **ABSTRACT**

A positive electrode active material which can improve cycle characteristics of a secondary battery is provided. Two kinds of regions are provided in a superficial portion of a positive electrode active material such as lithium cobaltate which has a layered rock-salt crystal structure. The inner region is a non-stoichiometric compound containing a transition metal such as titanium, and the outer region is a compound of representative elements such as magnesium oxide. The two kinds of regions each have a rock-salt crystal
(Continued)

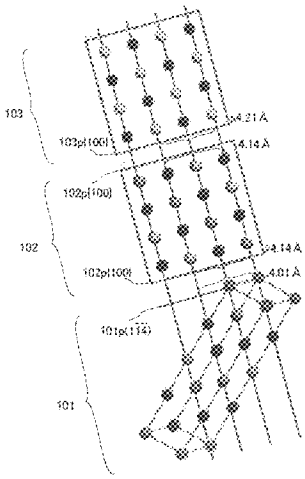

structure. The inner layered rock-salt crystal structure and the two kinds of regions in the superficial portion are topotaxy; thus, a change of the crystal structure of the positive electrode active material generated by charging and discharging can be effectively suppressed. In addition, since the outer coating layer in contact with an electrolyte solution is the compound of representative elements which is chemically stable, the secondary battery having excellent cycle characteristics can be obtained.

10 Claims, 58 Drawing Sheets

(30) **Foreign Application Priority Data**

Jan. 11, 2017	(JP)	2017-002831
Feb. 22, 2017	(JP)	2017-030693
Apr. 21, 2017	(JP)	2017-084321
Jun. 19, 2017	(JP)	2017-119272

(51) **Int. Cl.**

H01M 4/1391	(2010.01)
H01M 4/62	(2006.01)
H01M 4/13915	(2010.01)
H01M 4/134	(2010.01)
H01M 4/36	(2006.01)
H01M 4/525	(2010.01)
H01M 4/86	(2006.01)
H01M 4/02	(2006.01)
H01M 10/0525	(2010.01)

(52) **U.S. Cl.**
CPC ***H01M 4/1391*** (2013.01); ***H01M 4/13915*** (2013.01); ***H01M 4/366*** (2013.01); ***H01M 4/525*** (2013.01); ***H01M 4/625*** (2013.01); ***H01M 4/8657*** (2013.01); *H01M 10/0525* (2013.01); *H01M 2004/021* (2013.01); *H01M 2004/028* (2013.01)

(58) **Field of Classification Search**
USPC 429/231.3, 231.5, 231.6, 231.95
See application file for complete search history.

(56) **References Cited**

U.S. PATENT DOCUMENTS

5,240,794	A	8/1993	Thackeray et al.
5,443,929	A	8/1995	Yamamoto et al.
5,604,396	A	2/1997	Watanabe et al.
5,705,291	A	1/1998	Amatucci et al.
5,783,333	A	7/1998	Mayer
5,824,278	A	10/1998	Yao
5,834,139	A	11/1998	Shodai et al.
5,871,866	A	2/1999	Barker et al.
5,910,382	A	6/1999	Goodenough et al.
6,085,015	A	7/2000	Armand et al.
6,127,065	A	10/2000	Yamamoto et al.
6,218,050	B1	4/2001	Yoon et al.
6,277,521	B1	8/2001	Gao et al.
6,346,348	B1	2/2002	Nakajima et al.
6,458,487	B1	10/2002	Takeuchi et al.
6,514,640	B1	2/2003	Armand et al.
6,582,814	B2	6/2003	Swiler et al.
6,589,499	B2	7/2003	Gao et al.
6,680,143	B2	1/2004	Thackeray et al.
6,737,195	B2	5/2004	Kweon et al.
6,753,111	B2	6/2004	Kweon et al.
6,846,592	B2	1/2005	Kweon et al.
6,878,490	B2	4/2005	Gao et al.
6,919,144	B2	7/2005	Miyazaki et al.
6,974,601	B2	12/2005	Kweon et al.
6,984,469	B2	1/2006	Kweon et al.
7,018,741	B2	3/2006	Suhara et al.
7,138,209	B2	11/2006	Kweon et al.
7,294,435	B2	11/2007	Miyamoto et al.
7,303,840	B2	12/2007	Thackeray et al.
7,309,546	B2	12/2007	Kweon et al.
7,368,071	B2	5/2008	Dahn et al.
7,393,476	B2	7/2008	Shiozaki et al.
7,504,180	B2	3/2009	Tatsumi et al.
7,635,536	B2	12/2009	Johnson et al.
7,709,148	B2	5/2010	Kawasato et al.
7,709,151	B2	5/2010	Inoue et al.
7,736,807	B2	6/2010	Hasegawa et al.
7,790,308	B2	9/2010	Johnson et al.
7,892,679	B2	2/2011	Shimizu et al.
7,927,506	B2	4/2011	Park
7,935,270	B2	5/2011	Park
8,003,256	B2	8/2011	Ohishi
8,007,941	B2	8/2011	Kweon et al.
8,034,486	B2	10/2011	Kweon et al.
8,080,340	B2	12/2011	Thackeray et al.
RE43,276	E	3/2012	Kweon et al.
8,236,449	B2	8/2012	Nakura
8,470,477	B2	6/2013	Miwa et al.
8,476,510	B2	7/2013	Swager et al.
8,557,440	B2	10/2013	Yu et al.
8,685,569	B2	4/2014	Oguni et al.
8,685,570	B2	4/2014	Miwa et al.
8,709,654	B2	4/2014	Takeuchi et al.
8,753,532	B2	6/2014	Levasseur et al.
8,808,918	B2	8/2014	Jung et al.
8,877,377	B2	11/2014	Hosoya
8,877,381	B2	11/2014	Yasuda et al.
8,883,351	B2	11/2014	Todoriki et al.
8,906,547	B2	12/2014	Taniguchi et al.
8,927,148	B2	1/2015	Kawakami
8,945,770	B2	2/2015	Koo et al.
8,945,772	B2	2/2015	Kawakami et al.
8,951,448	B2	2/2015	Toyama et al.
9,105,926	B2	8/2015	Fujiki et al.
9,225,003	B2	12/2015	Yukawa
9,227,850	B2	1/2016	Ooishi
9,293,236	B2	3/2016	Kawakami et al.
9,362,557	B2	6/2016	Watanabe et al.
9,385,366	B2	7/2016	Yamakaji et al.
9,391,322	B2	7/2016	Liu et al.
9,478,796	B2	10/2016	Li et al.
9,505,631	B2	11/2016	Masukuni et al.
9,515,313	B2	12/2016	Umeyama et al.
9,614,225	B2	4/2017	Park
9,666,326	B2	5/2017	Kawakami et al.
9,698,420	B2	7/2017	Ishizaki et al.
9,786,903	B2	10/2017	Ryu et al.
9,812,709	B2	11/2017	Endoh et al.
9,871,246	B2	1/2018	Kim et al.
9,899,664	B2	2/2018	Yamaki et al.
9,923,244	B2	3/2018	Takanashi et al.
10,128,495	B2	11/2018	Satow et al.
10,243,215	B2	3/2019	Shitaba et al.
10,361,432	B2	7/2019	Takaichi et al.
10,777,815	B2	9/2020	Kanada et al.
2001/0010807	A1	8/2001	Matsubara
2002/0102459	A1	8/2002	Hosoya et al.
2002/0110736	A1	8/2002	Kweon et al.
2002/0164156	A1	11/2002	Bilbrey
2002/0195591	A1	12/2002	Ravet et al.
2003/0104279	A1	6/2003	Miyazaki et al.
2003/0134186	A1	7/2003	Shizuki
2004/0142241	A1	7/2004	Nagayama
2004/0229123	A1	11/2004	Takahashi et al.
2004/0229124	A1	11/2004	Miyamoto et al.
2004/0234857	A1	11/2004	Shiozaki et al.
2005/0019662	A1	1/2005	Suhara et al.
2006/0051671	A1	3/2006	Thackeray et al.
2006/0051673	A1	3/2006	Johnson et al.
2006/0121352	A1	6/2006	Kejha et al.
2006/0188780	A1	8/2006	Fujii et al.
2006/0263690	A1	11/2006	Suhara et al.

(56) **References Cited**

U.S. PATENT DOCUMENTS

2006/0275664 A1 12/2006 Ohzuku et al.
2006/0286459 A1 12/2006 Zhao et al.
2007/0026315 A1 2/2007 Lampe-Onnerud et al.
2007/0099086 A1 5/2007 Kang et al.
2007/0117014 A1 5/2007 Saito et al.
2007/0122712 A1 5/2007 Kang et al.
2007/0148546 A1 6/2007 Shimizu et al.
2007/0160906 A1 7/2007 Tooyama et al.
2007/0212609 A1 9/2007 Iwami
2007/0224506 A1 9/2007 Ooyama et al.
2008/0131780 A1 6/2008 Kawasato et al.
2008/0166637 A1 7/2008 Inagaki et al.
2008/0241693 A1 10/2008 Fukuchi et al.
2009/0011335 A1 1/2009 Takeda et al.
2009/0017383 A1 1/2009 Suhara et al.
2009/0087731 A1 4/2009 Fukui et al.
2009/0104532 A1 4/2009 Hosoya
2009/0123813 A1 5/2009 Chiang et al.
2009/0123842 A1 5/2009 Thackeray et al.
2009/0220862 A1 9/2009 Toyama et al.
2010/0019194 A1 1/2010 Fujiwara et al.
2010/0035147 A1 2/2010 Kotato et al.
2010/0086854 A1 4/2010 Kumar et al.
2010/0129714 A1 5/2010 Toyama et al.
2010/0129715 A1 5/2010 Saito et al.
2010/0143784 A1 6/2010 Johnson et al.
2010/0143799 A1 6/2010 Park
2010/0159330 A1 6/2010 Sugiura et al.
2010/0178464 A1 7/2010 Choi et al.
2010/0216024 A1 8/2010 Kanno et al.
2010/0233542 A1 9/2010 Endo et al.
2010/0247986 A1 9/2010 Toyama et al.
2010/0248033 A1 9/2010 Kumar et al.
2010/0294985 A1 11/2010 Suhara et al.
2011/0033749 A1 2/2011 Uchida et al.
2011/0059367 A1 3/2011 Morita et al.
2011/0076564 A1 3/2011 Yu et al.
2011/0200879 A1 8/2011 Saito et al.
2011/0229757 A1 9/2011 Kawakami et al.
2011/0256437 A1 10/2011 Katsuki et al.
2011/0269023 A1 11/2011 Kawakami et al.
2011/0297876 A1 12/2011 Masukuni et al.
2011/0300441 A1 12/2011 Kawakami
2012/0034516 A1 2/2012 Koo et al.
2012/0045692 A1 2/2012 Takemura et al.
2012/0064406 A1 3/2012 Sato et al.
2012/0064409 A1 3/2012 Zhamu et al.
2012/0088151 A1 4/2012 Yamazaki et al.
2012/0088156 A1 4/2012 Nomoto et al.
2012/0118149 A1 5/2012 Dabrowski et al.
2012/0244430 A1 9/2012 Yamazaki et al.
2012/0256337 A1 10/2012 Yokoyama et al.
2012/0258358 A1* 10/2012 Yura H01M 4/02 429/209
2012/0258365 A1 10/2012 Yokoyama et al.
2012/0258369 A1 10/2012 Yokoyama et al.
2012/0261622 A1 10/2012 Honma
2012/0295163 A1 11/2012 Yanagita et al.
2012/0308891 A1 12/2012 Todoriki et al.
2012/0315544 A1 12/2012 Yasuda et al.
2012/0328951 A1 12/2012 Hirohashi et al.
2012/0328956 A1 12/2012 Oguni et al.
2012/0330044 A1 12/2012 Hou
2013/0017435 A1 1/2013 Sato et al.
2013/0040193 A1 2/2013 Tsuchida et al.
2013/0045418 A1 2/2013 Oguni et al.
2013/0052534 A1 2/2013 Fujiki et al.
2013/0052547 A1 2/2013 Ogino et al.
2013/0065120 A1 3/2013 Miwa et al.
2013/0078516 A1 3/2013 Taniguchi et al.
2013/0084384 A1 4/2013 Yamakaji
2013/0089786 A1 4/2013 Jeong et al.
2013/0130103 A1 5/2013 Kim et al.
2013/0134051 A1 5/2013 Takahashi et al.
2013/0156683 A1 6/2013 Holzapfel et al.
2013/0156942 A1 6/2013 Yamakaji et al.
2013/0157034 A1 6/2013 Choi et al.
2013/0164619 A1 6/2013 Yamakaji et al.
2013/0177806 A1 7/2013 Caldwell et al.
2013/0183579 A1 7/2013 Kim et al.
2013/0189585 A1 7/2013 Kang et al.
2013/0190449 A1 7/2013 Kinloch et al.
2013/0202953 A1 8/2013 Sharma et al.
2013/0212879 A1 8/2013 Ogino
2013/0230770 A1 9/2013 Oya et al.
2013/0266858 A1 10/2013 Inoue et al.
2013/0266859 A1 10/2013 Todoriki et al.
2013/0313471 A1 11/2013 Endo et al.
2013/0316237 A1 11/2013 Miki
2013/0337320 A1 12/2013 Yukawa
2014/0004412 A1 1/2014 Ogino
2014/0023920 A1 1/2014 Yamazaki et al.
2014/0079995 A1 3/2014 Wakada
2014/0099554 A1 4/2014 Inoue et al.
2014/0127567 A1 5/2014 Kuriki et al.
2014/0127568 A1 5/2014 Kawakami et al.
2014/0131633 A1 5/2014 Ito et al.
2014/0162132 A1 6/2014 Ishii et al.
2014/0166946 A1 6/2014 Miwa et al.
2014/0184172 A1 7/2014 Momo et al.
2014/0212759 A1 7/2014 Blangero et al.
2014/0234700 A1 8/2014 Moriwaka et al.
2014/0242463 A1 8/2014 Song et al.
2014/0295068 A1 10/2014 Nanba et al.
2014/0332715 A1 11/2014 Kawakami et al.
2014/0370184 A1 12/2014 Takemura et al.
2015/0014581 A1 1/2015 Kawakami et al.
2015/0014605 A1 1/2015 Kawakami et al.
2015/0064565 A1 3/2015 Todoriki et al.
2015/0093648 A1 4/2015 Son et al.
2015/0099178 A1 4/2015 Kawakami et al.
2015/0099179 A1 4/2015 Ikenuma et al.
2015/0123050 A1 5/2015 Yamazaki et al.
2015/0155556 A1 6/2015 Kawakami et al.
2015/0166348 A1 6/2015 Ikenuma et al.
2015/0262762 A1 9/2015 Ikenuma et al.
2015/0325855 A1 11/2015 Kawakami et al.
2015/0333320 A1 11/2015 Tamaki et al.
2015/0333324 A1 11/2015 Umeyama et al.
2015/0357641 A1 12/2015 Sugie et al.
2015/0380737 A1 12/2015 Kawasato et al.
2016/0006032 A1 1/2016 Paulsen et al.
2016/0013478 A1 1/2016 Satow et al.
2016/0028080 A1 1/2016 Sugiura
2016/0064726 A1 3/2016 Ikenuma et al.
2016/0087315 A1 3/2016 Oyama
2016/0104880 A1* 4/2016 Gao H01M 4/505 429/217
2016/0118646 A1 4/2016 Ikenuma
2016/0118658 A1 4/2016 Kawakami et al.
2016/0156030 A1 6/2016 Sun et al.
2016/0164089 A1 6/2016 Kawakami et al.
2016/0276658 A1 9/2016 Choi et al.
2016/0276659 A1 9/2016 Choi et al.
2016/0285102 A1 9/2016 Shitaba et al.
2016/0329533 A1 11/2016 Tajima
2016/0336595 A1 11/2016 Choi et al.
2016/0349905 A1 12/2016 Momma et al.
2016/0380271 A1 12/2016 Ochiai et al.
2017/0005364 A1 1/2017 Yamazaki et al.
2017/0040594 A1 2/2017 Yamaki et al.
2017/0062819 A1 3/2017 Ikenuma
2017/0069907 A1 3/2017 Zhu et al.
2017/0117589 A1 4/2017 Tajima et al.
2017/0187035 A1 6/2017 Yanagihara et al.
2017/0207444 A1 7/2017 Yanagihara et al.
2017/0256817 A1 9/2017 Kadoma et al.
2017/0309910 A1 10/2017 Jo et al.
2018/0019462 A1 1/2018 Kadoma et al.
2018/0034045 A1 2/2018 Xia et al.
2018/0040888 A1 2/2018 Park et al.
2018/0040897 A1 2/2018 Park et al.
2018/0076489 A1 3/2018 Mikami et al.
2018/0102536 A1 4/2018 Kawakami et al.

(56) **References Cited**

U.S. PATENT DOCUMENTS

2018/0108944	A1	4/2018	Yamakaji
2018/0145317	A1	5/2018	Momma et al.
2018/0145368	A1	5/2018	Ochiai et al.
2018/0190976	A1	7/2018	Blangero et al.
2018/0254477	A1	9/2018	Horikawa et al.
2018/0366729	A1	12/2018	Yanagita et al.
2020/0144601	A1	5/2020	Takahashi et al.
2020/0152961	A1	5/2020	Momma et al.
2020/0176770	A1	6/2020	Takahashi et al.

FOREIGN PATENT DOCUMENTS

CN	101208269	A		6/2008
CN	101675547	A		3/2010
CN	102210045	A		10/2011
CN	102339998	A		2/2012
CN	102447107	A		5/2012
CN	102610806	A		7/2012
CN	102694201	A		9/2012
CN	102779976	A		11/2012
CN	103022502	A		4/2013
CN	103490060	A		1/2014
CN	102610806	B	*	11/2014
CN	104701534	A		6/2015
CN	105024047	A		11/2015
CN	106099098	A		11/2016
CN	102569775	B		1/2017
EP	0638625	A		2/1995
EP	2352190	A		8/2011
EP	2763218	A		8/2014
JP	05-314965	A		11/1993
JP	05-314995	A		11/1993
JP	07-316551	A		12/1995
JP	08-037007	A		2/1996
JP	08-100107	A		4/1996
JP	08-236114	A		9/1996
JP	11-025983	A		1/1999
JP	11-096993	A		4/1999
JP	3031546			4/2000
JP	2000-203842	A		7/2000
JP	3172388			6/2001
JP	2001-319692	A		11/2001
JP	2002-164053	A		6/2002
JP	2002-216760	A		8/2002
JP	2002-352802	A		12/2002
JP	2003-068306	A		3/2003
JP	2003-221235	A		8/2003
JP	2003-331824	A		11/2003
JP	2004-014381	A		1/2004
JP	2004-103566	A		4/2004
JP	2004-196604	A		7/2004
JP	2004-288579	A		10/2004
JP	2004-342554	A		12/2004
JP	2005-158612	A		6/2005
JP	2005-225734	A		8/2005
JP	2005-302510	A		10/2005
JP	2005-332629	A		12/2005
JP	2006-164758	A		6/2006
JP	2006-261132	A		9/2006
JP	2006-318928	A		11/2006
JP	2006-318929	A		11/2006
JP	2007-128714	A		5/2007
JP	2007-213866	A		8/2007
JP	3959333			8/2007
JP	2008-060033	A		3/2008
JP	2008-166156	A		7/2008
JP	2009-179501	A		8/2009
JP	2010-080407	A		4/2010
JP	2010-102895	A		5/2010
JP	2010-244847	A		10/2010
JP	2010-272239	A		12/2010
JP	2011-082133	A		4/2011
JP	2011-138718	A		7/2011
JP	4739780			8/2011
JP	2011-181527	A		9/2011
JP	2011-210694	A		10/2011
JP	2012-018914	A		1/2012
JP	2012-043794	A		3/2012
JP	2012-066944	A		4/2012
JP	2012-074366	A		4/2012
JP	2012-084257	A		4/2012
JP	2012-508444			4/2012
JP	2012-169217	A		9/2012
JP	2012-209077	A		10/2012
JP	2013-012410	A		1/2013
JP	2013-062082	A		4/2013
JP	2013-087040	A		5/2013
JP	2013-091581	A		5/2013
JP	2013-100197	A		5/2013
JP	2013-246936	A		12/2013
JP	2014-049239	A		3/2014
JP	2014-063707	A		4/2014
JP	2014-063708	A		4/2014
JP	2014-116111	A		6/2014
JP	2015-069958	A		4/2015
JP	2015-082374	A		4/2015
JP	2015-088450	A		5/2015
JP	2015-099722	A		5/2015
JP	2015-156363	A		8/2015
JP	2015-527707			9/2015
JP	2015-201432	A		11/2015
JP	2016-054151	A		4/2016
JP	2016-076454	A		5/2016
JP	2017-021942	A		1/2017
JP	2017-091777	A		5/2017
JP	2018-092934	A		6/2018
JP	2018-147726	A		9/2018
KR	10-0696619			3/2007
KR	2008-0024105	A		3/2008
KR	2009-0086440	A		8/2009
KR	2009-0111130	A		10/2009
KR	10-0944137			2/2010
KR	2010-0052419	A		5/2010
KR	2011-0134852	A		12/2011
KR	2013-0033154	A		4/2013
KR	2014-0125856	A		10/2014
KR	2015-0062724	A		6/2015
KR	2016-0092946	A		8/2016
WO	WO-2007/052712			5/2007
WO	WO-2009/057722			5/2009
WO	WO-2010/053328			5/2010
WO	WO-2011/141486			11/2011
WO	WO-2011/155781			12/2011
WO	WO-2012/005180			1/2012
WO	WO-2012/029729			3/2012
WO	WO-2012/124242			9/2012
WO	WO-2012/132387			10/2012
WO	WO-2014/015139			1/2014
WO	WO-2014/061653			4/2014
WO	WO-2014/098238			6/2014
WO	WO-2015/136881			9/2015
WO	WO-2015/163356			10/2015
WO	WO-2016/017077			2/2016
WO	WO-2016/017079			2/2016
WO	WO-2018/211375			11/2018

OTHER PUBLICATIONS

Taguchi.N. et al., "Characterization of MgO-coated-LiCoO2 particles by analytical transmission electron microscopy", Journal of Power Sources, 2016, vol. 328, pp. 161-166, Elsevier.

Thackeray.M et al., "Li2MnO3-stabilized LiMO2(M=Mn, Ni, Co) electrodes for lithium-ion batteries", J. Mater. Chem. (Journal of Materials Chemistry), 2007, vol. 17, pp. 3112-3125.

Berbenni.V et al., "Thermogravimetry and X-Ray Diffraction Study of the Thermal Decomposition Processes in Li2CO3-MnCO3 Mixtures", Journal of Analytical and Applied Pyrolysis, 2002, vol. 62, pp. 45-62.

Johnson.C et al., "Lithium-manganese oxide electrodes with layered-spinel composite structures xLi2MnO3 • (1-x)Li1+yMn2-yO4(0<x<1,0≤y≤0.33) for lithium batteries", Electrochemistry Communications, May 1, 2005, vol. 7, No. 5, pp. 528-536, Elsevier.

(56) **References Cited**

OTHER PUBLICATIONS

Khedr.A et al., "Synthesis, Structure, and Electrochemistry of Sm-Modified LiMn2O4 Cathode Materials for Lithium-Ion Batteries", J. Electron. Mater.(Journal of Electronic Materials), Apr. 23, 2013, vol. 42, No. 6, pp. 1275-1281.
Lee.S et al., "Antiferromagnetic ordering in Li2MnO3 single crystals with a two-dimensional honeycomb lattice", Journal of Physics: Condensed Matter, Nov. 14, 2012, vol. 24, No. 45, pp. 456004-1-456004-9.
Mukai.K et al., "Magnetic properties of the chemically delithiated LixMn2O4 with 0.07≤x≤1", Journal of Solid State Chemistry, May 1, 2011, vol. 184, No. 5, pp. 1096-1104.
Wang.Z et al., "EELS analysis of cation valence states and oxygen vacancies in magnetic oxides", Micron, Oct. 1, 2000, vol. 31, No. 5, pp. 571-580, Elsevier.
Tan.H et al., "Oxidation state and chemical shift investigation in transition metal oxides by EELS", Ultramicroscopy, May 1, 2012, vol. 116, pp. 24-33, Elsevier.
McCalla.E et al., "The spinel and cubic rocksalt solid-solutions in the Li—Mn—Ni oxide pseudo-ternary system", Solid State Ionics, May 2, 2013, vol. 242, pp. 1-9, Elsevier.
Dreyer.D et al., "The Chemistry of Graphene Oxide", Chemical Society Reviews, Nov. 3, 2009, vol. 39, No. 1, pp. 228-240.
International Search Report (Application No. PCT/IB2017/053896) dated Oct. 3, 2017.
Written Opinion (Application No. PCT/IB2017/053896) dated Oct. 3, 2017.
Sun.Y et al., "High-energy cathode material for long-life and safe lithium batteries", Nature Materials, Mar. 22, 2009, vol. 8, pp. 320-324.
Joshi.T et al., "Effects of Dissolved Transition Metals on the Electrochemical Performance and SEI Growth in Lithium-Ion Batteries", J. Electrochem. Soc. (Journal of the Electrochemical Society), 2014, vol. 161, No. 12, pp. A1915-A1921.
Chung.K et al., "Structural Studies on the Effects of ZrO2 Coating on LiCoO2 during Cycling Using in Situ X-Ray Diffraction Technique", J. Electrochem Soc. (Journal of the Electrochemical Society), 2006, vol. 153, No. 11, pp. A2152-A2157.
Liu.L et al., "Electrochemical and In Situ Synchrotron XRD Studies on Al2O3-Coated LiCoO2 Cathode Material", J. Electrochem. Soc. (Journal of the Electrochemical Society), 2004, vol. 151, No. 9, pp. A1344-A1351.
Yano.A et al., "LiCoO2 Degradation Behavior in the High-Voltage Phase Transition Region and Improved Reversibility with Surface Coating", J. Electrochem. SOC. (Journal of the Electrochemical Society), 2017, vol. 164, No. 1, pp. A6116-A6122.
Chen.Z et al., "Staging Phase Transitions in LixCoO2", J. Electrochem. Soc. (Journal of the Electrochemical Society), 2002, vol. 149, No. 12, pp. A1604-A1609.
Shim.J et al., "Characterization of Spinel LixCo204-Coated LiCo02 Prepared with Post-Thermal Treatment as a Cathode Material for Lithium Ion Batteries", Chem Mater. (Chemistry of Materials), Apr. 10, 2015, vol. 27, No. 9, pp. 3273-3279.
Okumura.T et al., "Correlation of lithium ion distribution and X-ray absorption near-edge structure in O3- and O2-lithium cobalt oxides from first-principle calculation", Journal of Materials Chemistry, 2012, vol. 22, pp. 17340-17348.
Motohashi.T et al., "Electronic phase diagram of the layered cobalt oxide system LixCoO2 (0.0≤x≤1.0)", Phys. Rev. B (Physical Review. B), Oct. 9, 2009, vol. 80, No. 16, pp. 165114-1-155114-9.
Gabrisch.H et al., "Hexagonal to Cubic Spinel Transformation in Lithiated Cobalt Oxide TEM Investigation", J. Electrochem. Soc. (Journal of the Electrochemical Society), 2004, vol. 151, No. 6, pp. A891-A897.
Counts.W et al., "Fluoride Model Systems: II, The Binary Systems CaF2—BeF2, MgF2—BeF2, and LiF—MgF2", J. Am. Ceram. Soc. (Journal of the American Ceramic Society), 1953, vol. 36, No. 1, pp. 12-17.
Liu.A et al., "Synthesis of Mg and Mn Doped LiCoO2 and Effects on High Voltage Cycling", J. Electrochem. SOC/ (Journal of the Electrochemical Society), Jun. 2, 2017,vol. 164, No. 7, pp. A1655-A1664.
Tukamoto.H et al., "Electronic Conductivity of LiCoO2 and Its Enhancement by Magnesium Doping", J. Electrochem. Soc. (Journal of the Electrochemical Society), Sep. 1, 1997, vol. 144, No. 9, pp. 3164-3168.
Ohzuku.T et al., "Solid-State Redox Reactions of LiCoO2 (R-3m) for 4 Volt Secondary Lithium Cells", J. Electrochem. Soc. (Journal of the Electrochemical Society), Nov. 1, 1994, vol. 141, No. 11, pp. 2972-2977.
Amatucci.G et al., "CoO2, The End Member of the LixCoO2 Solid Solution", J. Electrochem. Soc. (Journal of the Electrochemical Society), Mar. 1, 1996, vol. 143, No. 3, pp. 1114-1123.
Wang.Z et al., "Structural and electrochemical characterizations of surface-modified LiCoO2 cathode materials for Li-ion batteries", Solid State Ionics, Jun. 2, 2002, vol. 148, No. 3-4, pp. 335-342, Elsevier.
Zou.M et al., "Synthesis and Electrochemical Performance of High Voltage Cycling LiM0.05Co0.95O2 as Cathode Material for Lithium Rechargeable Cells", Electrochemical and Solid-State Letters, 2004, vol. 7, No. 7, pp. A176-A179.
Wang.Z et al., "Improving the cycling stability of LiCoO2 at 4.5 V through co-modification by Mg doping and zirconium oxyfluoride coating", Ceramics Internationa,, 2015, vol. 41, No. 1, pp. 469-474.
Cho.Y et al., "High Performance LiCoO2 Cathode Materials at 60° C. for Lithium Secondary Batteries Prepared by the Facile Nanoscale Dry-Coating Method", J. Electrochem. Soc. (Journal of the Electrochemical Society), 2010, vol. 157, No. 5, pp. A617-A624.
Wang.Z et al., "Mg doping and zirconium oxyfluoride coating co-modification to enhance the high-voltage performance of LiCoO2 for lithium ion battery", Journal of Alloys and Compounds, Feb. 5, 2015, vol. 621, pp. 212-219.
Mladenov.M et al., "Effect of Mg doping and MgO-surface modification on the cycling stability of LiCoO2 electrodes.", Electrochemistry Communications, Aug. 1, 2001, vol. 3, No. 8, pp. 410-416.
Kweon.H et al., "Effects of metal oxide coatings on the thermal stability and electrical performance of LiCoCO2 in a Li-ion cell", Journal of Power Sources, Feb. 16, 2004, vol. 126, pp. 156-162, Elsevier.
Shim.J et al., "Effects of MgO Coating on the Structural and Electrochemical Characteristics of LiCoO2 as Cathode Materials for Lithium Ion Battery", Chem. Mater. (Chemistry of Materials), Mar. 24, 2014, vol. 26, No. 8, pp. 2537-2543.
Zhao.H et al., "Improvement of electrochemical stability of LiCoO2 cathode by a nano-crystalline coating", Journal of Power Sources, May 20, 2004, vol. 132, pp. 195-200, Elsevier.
Iriyama.Y et al., "Effects of surface modification by MgO on interfacial reaction of lithium cobalt oxide thin film electrode", Journal of Power Sources, Oct. 5, 2004, vol. 137, pp. 111-116, Elsevier.
Shim.J et al., "Effects of MgO Coating on the Structural and Electrochemical Characteristics of LiCoO2 as Cathode Materials for Lithium Ion Battery", Chem. Mater. (Chemistry of Materials), [e.g.), Suppor] Supporting Information, Mar. 24, 2014, vol. 26, No. 8, pp. 31-33.
Orikasa.Y et al., "Origin of Surface Coating Effect for MgO on LiCoO2 to Improve the Interfacial Reaction between Electrode and Electrolyte", Adv. Mater.Interfaces (Advanced Materials Interfaces), Aug. 28, 2014, vol. 1, No. 9, pp. 1400195-1-1400195-8.
Yamamoto.K et al., "Stabilization of the Electronic Structure at the Cathode/Electrolyte Interface via MgO Ultra-thin Layer during Lithium-ions Insertion/Extraction", Electrochemistry, Oct. 5, 2014, vol. 82, No. 10, pp. 891-896.
Shim.J et al., "Synergistic effects of coating and doping for lithium ion battery cathode materials: synthesis and characterization of lithium titanate-coating LiCoO2 with Mg doping", Electrochimica Acta, Dec. 20, 2015, vol. 186, pp. 201-208, Elesevier.
Yamamoto.K et al., "In situ Total-Reflection Fluorescence X-Ray Absorption Spectroscopic Study on Stability at LiFePO4 / Elecrtrolyte Interface", 224th ECS Meeting Abstract, Oct. 27, 2013, p. 923.

(56) **References Cited**

OTHER PUBLICATIONS

Wang.Z et al., "Electrochemical Evaluation and Structural Characterization of Commercial LiCoO2 Surfaces Modified with MgO with Lithion-Ion Batteries", J. Electrochem. Soc. (Journal of the Electrochemical Society), Mar. 4, 2002, vol. 149, No. 4, pp. A466-A471.
Lee.Y et al., "Phase Transitions of Bare and Coated LixCoO2 (x=0.4 and 0.24) at 300° C.", J. Electrochem. Soc. (Journal of the Electrochemical Society), Jul. 28, 2005, vol. 152, No. 9, pp. A1824-A1827.
Geder.J et al., "Impact of active material surface area on thermal stability of LiCoO2 cathode", Journal of Power Sources, Jul. 1, 2014, vol. 257, pp. 285-292, Elsevier.
Benecke.M et al., "Effect of LiF on Hot-Pressing of MgO", J. Am. Ceram. Soc. (Journal of the American Ceramic Society), Jul. 1, 1967, vol. 50, No. 7, pp. 365-368.
Hart.P. et al., "Densification Mechanisms in Hot-Pressing of Magnesia with a Fugitive Liquid", J. Am. Ceram. Soc. (Journal of the American Ceramic Society), Feb. 1, 1970, vol. 53, No. 2, pp. 83-86.
Belsky.A et al., "New developments in the Inorganic Crystal Structure Database (ICSD): Accessibility in support of materials research and design.", ACTA Cryst. (ACTA Crystallographic SectionB), Jun. 1, 2002, vol. B58, No. 3, pp. 364-369.
Alcantara.R et al., "SPES, 6Li MAS NMR, and Ni3+EPR evidence for the formation of Co2+-containing spinel phases in LiCoO2 cycled electrode materials", Journal of Electroanalytical Chemistry, Aug. 28, 1998, vol. 454, No. 1-2, pp. 173-181.
Shi.S et al., "Enhanced cycling stability of Li[Li 0.2Mn0.54Ni0.13Co0.13]O2 by surface modification of MgO with melting impregnation method", Electrochimica Acta, Nov. 1, 2012, vol. 88, pp. 671-679.
Antaya.M et al., "Preparation and Characterization of LiCoO2 Thin Films by Laser Ablation Deposition", J. Electrochem. Soc. (Journal of the Electrochemical Society), Mar. 1, 1993, vol. 140, No. 3, pp. 575-578.
Koyama.Y et al., "Co K-edge XANES of LiCoO2 and CoO2 with a variety of structures by supercell density functional calculations with a core hold", Phys. Rev. B (Physical Review. B), Feb. 27, 2012, vol. 85, No. 7, pp. 075129-1-075129-7.
Quinlan.R et al., "XPS Investigation of the Electrolyte Induced Stabilization of LiCoO2 and "AlPO4"-Coated LiCoO2 Composite Electrodes", J. Electrochem. Soc. (Journal of the Electrochemical Society), Dec. 3, 2015, vol. 163, No. 2, pp. A300-A308.
Cho.J et al., "Comparison of Al2O3- and AlPO4-coated LiCoO2 cathode materials for a Li-ion cell", Journal of Power Sources, 2005, vol. 146, pp. 58-64, Elsevier.
Jin.Y et al., "Electrochemical Characterizations of Commercial LiCoO2 Powders with Surface Modified by Li3PO4 Nanoparticles", Electrochemical and Solid-State Letters, Apr. 3, 2006, vol. 9, No. 6, pp. A273-A276.
Hong.W et al., "Modification of LiCoO2 by Surface Coating with MgO/TiO2/SiO2 for High-Performance Lithium-Ion Battery", Electrochemical and Solid-State Letters, Dec. 20, 2005, vol. 9, No. 2, pp. A82-A85.
Eom.J et al., "M3(PO4)2-Nanoparticle-Coated LiCoO2 vs LiCo0.96M0.04O2(M=Mg and Zn) on Electrochemical and Storage Characteristics", J. Electrochem. Soc. (Journal of the Electrochemical Society), Jan. 8, 2008, vol. 155, No. 3, pp. A201-A205.
Kim.Y et al., "Suppression of Cobalt Dissolution from the LiCoO2 Cathodes with Various Metal-Oxide Coatings", J. Electrochem. Soc. (Journal of the Electrochemical Society), 2003, vol. 150, No. 12, pp. A1723-A1725.
Fang.T et al., "Effect of calcination temperature on the electrochemical behavior of ZnO-coated LiCoO2 cathode", Surface & Coatings Technology , Apr. 19, 2006, vol. 201, No. 3-4, pp. 1886-1893, Elsevier.
Park.S et al., "Novel Surface Modification Technique to Improve Electrochemical Performance of LiCoO2 at High Voltage", Electrochemical and Solid-State Letters, Apr. 21, 2005, vol. 8, No. 6, pp. A299-A302.
Jo.C et al., "An effective method to reduce residual lithium compounds on Ni-rich Li[Ni0.6Co0.2Mn0.2]O2 active material using a phosphoric acid derived Li3PO4 nanolayer", Nano Research, Dec. 4, 2014, vol. 8, No. 5, pp. 1464-1479, Springer.
Tebbe.J et al., "Mechanisms of LiCoO2 Cathode Degradation by Reaction with HF and Protection by Thin Oxide Coatings", ACS Applied Materials & Interfaces, Oct. 12, 2015, vol. 7, No. 43, pp. 24265-24278.
Bensalah.N et al., "Review on Synthesis, Characterizations, and Electrochemical Properties of Cathode Materials for Lithium Ion Batteries", Journal of Material Science & Engineering, 2016, vol. 5, No. 4, pp. 1000258-1-1000258-21.
Lu.Y et al., "Recent progress on lithium-ion batteries with high electrochemical performance", Science China Chemistry, Feb. 25, 2019, vol. 62, No. 5, pp. 533-548.
Xiao.B, "Surface Modifification of Electrode Materials for Lithium-Ion Batteries", Graduate Program in Mechanical and Materials Engineering, 2006, pp. 1-235.
Ohnishi.M et al., "Investigation of the surface degradation of LiCoO2 particles in the cathode materials of Li-ion batteries using FIB-TOF-SIMS", Journal of Surface Analysis, 2013, vol. 20, No. 2, pp. 99-110.
Iwaya.K et al., "Impact of Lithium-Ion Ordering on Surface Electronic States of LixCoO2", Phys. Rev. Lett. (Physical Review Letters), Sep. 20, 2013, vol. 111, No. 12, pp. 126104-1-126104-5.
Zou.M et al., "Synthesis of High-Voltage (4.5 V) Cycling Doped LiCoO2 for Use in Lithium Rechargeable Cells", Chem. Mater. (Chemistry of Materials), Dec. 16, 2003, vol. 15, No. 25, pp. 4699-4702.
Schipper.F et al., "Study of Cathode Materials for Lithium-Ion Batteries: Recent Progress and New Challenges", Inorganics, Apr. 28, 2017, vol. 5, No. 2, pp. 1-29.
Xia.H et al., "Phase Transitions and High-Voltage Electrochemical Behavior of LiCoO2 Thin Films Grown by Pulsed Laser Deposition", J. Electrochem. Soc. (Journal of the Electrochemical Society), 2007, vol. 154, No. 4, pp. A337-A342.
Sun.Y et al., "Role of AlF3 Coating on LiCoO2 Particles during Cycling to Cutoff Voltage above 4.5 V", J. Electrochem. Soc. (Journal of the Electrochemical Society), 2009, vol. 156, No. 12, pp. A1005-A1010.
Araki.K et al., "Electrochemical properties of LiNi1/3Co1/3Mn1/3O2 cathode material modified by coating with Al2O3 nanoparticles", Journal of Power Sources, 2014, vol. 269, pp. 236-243.
Kim.H et al., "Capacity fading behavior of Ni-rich layered cathode materials in Li-ion full cells", Journal of Electroanalytical Chemistry, 2016, vol. 782, pp. 168-173.
Lin.F et al., "Surface reconstruction and chemical evolution of stoichiometric layered cathode materials for lithium-ion batteries", Nature Communications, Mar. 27, 2014, vol. 5, pp. 3529-1-3529-9.
Yano.A et al., "Surface Structure and High-Voltage Charge/Discharge Characteristics of Al-Oxide Coated LiNi1/3Co1/3Mn1/3O2 Cathodes", J. Electrochem. Soc. (Journal of the Electrochemical Soceity), 2015, vol. 162, No. 2, pp. A3137-A3144.
Yano.A et al., "Surface Structure and High-Voltage Charging/Discharging Performance of Low-Content Zr-Oxide-Coated LiNi1/3Co1/3Mn1/3O2", J. Electrochem. Soc. (Journal of the Electrochemical Society), 2016, vol. 163, No. 2, pp. A75-A82.
Antolini.E, "LiCoO2: formation, structure, lithium and oxygen nonstoichiometry, electrochemical behaviour and transport properties", Solid State Ionics, 2004, vol. 170, No. 3-4, pp. 159-171.
Ceder.G et al., "Identification of cathode materials for lithium batteries guided by first-principles calculations", Nature, Apr. 16, 1998, vol. 392, pp. 694-696.
Gopukumar.S et al., "Synthesis and electrochemical performance of tetravalent doped LiCoO2 in lithium rechargeable cells", Solid State Ionics, 2003, vol. 159, pp. 223-232, Elsevier.
Ding.Y et al., "Preparation of nano-structured LiFePO4/graphene composites by co-precipitation method", Electrochemistry Communications, 2010, vol. 12, No. 1, pp. 10-13, Elsevier.

* cited by examiner

FIG. 1A

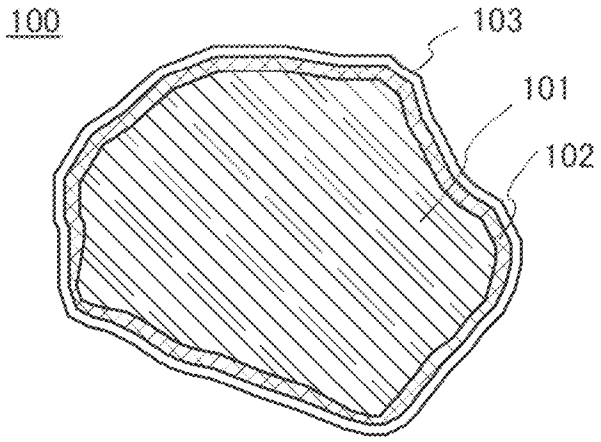

FIG. 1B

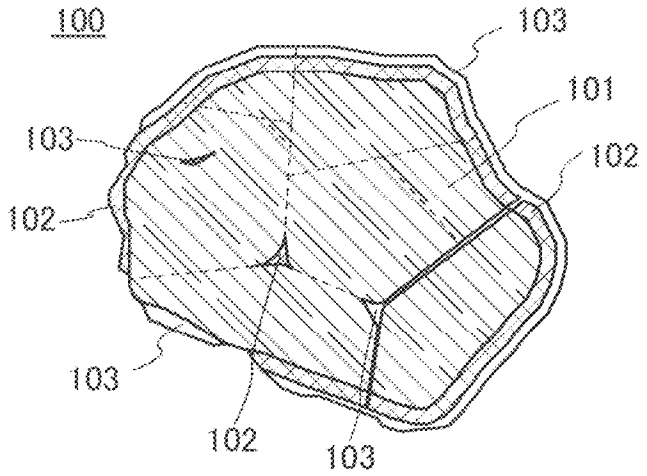

FIG. 1C

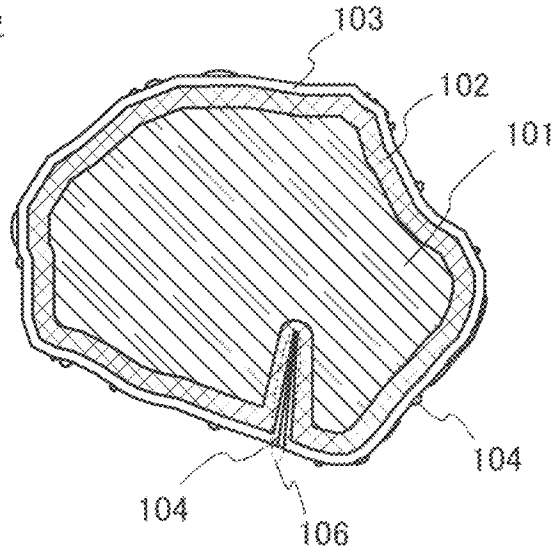

FIG. 2A

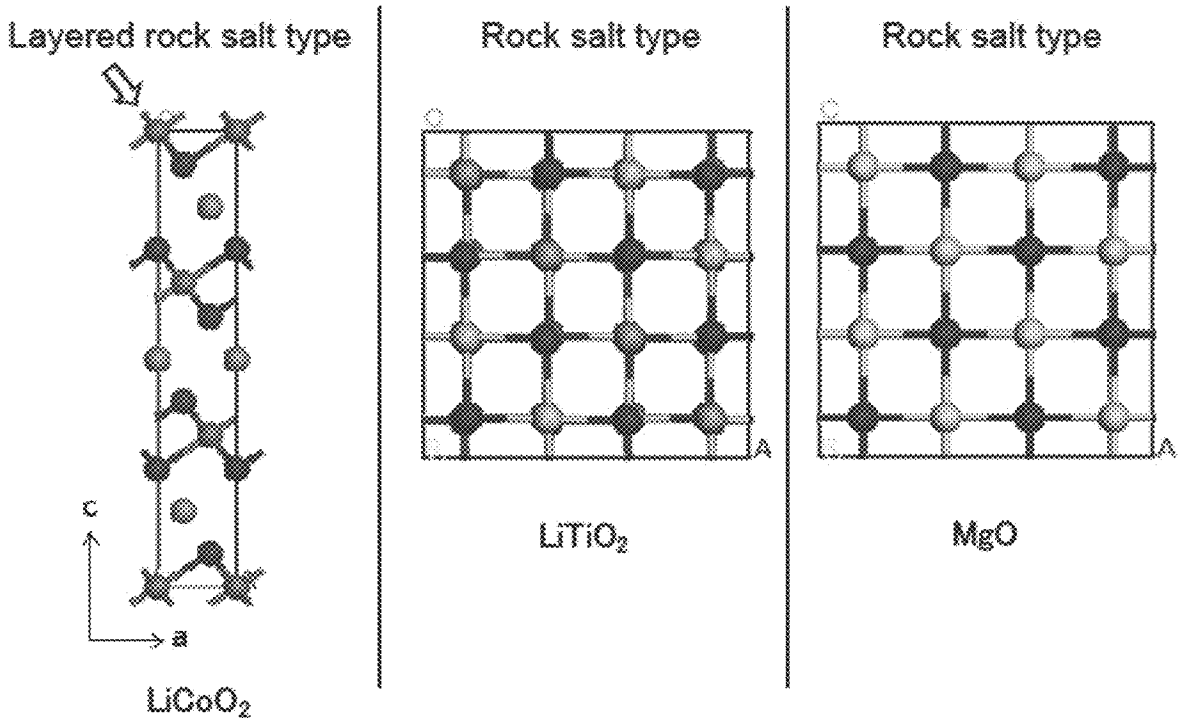
Layered rock salt type
Rock salt type
Rock salt type
c
a
LiCoO2
LiTiO2
MgO

FIG. 2B

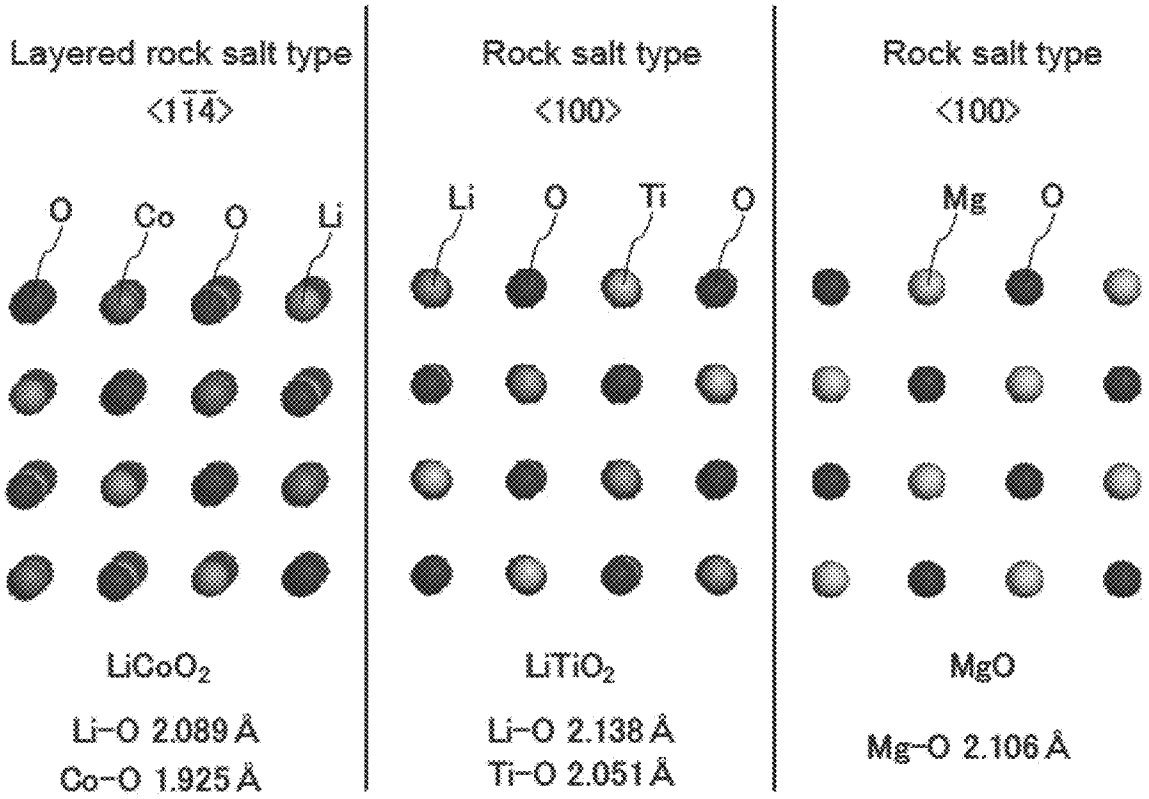
Layered rock salt type
<1$\bar{1}$4>
Rock salt type
<100>
Rock salt type
<100>
O
Co
O
Li
Li
O
Ti
O
Mg
O
LiCoO2
Li–O 2.089 Å
Co–O 1.925 Å
LiTiO2
Li–O 2.138 Å
Ti–O 2.051 Å
MgO
Mg–O 2.106 Å

FIG. 3

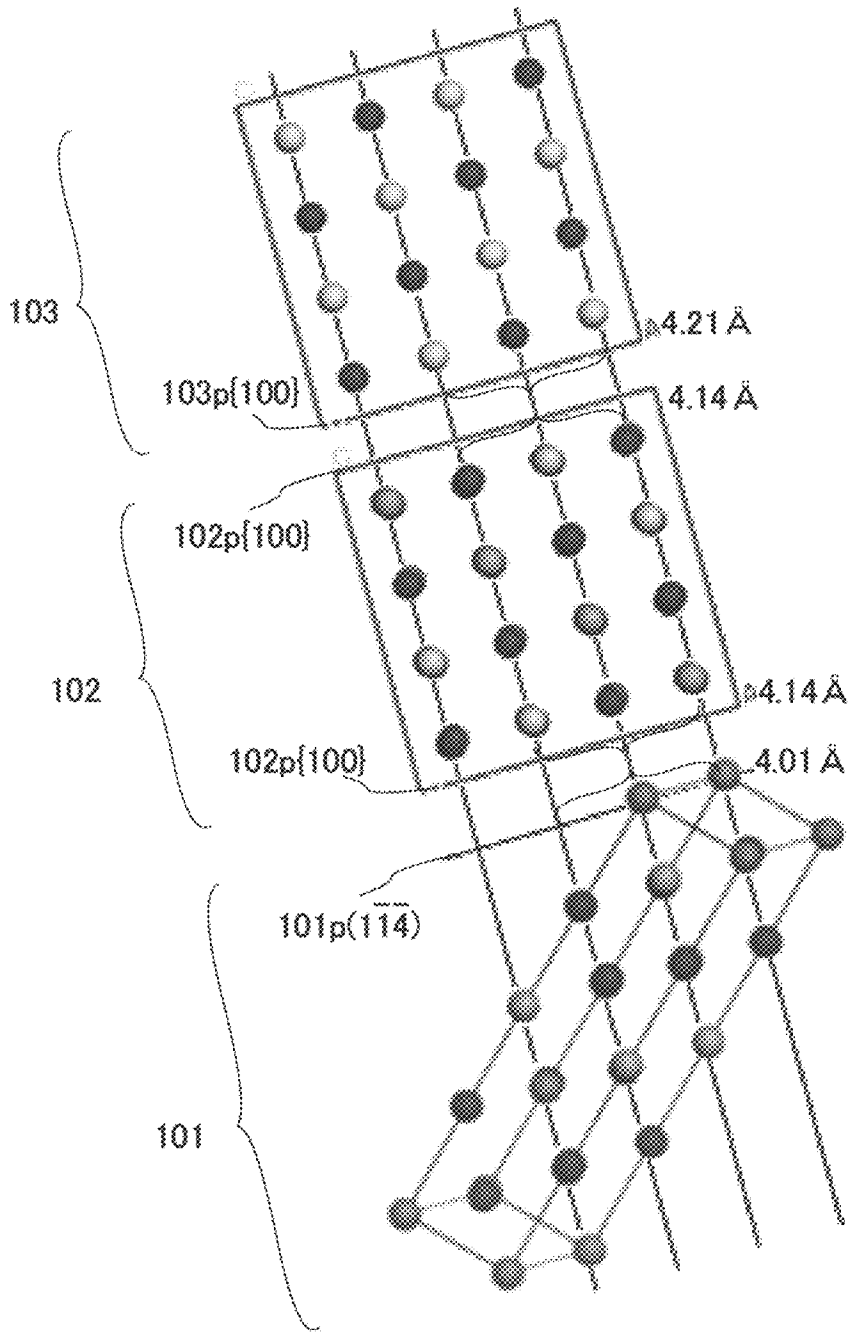
103
103p(100)
4.21 Å
4.14 Å
102p(100)
102
4.14 Å
102p(100)
4.01 Å
101p(1̄1̄4)
101

FIG. 4A-1

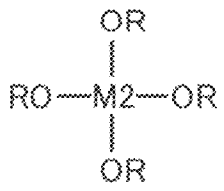

$M2(OR)_4$

FIG. 4A-2

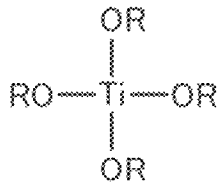

$Ti(OR)_4$

FIG. 4A-3

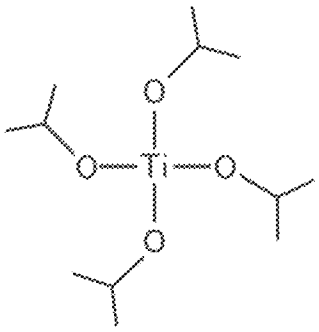

TTIP

FIG. 4B

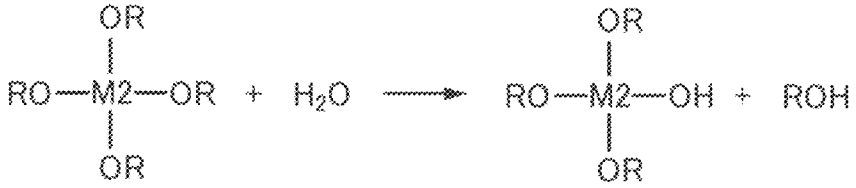

FIG. 4C

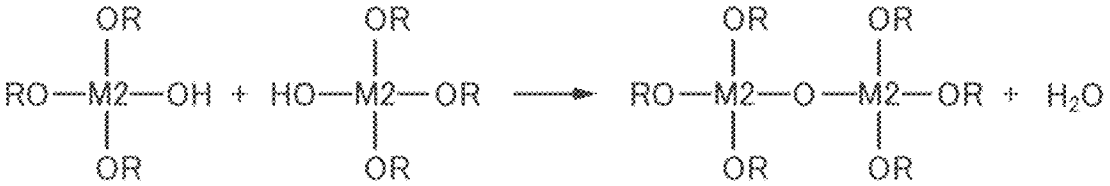

FIG. 4D-1

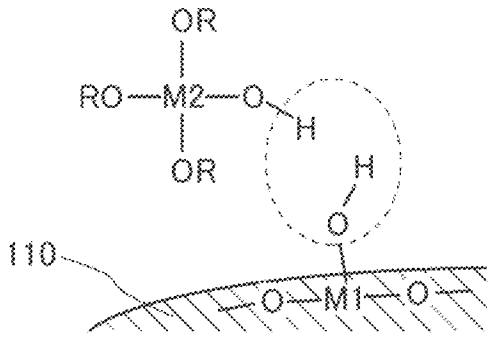

FIG. 4D-2

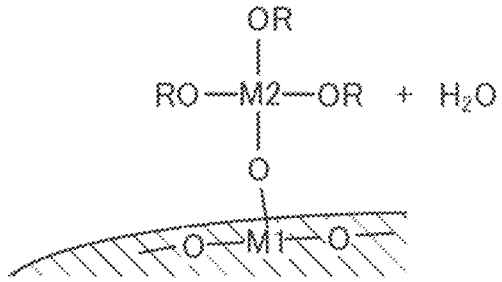

FIG. 5A

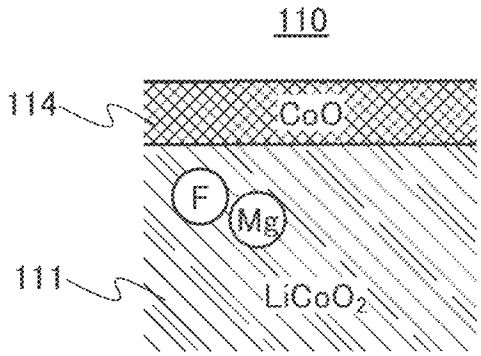

FIG. 5B

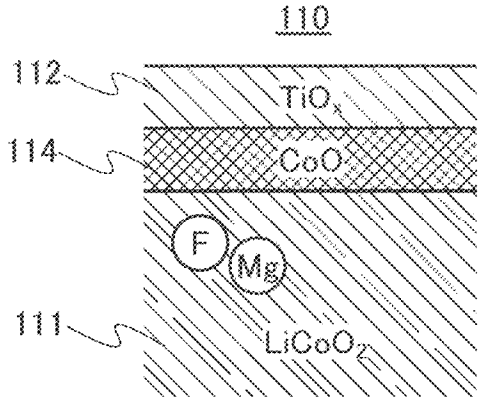

FIG. 5C

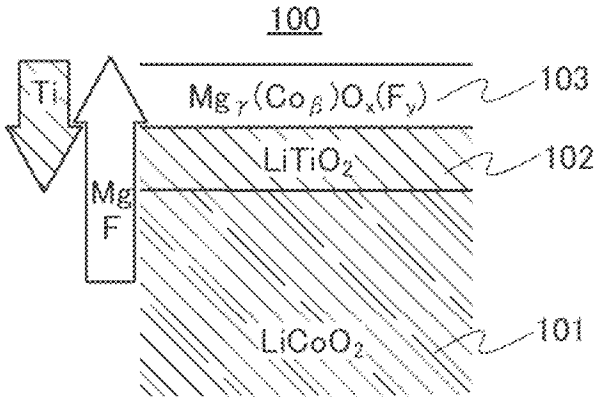

FIG. 6A

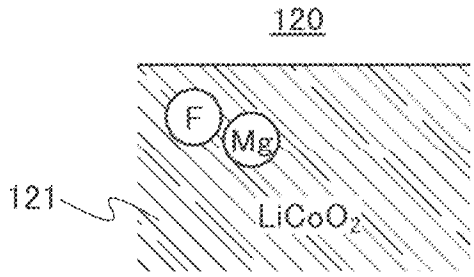

FIG. 6B

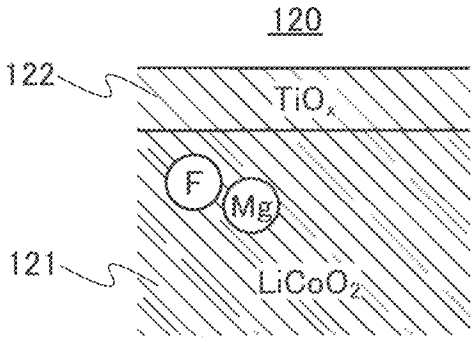

FIG. 6C

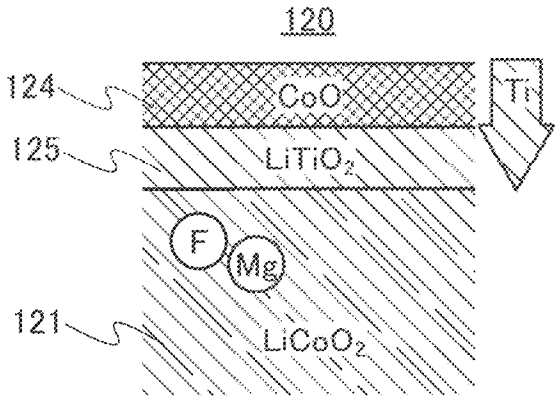

FIG. 6D

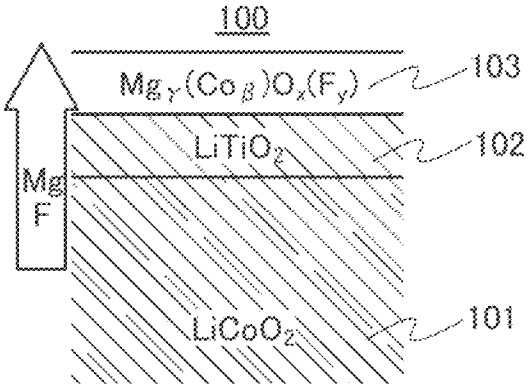

FIG. 7A

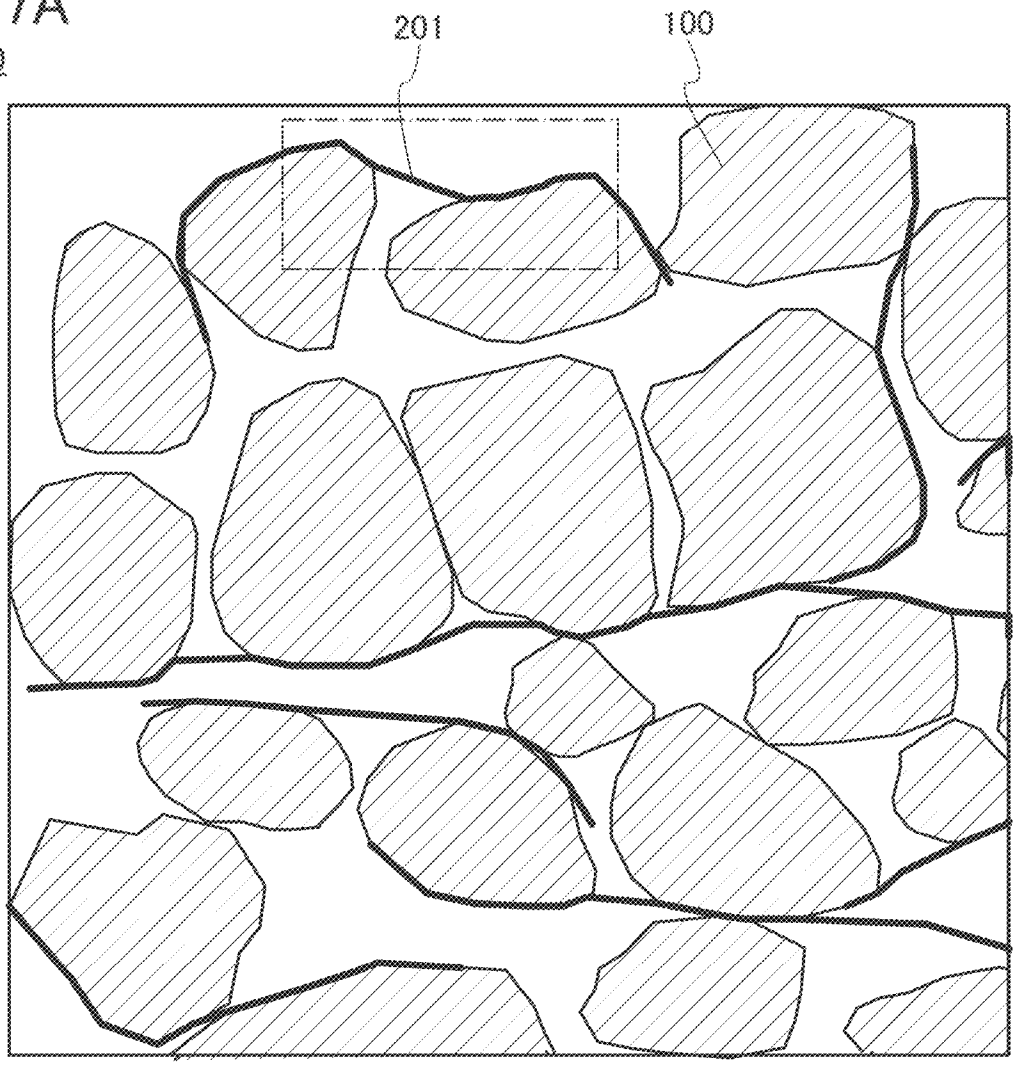

FIG. 7B

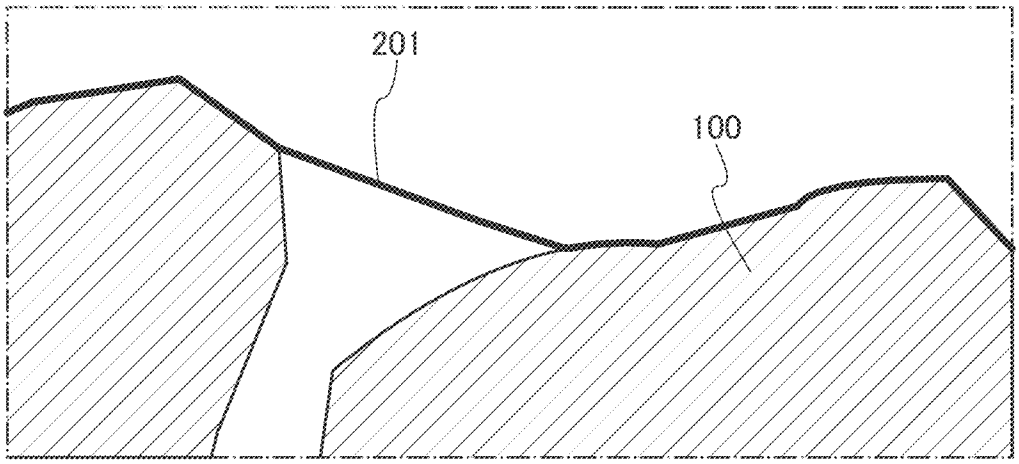

FIG. 8A

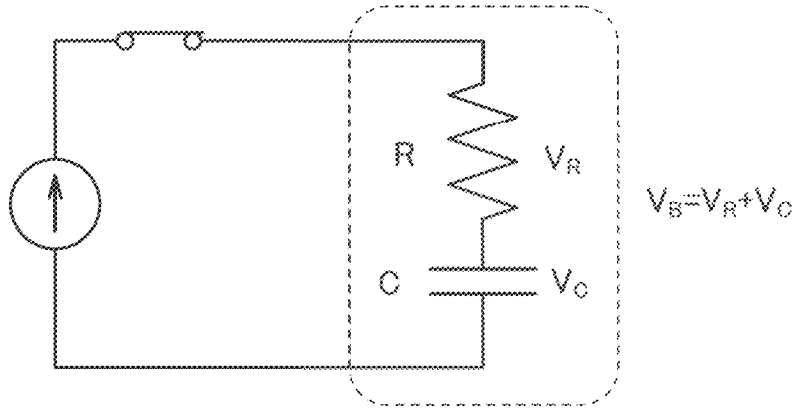

FIG. 8B

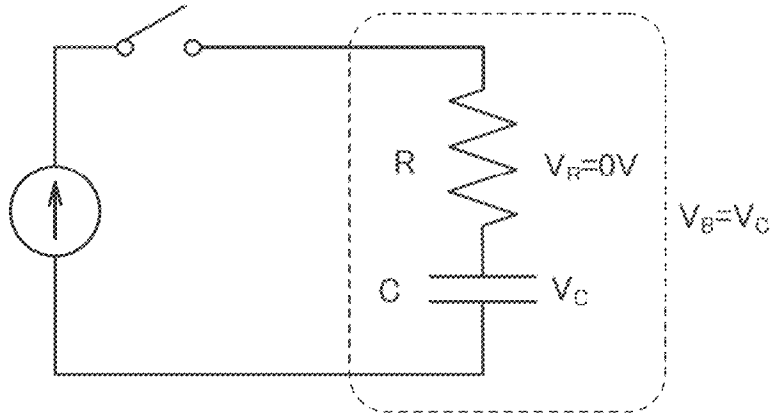

FIG. 8C

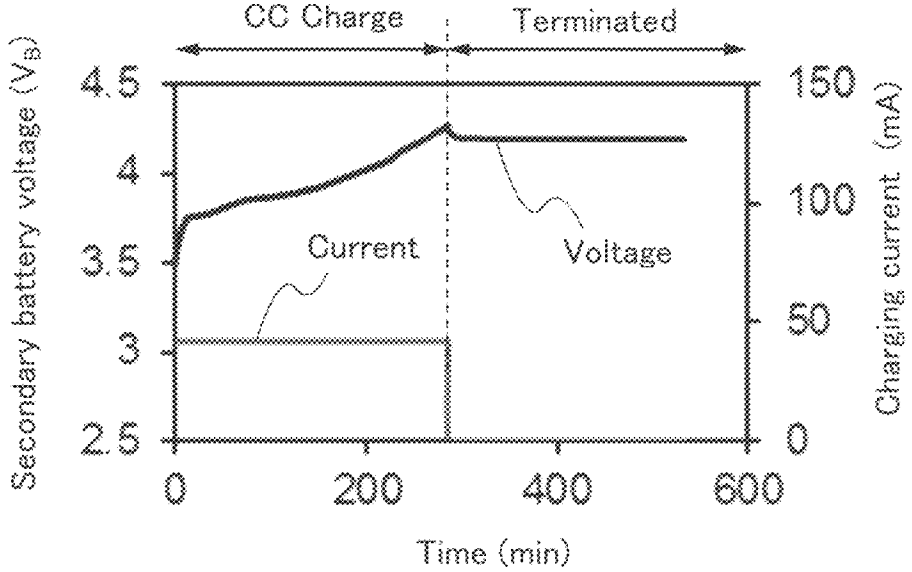

FIG. 9A

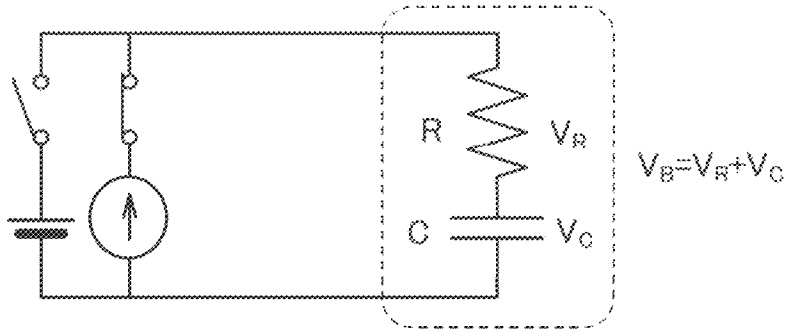

FIG. 9B

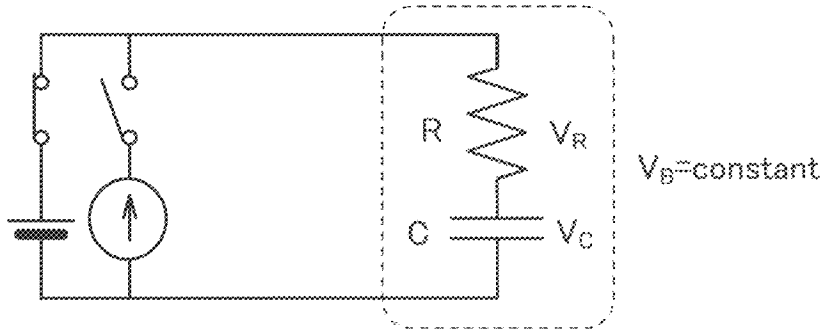

FIG. 9C

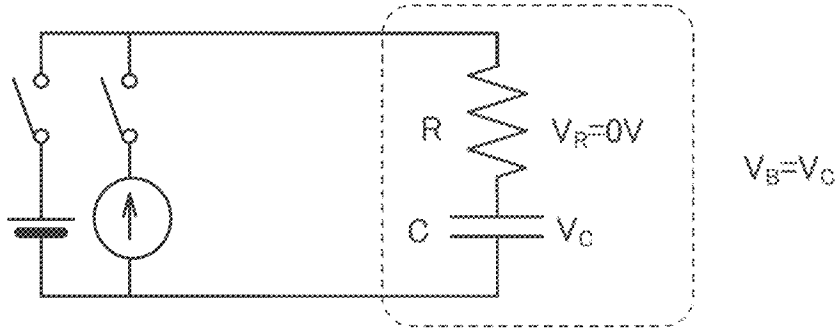

FIG. 9D

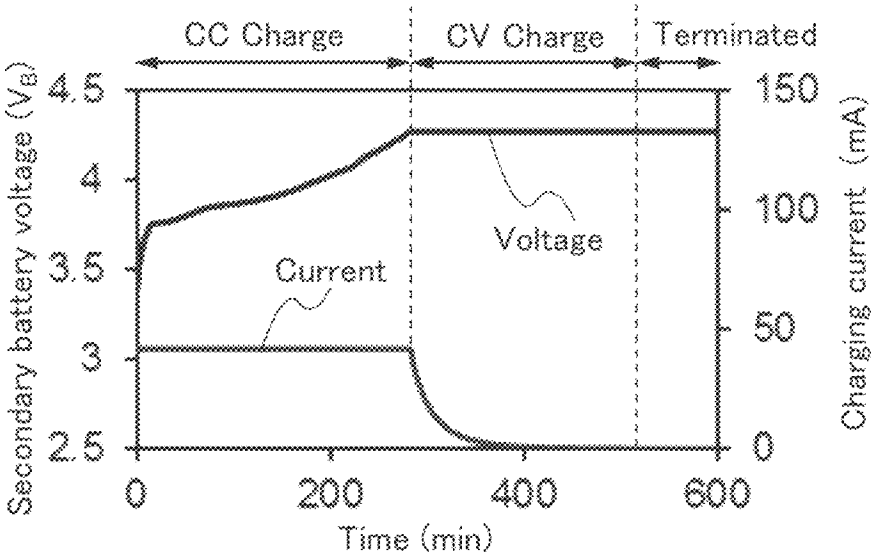

FIG. 10

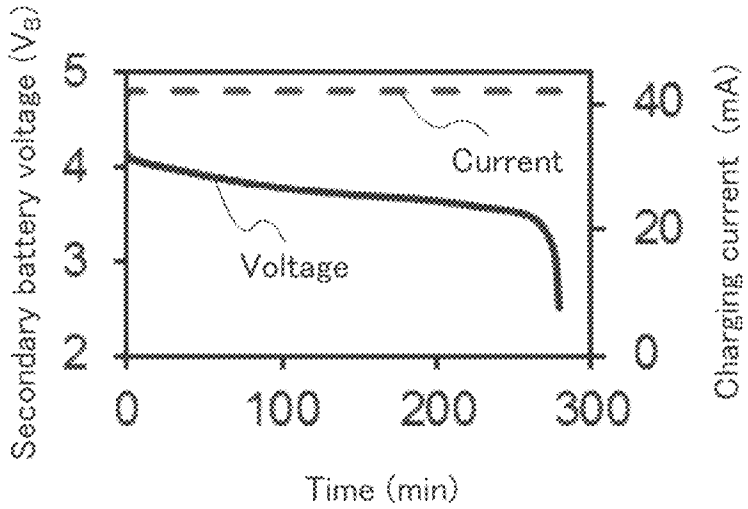
Secondary battery voltage (V_B)
5
4
3
2
Voltage
Current
40
20
0
Charging current (mA)
0
100
200
300
Time (min)

FIG. 11A

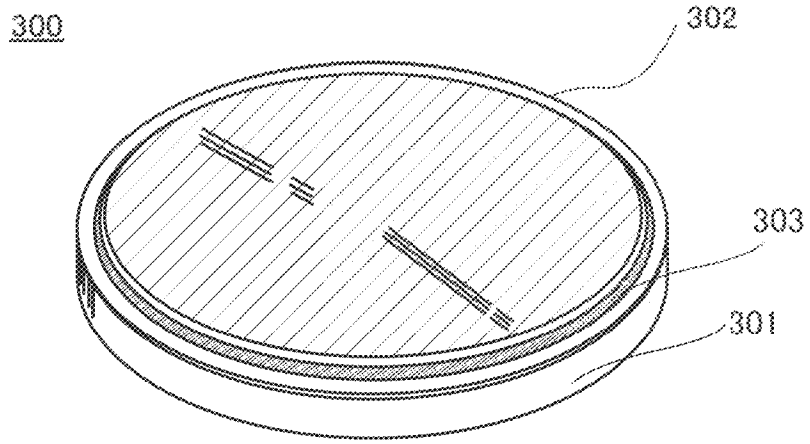

FIG. 11B

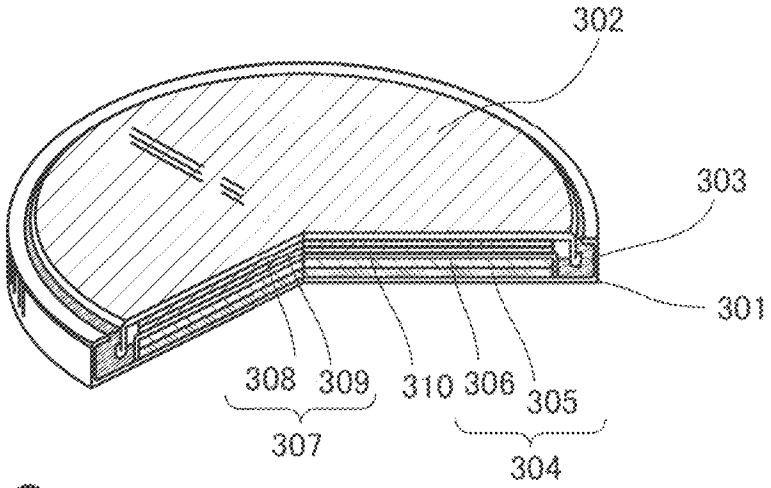

FIG. 11C

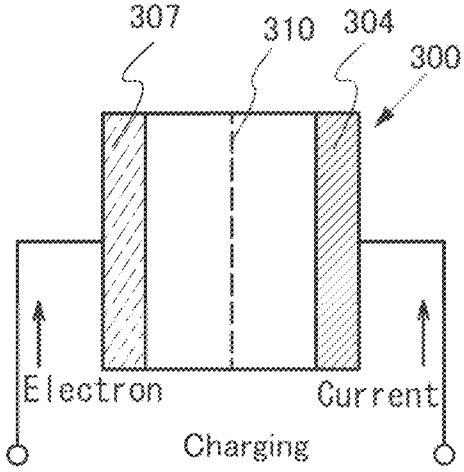

FIG. 12A

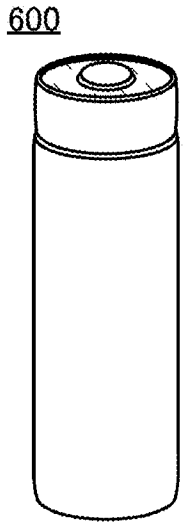

FIG. 12B

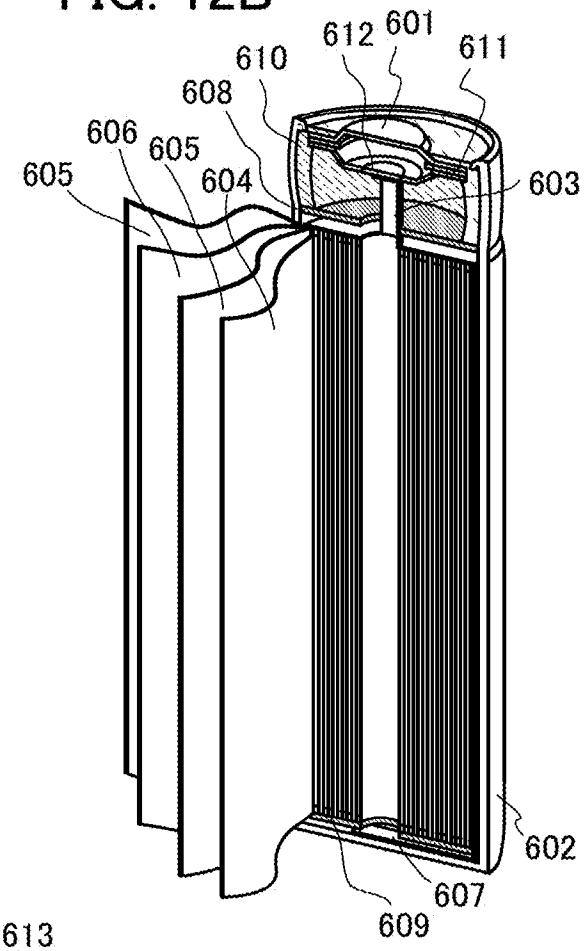

FIG. 12C

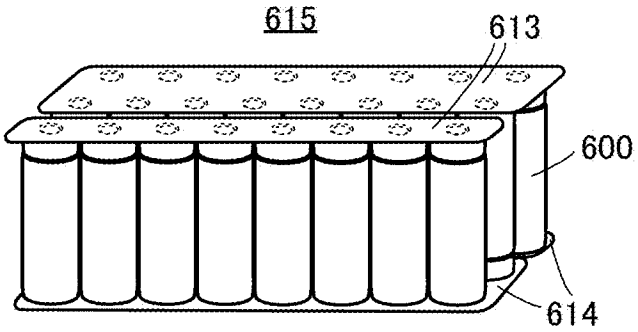

FIG. 12D

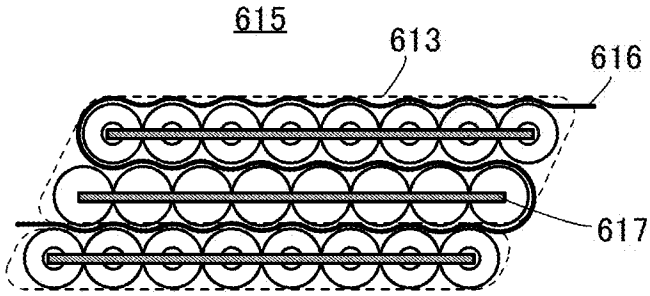

FIG. 13A

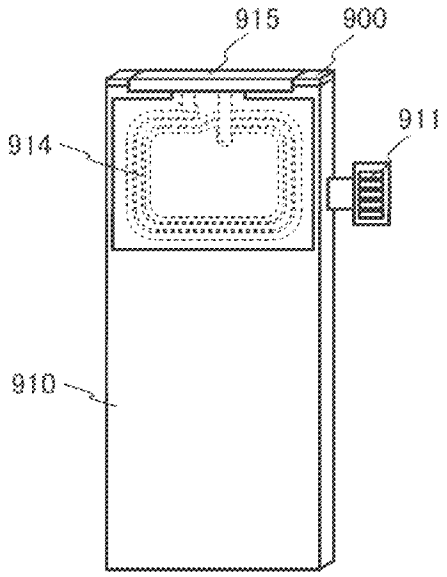

FIG. 13B

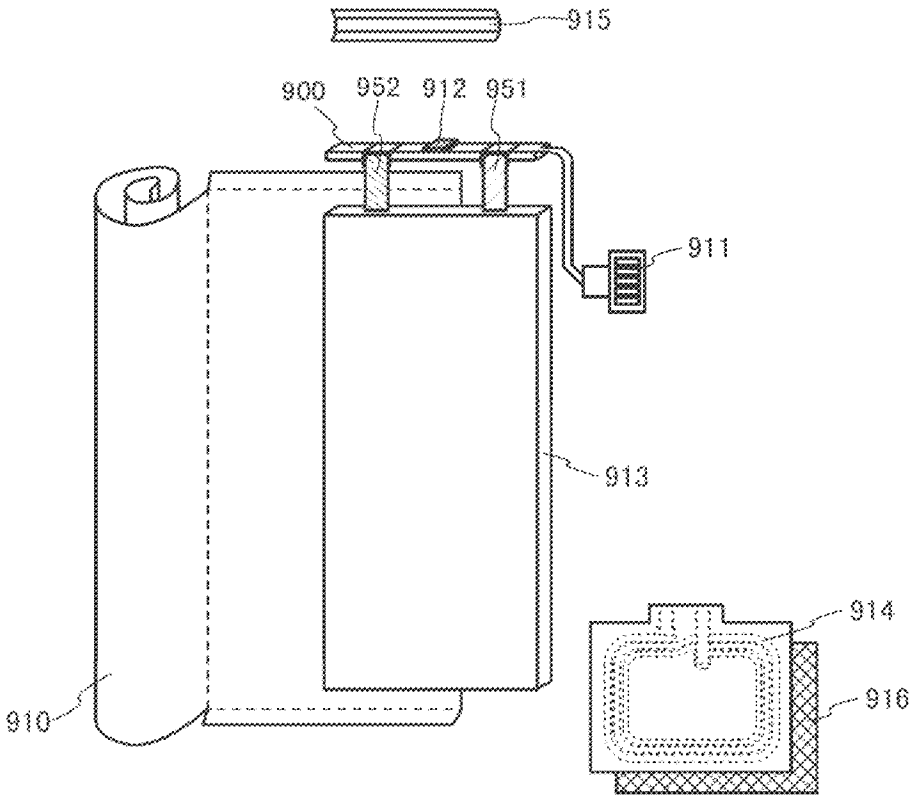

FIG. 14A-1

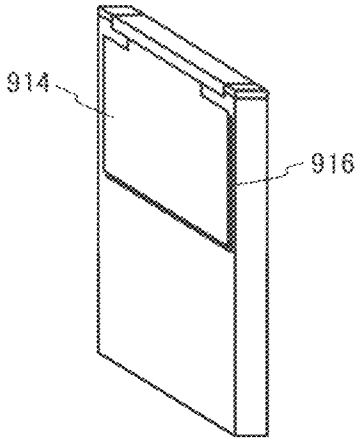

FIG. 14A-2

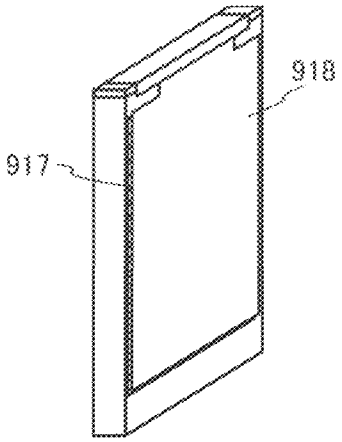

FIG. 14B-1

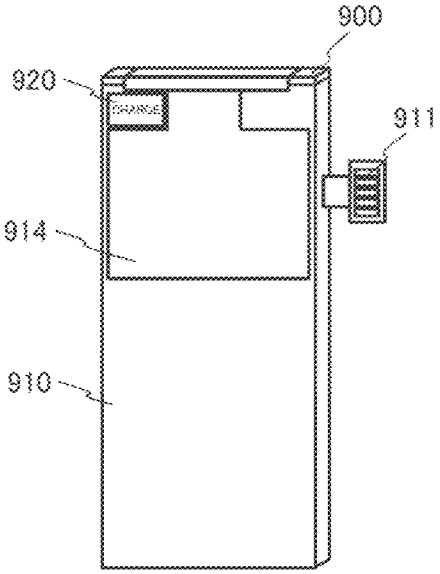

FIG. 14B-2

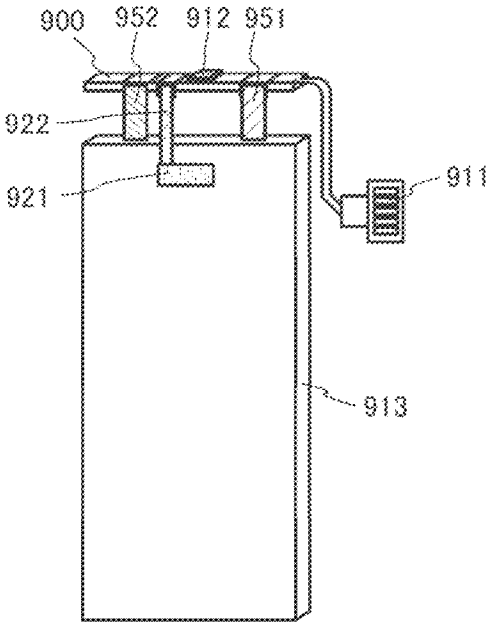

FIG. 15A

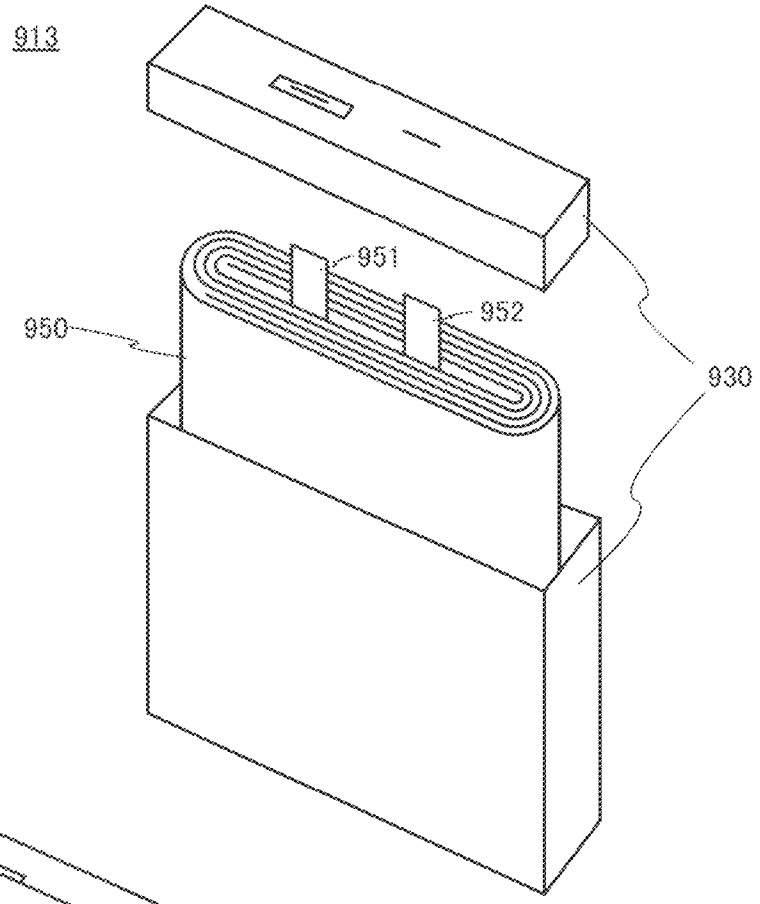

FIG. 15B

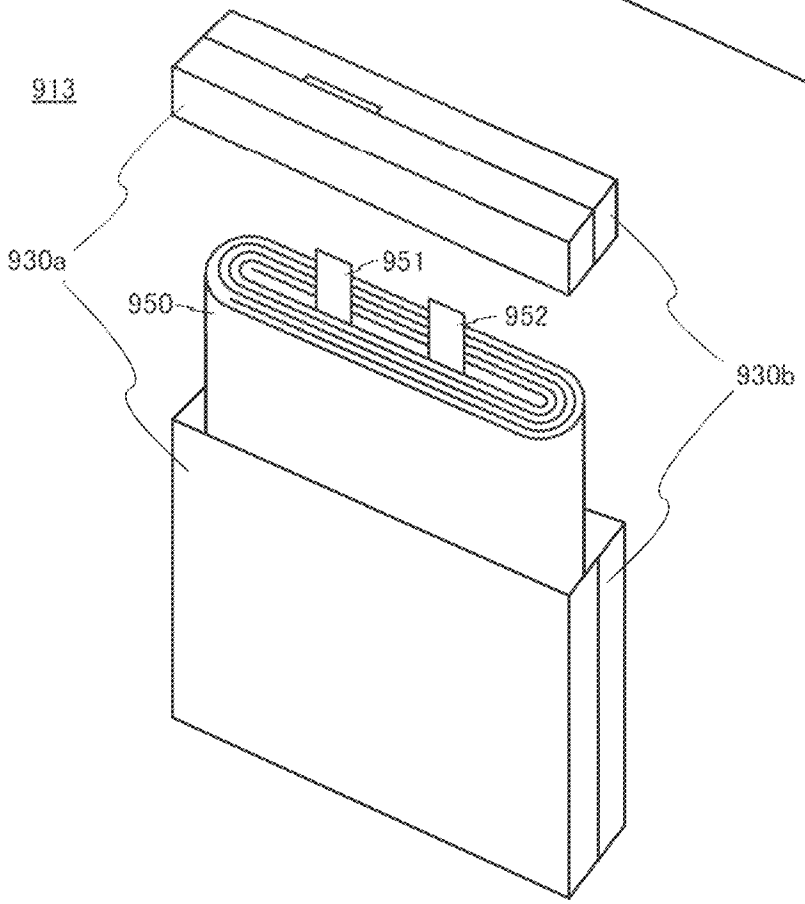

FIG. 16

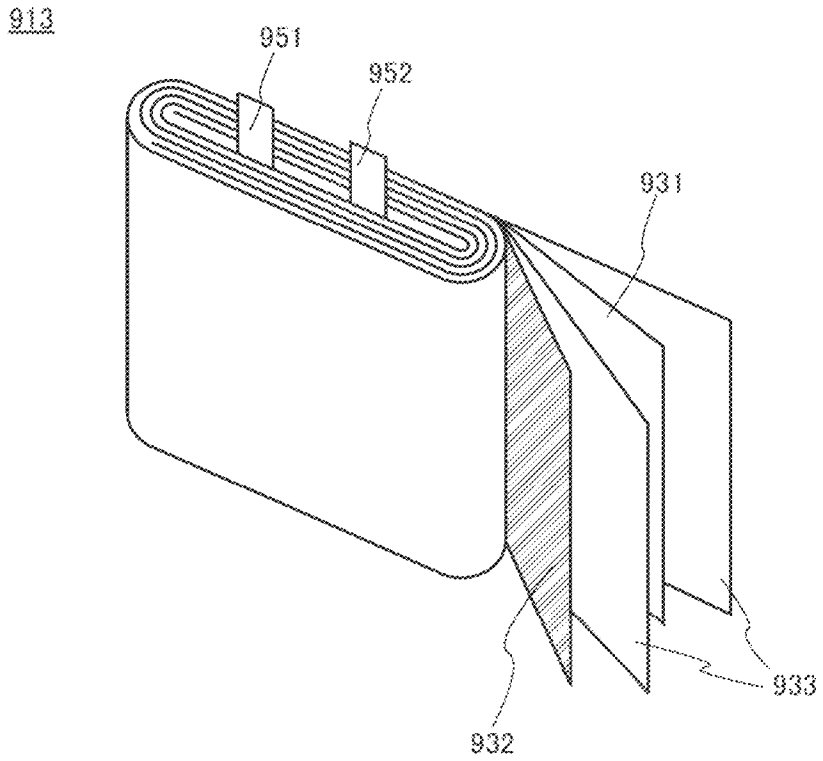

FIG. 17A

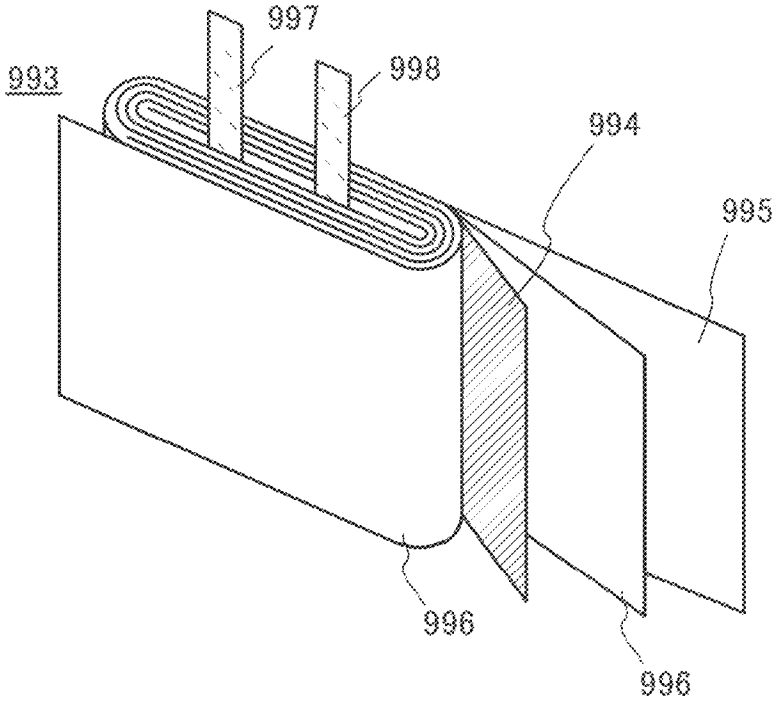

FIG. 17B

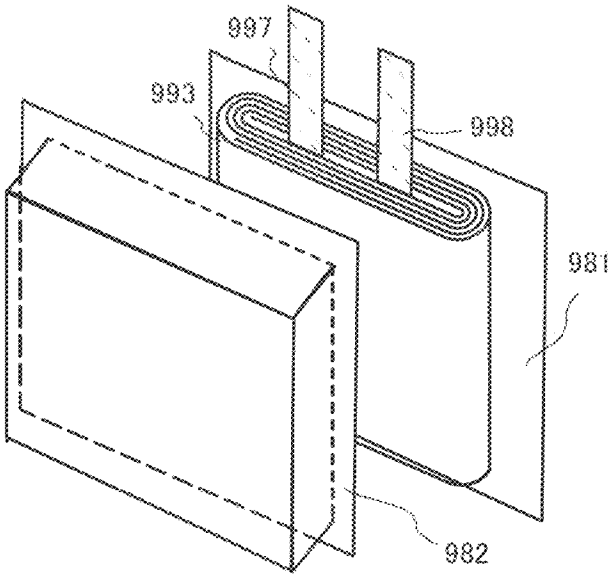

FIG. 17C

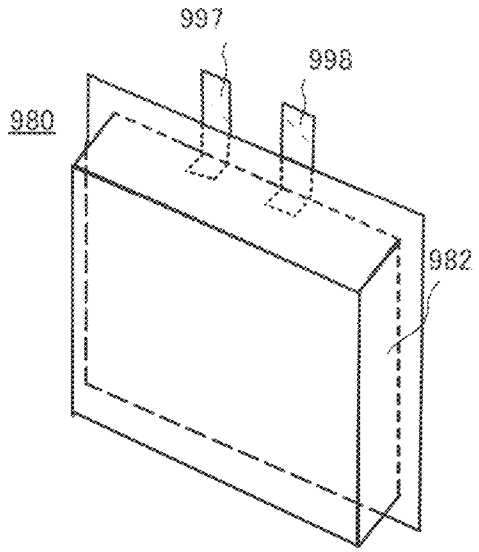

FIG. 18A

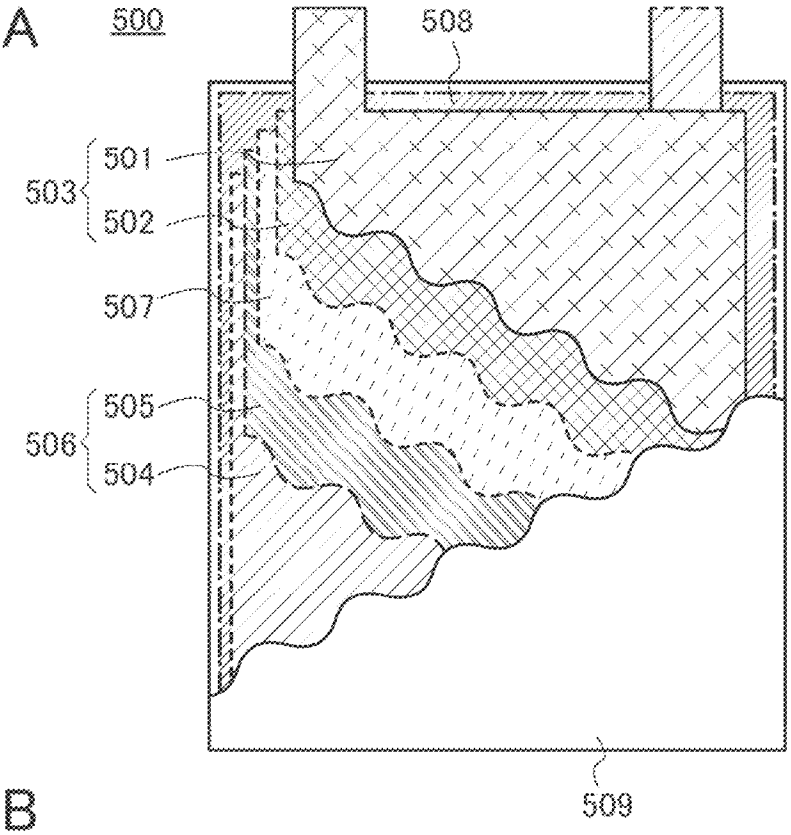

FIG. 18B

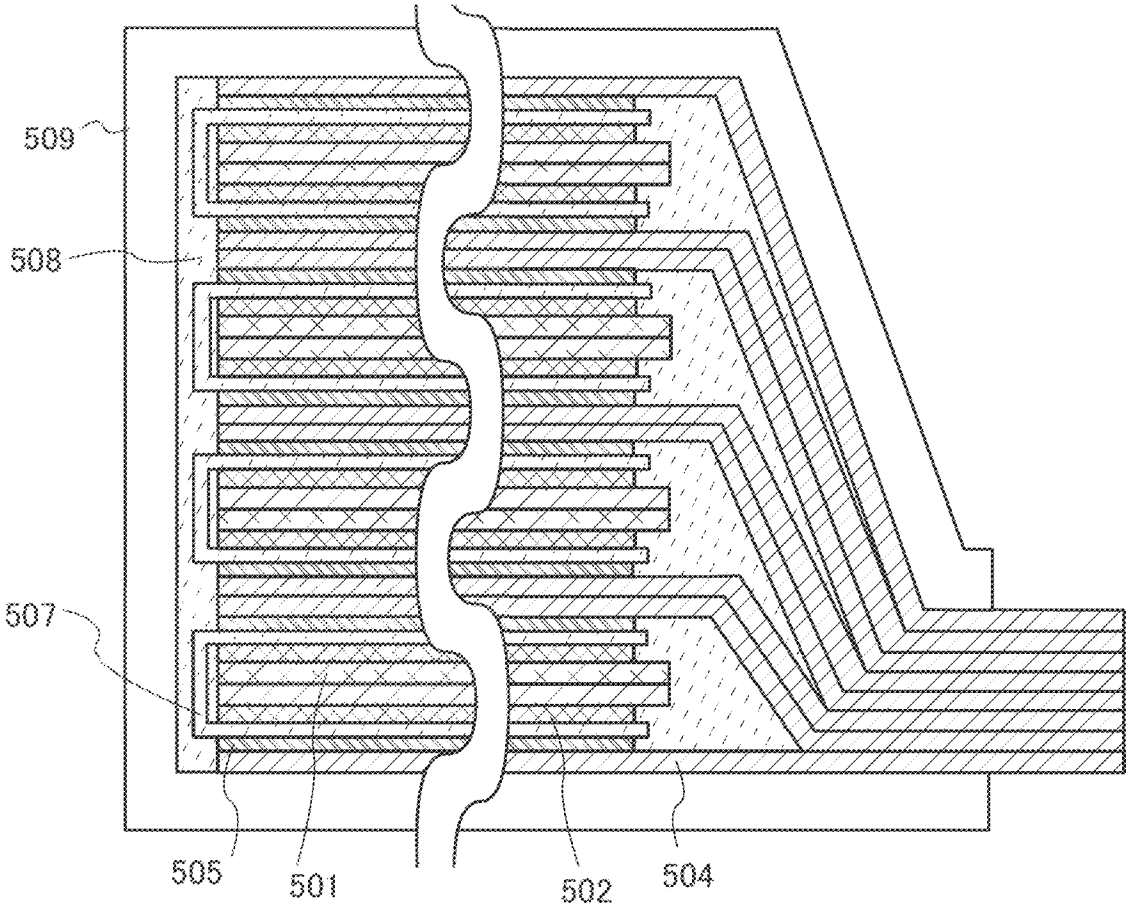

FIG. 19

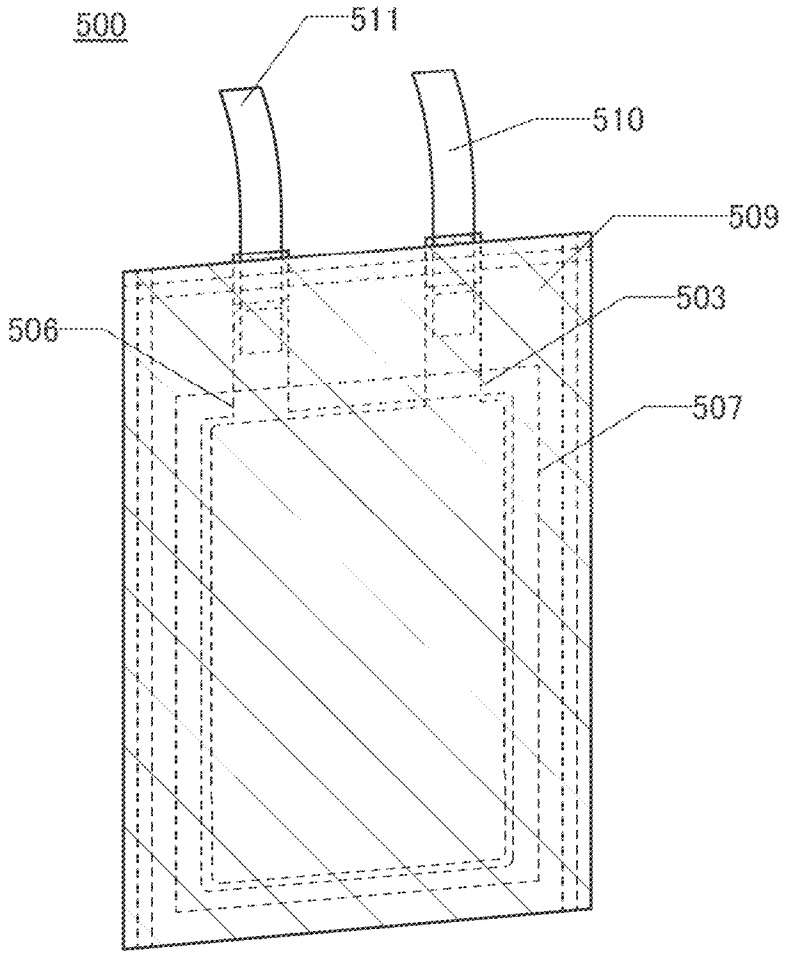

FIG. 20

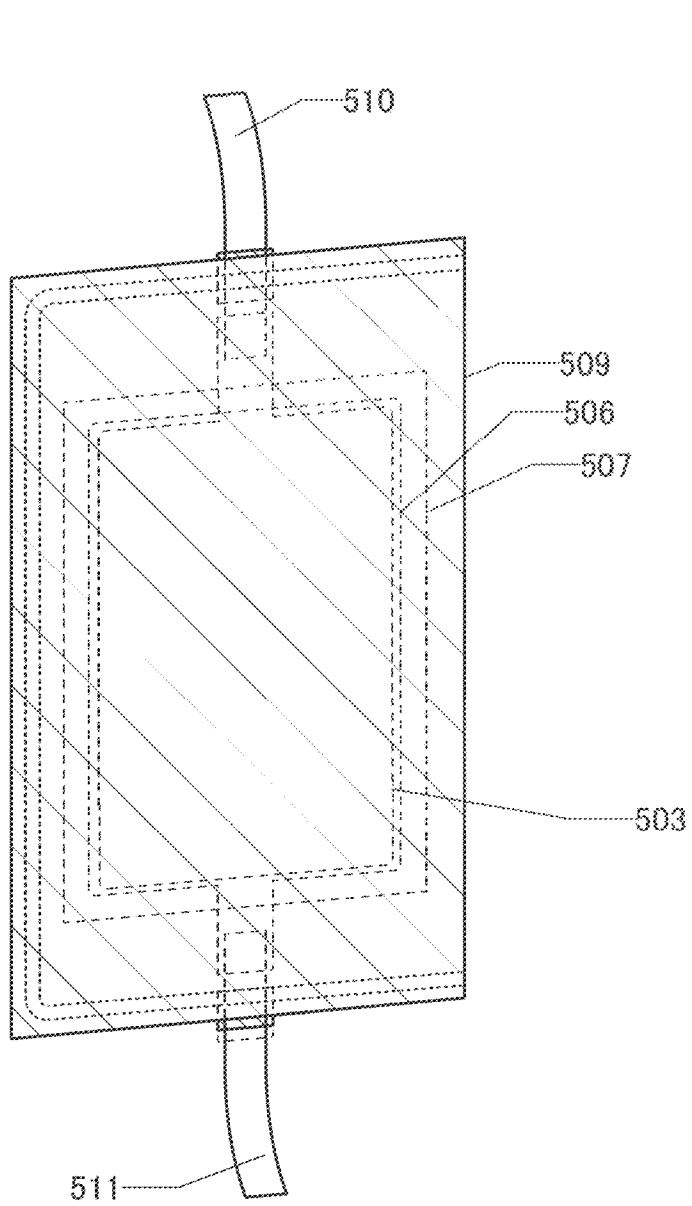

FIG. 21A

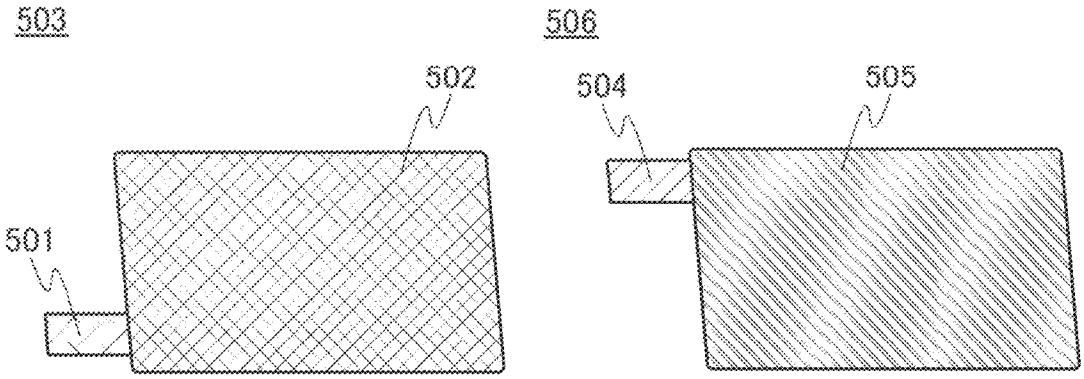

FIG. 21B

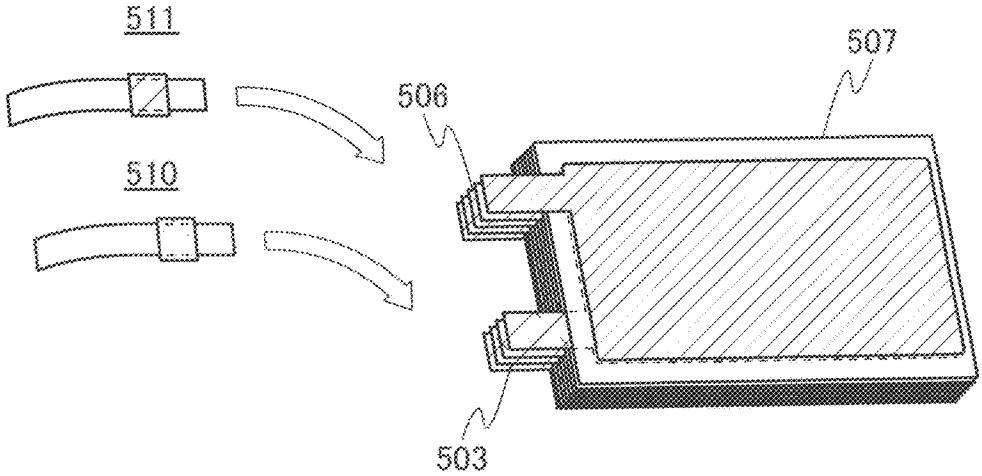

FIG. 21C

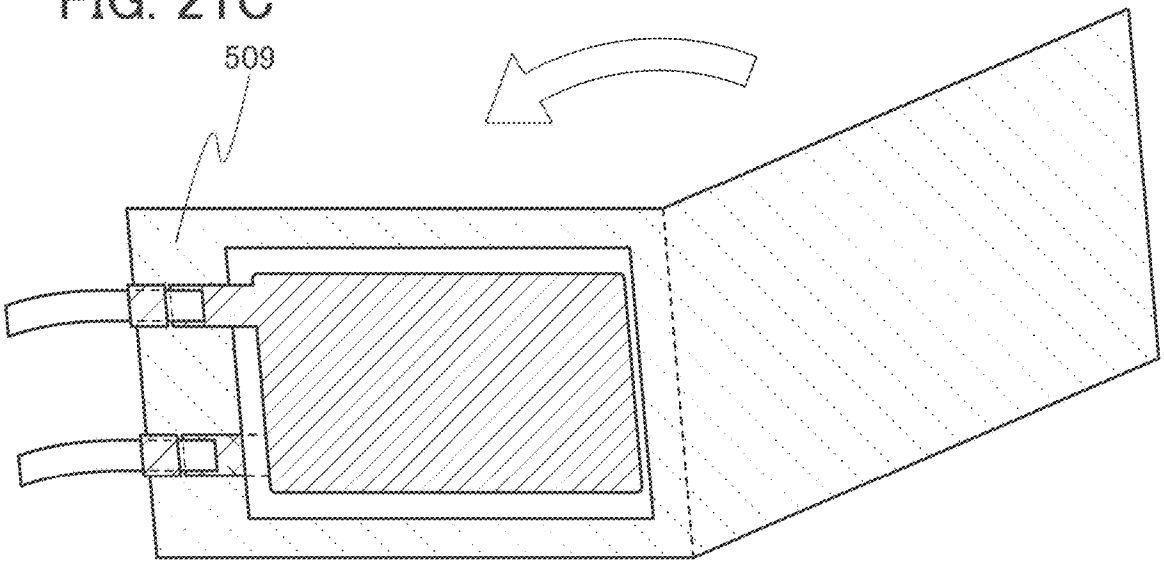

FIG. 22A

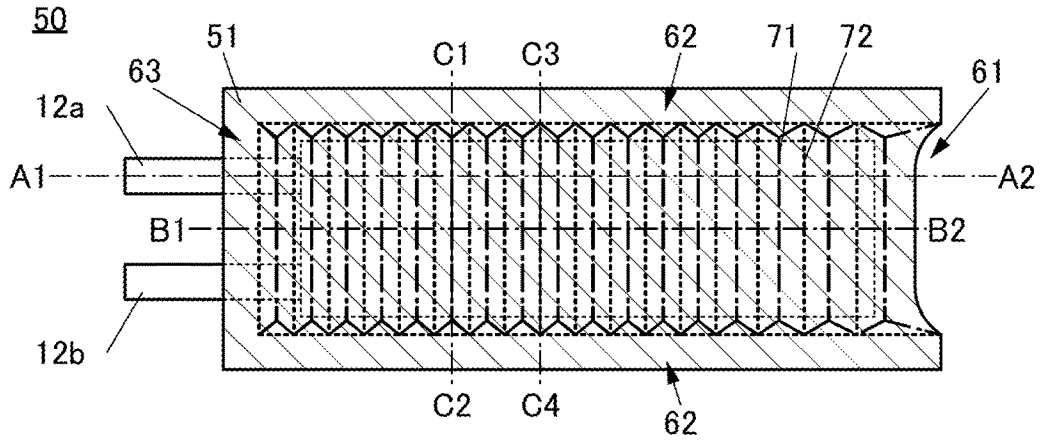

FIG. 22B1

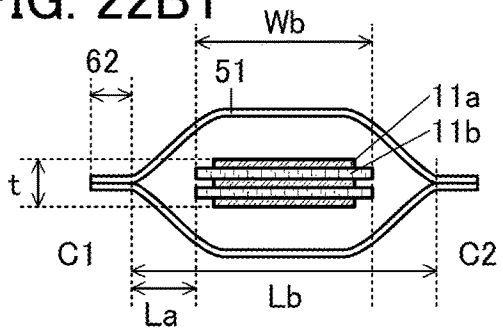

FIG. 22B2

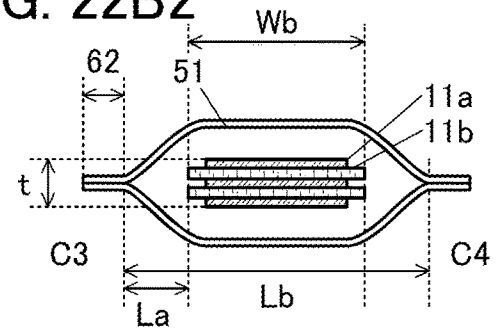

FIG. 22C

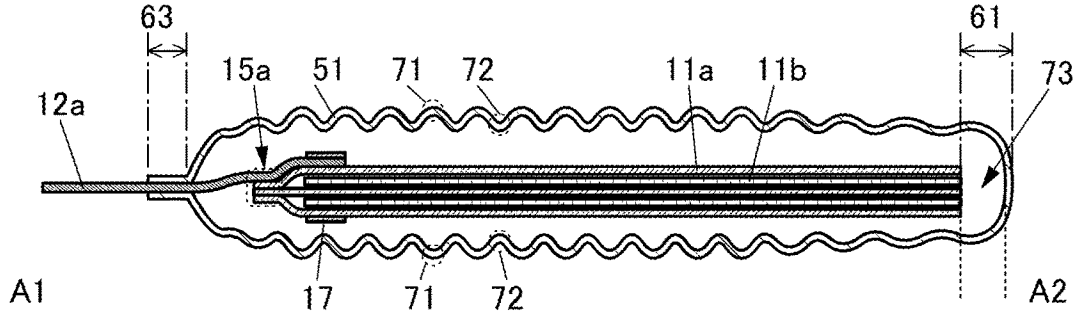

FIG. 22D

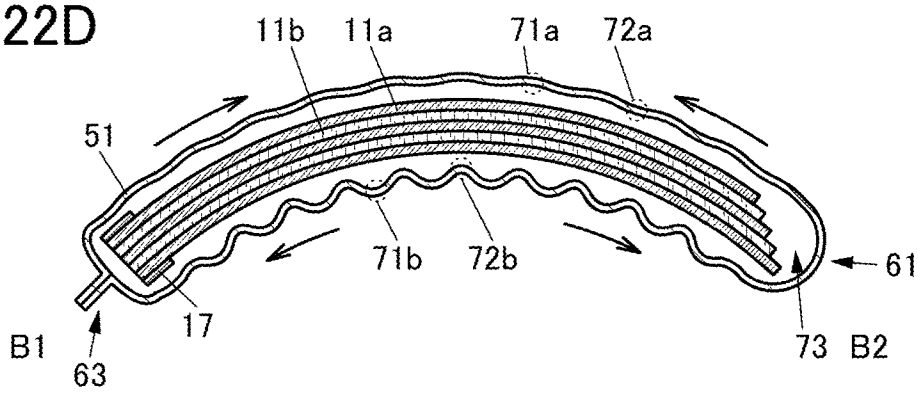

FIG. 23A

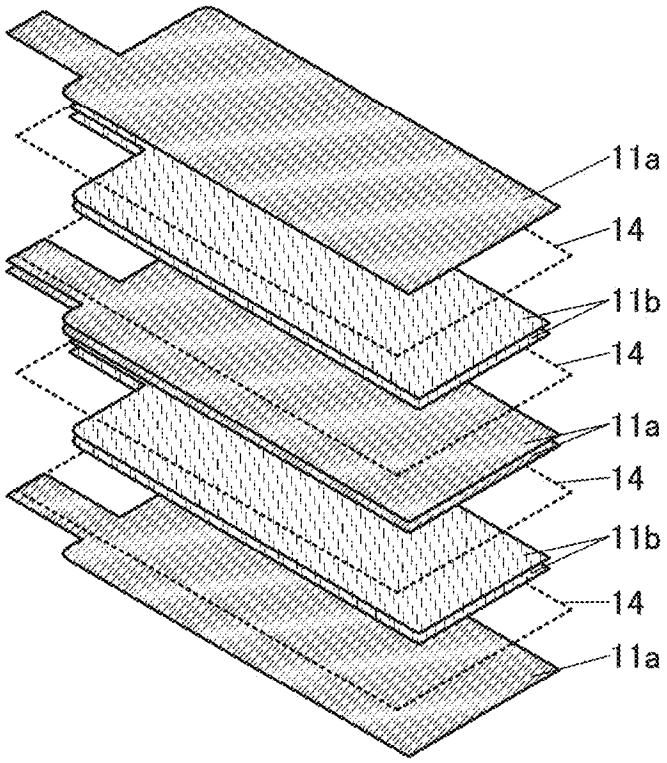

FIG. 23B

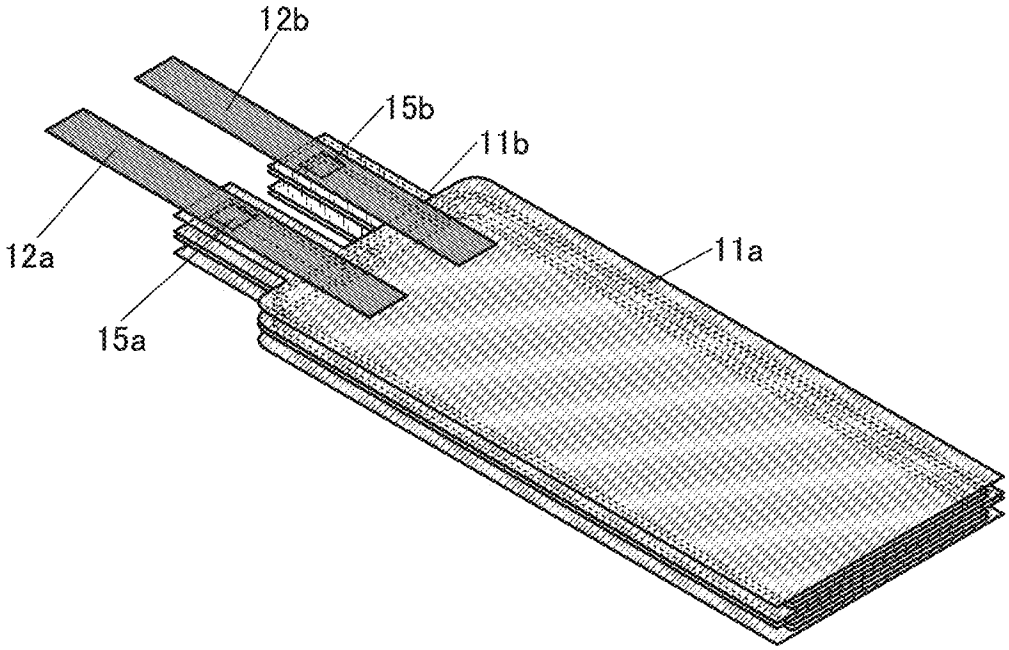

FIG. 24A

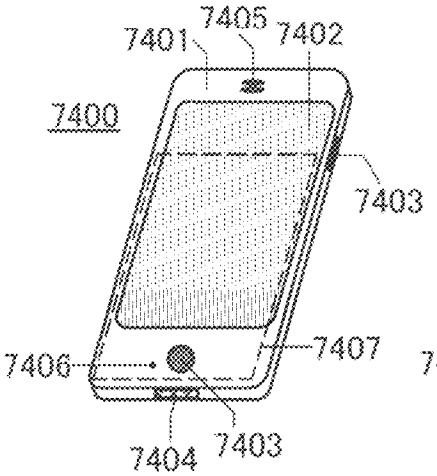

FIG. 24B

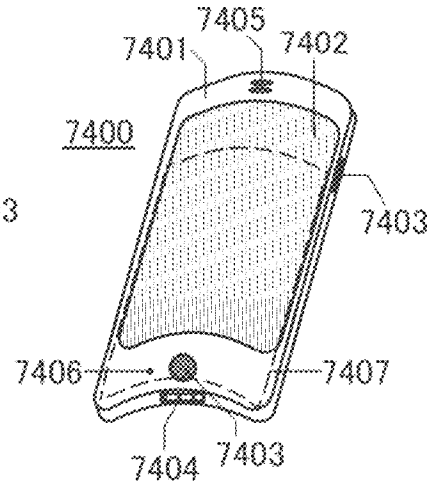

FIG. 24C

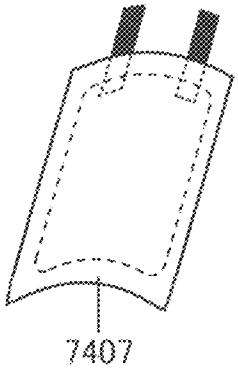

FIG. 24D

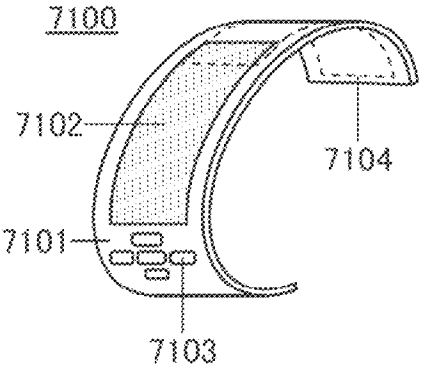

FIG. 24E

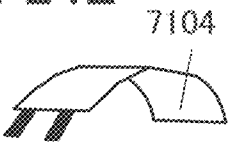

FIG. 24F

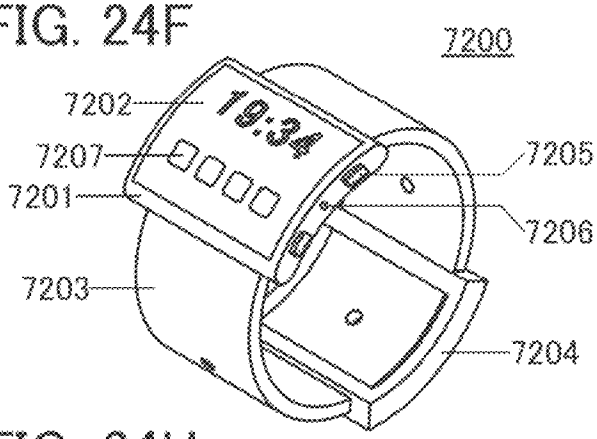

FIG. 24G

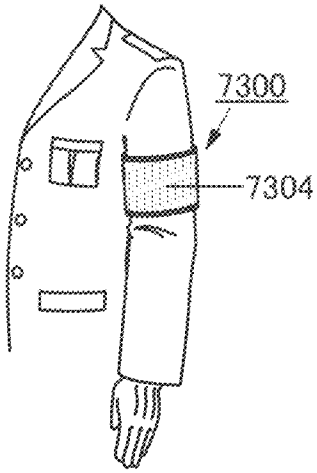

FIG. 24H

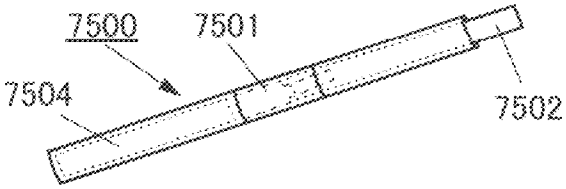

FIG. 25A

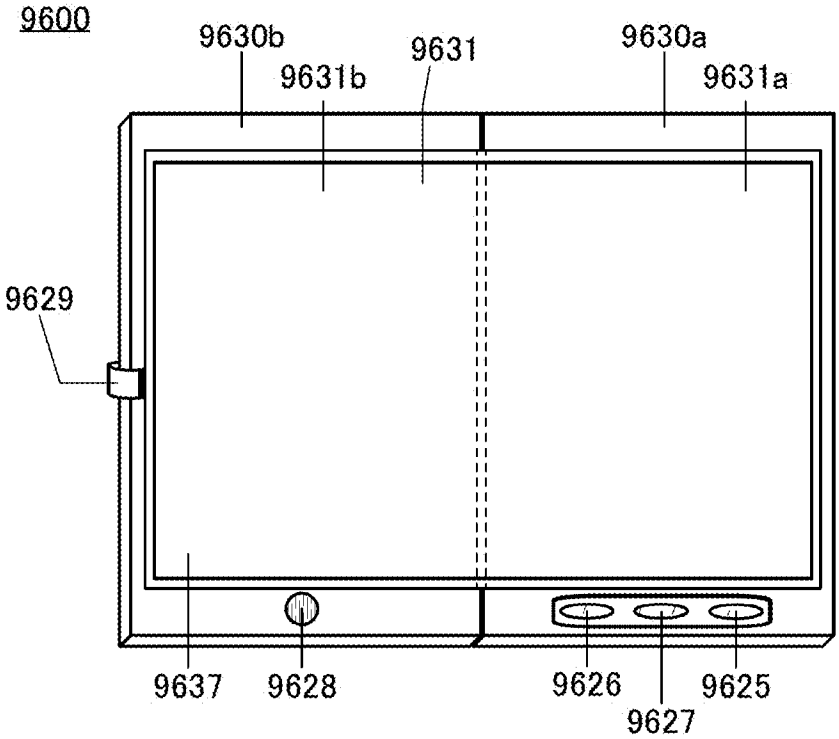

FIG. 25B

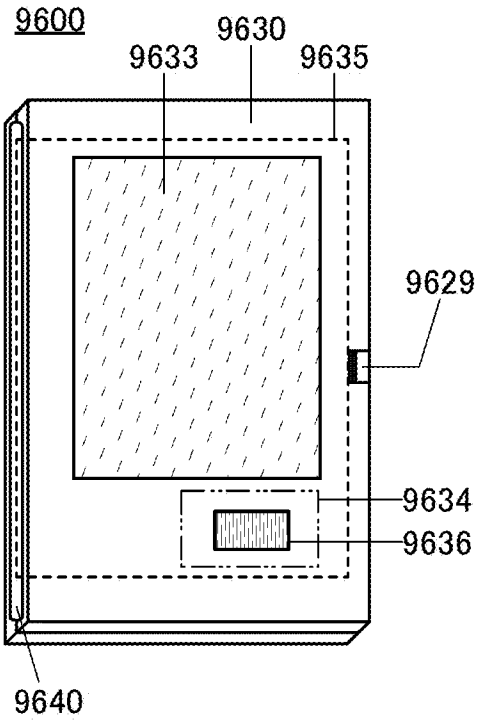

FIG. 25C

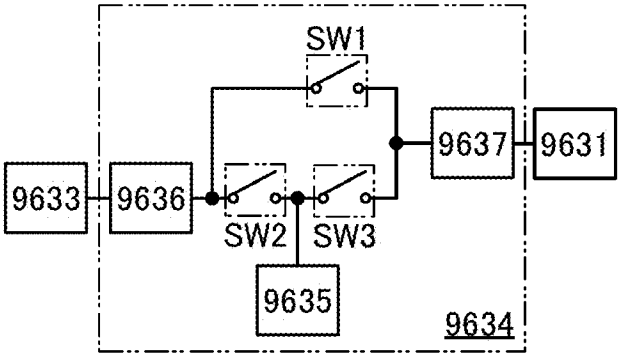

FIG. 26

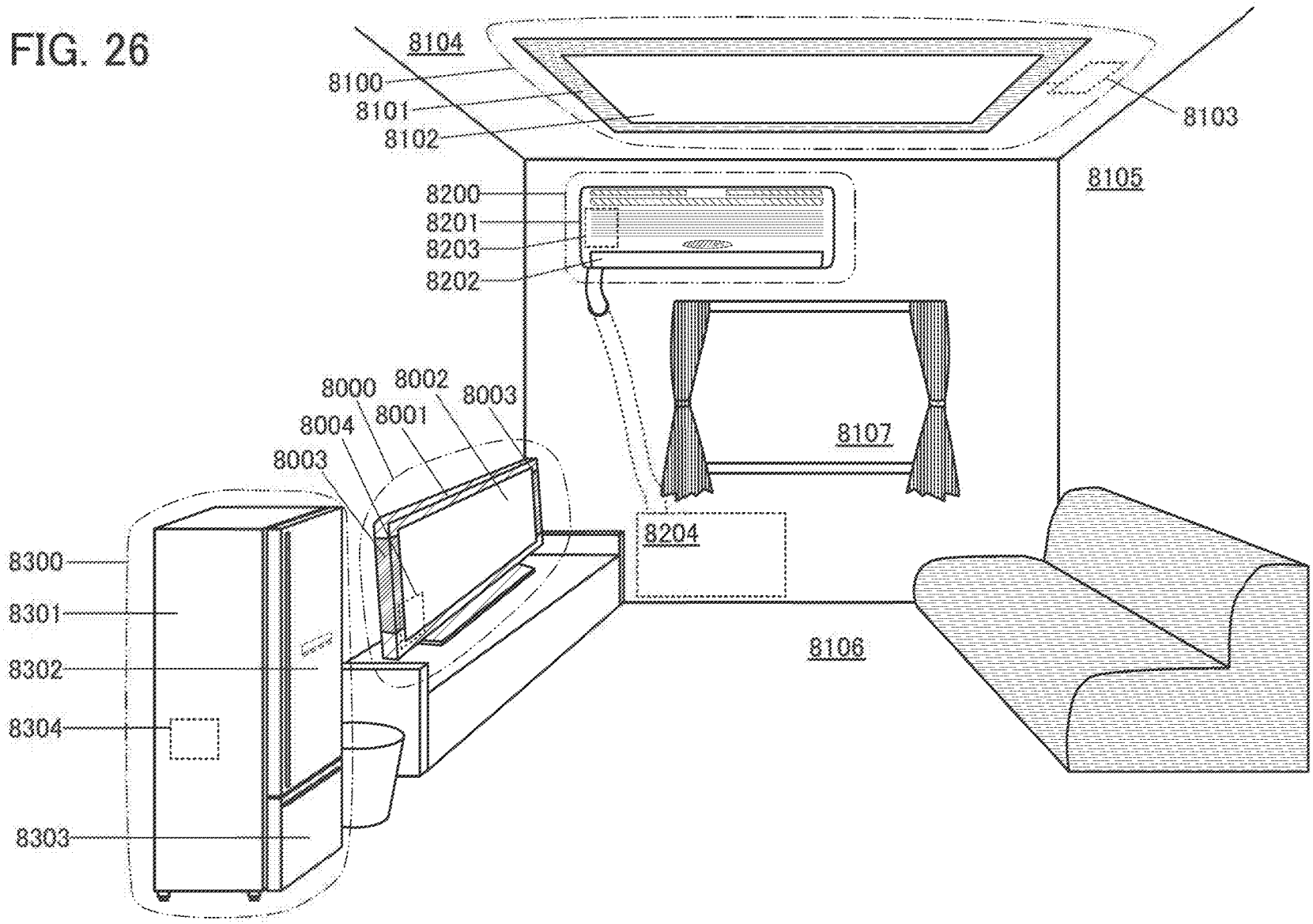
8104
8100
8101
8102
8103
8105
8200
8201
8203
8202
8000
8002
8003
8004
8001
8003
8107
8204
8300
8301
8302
8304
8303
8106

FIG. 27A

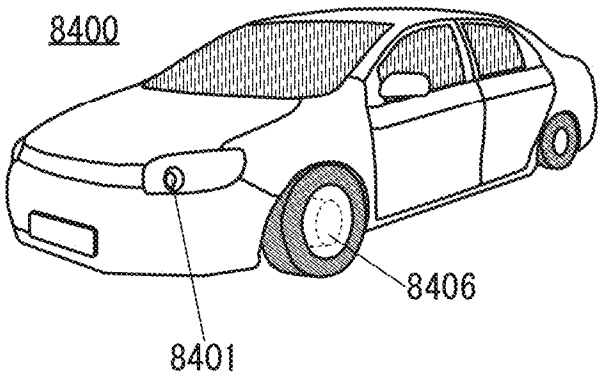

FIG. 27B

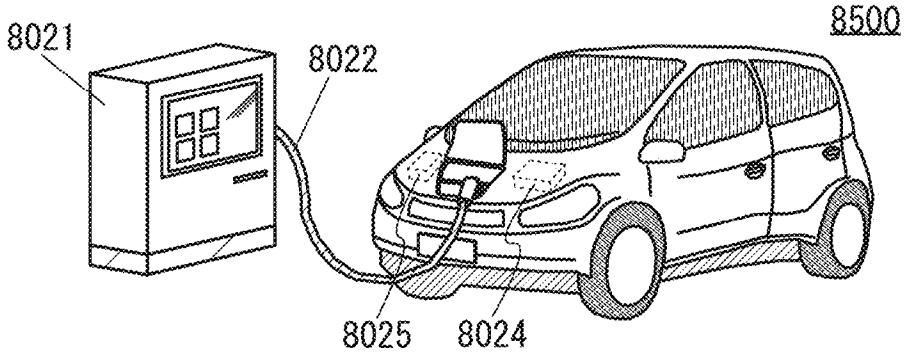

FIG. 27C

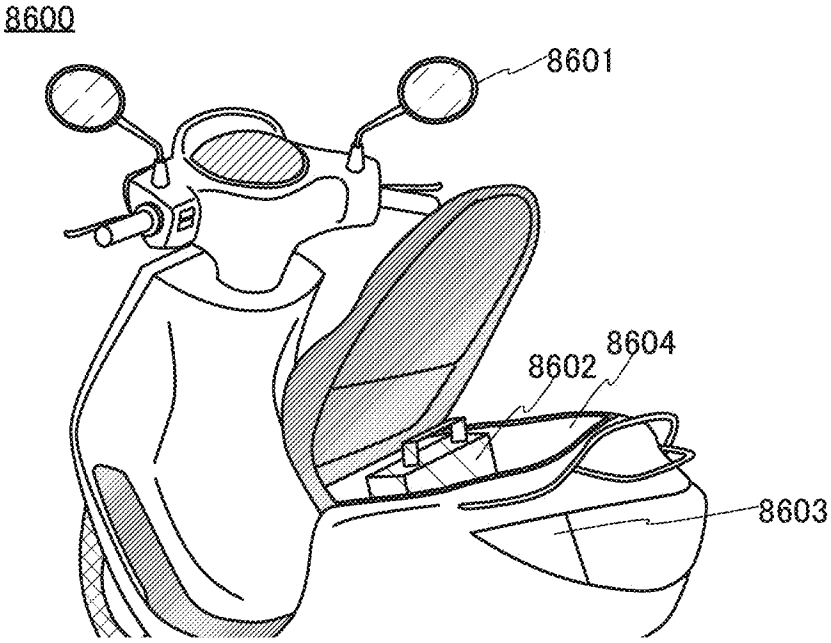

FIG. 28

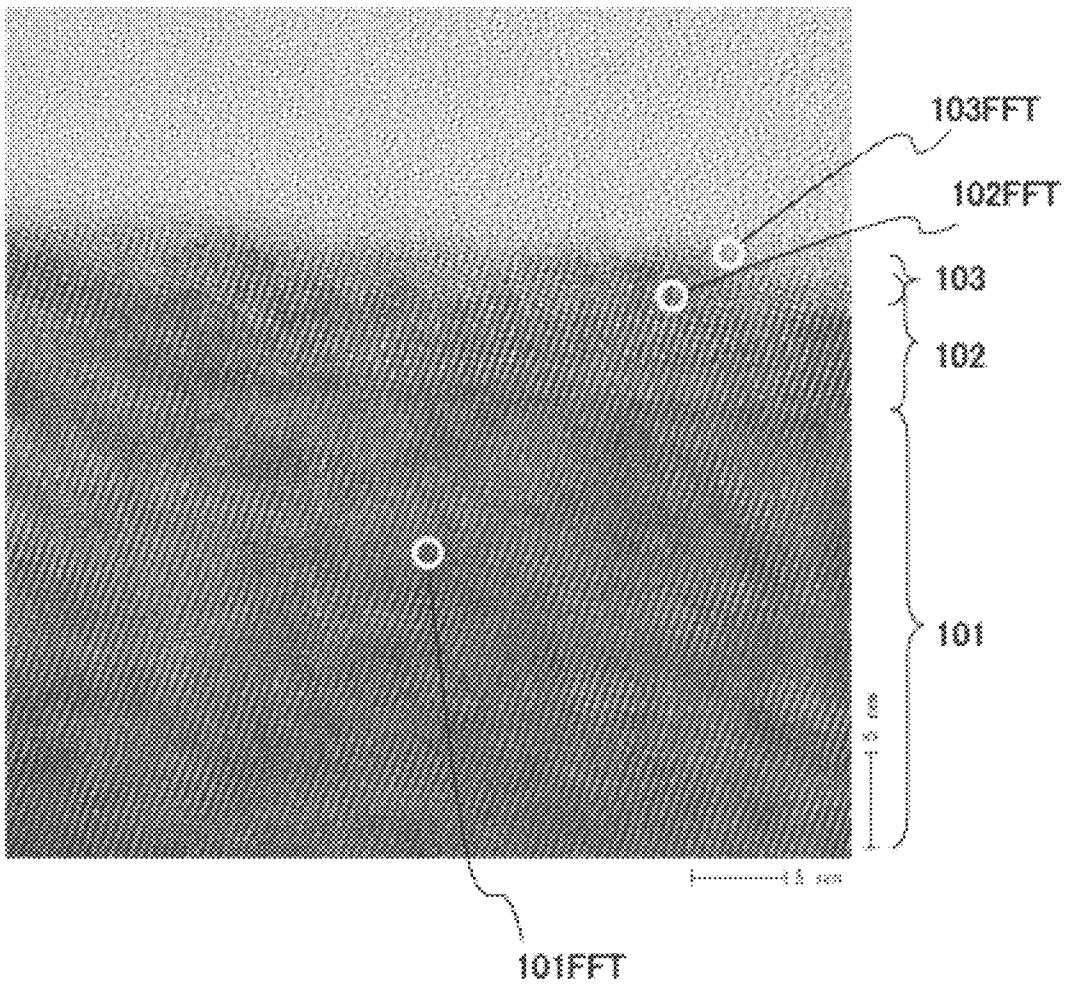

FIG. 29A1

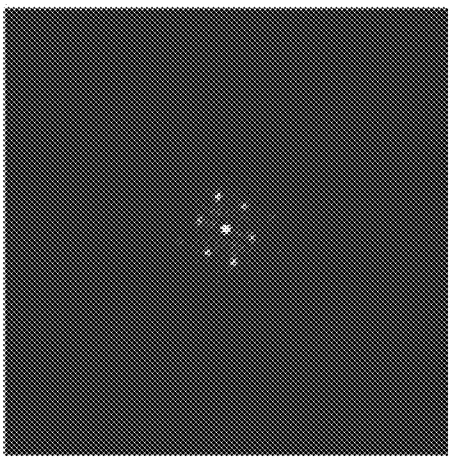

FIG. 29A2

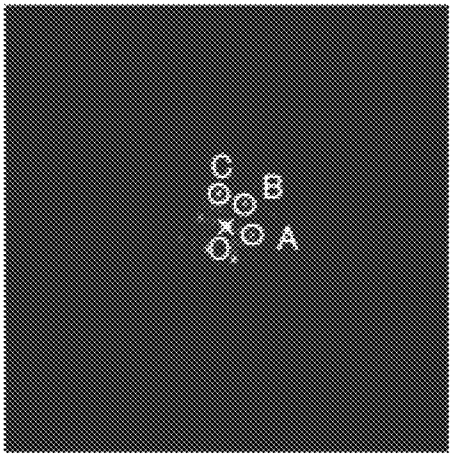

FIG. 29B1

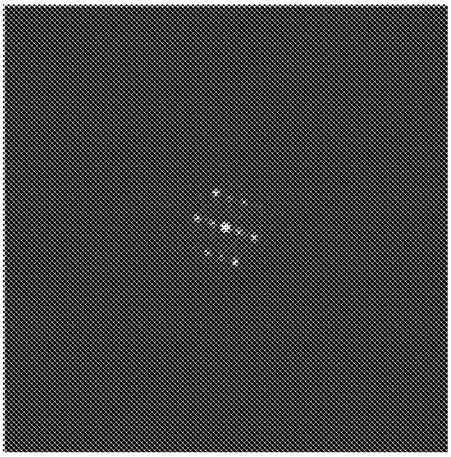

FIG. 29B2

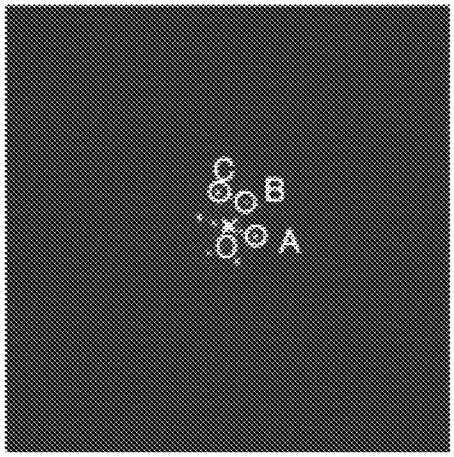

FIG. 29C1

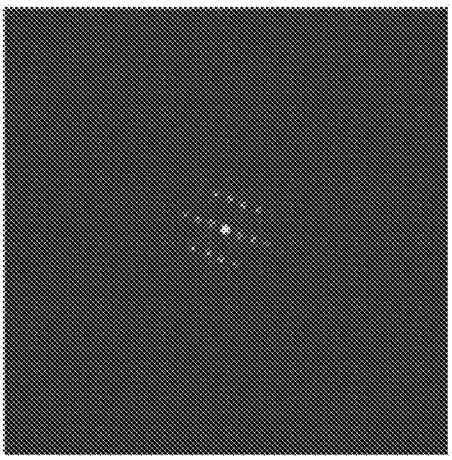

FIG. 29C2

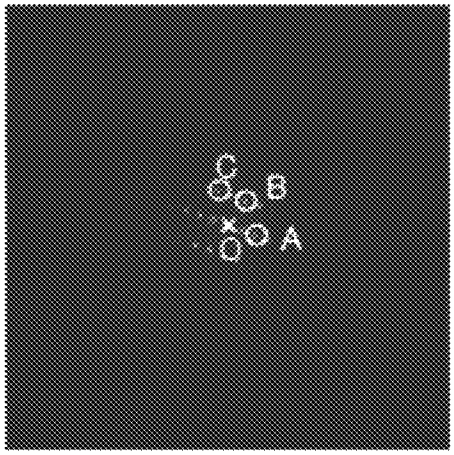

FIG. 30A1

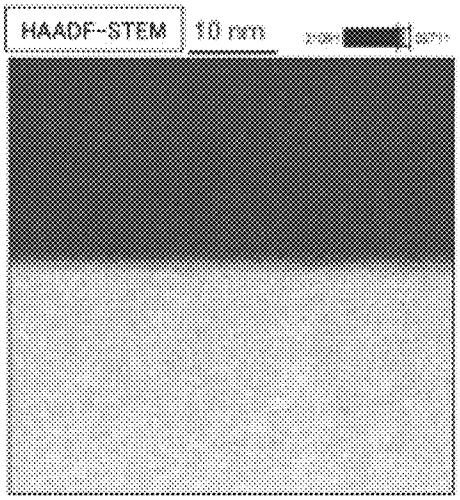

FIG. 30A2

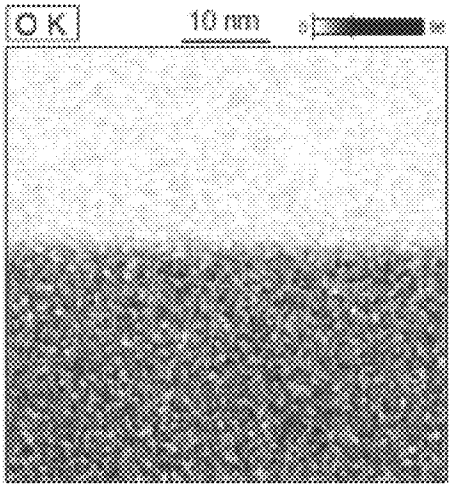

FIG. 30B1

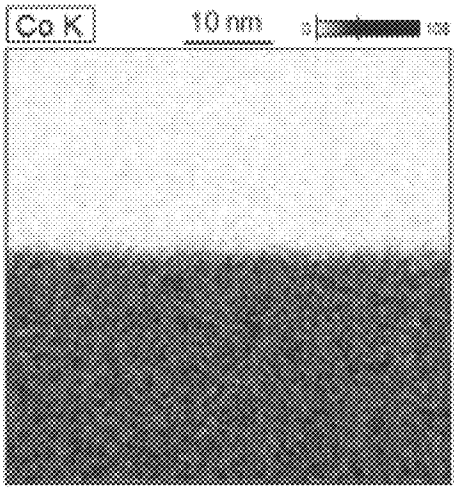

FIG. 30B2

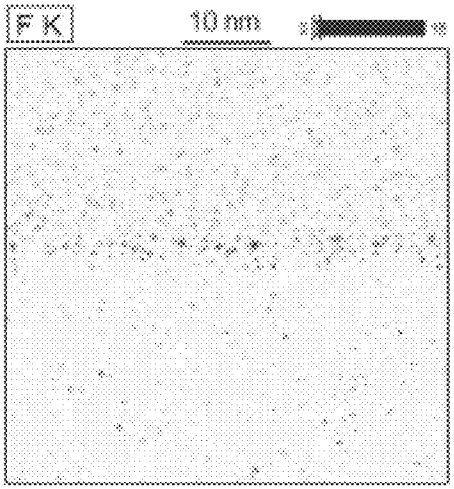

FIG. 30C1

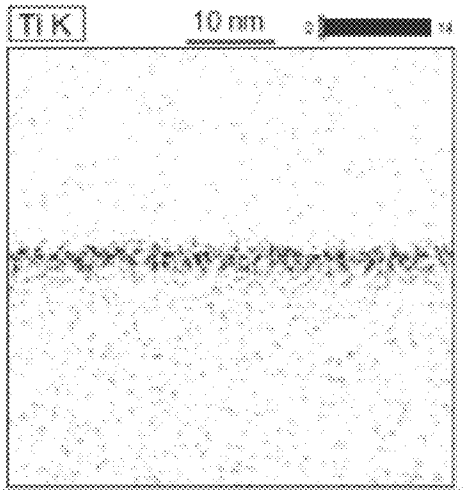

FIG. 30C2

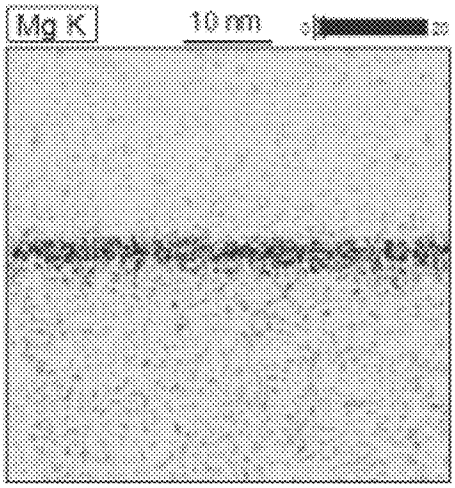

FIG. 31A1

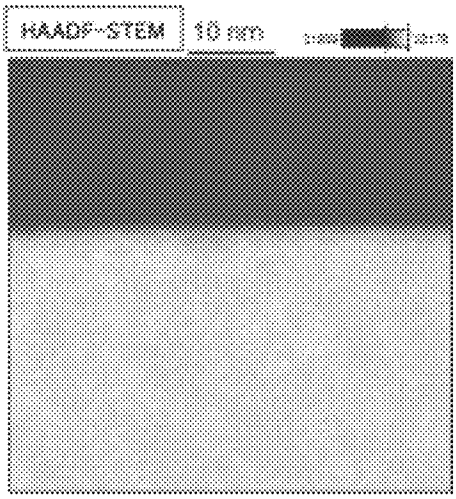

FIG. 31A2

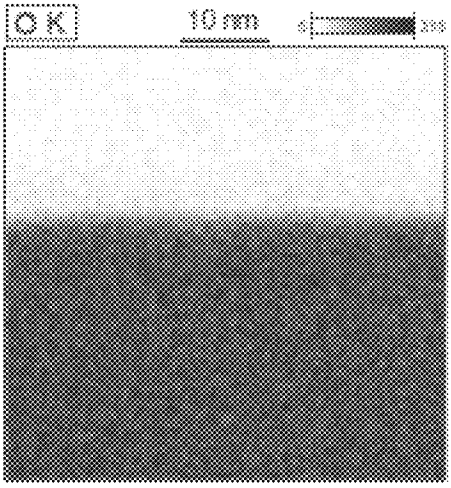

FIG. 31B1

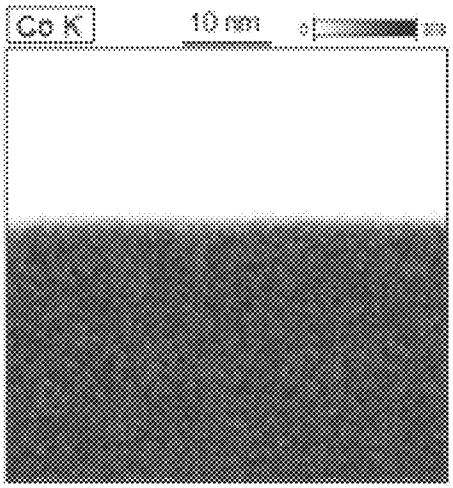

FIG. 31B2

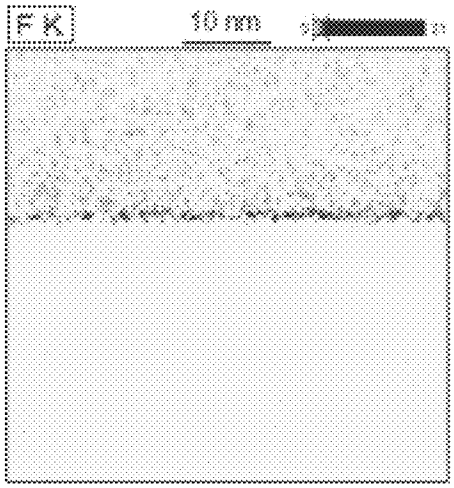

FIG. 31C1

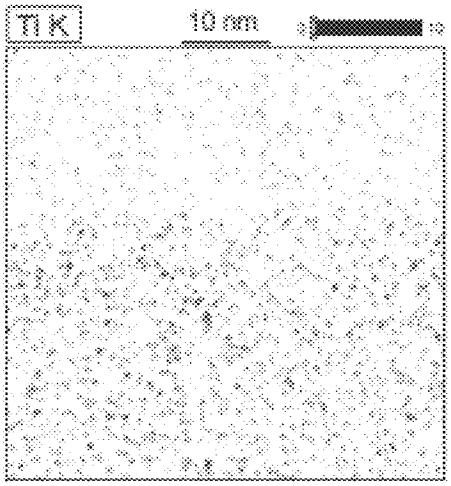

FIG. 31C2

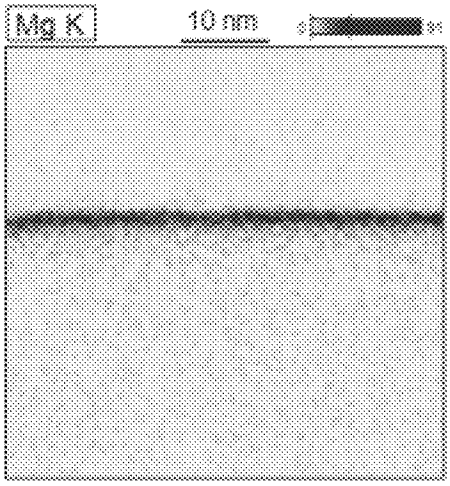

FIG. 32

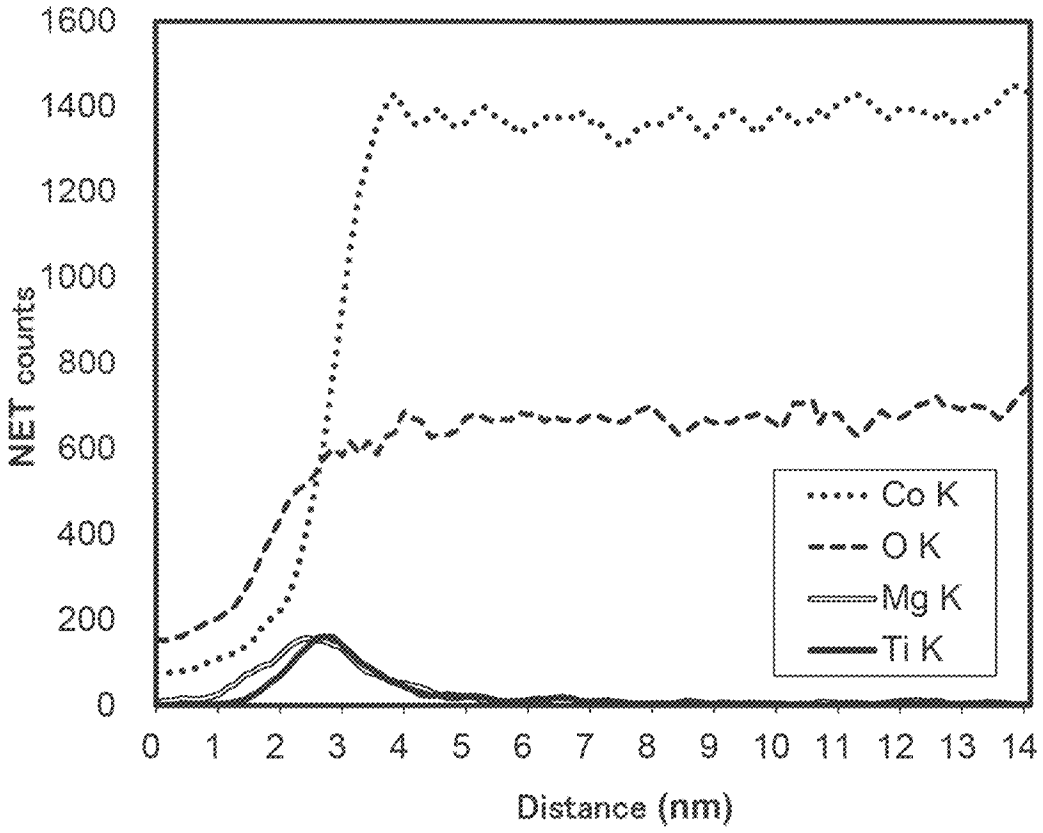
1600
1400
1200
1000
800
600
400
200
0
NET counts
0 1 2 3 4 5 6 7 8 9 10 11 12 13 14
Distance (nm)
Co K
O K
Mg K
Ti K

FIG. 33

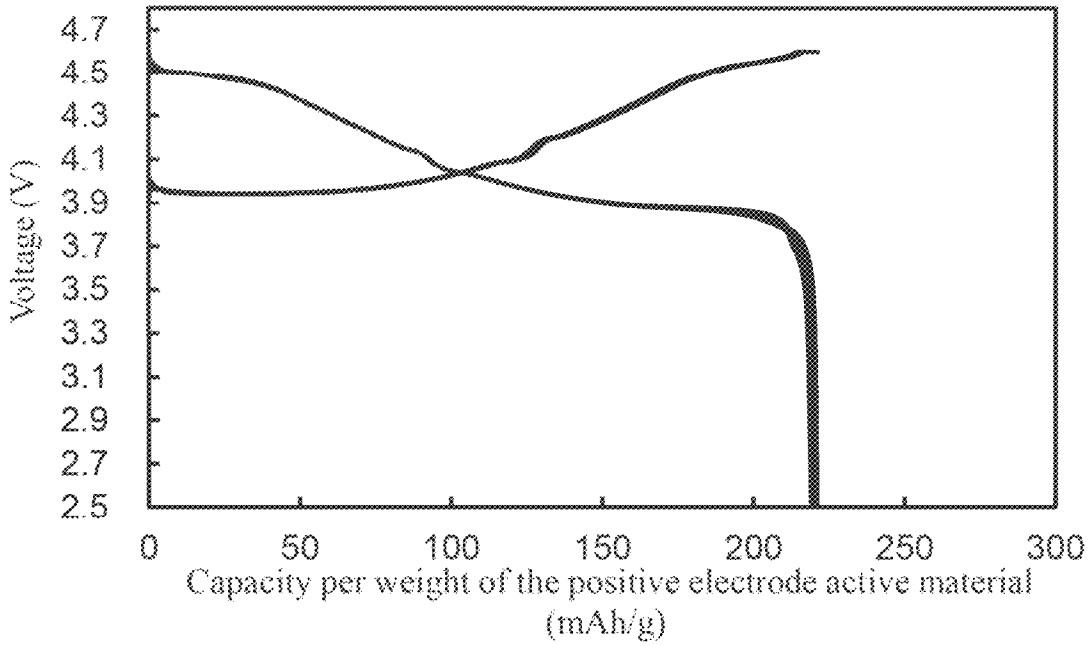
4.7
4.5
4.3
4.1
3.9
3.7
3.5
3.3
3.1
2.9
2.7
2.5
Voltage (V)
0
50
100
150
200
250
300
Capacity per weight of the positive electrode active material
(mAh/g)

FIG. 34

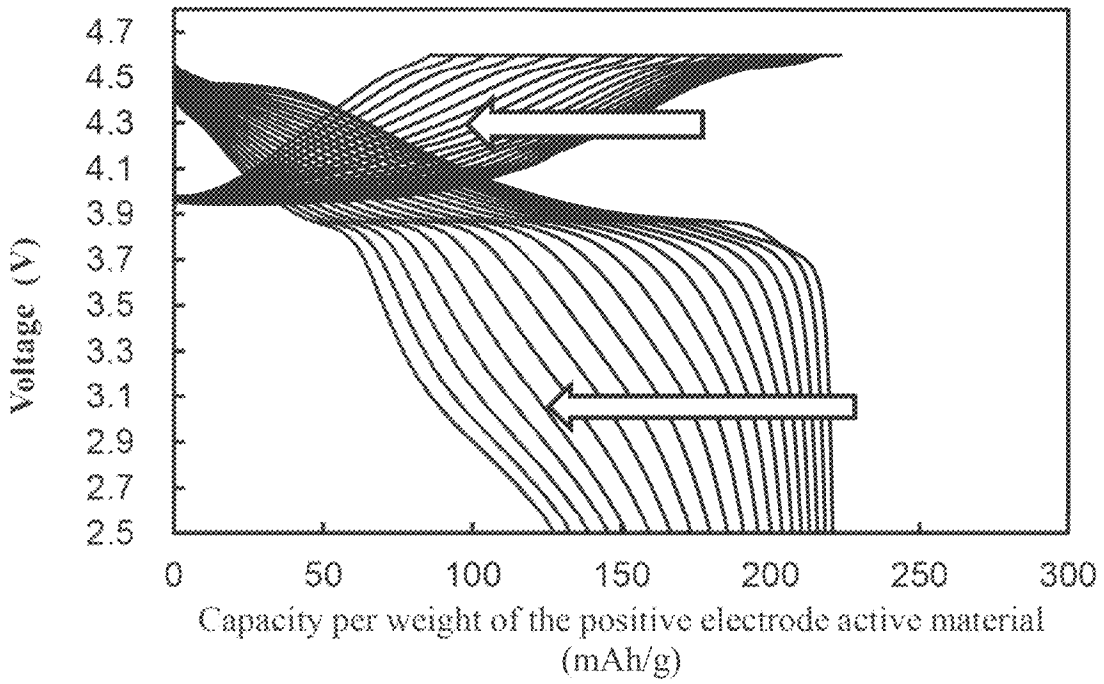
4.7
4.5
4.3
4.1
3.9
3.7
3.5
3.3
3.1
2.9
2.7
2.5
Voltage (V)
0
50
100
150
200
250
300
Capacity per weight of the positive electrode active material
(mAh/g)

FIG. 35

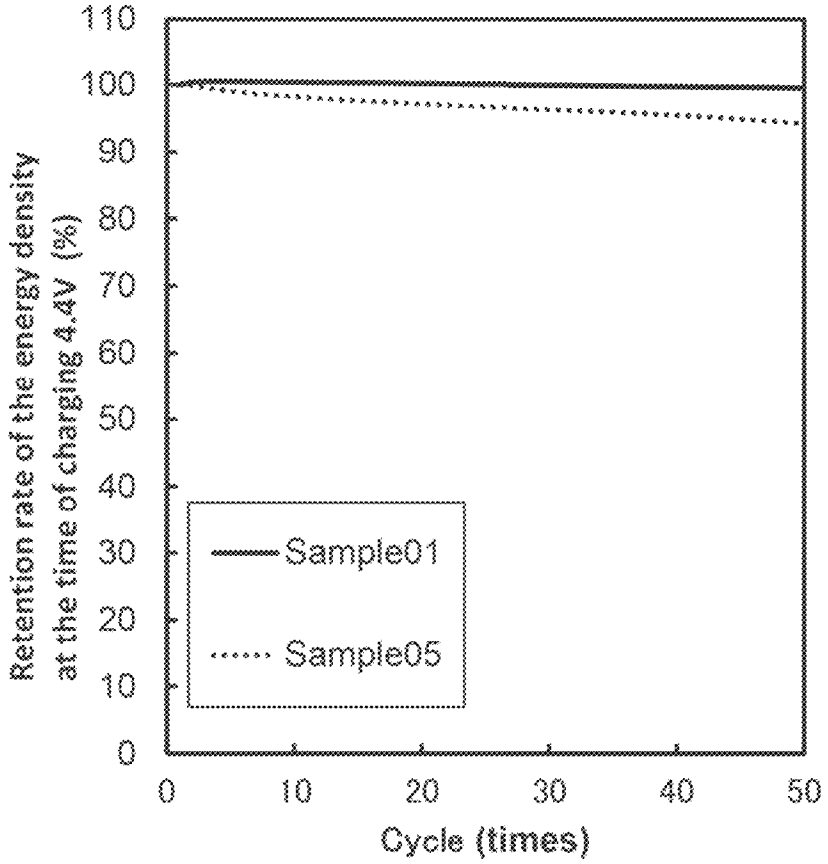
110
100
90
80
70
60
50
40
30
20
10
0
Retention rate of the energy density at the time of charging 4.4V (%)
Sample01
Sample05
0
10
20
30
40
50
Cycle (times)

FIG. 36

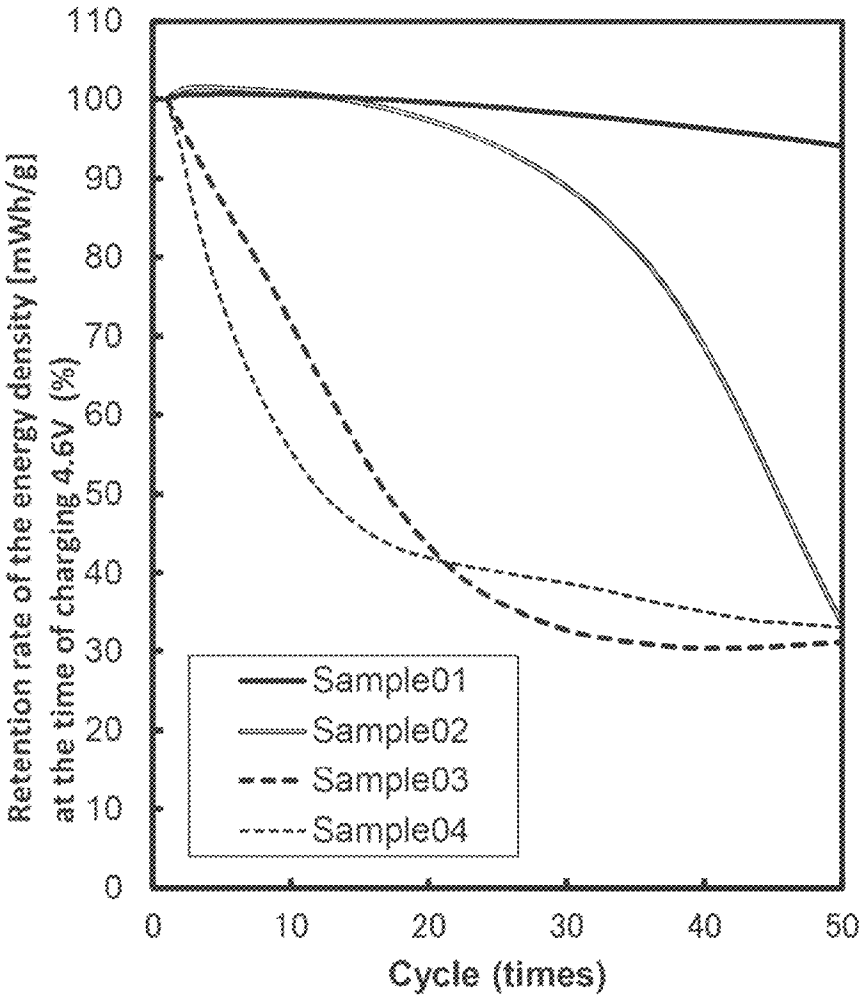
110
100
90
80
70
60
50
40
30
20
10
0
Retention rate of the energy density [mWh/g]
at the time of charging 4.6V (%)
0
10
20
30
40
50
Cycle (times)
Sample01
Sample02
Sample03
Sample04

before Ti heating (Sample06)

FIG. 37A

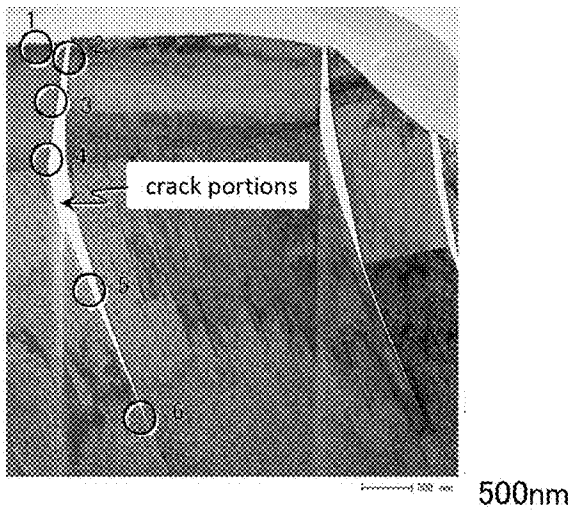

FIG. 37B1

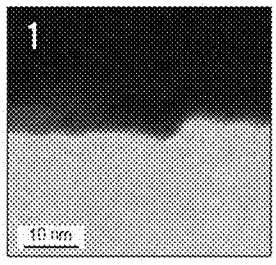

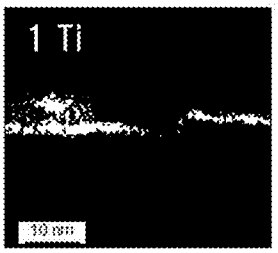

FIG. 37B2

FIG. 37C1

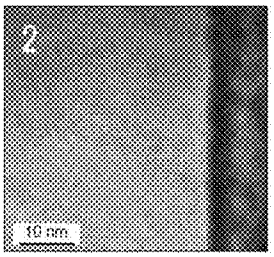

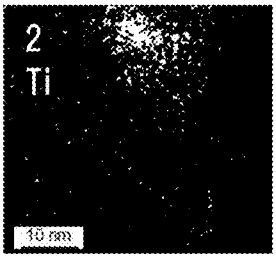

FIG. 37C2

FIG. 37D1

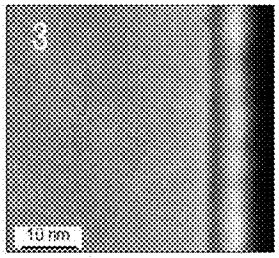

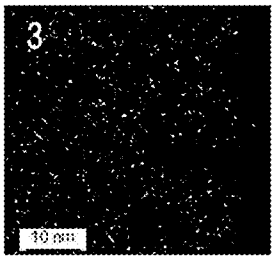

FIG. 37D2

FIG. 37E1

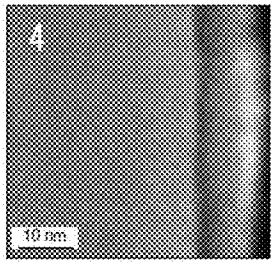

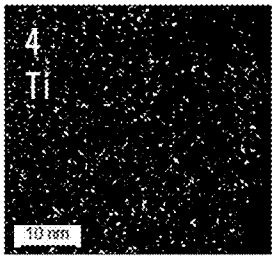

FIG. 37E2

after Ti heating (Sample07)

FIG. 38A

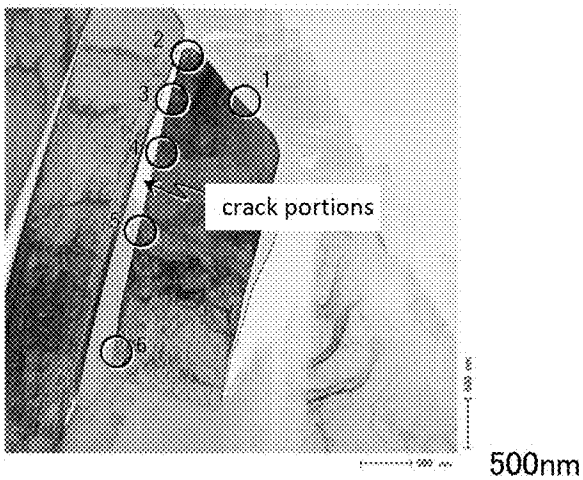

FIG. 38B1

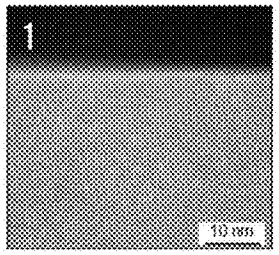

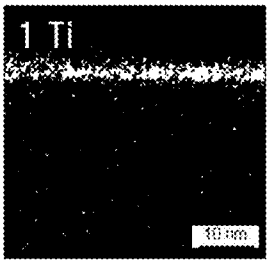

FIG. 38B2

FIG. 38C1

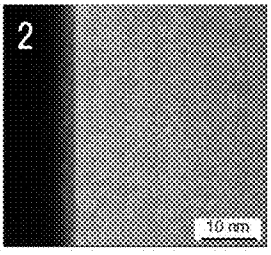

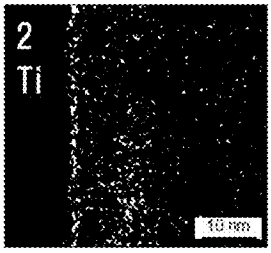

FIG. 38C2

FIG. 38D1

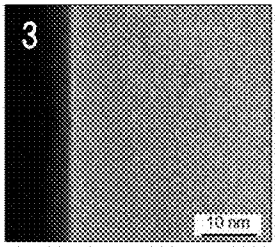

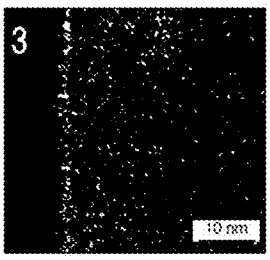

FIG. 38D2

FIG. 38E1

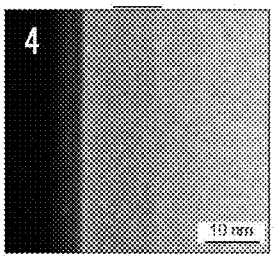

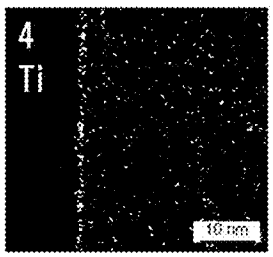

FIG. 38E2

before Mg heating (Sample06)

FIG. 39A

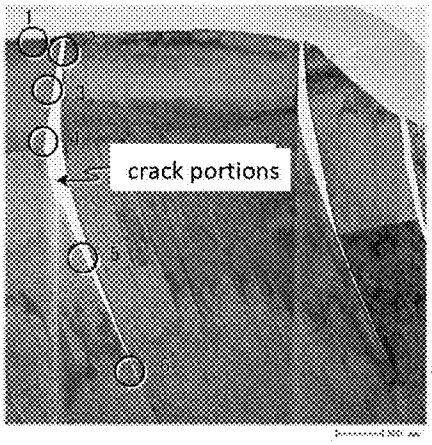

FIG. 39B1

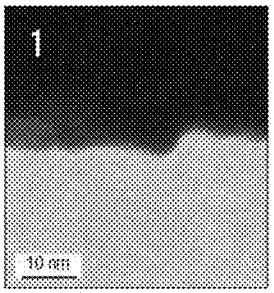

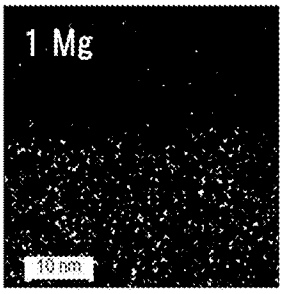

FIG. 39B2

FIG. 39C1

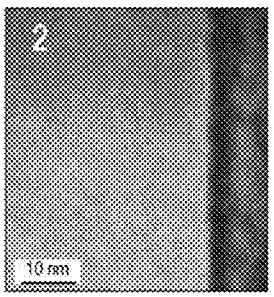

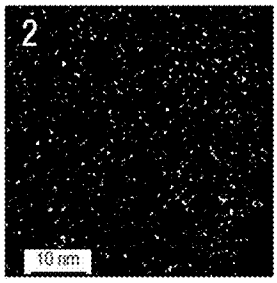

FIG. 39C2

FIG. 39D1

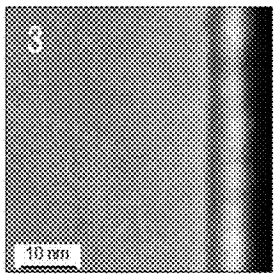

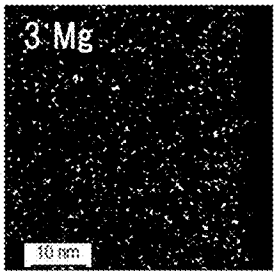

FIG. 39D2

FIG. 39E1

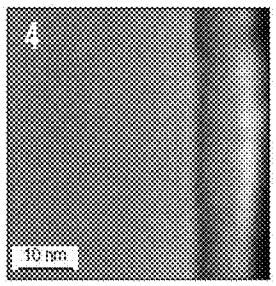

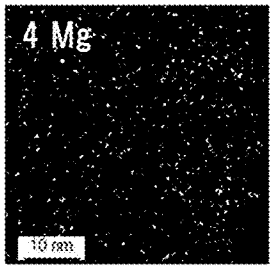

FIG. 39E2

after Mg heating (Sample07)

FIG. 40A

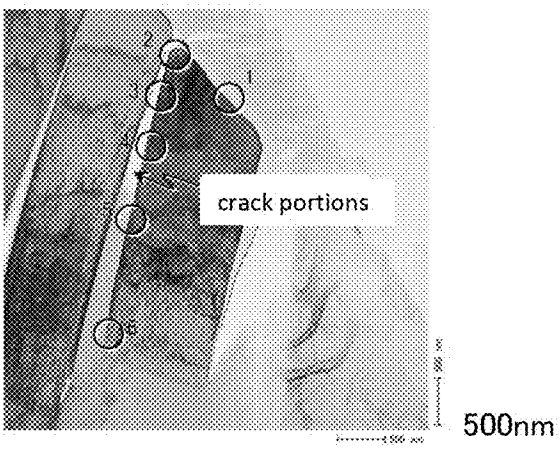

FIG. 40B1

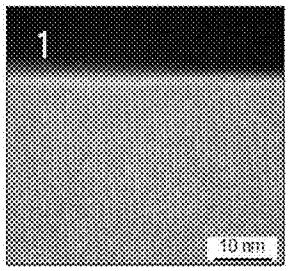

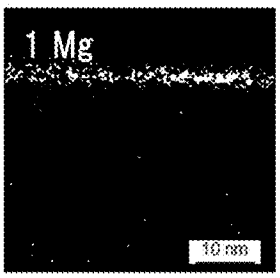

FIG. 40B2

FIG. 40C1

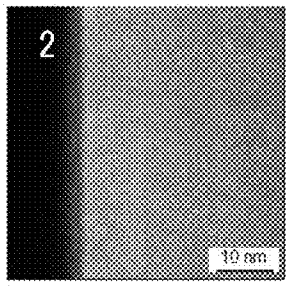

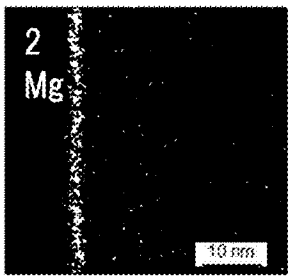

FIG. 40C2

FIG. 40D1

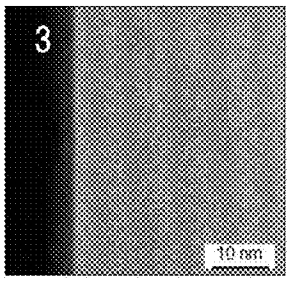

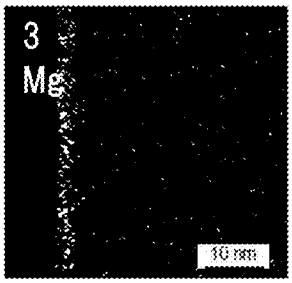

FIG. 40D2

FIG. 40E1

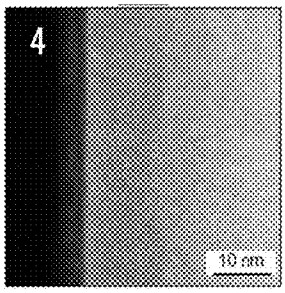

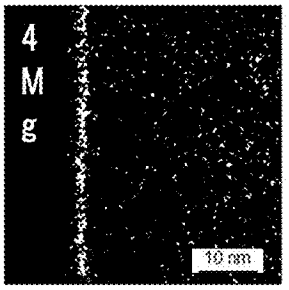

FIG. 40E2

AMPEREX Ex. 1001
Page 47

FIG. 41A

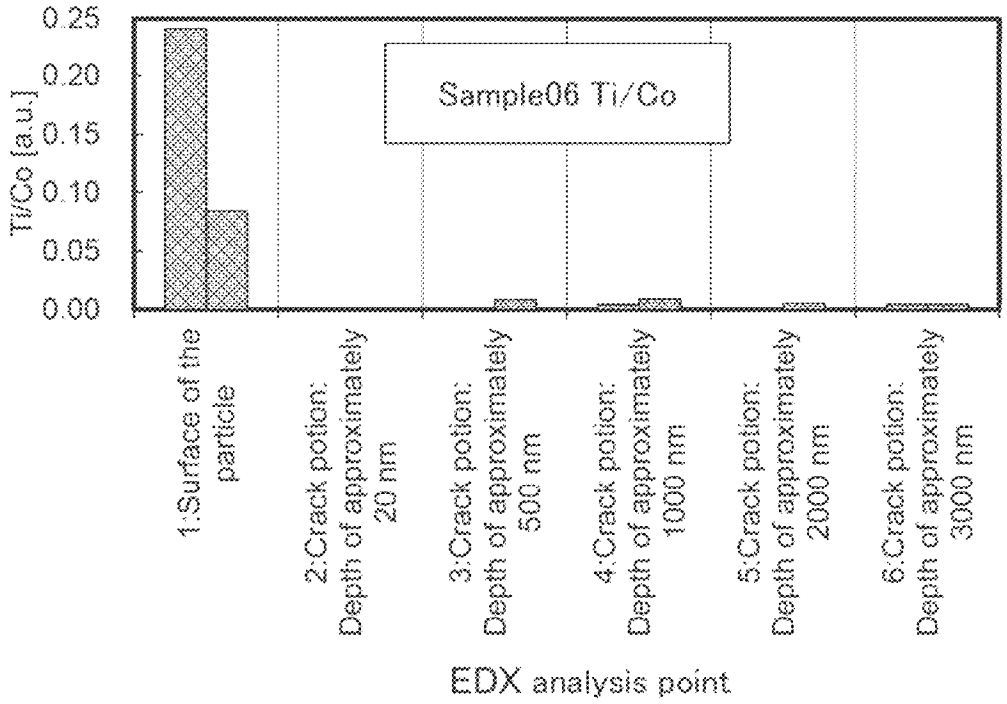

FIG. 41B

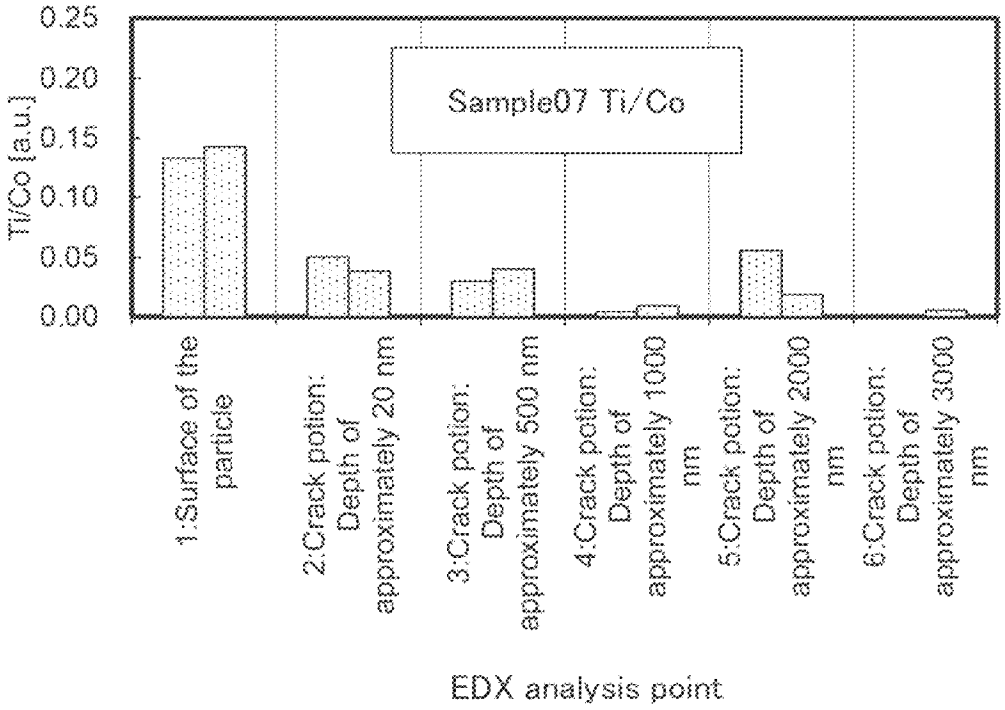

AMPEREX Ex. 1001
Page 48

FIG. 42A

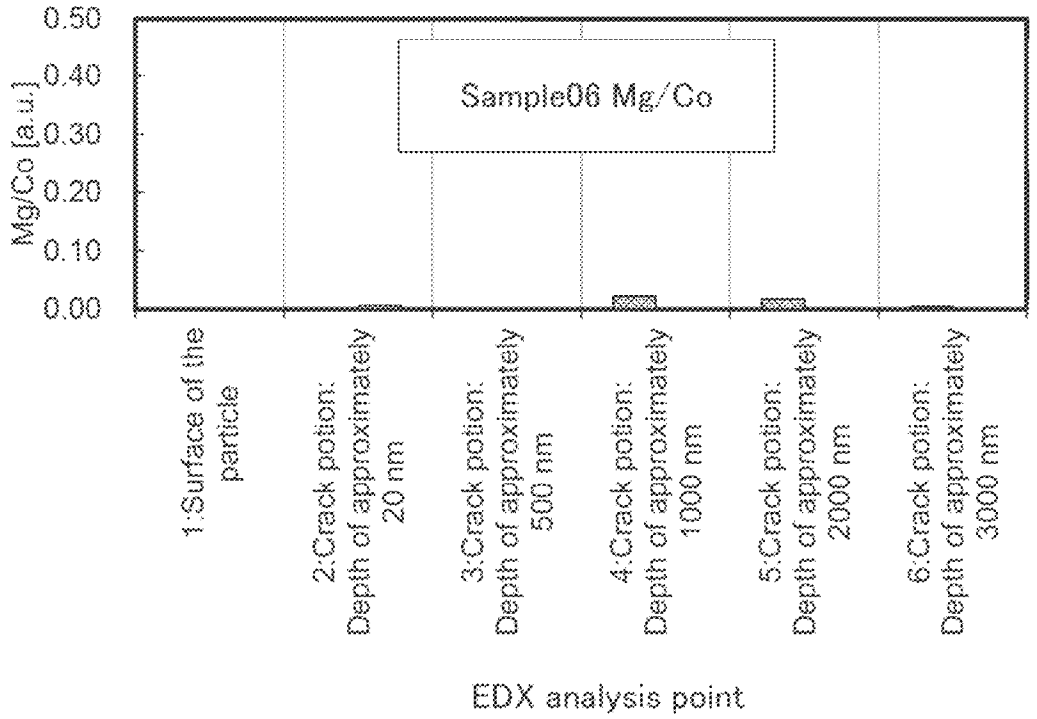

FIG. 42B

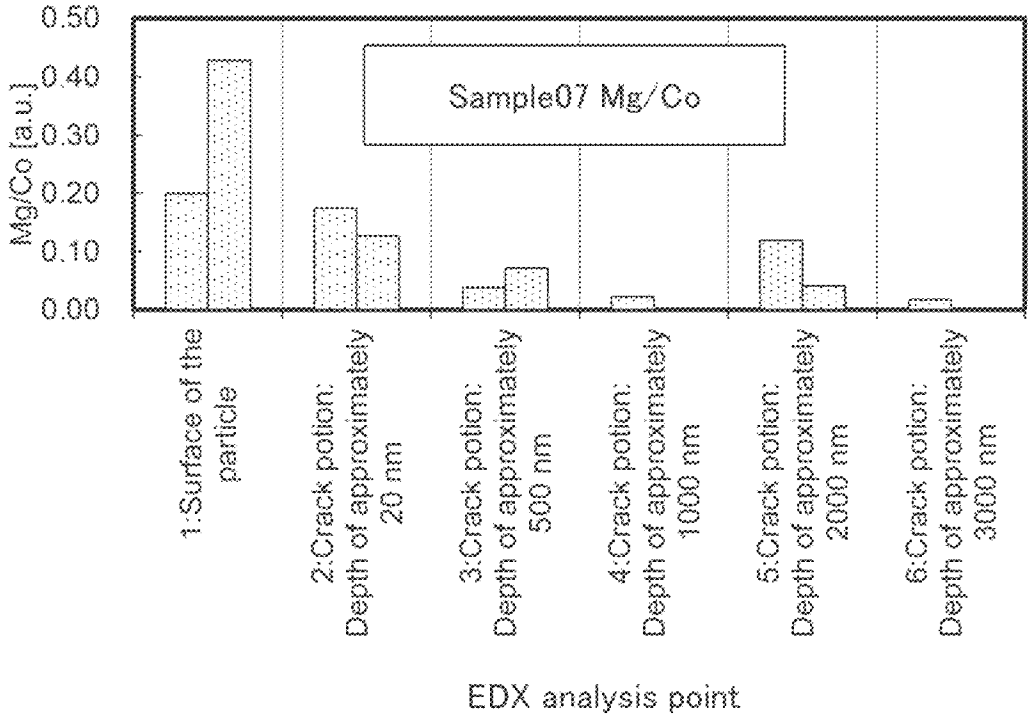

FIG. 43

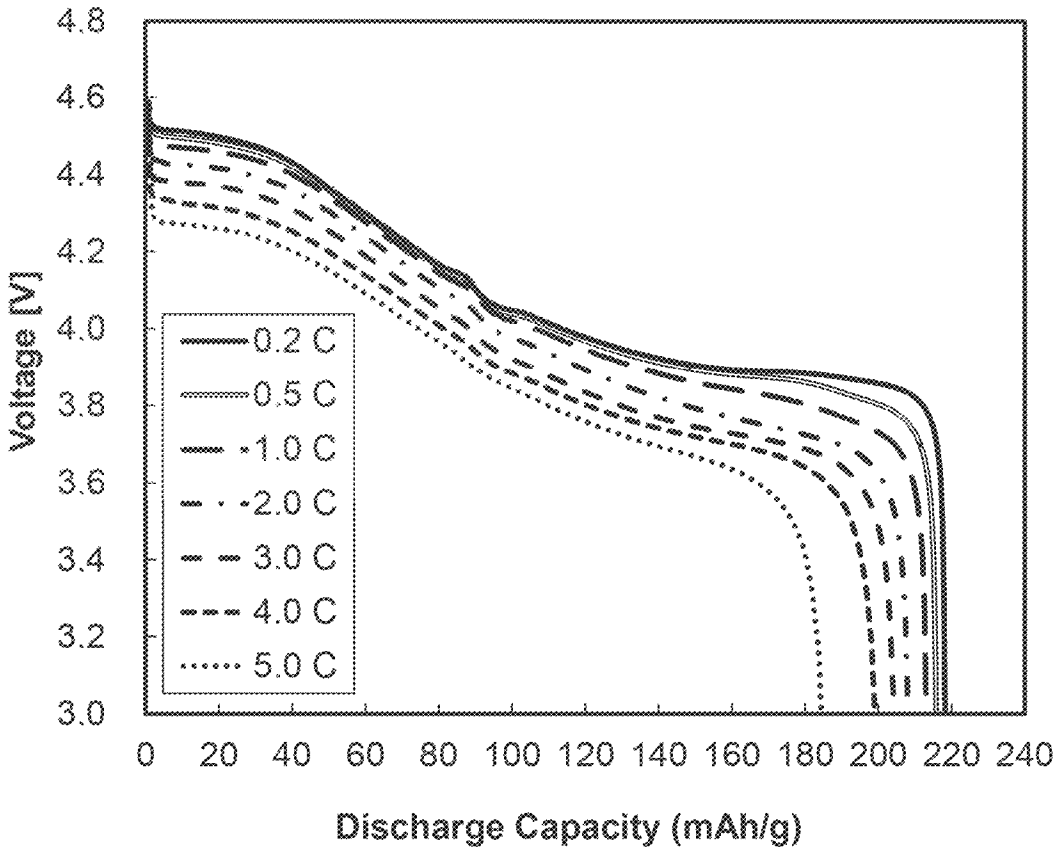
4.8
4.6
4.4
4.2
4.0
3.8
3.6
3.4
3.2
3.0
Voltage [V]
0.2 C
0.5 C
1.0 C
2.0 C
3.0 C
4.0 C
5.0 C
0 20 40 60 80 100 120 140 160 180 200 220 240
Discharge Capacity (mAh/g)

FIG. 44

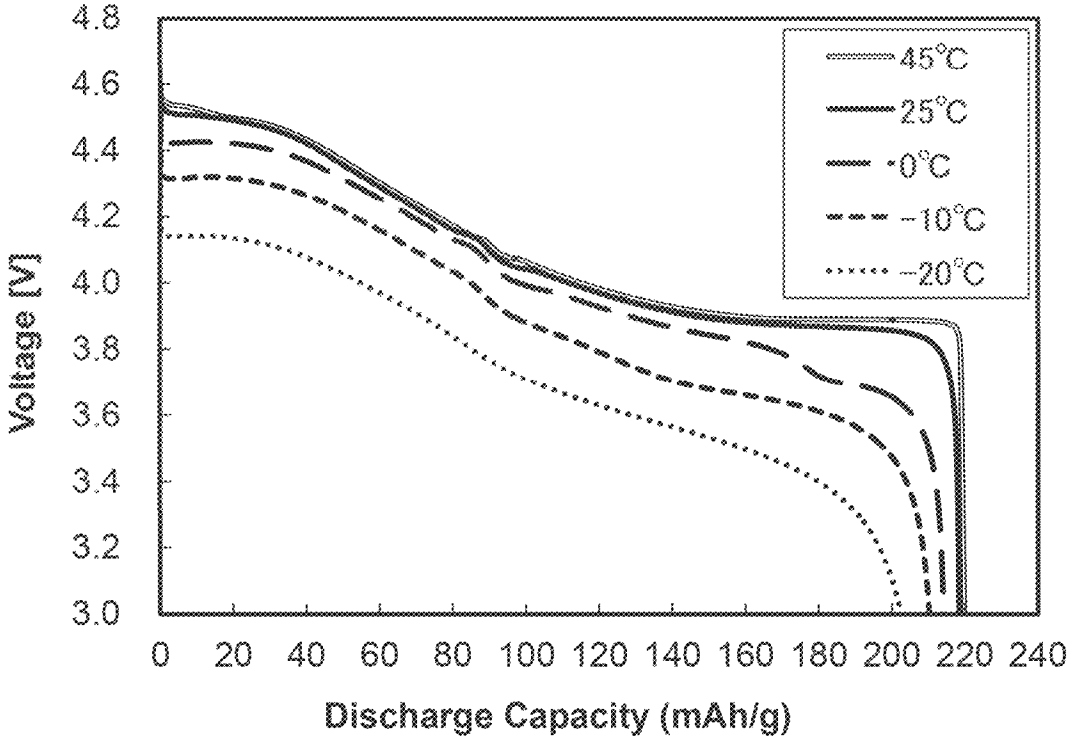
4.8
4.6
4.4
4.2
4.0
3.8
3.6
3.4
3.2
3.0
Voltage [V]
0 20 40 60 80 100 120 140 160 180 200 220 240
Discharge Capacity (mAh/g)
45°C
25°C
0°C
−10°C
−20°C

FIG. 45

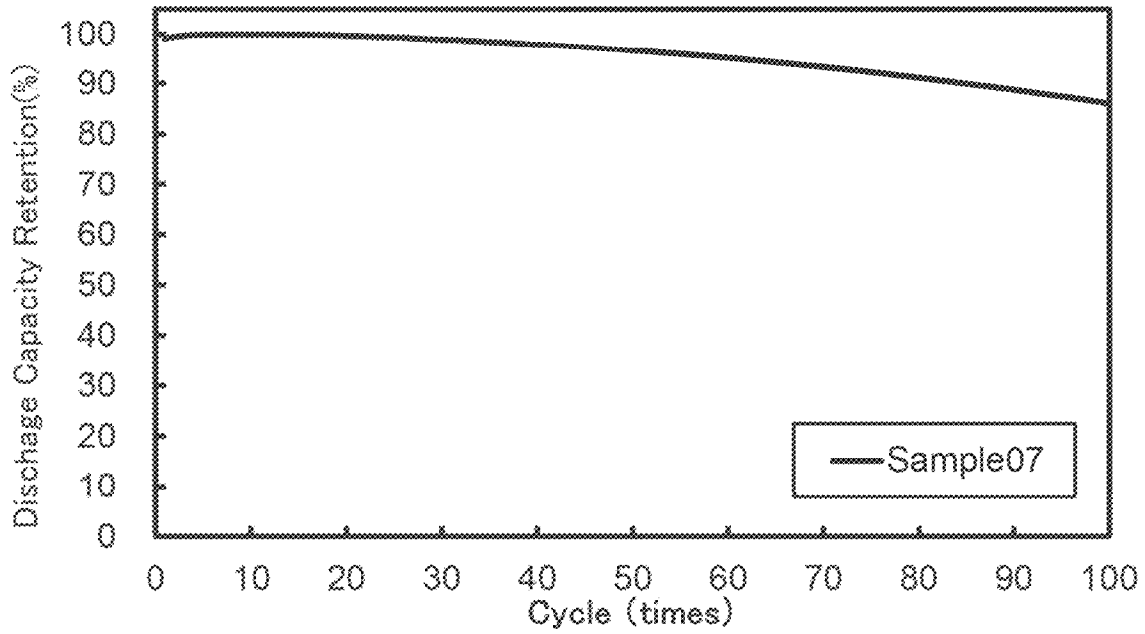
Dischage Capacity Retention(%)
100
90
80
70
60
50
40
30
20
10
0
0
10
20
30
40
50
60
70
80
90
100
Cycle (times)
Sample07

FIG. 46A

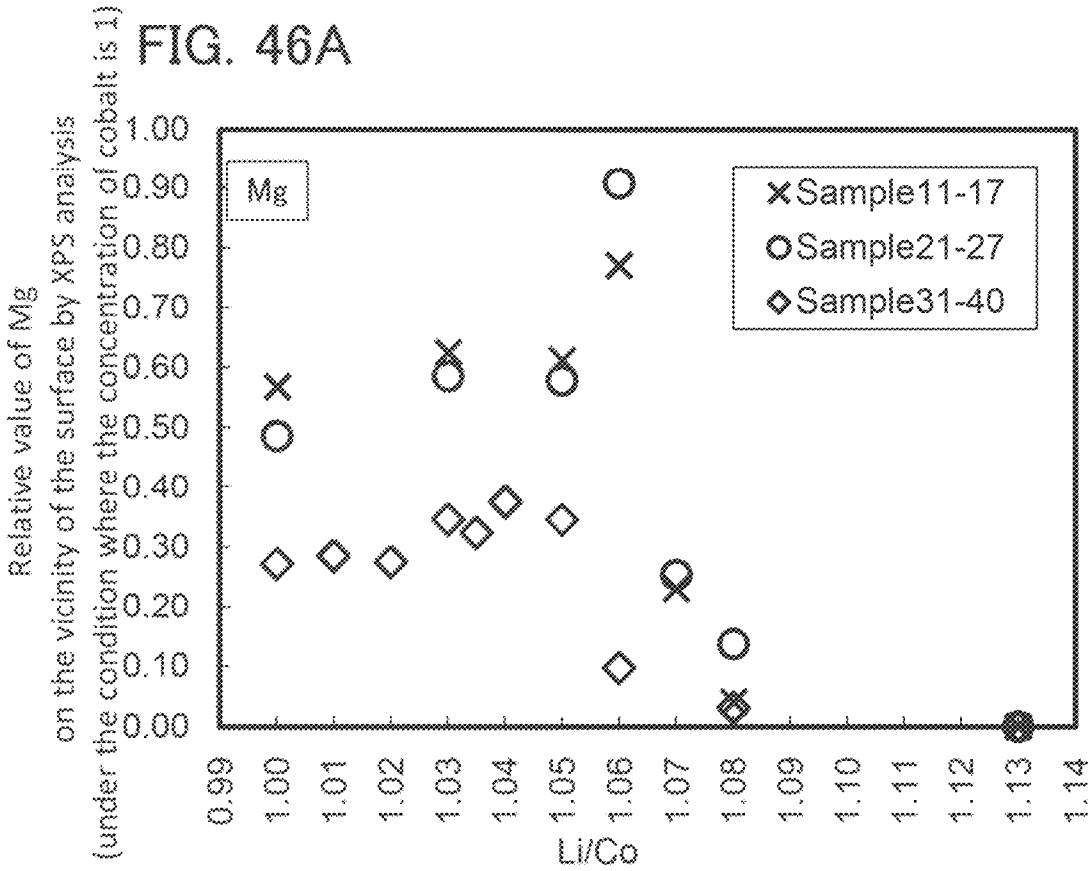

FIG. 46B

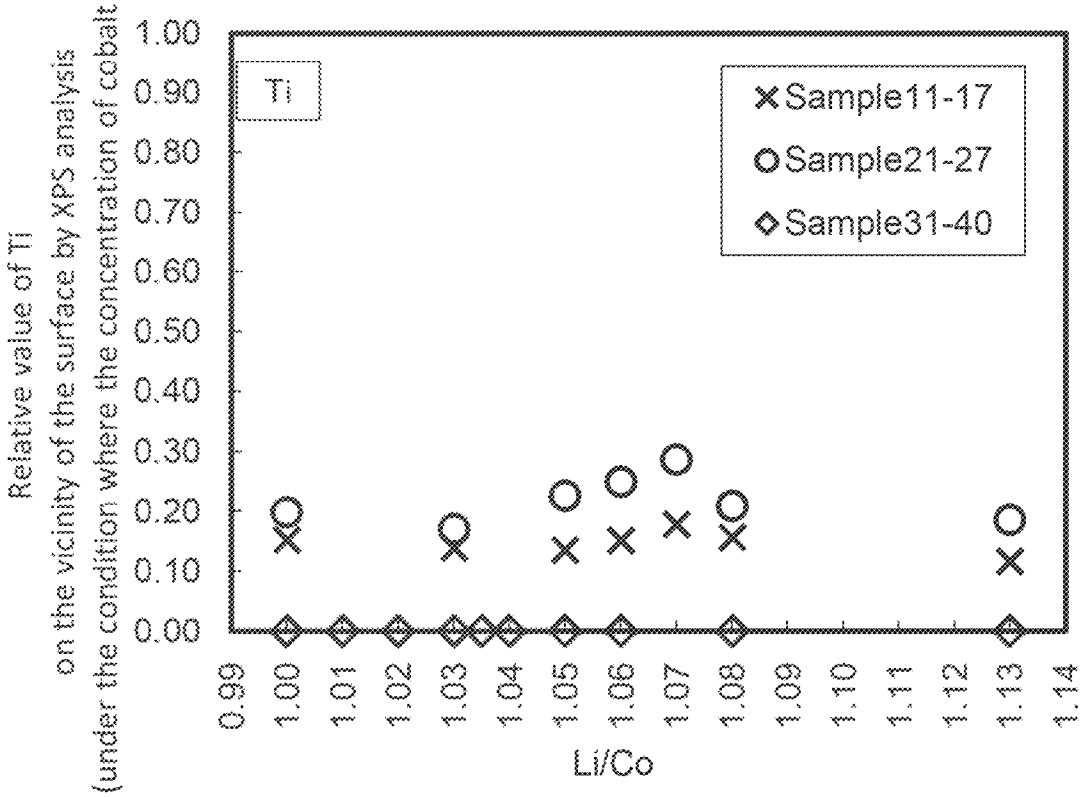

FIG. 47A

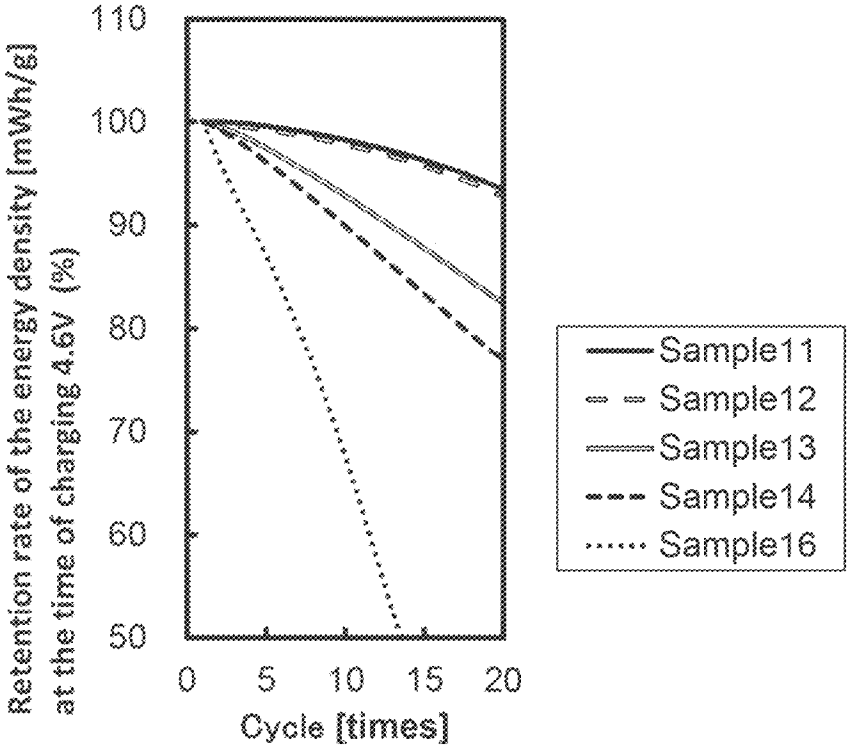

FIG. 47B

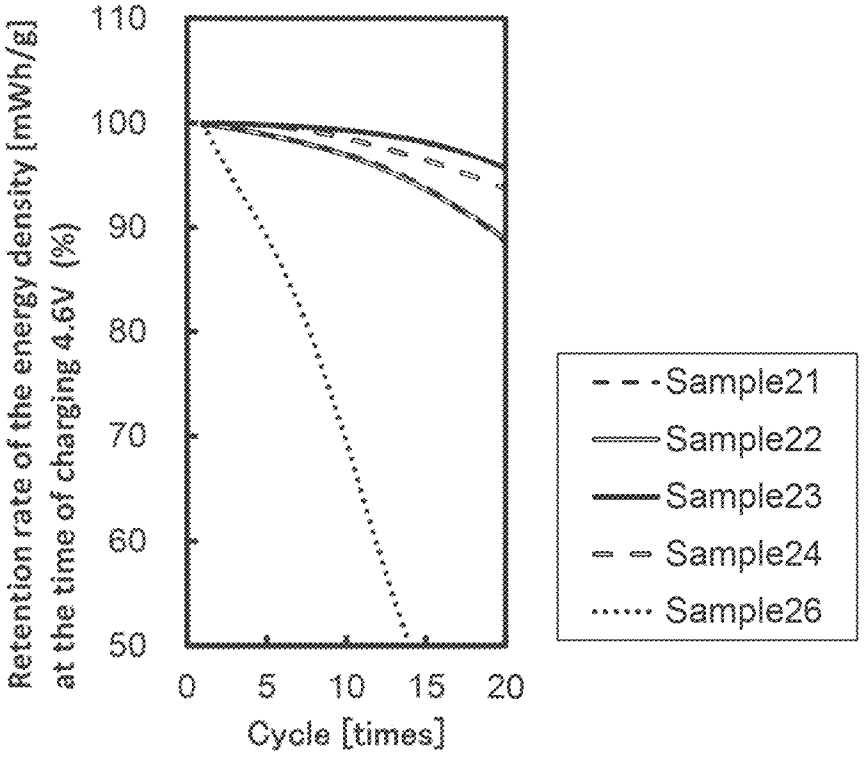

FIG. 48

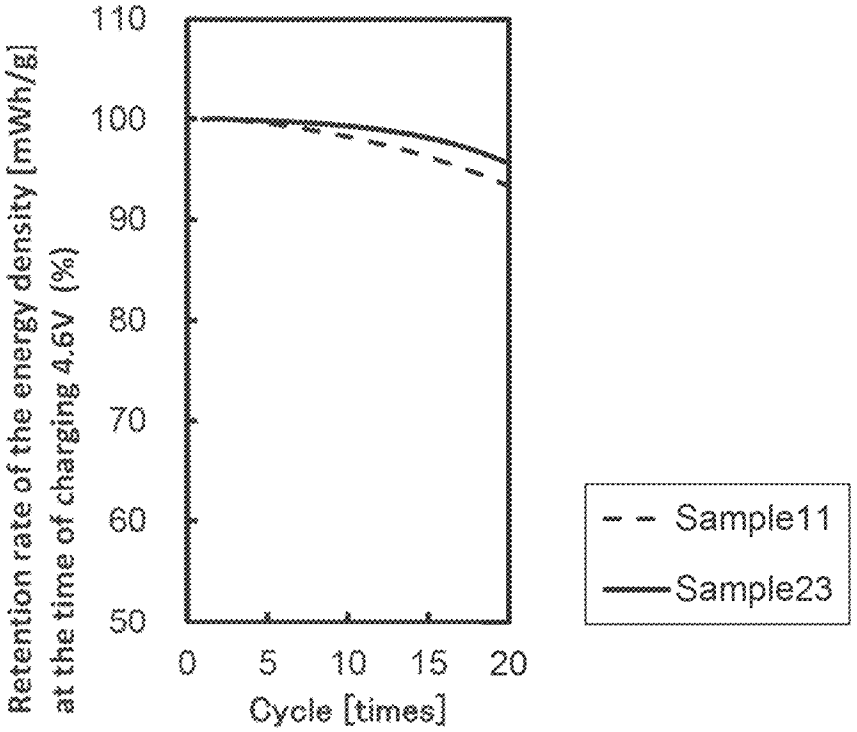
Retention rate of the energy density [mWh/g]
at the time of charging 4.6V (%)
110
100
90
80
70
60
50
0
5
10
15
20
Cycle [times]
Sample11
Sample23

FIG. 49

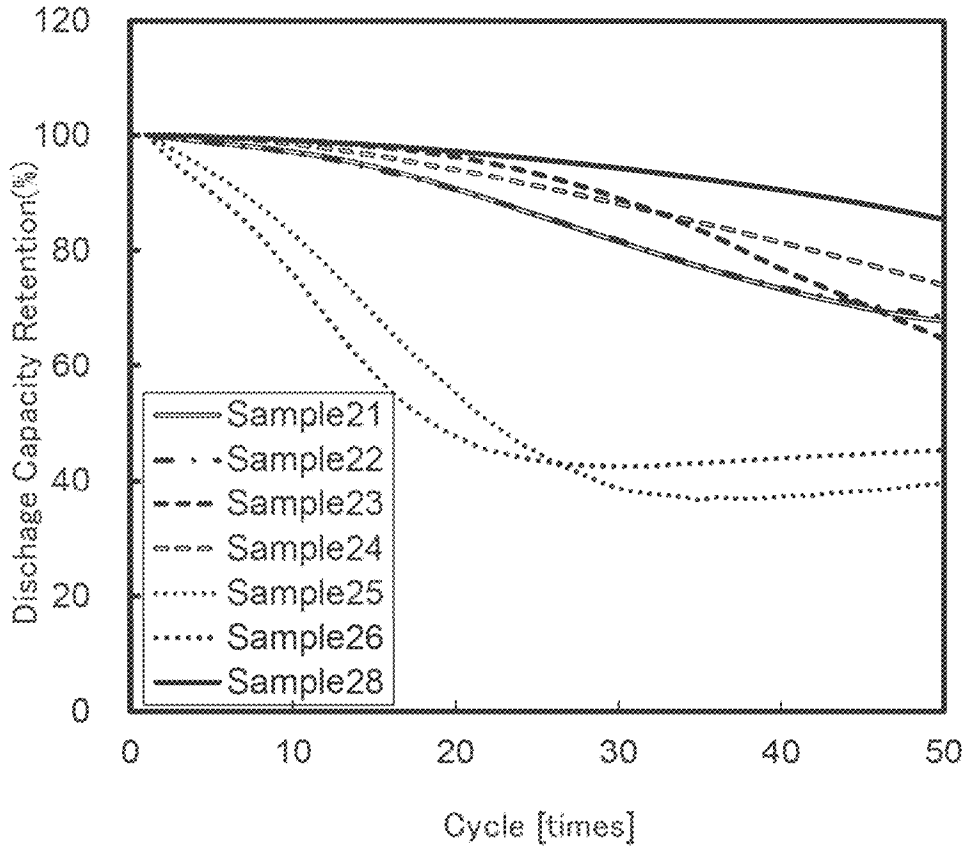
120
100
80
60
40
20
0
Dischage Capacity Retention(%)
0
10
20
30
40
50
Cycle [times]
Sample21
Sample22
Sample23
Sample24
Sample25
Sample26
Sample28

FIG. 50A

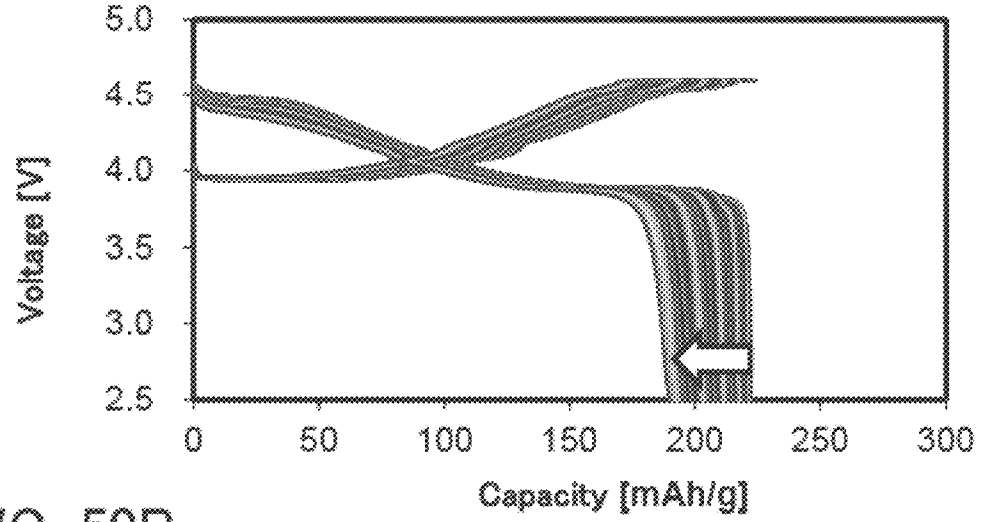

FIG. 50B

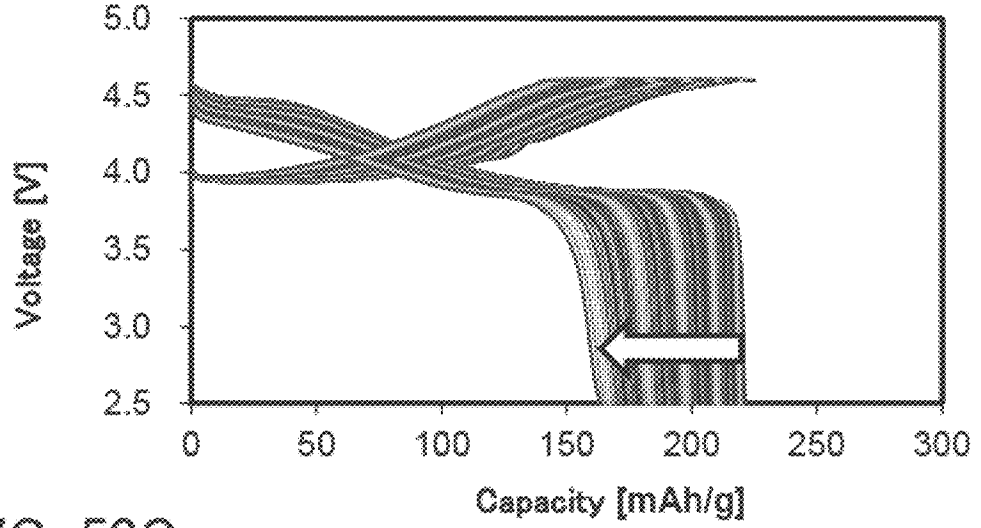

FIG. 50C

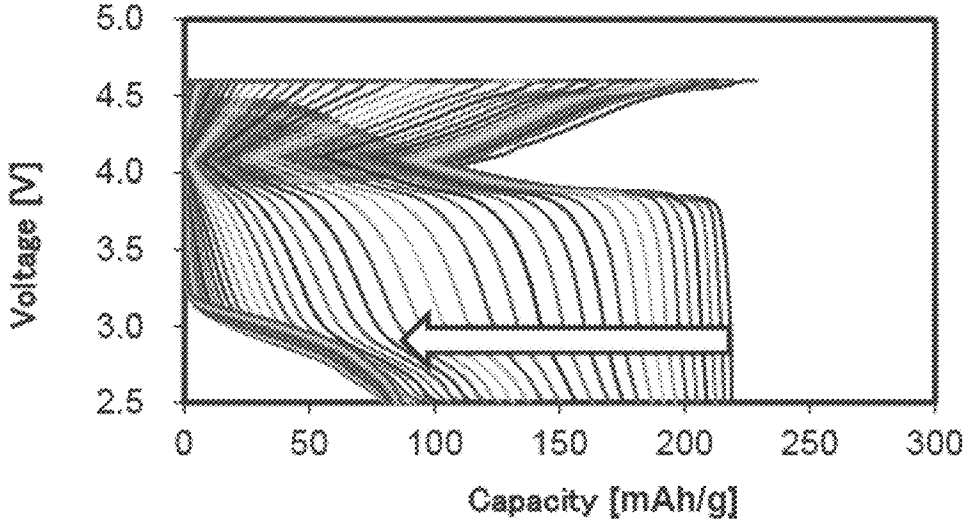

FIG. 51A

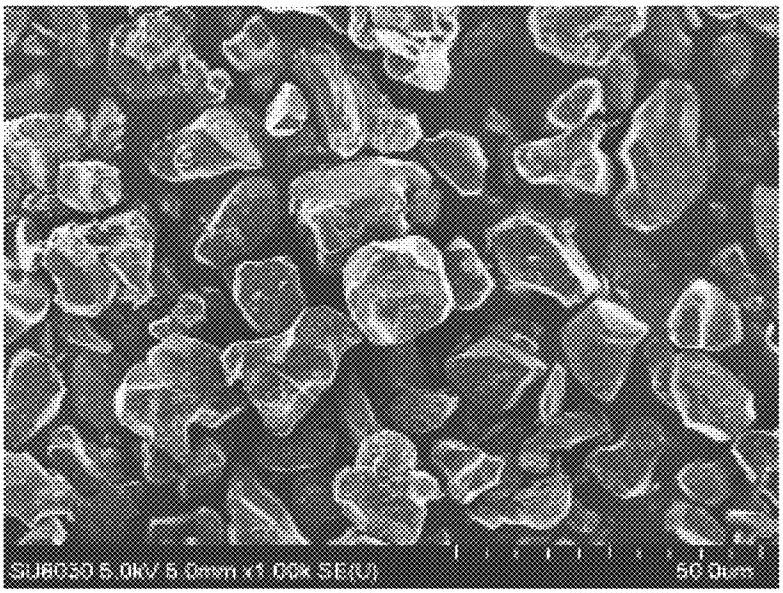

FIG. 51B

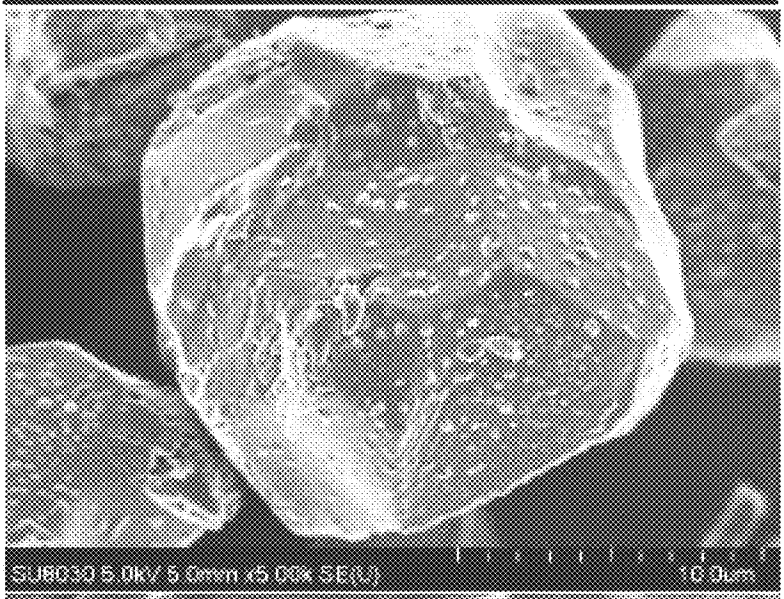

FIG. 51C

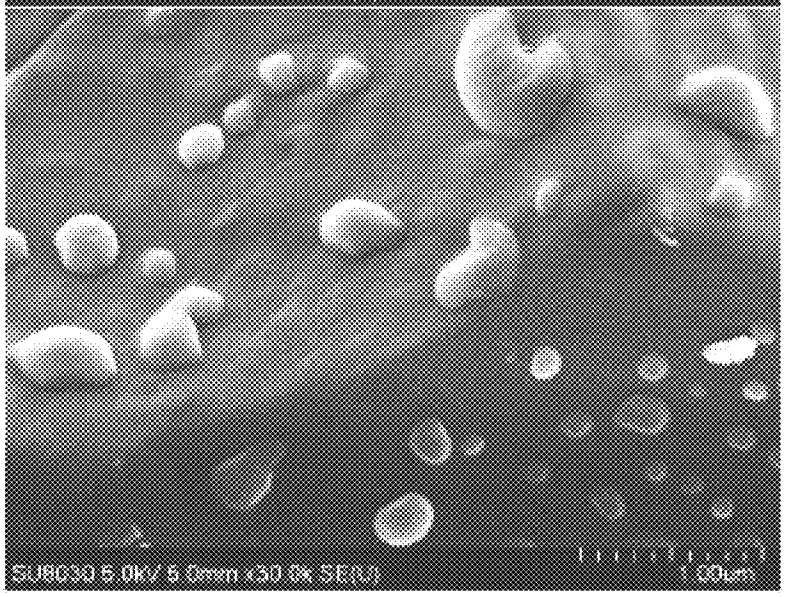

FIG. 52A-1

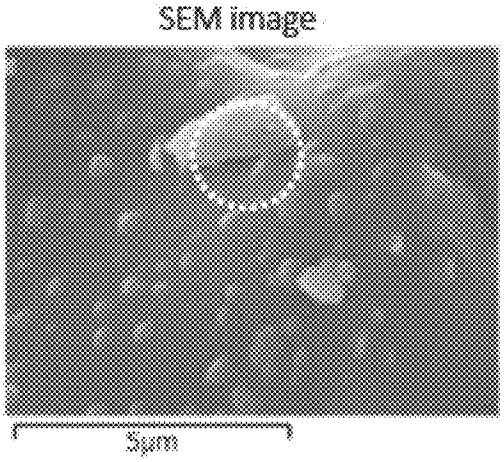

FIG. 52A-2

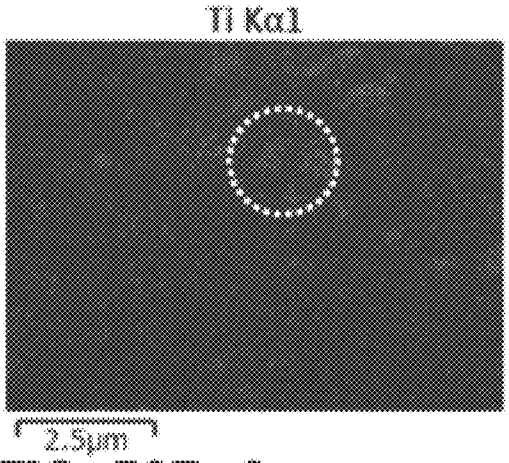

FIG. 52B-1

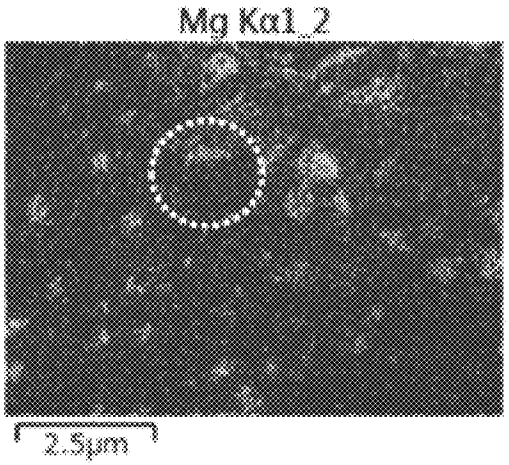

FIG. 52B-2

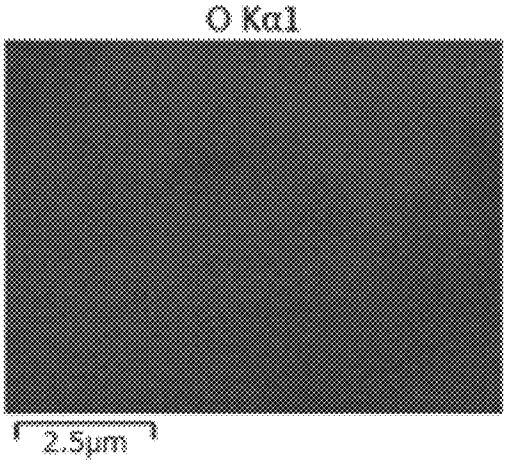

FIG. 52C-1

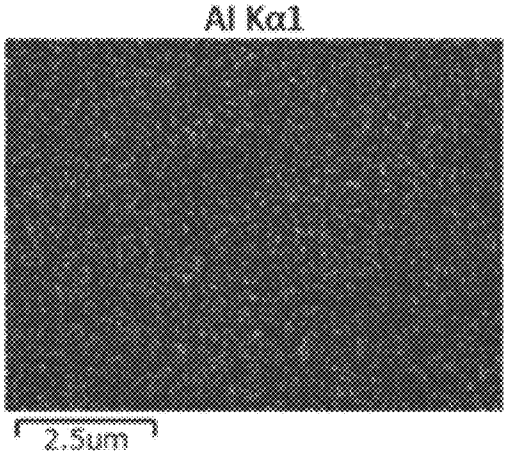

FIG. 52C-2

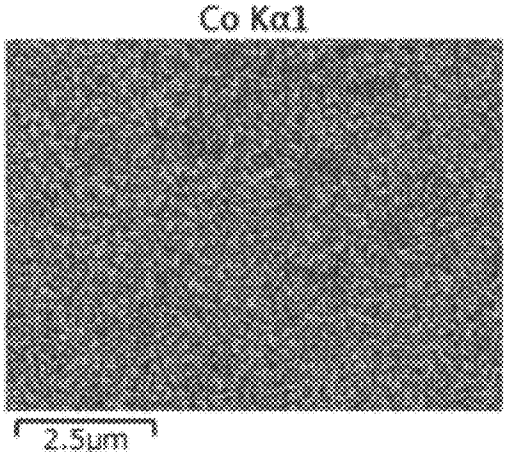

FIG. 53

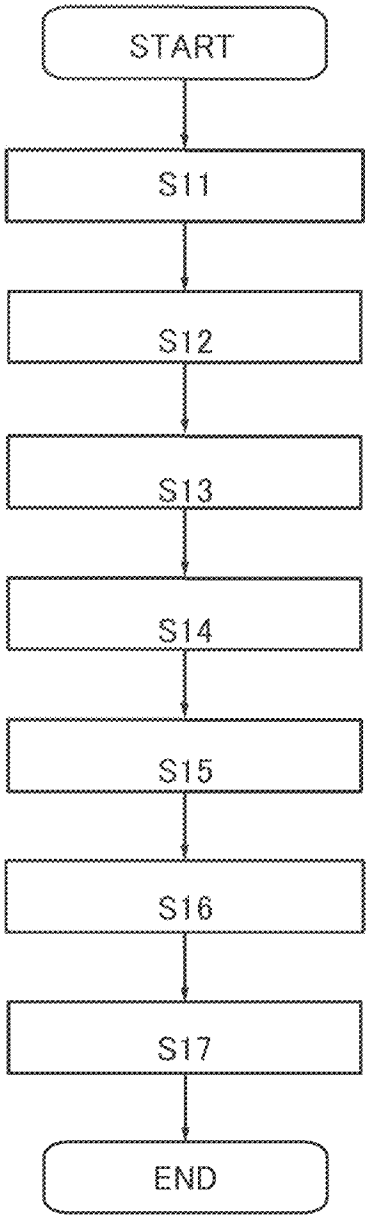

FIG. 54

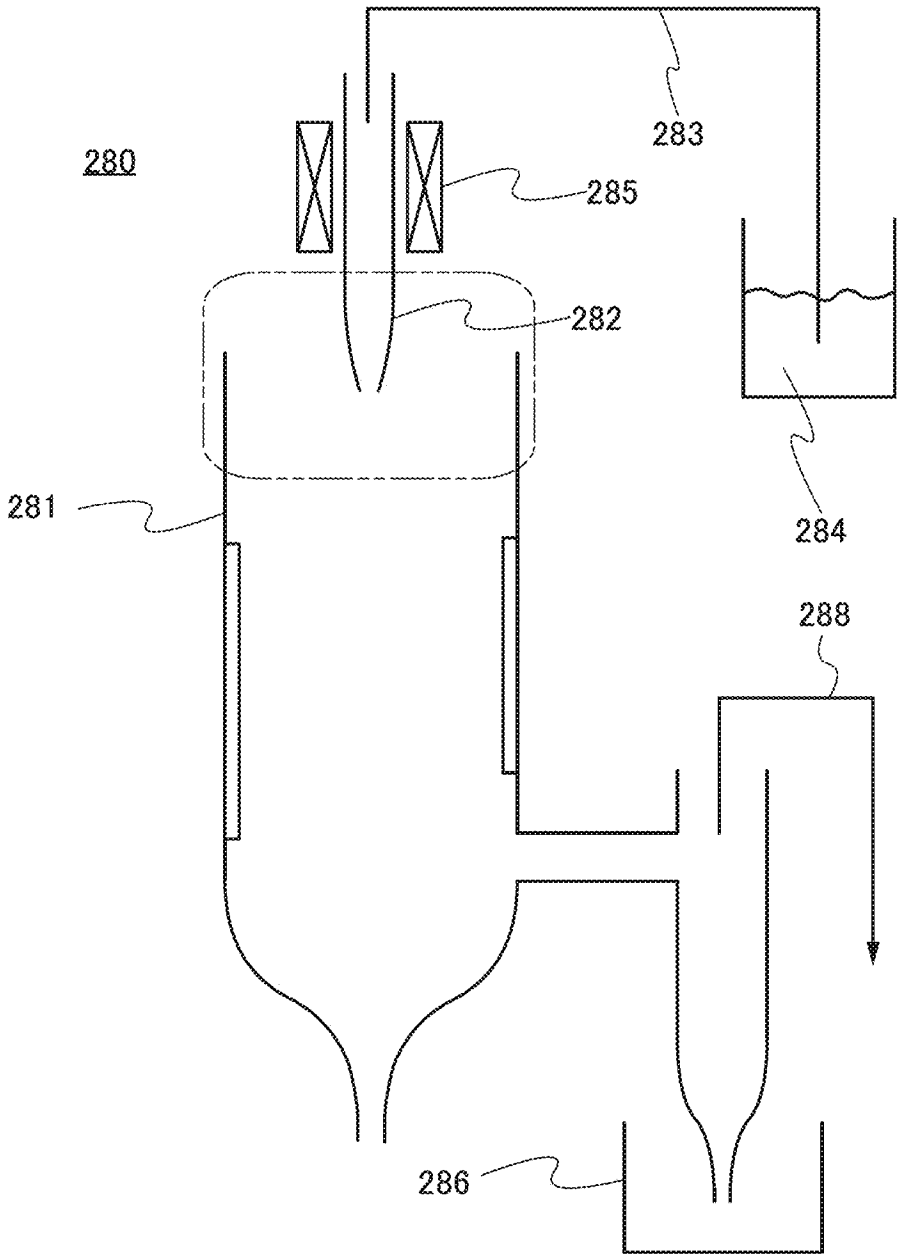

FIG. 55

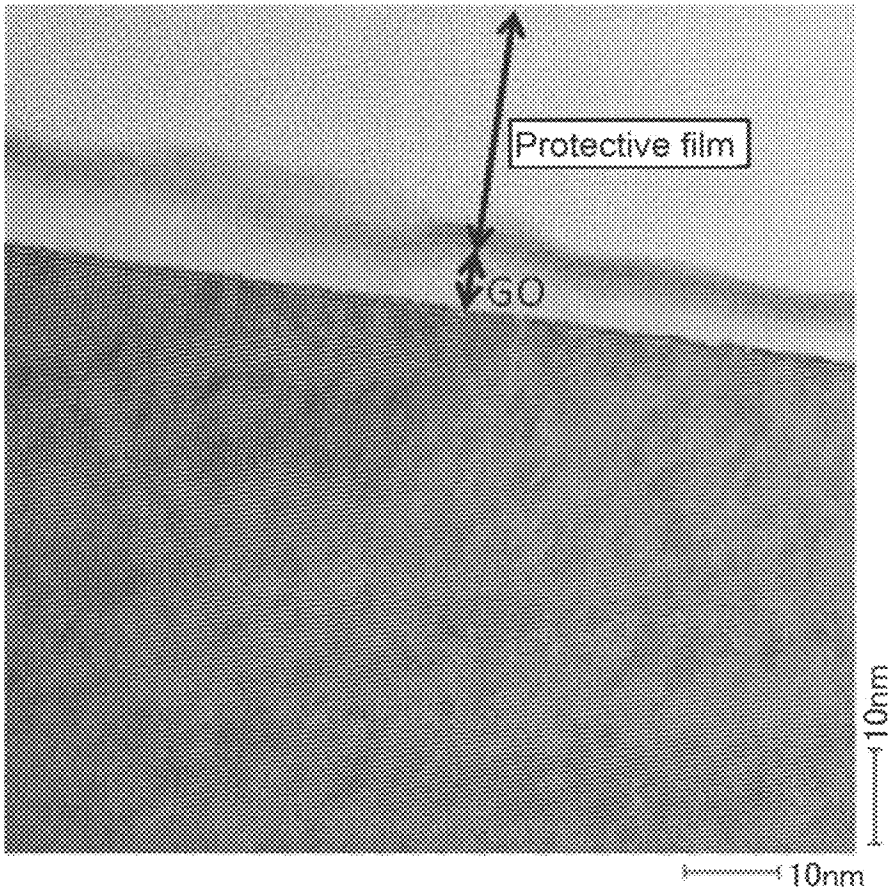

FIG. 56

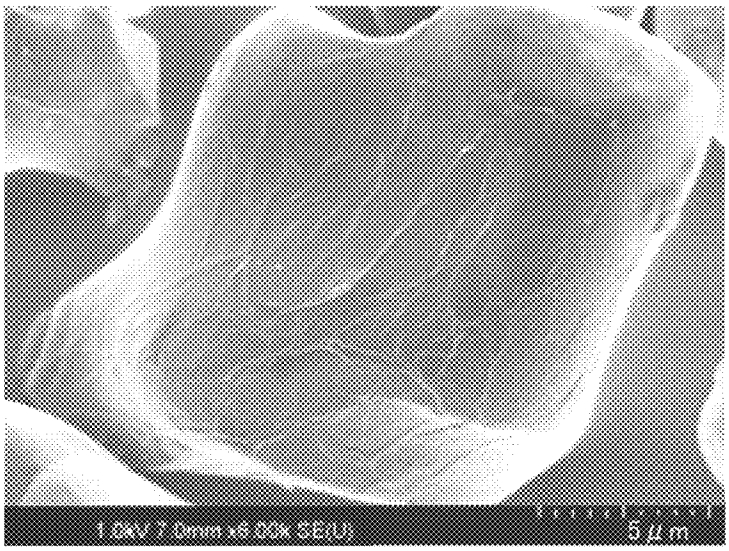

FIG. 57

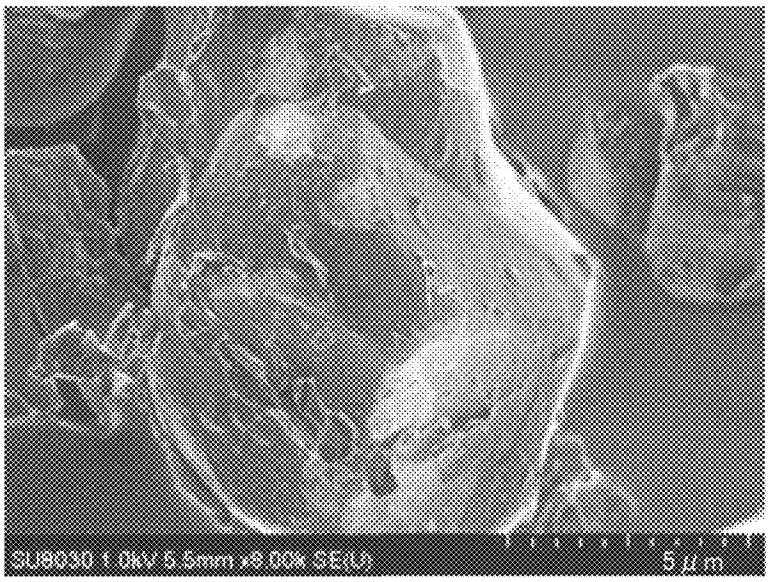

FIG. 58A

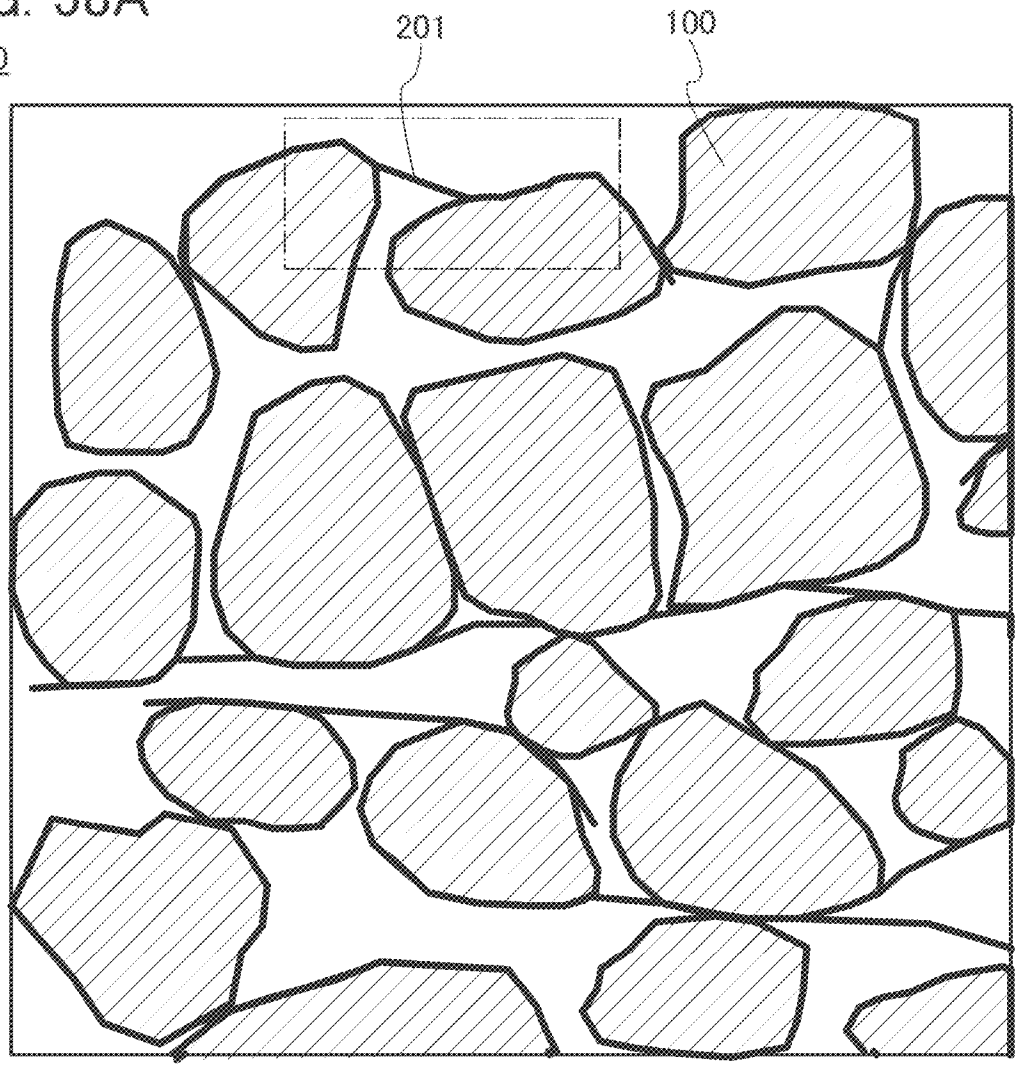

FIG. 58B

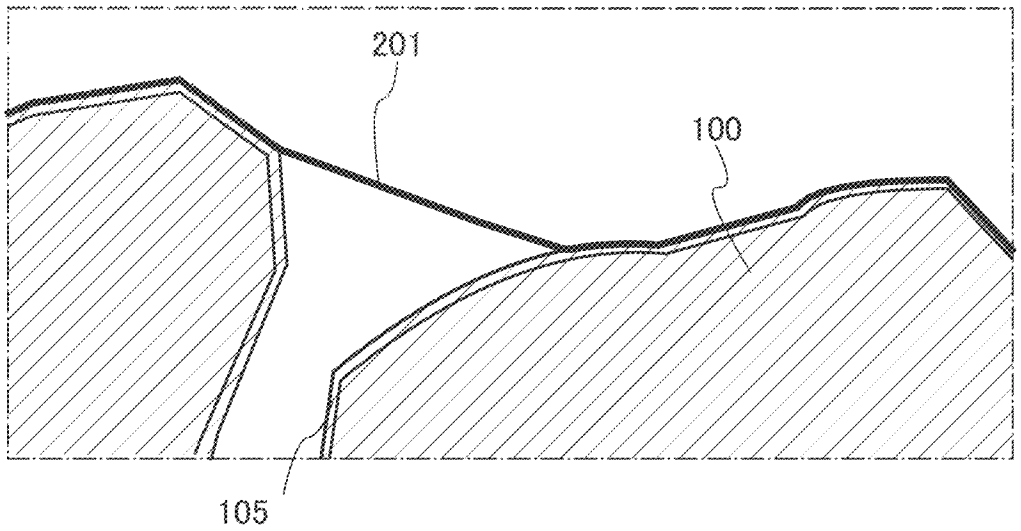

POSITIVE ELECTRODE ACTIVE MATERIAL INCLUDING LITHIUM COBALTATE COATED WITH LITHIUM TITANATE AND MAGNESIUM OXIDE

CROSS-REFERENCE TO RELATED APPLICATIONS

This application is a continuation of U.S. application Ser. No. 15/638,449, filed Jun. 30, 2017, now allowed, which claims the benefit of foreign priority applications filed in Japan as Serial No. 2016-133143 on Jul. 5, 2016, Serial No. 2016-133997 on Jul. 6, 2016, Serial No. 2017-002831 on Jan. 11, 2017, Serial No. 2017-030693 on Feb. 22, 2017, Serial No. 2017-084321 on Apr. 21, 2017, and Serial No. 2017-119272 on Jun. 19, 2017, all of which are incorporated by reference.

TECHNICAL FIELD

One embodiment of the present invention relates to an object, a method, or a manufacturing method. The present invention relates to a process, a machine, manufacture, or a composition of matter. One embodiment of the present invention relates to a semiconductor device, a display device, a light-emitting device, a power storage device, a lighting device, an electronic device, or a manufacturing method thereof. In particular, one embodiment of the present invention relates to a positive electrode active material that can be used in a secondary battery, a secondary battery, and an electronic device including a secondary battery.

In this specification, the power storage device is a collective term describing elements and devices having a power storage function. For example, a storage battery such as a lithium-ion secondary battery (also referred to as secondary battery), a lithium-ion capacitor, and an electric double layer capacitor are included in the category of the power storage device.

Note that electronic devices in this specification mean all devices including power storage devices, and electro-optical devices including power storage devices, information terminal devices including power storage devices, and the like are all electronic devices.

BACKGROUND ART

In recent years, a variety of power storage devices such as lithium-ion secondary batteries, lithium-ion capacitors, and air batteries have been actively developed. In particular, demand for lithium-ion secondary batteries with high output and high energy density has rapidly grown with the development of the semiconductor industry, for portable information terminals such as mobile phones, smartphones, tablets, and laptop computers; portable music players; digital cameras; medical equipment; next-generation clean energy vehicles such as hybrid electric vehicles (HEV), electric vehicles (EV), and plug-in hybrid electric vehicles (PHEV); and the like. The lithium-ion secondary batteries are essential as rechargeable energy supply sources for today's information society.

The performance required for lithium-ion secondary batteries includes increased energy density, improved cycle performance, safe operation under a variety of environments, and longer-term reliability.

Thus, improvement of a positive electrode active material has been studied to increase the cycle performance and the

capacity of the lithium ion secondary battery (Patent Document 1 and Patent Document 2).

REFERENCE

Patent Documents

[Patent Document 1] Japanese Published Patent Application No. 2012-018914

[Patent Document 2] Japanese Published Patent Application No. 2015-201432

DISCLOSURE OF INVENTION

Development of lithium ion secondary batteries and positive electrode active materials used therein is susceptible to improvement in terms of charge and discharge characteristics, cycle characteristics, reliability, safety, cost, and the like.

An object of one embodiment of the present invention is to provide a positive electrode active material which suppresses a reduction in capacity due to charge and discharge cycles when used in a lithium ion secondary battery. Another object of one embodiment of the present invention is to provide a high-capacity secondary battery. Another object of one embodiment of the present invention is to provide a secondary battery with excellent charge and discharge characteristics. Another object of one embodiment of the present invention is to provide a highly safe or highly reliable secondary battery.

Another object of one embodiment of the present invention is to provide a novel material, a novel active material particle, a novel secondary battery, or a formation method thereof.

Note that the descriptions of these objects do not disturb the existence of other objects. In one embodiment of the present invention, there is no need to achieve all the objects. Other objects can be derived from the description of the specification, the drawings, and the claims.

To achieve the above objects, in one embodiment of the present invention, two kinds of regions which are different from a region inside the positive electrode active material are provided in a superficial portion of the positive electrode active material. It is preferable that the inner region contain a non-stoichiometric compound and the outer region contain a stoichiometric compound.

In addition, it is preferable that the inner region contain titanium and the outer region contain magnesium. Furthermore, these two kinds of regions may overlap.

In addition, it is preferable that the inner region be formed through a coating process such as a sol-gel method and the outer region be formed by segregation due to heating.

One embodiment of the present invention is a positive electrode active material including a first region, a second region, and a third region. The first region is present inside the positive electrode active material. The second region and the third region are present in a superficial portion of the positive electrode active material. The third region is present in a region closer to a surface of the positive electrode active material than the second region is. The first region contains an oxide of lithium and a first transition metal and has a layered rock-salt crystal structure. The second region contains a non-stoichiometric compound containing an oxide of a second transition metal and the non-stoichiometric compound has a rock-salt crystal structure. The third region

contains a compound of representative elements and the compound of representative elements has a rock-salt crystal structure.

In the above structure, it is preferable that the first transition metal be cobalt, the second transition metal be titanium, and the compound of representative elements be magnesium oxide.

In the above structure, the third region may contain fluorine. Furthermore, the second region and the third region may each contain cobalt.

In the above structure, it is preferable that crystal orientations of the first region and the second region be partly aligned with each other and crystal orientations of the second region and the third region be partly aligned with each other.

In the above structure, a degree of a mismatch between a (1-1-4) plane of the layered rock-salt crystal structure in the first region or a plane orthogonal to the (1-1-4) plane and a {100} plane of the rock-salt crystal structure in the second region is preferably less than or equal to 0.12, and a degree of a mismatch between the {100} plane of the rock-salt crystal structure in the second region and a {100} plane of the rock-salt crystal structure in the third region is preferably less than or equal to 0.12.

Another embodiment of the present invention is a positive electrode active material containing lithium, titanium, cobalt, magnesium, oxygen, and fluorine. When the concentration of cobalt which is present in a superficial portion of the positive electrode active material and is measured by X-ray photoelectron spectroscopy is 1, the concentration of titanium is greater than or equal to 0.05 and less than or equal to 0.4, the concentration of magnesium is greater than or equal to 0.4 and less than or equal to 1.5, and the concentration of fluorine is greater than or equal to 0.05 and less than or equal to 1.5.

Another embodiment of the present invention is a method for forming a positive electrode active material including: a step of mixing a source of lithium, a source of cobalt, a source of magnesium, and a source of fluorine; a step of heating the mixture of the source of lithium, the source of cobalt, the source of magnesium, and the source of fluorine at 800° C. or higher and 1100° C. or lower for 2 hours or longer and 20 hours or shorter to obtain particles containing lithium, cobalt, magnesium, oxygen, and fluorine; a step of dissolving titanium alkoxide into alcohol; a step of mixing the particles containing lithium, cobalt, magnesium, oxygen, and fluorine into the alcohol solution of the titanium alkoxide and stirring the mixed solution in an atmosphere containing water vapor; a step of collecting precipitate from the mixed solution; and a step of heating the collected precipitate at 500° C. or higher and 1200° C. or lower in an atmosphere containing oxygen under a condition where a retention time is 50 hours or shorter.

In the above formation method, a ratio of the number of atoms of lithium in the source of lithium to the number of atoms of cobalt in the source of cobalt is preferably greater than or equal to 1.00 and less than 1.07.

In the above formation method, a ratio between the number of atoms of magnesium in the source of magnesium and the number of atoms of fluorine in the source of fluorine is preferably Mg:F=1:x ($1.5 \leq x \leq 4$).

In the above formation method, the number of atoms of magnesium in the source of magnesium is preferably greater than or equal to 0.5 atomic % and less than or equal to 1.5 atomic % of the number of atoms of cobalt in the source of cobalt.

In the above formation method, lithium carbonate, cobalt oxide, magnesium oxide, and lithium fluoride can be used as a source of lithium, a source of cobalt, a source of magnesium, and a source of fluorine, respectively.

When the surface of the positive electrode active material is covered with a coating film to protect the above crystal structure, a decrease in capacity due to charge and discharge cycles can be suppressed. As the coating film covering the surface of the positive electrode active material, a coating film containing carbon (a film containing a graphene compound) or a coating film containing lithium or a decomposition product of an electrolyte solution is used.

In particular, powder in which the surface of the positive electrode active material is coated with graphene oxide using a spray dry apparatus is preferably obtained. The spray dry apparatus is a manufacturing apparatus using a spray dry method by which a dispersion medium is removed by supplying a hot wind to a suspension.

When charge and discharge cycles are repeated, deformation of the particles of the positive electrode active materials, such as cracking or breaking, might occur. It is said that such deformation makes a new surface of the positive electrode active material exposed, and the surface is in contact with an electrolyte solution to cause a decomposition reaction or the like, so that the cycle characteristics and the charge and discharge characteristics of the secondary battery are degraded.

Thus, a coating film is preferably provided to prevent the deformation of the particles of the positive electrode active materials, such as cracking or breaking.

However, when suspension is formed and stirred by a rotary and revolutionary mixer to coat the surface of the positive electrode active material whose weight per unit volume is large with graphene oxide whose weight is relatively small, coating is insufficient.

Thus, to coat the surfaces of the particles of the positive electrode active materials with the graphene oxide, a method in which the graphene oxide and a polar solvent (such as water) are mixed and ultrasonic treatment is performed, the particles of the positive electrode active materials are mixed therein to prepare the suspension, and dried powder is produced with a spray dry apparatus is preferably used. The dried powder produced in this manner is referred to as a composite in some cases.

The size of one drop of spray liquid sprayed from a nozzle of the spray dry apparatus depends on a nozzle diameter.

When the particle diameter is smaller than the nozzle diameter, there are a plurality of particles in one drop of the spray liquid sprayed from the nozzle. When the surface of the particle after drying under the condition where the largest particle size is smaller than the nozzle diameter is observed, there are some portions where the surface is coated with the graphene oxide; however, the coating is insufficient.

The nozzle diameter of the spray dry apparatus is preferably substantially equal to the largest particle size of the active material because the coverage of the active material can be improved. Moreover, the largest particle size of the positive electrode active material is preferably adjusted to be substantially equal to the nozzle diameter in forming the positive electrode active material.

Since the graphene oxide is well dispersed into water, the suspension of water and the graphene oxide can be formed by stirring using ultrasonic waves. The positive electrode active material is added to the suspension, and the suspension is sprayed with the spray dry apparatus, whereby

powder in which the surface of the positive electrode active material is coated with the graphene oxide can be obtained.

Note that the suspension becomes more acidic as the amount of graphene oxide is increased. Thus, part of the surface of the positive electrode active material (e.g., $LiCoO_2$ containing Mg and F) might be etched. Then, a hydrogen ion exponent (pH) of the suspension before being sprayed is preferably adjusted to be close to approximately pH7, that is, close to neutral, or higher than or equal to pH8, that is, alkaline. For the pH adjustment, a LiOH aqueous solution is preferably used. For example, in the case where $LiCoO_2$ is used for the positive electrode active material and only pure water is used as the dispersion medium of the suspension, the surface of the positive electrode active material may be damaged. Thus, a mixed solution of ethanol and water is used as the dispersion medium of the suspension, whereby damage to the surface of the active material may be reduced.

The suspension is formed in the above manner, whereby the positive electrode active material whose surface is coated with the graphene oxide can be prepared efficiently. When the surface is coated with the graphene oxide, the deformation of the particles of the positive electrode active materials, such as cracking or breaking can be prevented. Moreover, even if the positive electrode active material whose surface is coated with the graphene oxide is exposed to the air after the formation, the change of properties or degradation can be suppressed. Here, "after the formation" refers to a period from the termination of the formation of the positive electrode active material to the start of the fabrication of the secondary battery containing the positive electrode active material and includes the storing, the transporting, and the like of the positive electrode active material. In addition, when the coating film is formed, the positive electrode active material and the electrolyte solution can be prevented from being in direct contact with each other to react; thus, the secondary battery using the coating film has high reliability.

For the spray dry method, a known apparatus can be utilized, for example, a countercurrent pressure-nozzle-type spray dry apparatus and a counter-cocurrent pressure-nozzle-type spray dry apparatus can be utilized.

Note that the graphene oxide coating the surface of the active material may be reduced when used in the secondary battery. The reduced graphene oxide is referred to as "RGO" in some cases. In RGO, in some cases, part of oxygen atoms remains in a state of oxygen or atomic group containing oxygen that is bonded to carbon. For example, RGO includes a functional group, e.g., an epoxy group, a carbonyl group such as a carboxyl group, or a hydroxyl group.

Another embodiment of the present invention is a secondary battery which includes a positive electrode containing the above-described positive electrode active material or the above-described positive electrode active material coated with a coating film and a negative electrode.

The secondary battery can have any of a variety of shapes to fit the form of the device to be used, for example, a cylindrical shape, a rectangular shape, a coin-type shape, and a laminated (flat plate) shape.

According to one embodiment of the present invention, a positive electrode active material which suppresses a reduction in capacity due to charge and discharge cycles when used in a lithium ion secondary battery is provided. In addition, a secondary battery with excellent charge and discharge characteristics is provided. In addition, a highly safe or highly reliable secondary battery is provided. In addition, a novel material, a novel active material particle, a novel secondary battery, or a formation method thereof is provided.

BRIEF DESCRIPTION OF DRAWINGS

In the accompanying drawings:

FIGS. **1**A to **1**C show examples of a positive electrode active material;

FIGS. **2**A and **2**B illustrate crystal structures of a positive electrode active material;

FIG. **3** illustrates crystal structures of a positive electrode active material;

FIGS. **4**A-**1**, **4**A-**2**, **4**A-**3**, **4**B, **4**C, **4**D-**1**, and **4**D-**2** show a sol-gel method;

FIGS. **5**A to **5**C illustrate a segregation model of elements contained in a positive electrode active material;

FIGS. **6**A to **6**D illustrate a segregation model of elements contained in a positive electrode active material;

FIGS. **7**A and **7**B are cross-sectional views of an active material layer containing a graphene compound as a conductive additive;

FIGS. **8**A to **8**C illustrate a method for charging a secondary battery;

FIGS. **9**A to **9**D illustrate a method for charging a secondary battery;

FIG. **10** illustrates a method for discharging a secondary battery;

FIGS. **11**A to **11**C illustrate a coin-type secondary battery;

FIGS. **12**A to **12**D illustrate a cylindrical secondary battery;

FIGS. **13**A and **13**B illustrate an example of a secondary battery;

FIGS. **14**A-**1**, **14**A-**2**, **14**B-**1**, and **14**B-**2** illustrate examples of secondary batteries;

FIGS. **15**A and **15**B illustrate examples of secondary batteries;

FIG. **16** illustrates an example of a secondary battery;

FIGS. **17**A to **17**C illustrate a laminated secondary battery;

FIGS. **18**A and **18**B illustrate a laminated secondary battery;

FIG. **19** is an external view of a secondary battery;

FIG. **20** is an external view of a secondary battery;

FIGS. **21**A to **21**C illustrate a formation method of a secondary battery;

FIGS. **22**A, **22**B**1**, **22**B**2**, **22**C, and **22**D illustrate a bendable secondary battery;

FIGS. **23**A and **23**B illustrate a bendable secondary battery;

FIGS. **24**A to **24**H illustrate examples of electronic devices;

FIGS. **25**A to **25**C illustrate an example of an electronic device;

FIG. **26** illustrates examples of electronic devices;

FIGS. **27**A to **27**C illustrate examples of electronic devices;

FIG. **28** is a transmission electron microscope image of a positive electrode active material in Example 1;

FIGS. **29**A**1**, **29**A**2**, **29**B**1**, **29**B**2**, **29**C**1**, and **29**C**2** are FFT images of transmission electron microscope images of a positive electrode active material in Example 1;

FIGS. **30**A**1**, **30**A**2**, **30**B**1**, **30**B**2**, **30**C**1**, and **30**C**2** are element mapping images of a positive electrode active material in Example 1;

FIGS. **31**A**1**, **31**A**2**, **31**B**1**, **31**B**2**, **31**C**1**, and **31**C**2** are element mapping images of a positive electrode active material of a comparative example in Example 1;

FIG. **32** is a graph showing TEM-EDX line analysis results of a positive electrode active material in Example 1;

FIG. **33** is a graph showing charge and discharge characteristics of a secondary battery in Example 1;

FIG. **34** is a graph showing charge and discharge characteristics of a secondary battery of a comparative example in Example 1;

FIG. **35** is a graph showing cycle characteristics of a secondary battery in Example 1;

FIG. **36** is a graph showing cycle characteristics of a secondary battery in Example 1;

FIGS. **37**A, **37**B**1**, **37**B**2**, **37**C**1**, **37**C**2**, **37**D**1**, **37**D**2**, **37**E**1**, and **37**E**2** are TEM-EDX plane analysis images of a comparative example in Example 2;

FIGS. **38**A, **38**B**1**, **38**B**2**, **38**C**1**, **38**C**2**, **38**D**1**, **38**D**2**, **38**E**1**, and **38**E**2** are TEM-EDX plane analysis images of a positive electrode active material in Example 2;

FIGS. **39**A, **39**B**1**, **39**B**2**, **39**C**1**, **39**C**2**, **39**D**1**, **39**D**2**, **39**E**1**, and **39**E**2** are TEM-EDX plane analysis images of a comparative example in Example 2;

FIGS. **40**A, **40**B**1**, **40**B**2**, **40**C**1**, **40**C**2**, **40**D**1**, **40**D**2**, **40**E**1**, and **40**E**2** are TEM-EDX plane analysis images of a positive electrode active material in Example 2;

FIGS. **41**A and **41**B are each a graph showing EDX point analysis results in Example 2;

FIGS. **42**A and **42**B are each a graph showing EDX point analysis results in Example 2;

FIG. **43** is a graph showing rate characteristics of a secondary battery in Example 2;

FIG. **44** is a graph showing temperature characteristics of a secondary battery in Example 2;

FIG. **45** is a graph showing cycle characteristics of a secondary battery in Example 2;

FIGS. **46**A and **46**B are each a graph showing XPS analysis results of a positive electrode active material in Example 3;

FIGS. **47**A and **47**B are each a graph showing cycle characteristics of a secondary battery containing a positive electrode active material in Example 3;

FIG. **48** is a graph showing cycle characteristics of a secondary battery containing a positive electrode active material in Example 3;

FIG. **49** is a graph showing cycle characteristics of a secondary battery containing a positive electrode active material in Example 3;

FIGS. **50**A to **50**C are each a graph showing charge and discharge characteristics of a secondary battery containing a positive electrode active material in Example 3;

FIGS. **51**A to **51**C are SEM images of a positive electrode active material in Example 4;

FIGS. **52**A-**1**, **52**A-**2**, **52**B-**1**, **52**B-**2**, **52**C-**1**, and **52**C-**2** are SEM-EDX images of a positive electrode active material in Example 4;

FIG. **53** is a process flow chart of Example 5;

FIG. **54** illustrates a spray dry apparatus in Example 5;

FIG. **55** is a TEM image showing one embodiment of the present invention in Example 5;

FIG. **56** is a SEM image showing one embodiment of the present invention in Example 5;

FIG. **57** is a SEM image showing a comparative example in Example 5; and

FIGS. **58**A and **58**B are cross-sectional views of an active material layer containing a graphene compound as a conductive additive in Example 5.

BEST MODE FOR CARRYING OUT THE INVENTION

Embodiments of the present invention will be described below in detail with reference to the drawings. Note that the present invention is not limited to the description below, and it is easily understood by those skilled in the art that modes and details of the present invention can be modified in various ways. In addition, the present invention should not be construed as being limited to the description in the embodiments given below.

Note that in drawings used in this specification, the sizes, thicknesses, and the like of components such as a positive electrode, a negative electrode, an active material layer, a separator, and an exterior body are exaggerated for simplicity in some cases. Therefore, the sizes of the components are not limited to the sizes in the drawings and relative sizes between the components.

Note that in structures of the present invention described in this specification and the like, the same portions or portions having similar functions are denoted by common reference numerals in different drawings, and descriptions thereof are not repeated. Further, the same hatching pattern is applied to portions having similar functions, and the portions are not especially denoted by reference numerals in some cases.

In this specification and the like, the Miller index is used for the expression of crystal planes and orientations. In the crystallography, a superscript bar is placed over a number in the expression using the Miller index; however, in this specification and the like, crystal planes and orientations are expressed by placing a minus sign (−) at the front of a number instead of placing the bar over a number because of expression limitations. Furthermore, an individual direction which shows an orientation in crystal is denoted by "[ ]", a set direction which shows all of the equivalent orientations is denoted by "< >", an individual direction which shows a crystal plane is denoted by "( )", and a set plane having equivalent symmetry is denoted by "{ }". In the drawings, the crystal planes and orientations are expressed by a number with a bar placed thereover, which is an original crystallographic expression. Note that 1 Å is 10^{-10} m.

In this specification and the like, segregation refers to a phenomenon in which, in a solid made of a plurality of elements (e.g., A, B, and C), a certain element (for example, B) is non-uniformly distributed.

In this specification and the like, a layered rock-salt crystal structure included in a composite oxide containing lithium and a transition metal refers to a crystal structure in which a rock-salt ion arrangement where cations and anions are alternately arranged is included and the lithium and the transition metal are regularly arranged to form a two-dimensional plane, so that lithium can be two-dimensionally diffused. Note that a defect such as a cation or anion vacancy can exist. In the layered rock-salt crystal structure, strictly, a lattice of a rock-salt crystal is distorted in some cases.

In this specification and the like, a rock-salt crystal structure refers to a structure in which cations and anions are alternately arranged. Note that a cation or anion vacancy may exist.

Anions of a layered rock-salt crystal and anions of a rock-salt crystal each form a cubic closest packed structure (face-centered cubic lattice structure). When a layered rock-salt crystal and a rock-salt crystal are in contact with each other, there is a crystal plane at which directions of cubic closest packed structures formed of anions are aligned with each other. A space group of the layered rock-salt crystal is

R-3m, which is different from a space group Fm-3m of a general rock-salt crystal and a space group Fd-3m of a rock-salt crystal having the simplest symmetry; thus, the Miller index of the crystal plane satisfying the above conditions in the layered rock-salt crystal is different from that in the rock-salt crystal. In this specification, in the layered rock-salt crystal and the rock-salt crystal, a state where the directions of the cubic closest packed structures formed of anions are aligned with each other is referred to as a state where crystal orientations are substantially aligned with each other.

Whether the crystal orientations in two regions are aligned with each other or not can be judged by a transmission electron microscope (TEM) image, a scanning transmission electron microscope (STEM) image, a high-angle annular dark field scanning transmission electron microscopy (HAADF-STEM) image, an annular bright-field scan transmission electron microscopy (ABF-STEM) image, and the like. X-ray diffraction, electron diffraction, neutron diffraction, and the like can be used for judging. In the TEM image and the like, alignment of cations and anions can be observed as repetition of bright lines and dark lines. When the orientations of cubic closest packed structures of the layered rock-salt crystal and the rock-salt crystal are aligned with each other, a state where an angle between the repetition of bright lines and dark lines in the layered rock-salt crystal and the repetition of bright lines and dark lines in the rock-salt crystal is less than or equal to 5°, preferably less than or equal to 2.5° is observed. Note that, in the TEM image and the like, a light element such as oxygen or fluorine is not clearly observed in some cases; however, in such a case, alignment of orientations can be judged by arrangement of metal elements.

Furthermore, in this specification and the like, a state where structures of two-dimensional interfaces have similarity is referred to as "epitaxy". Crystal growth in which structures of two-dimensional interfaces have similarity is referred to as "epitaxial growth". In addition, a state where three-dimensional structures have similarity or orientations are crystallographically the same is referred to as "topotaxy". Thus, in the case of topotaxy, when part of a cross section is observed, orientations of crystals in two regions (e.g., a region serving as a base and a region formed through growth) are substantially aligned with each other.

Embodiment 1

[Structure of Positive Electrode Active Material]

First, a positive electrode active material **100**, which is one embodiment of the present invention, is described with reference to FIGS. **1**A to **1**C. The positive electrode active material **100** refers to a substance containing a transition metal which can receive and release lithium ion electrochemically. As illustrated in FIG. **1**A, the positive electrode active material **100** includes a first region **101** inside and a second region **102** and a third region **103** in a superficial portion.

As illustrated in FIG. **1**B, the second region **102** does not necessarily cover the entire first region **101**. Similarly, the third region **103** does not necessarily cover the entire second region **102**. In addition, the third region **103** may be present in contact with the first region **101**.

The thicknesses of the second region **102** and the third region **103** may each differ depending on the positions.

Furthermore, the third region **103** may be present inside the positive electrode active material **100**. For example, in the case where the first region **101** is a polycrystal, the third region **103** may be present in the vicinity of a grain boundary. Furthermore, the third region **103** may be present in a portion which includes crystal defects or a crack portion in the positive electrode active material **100** or in the vicinity thereof. In FIG. **1**B, parts of grain boundaries are shown by dotted lines. In this specification and the like, crystal defects refer to defects which can be observed from a TEM image and the like, that is, a structure in which another element enters crystal, a cavity, and the like. In addition, a crack portion refers to a crack or a break formed in a particle like a crack portion **106** illustrated in FIG. **1**C, for example.

Similarly, as illustrated in FIG. **1**B, the second region **102** may be present inside the positive electrode active material **100**. For example, in the case where the first region **101** is a polycrystal, the second region **102** may be present in the vicinity of a grain boundary. Furthermore, the second region **102** may be present in a portion which includes crystal defects or a crack portion in the positive electrode active material **100** or in the vicinity thereof. Moreover, the third region **103** and the second region **102** inside the positive electrode active material **100** may overlap.

<First Region **101**>

The first region **101** contains a composite oxide of lithium and a first transition metal. In other words, the first region **101** contains lithium, a first transition metal, and oxygen.

The composite oxide of lithium and a first transition metal preferably has a layered rock-salt crystal structure.

As the first transition metal, only cobalt may be used, cobalt and manganese may be used, or cobalt, manganese, and nickel may be used.

That is, the first region can include lithium cobalt oxide, lithium manganese oxide, lithium nickel oxide, lithium cobalt oxide in which manganese is substituted for part of cobalt, lithium nickel-manganese-cobalt oxide, or the like. In addition to the transition metal, the first region **101** may include a metal other than the transition metal, such as aluminum.

The first region **101** serves as a region which particularly contributes to a charge and discharge reaction in the positive electrode active material **100**. To increase capacity of a secondary battery containing the positive electrode active material **100**, the volume of the first region **101** is preferably larger than those of the second region and the third region.

A material having a layered rock-salt crystal structure has features such as high discharge capacity and low resistance due to lithium that can be diffused two-dimensionally, which is preferably used for the first region **101**. In addition, in the case where the first region **101** has a layered rock-salt crystal structure, a segregation of a representative element such as magnesium, which is described later, tends to occur unexpectedly.

Note that the first region **101** may be a single crystal or a polycrystal. For example, the first region **101** may be a polycrystal in which an average crystallite size is greater than or equal to 280 nm and less than or equal to 630 nm. In the case of a polycrystal, a grain boundary can be observed from the TEM or the like in some cases. In addition, the average of crystal grain sizes can be calculated from the half width of XRD.

The polycrystal has a clear crystal structure; thus, a two-dimensional diffusion path of lithium ions can be sufficiently ensured. In addition, a polycrystal is easily produced as compared with a single crystal; thus, a polycrystal is preferably used for the first region **101**.

Furthermore, the entire first region **101** does not necessarily have a layered rock-salt crystal structure. For example, part of the first region **101** may be amorphous or has another crystal structure.

<Second Region **102**>

The second region **102** contains an oxide of a second transition metal. In other words, the second region **102** contains a second transition metal and oxygen.

As the second transition metal, a non-stoichiometric metal is preferably used. In other words, the second region **102** preferably includes a non-stoichiometric compound. For example, as the second transition metal, at least one of titanium, vanadium, manganese, iron, chromium, niobium, cobalt, zinc, zirconium, nickel, and the like can be used. Note that the second transition metal is preferably an element different from that of the first transition metal.

In this specification and the like, a non-stoichiometric metal refers to a metal that can have a plurality of valences. In addition, a non-stoichiometric compound refers to a compound of a metal that can have a plurality of valences and another element.

The second region **102** preferably has a rock-salt crystal structure.

The second region **102** serves as a buffer region which connects the first region **101** to the third region **103** which is described later. In the non-stoichiometric compound, an interatomic distance can be changed in accordance with a change in valence of a metal contained in the non-stoichiometric compound. In addition, in the non-stoichiometric compound, a cation or anion vacancy and dislocation (what is called Magneli phase) are often formed. Thus, the second region **102**, which serves as a buffer region, can absorb a strain generated between the first region **101** and the third region **103**.

Furthermore, the second region **102** may contain lithium in addition to the second transition metal and oxygen. For example, lithium titanate or lithium manganite may be contained. Moreover, the second region **102** may contain a representative element contained in the third region **103** which is described later. The second region **102** that contains an element contained in the first region **101**, such as lithium, and an element contained in the third region **103** is preferable because the second region **102** serves as a buffer region.

That is, the second region **102** can contain lithium titanate, titanium oxide, vanadium oxide, manganese oxide, iron oxide, copper oxide, chromium oxide, niobium oxide, cobalt oxide, zinc oxide, or the like.

In addition, the second region **102** may contain the first transition metal. For example, the second transition metal may be present in part of a first transition metal site of the composite oxide including the first transition metal.

For example, in the case where the second transition metal is titanium, titanium may be present as titanium oxide (TiO_2) or lithium titanate ($LiTiO_2$) in the second region **102**. Alternatively, in the second region **102**, titanium may be substituted for part of the first transition metal site of the composite oxide of lithium and the first transition metal.

Moreover, the second region **102** may contain fluorine.

The second region **102** preferably has a crystal structure which is the same as that of the third region **103** which is described later. In this case, orientations of crystals of the second region **102** and the third region **103** are likely to be aligned with each other.

The second region **102** preferably has a rock-salt crystal structure; however, the entire second region **102** does not necessarily have a rock-salt crystal structure. For example, the second region **102** may have another crystal structure such as a spinel crystal structure, an olivine crystal structure, a corundum crystal structure, or a rutile crystal structure.

Furthermore, a crystal structure may have a strain as long as a structure where six oxygen atoms are adjacent to cations is kept. In addition, a cation vacancy may be present in part of the second region **102**.

Moreover, part of the second region **102** may be amorphous.

When the thickness of the second region **102** is too small, the function as the buffer region is degraded; however, when the thickness of the second region **102** is too large, the capacity might be decreased. Thus, the second region **102** is preferably provided in a range from the surface of the positive electrode active material **100** to a depth of 20 nm, preferably a depth of 10 nm, in a depth direction. The second transition metal may have a concentration gradient.

<Third Region **103**>

The third region **103** contains a compound of representative elements. A compound of representative elements is a stoichiometric compound. As the compound of representative elements, a compound made of representative elements which are electrochemically stable is preferable, and at least one of magnesium oxide, calcium oxide, beryllium oxide, lithium fluoride, and sodium fluoride can be used, for example.

The third region **103** is in contact with an electrolyte solution when the positive electrode active material **100** is used in a secondary battery. Thus, for the third region **103**, a material which is hardly changed electrochemically in the process of charging and discharging and is not easily transformed by contact with the electrolyte solution is preferably used. The compound of representative elements which is a stoichiometric compound and electrochemically stable is preferably used for the third region **103**. The positive electrode active material **100** includes the third region **103** in a superficial portion to improve stability in charging and discharging of the secondary battery. Here, a state where stability of a secondary battery is high refers to a state where the crystal structure of the composite oxide of lithium and the first transition metal contained in the first region **101** is more stable. Alternatively, it refers to a state where a change in capacity of the secondary battery is small even if charging and discharging are repeated or a state where a change in valence of a metal contained in the positive electrode active material **100** is suppressed even after charging and discharging are repeated.

The third region **103** may contain fluorine. In the case where the third region **103** contains fluorine, fluorine may be substituted for some anions in the compound of the representative elements.

Fluorine is substituted for some anions in the compound of the representative elements, whereby diffusion properties of lithium can be improved. Thus, the third region **103** is less likely to prevent charging and discharging. In addition, when fluorine is present in a superficial portion of a positive electrode active material particle, corrosion resistance against a hydrofluoric acid generated by decomposition of an electrolyte solution is increased in some cases.

Moreover, the third region **103** may include lithium, the first transition metal, and the second transition metal.

The compound of the representative elements contained in the third region **103** preferably has a rock-salt crystal structure. When the third region **103** has a rock-salt crystal structure, orientations of crystals are likely to be aligned with those of the second region **102**. The orientations of crystals of the first region **101**, the second region **102**, and the third region **103** are substantially aligned with each

other, whereby the second region **102** and the third region **103** can serve as a more stable coating layer.

However, the entire third region **103** does not necessarily have a rock-salt crystal structure. For example, the third region **103** may have another crystal structure such as a spinel crystal structure, an olivine crystal structure, a corundum crystal structure, or a rutile crystal structure.

Furthermore, a crystal structure may have a strain as long as a structure where six oxygen atoms are adjacent to cations is kept. In addition, a cation vacancy may be present in part of the third region **103**.

Moreover, part of the third region **103** may be amorphous.

When the thickness of the third region **103** is too small, the function of increasing stability in charging and discharging is degraded; however, when the thickness of the third region **103** is too large, the capacity might be decreased. Thus, the thickness of the third region **103** is preferably greater than or equal to 0.5 nm and less than or equal to 50 nm, further preferably greater than or equal to 0.5 nm and less than or equal to 2 nm.

In the case where the third region **103** contains fluorine, fluorine is preferably present in a bonding state other than magnesium fluoride (MgF_2), lithium fluoride (LiF), and cobalt fluoride (CoF_2). Specifically, when an XPS analysis is performed on the vicinity of the surface of the positive electrode active material **100**, a peak position of bonding energy with fluorine is preferably higher than or equal to 682 eV and lower than or equal to 685 eV, further preferably approximately 684.3 eV. The bonding energy does not correspond to those of MgF_2, LiF, and CoF_2.

In this specification and the like, a peak position of bonding energy with an element in an XPS analysis refers to a value of bonding energy at which the maximum intensity of an energy spectrum is obtained in a range corresponding to bonding energy of the element.

In general, when charging and discharging are repeated, a side reaction occurs in a positive electrode active material, for example, a first transition metal such as manganese, cobalt, or nickel is dissolved in an electrolyte solution, oxygen is released, and a crystal structure becomes unstable, so that the positive electrode active material deteriorates. However, the positive electrode active material **100** of one embodiment of the present invention includes the second region **102** serving as a buffer region and the third region **103** which is electrochemically stable. Thus, the dissolution of the first transition metal can be effectively suppressed, and the crystal structure of the composite oxide of lithium and the transition metal contained in the first region **101** can be more stable. As a result, the cycle characteristics of the secondary battery including the positive electrode active material **100** can be significantly improved. In addition, in the case where charging and discharging are performed at a voltage higher than 4.3 V (vs. Li/Li^+), in particular, a high voltage of 4.5 V (vs. Li/Li^+) or more, the structure of one embodiment of the present invention is significantly effective.

<Heteroepitaxial Growth and Topotaxy>

The second region **102** is preferably formed by heteroepitaxial growth from the first region **101**. Furthermore, the third region **103** is preferably formed by heteroepitaxial growth from the second region **102**. A region formed by heteroepitaxial growth becomes topotaxy which has crystal orientations substantially three-dimensionally aligned with those of a region serving as a base. Thus, the first region **101**, the second region **102**, and the third region **103** can be topotaxy.

When the crystal orientations of the first region **101**, the second region **102**, and the third region **103** are substantially aligned with each other, the second region **102** and the third region **103** serve as a coating layer which has a stable bond with the first region **101**. As a result, the positive electrode active material **100** including a strong coating layer can be provided.

Since the second region **102** and the third region **103** have a stable bond with the first region **101**, when the positive electrode active material **100** is used for the secondary battery, a change of the crystal structure in the first region **101** which is caused by charging and discharging can be effectively suppressed. Even when lithium is released from the first region **101** due to charging, the coating layer having a stable bond can suppress release of cobalt and oxygen from the first region **101**. Furthermore, a chemically stable material can be used for a region in contact with the electrolyte solution. Thus, a secondary battery having excellent cycle characteristics can be provided.

<Degree of Mismatch Between Regions>

To perform heteroepitaxial growth, the degree of a mismatch between crystals in a region serving as a base and crystals on which crystal growth is performed is important.

In this specification and the like, the degree of a mismatch f is defined by the following Formula 1. The average of the nearest neighbor distances between oxygen and cations of the crystals in the region serving as a base is represented by a, and the average of the natural nearest neighbor distances between anions and cations of the crystals on which crystal growth is performed is represented by b.

[Formula 1]

$$f=|b-a/a| \quad \text{(Formula 1)}$$

To perform heteroepitaxial growth, the degree of a mismatch f between crystals in a region serving as a base and crystals on which crystal growth is performed needs to be less than or equal to 0.12. To perform more stable heteroepitaxial growth to form a layered shape, the degree of a mismatch f is preferably less than or equal to 0.08, further preferably less than or equal to 0.04.

Thus, materials of the first region **101** and the second region **102** are preferably selected so that the degree of a mismatch f between the layered rock-salt crystal structure in the first region **101** and the rock-salt crystal structure in the second region **102** is less than or equal to 0.12.

Furthermore, materials of the second region **102** and the third region **103** are preferably selected so that the degree of a mismatch f between the rock-salt crystal structure in the second region **102** and the rock-salt crystal structure in the third region **103** is less than or equal to 0.12.

Examples of materials and crystal planes of the first region **101**, the second region **102**, and the third region **103** are shown below, which satisfy the above-described conditions: the degree of a mismatch f between the layered rock-salt crystal structure in the first region **101** and the rock-salt crystal structure in the second region **102** is less than or equal to 0.12; and the degree of a mismatch f between the rock-salt crystal structure in the second region **102** and the rock-salt crystal structure in the third region **103** is less than or equal to 0.12.

Example 1

Lithium Cobaltate, Lithium Titanate, and Magnesium Oxide

First, FIGS. **2**A and **2**B and FIG. **3** show an example in which the first transition metal is cobalt, the first region **101**

contains lithium cobaltate having a layered rock-salt crystal structure, the second transition metal is titanium, the second region **102** contains lithium titanate having a rock-salt crystal structure, and the compound of the representative elements in the third region **103** is magnesium oxide having a rock-salt crystal structure.

FIG. **2**A illustrates a model of a layered rock-salt crystal structure (a space group R-3mH) of lithium cobaltate ($LiCoO_2$), a model of a rock-salt crystal structure (a space group Fd-3mZ) of lithium titanate ($LiTiO_2$), and a model of a rock-salt crystal structure (a space group Fd-3mZ) of magnesium oxide. FIG. **2**A illustrates models each of which is seen from the b-axis direction.

From FIG. **2**A, it is not seen that the layered rock-salt crystals and the rock-salt crystals make topotaxy. Then, here, the layered rock-salt crystals are seen from a different direction (e.g., a direction indicated by an arrow in FIG. **2**A). FIG. **2**B illustrates a model of the layered rock-salt crystals seen from the <1-1-4> plane direction and models of the rock-salt crystals seen from the <100> plane direction.

As illustrated in FIG. **2**B, when the layered rock-salt crystals are seen from the <1-1-4> plane direction, atomic arrangement of the layered rock-salt crystals is highly similar to those of the rock-salt crystals seen from the <100> plane direction. In addition, the nearest neighbor distances between metal and oxygen have similar values. For example, in the layered rock-salt lithium cobaltate, a distance between Li and O is 2.089 Å and a distance between Co and O is 1.925 Å. In the rock-salt lithium titanate, a distance between Li and O is 2.138 Å and a distance between Ti and O is 2.051 Å. In the rock-salt magnesium oxide, a distance between Mg and O is 2.106 Å.

Then, with reference to FIG. **3**, the degree of a mismatch between the regions when the (1-1-4) crystal plane of the layered rock-salt crystal and the {100} crystal plane of the rock-salt crystal are in contact with each other is described.

As illustrated in FIG. **3**, a distance between metals through oxygen in a (1-1-4) crystal plane **101***p* (1-1-4) of lithium cobaltate having the layered rock-salt crystal structure in the first region **101** is 4.01 Å. Furthermore, a distance between metals through oxygen in a {100} crystal plane **102***p* {100} of lithium titanate having the rock-salt crystal structure in the second region **102** is 4.19 Å. Thus, the degree of a mismatch f between the crystal plane **101***p* (1-1-4) and the crystal plane **102***p* {100} is 0.04.

In addition, a distance between metals through oxygen in a {100} crystal plane **103***p* {100} of magnesium oxide having the rock-salt crystal structure in the third region **103** is 4.21 Å. Thus, the degree of a mismatch f between the crystal plane **102***p* {100} and the crystal plane **103***p* {100} is 0.02.

In this manner, the degree of a mismatch between the first region **101** and the second region **102** and the degree of a mismatch between the second region **102** and the third region **103** are sufficiently small; thus, the first region **101**, the second region **102**, and the third region **103** can be topotaxy.

Although not illustrated in FIG. **3**, if the crystal plane **101***p* (1-1-4) in the first region **101** and the crystal plane **103***p* {100} in the third region **103** are in contact with each other, the degree of a mismatch f is 0.05. That is, owing to the second region **102**, the degree of a mismatch can be small. Moreover, with the second region **102** that is a non-stoichiometric transition metal oxide, the first region **101**, the second region **102**, and the third region **103** can be more stable topotaxy. Thus, the second region **102** and the third region **103** can serve as a coating layer having a stable bond with the first region **101**.

In this embodiment, the (1-1-4) plane of the layered rock-salt crystal and the {100} plane of the rock-salt crystal are in contact with each other; however, one embodiment of the present invention is not limited thereto as long as crystal planes which can be topotaxy are in contact with each other.

Example 2

Lithium Cobaltate, Manganese Oxide, and Calcium Oxide

Next, an example in which the first transition metal is cobalt, the first region **101** contains lithium cobaltate having a layered rock-salt crystal structure, the second transition metal is manganese, the second region **102** contains manganese oxide having a rock-salt crystal structure, and the compound of the representative elements in the third region **103** is calcium oxide having a rock-salt crystal structure is shown.

Also in this case, as in FIGS. **2**A and **2**B and FIG. **3**, when the layered rock-salt crystals are seen from the <1-1-4> plane direction, atomic arrangement of the layered rock-salt crystals in the first region **101** is highly similar to those of the rock-salt crystals in the second region **102** and the third region **103** seen from the <100> plane direction.

The degree of a mismatch between the regions when the (1-1-4) crystal plane of the layered rock-salt crystal and the {100} crystal plane of the rock-salt crystal are in contact with each other is described. A distance between metals through oxygen in a crystal plane (1-1-4) of lithium cobaltate having the layered rock-salt crystal structure in the first region **101** is 4.01 Å. Furthermore, a distance between metals through oxygen in a crystal plane {100} of manganese oxide having the rock-salt crystal structure in the second region **102** is 4.45 Å. Thus, the degree of a mismatch f between the crystal plane (1-1-4) in the first region **101** and the crystal plane {100} in the second region **102** is 0.11.

In addition, a distance between metals through oxygen in a crystal plane {100} of calcium oxide having the rock-salt crystal structure in the third region **103** is 4.82 Å. Thus, the degree of a mismatch f between the crystal plane {100} in the second region **102** and the crystal plane {100} in the third region **103** is 0.08.

In this manner, the degree of a mismatch between the first region **101** and the second region **102** and the degree of a mismatch between the second region **102** and the third region **103** are sufficiently small; thus, the first region **101**, the second region **102**, and the third region **103** can be topotaxy.

If the crystal plane (1-1-4) in the first region **101** and the crystal plane {100} in the third region **103** are in contact with each other, the degree of a mismatch f is 0.20; thus, it is difficult to perform the heteroepitaxial growth. That is, owing to the second region **102**, the heteroepitaxial growth from the first region to the third region can be performed. Thus, the second region **102** and the third region **103** can serve as a coating layer having a stable bond with the first region **101**.

Example 3

Lithium Nickel-Manganese-Cobalt Oxide, Manganese Oxide, and Calcium Oxide

Next, an example in which the first transition metals are nickel, manganese, and cobalt, the first region **101** contains

lithium nickel-manganese-cobalt oxide ($LiNi_{0.33}Co_{0.33}Mn_{0.33}O_2$) having a layered rock-salt crystal structure, the second transition metal is manganese, the second region **102** contains manganese oxide having a rock-salt crystal structure, and the compound of the representative elements in the third region **103** is calcium oxide having a rock-salt crystal structure is shown.

Also in this case, as illustrated in FIGS. **2**A and **2**B and FIG. **3**, when the layered rock-salt crystals are seen from the <1-1-4> plane direction, atomic arrangement of the layered rock-salt crystals is highly similar to those of the rock-salt crystals seen from the <100> plane direction. The degree of a mismatch between the regions when the (1-1-4) crystal plane of the layered rock-salt crystal and the {100} crystal plane of the rock-salt crystal are in contact with each other is described.

A distance between metals through oxygen in a crystal plane (1-1-4) of lithium nickel-manganese-cobalt oxide having the layered rock-salt crystal structure in the first region **101** is 4.07 Å. Furthermore, a distance between metals through oxygen in a crystal plane {100} of manganese oxide having the rock-salt crystal structure in the second region **102** is 4.45 Å. Thus, the degree of a mismatch f between the crystal plane (1-1-4) in the first region **101** and the crystal plane {100} in the second region **102** is 0.09.

In addition, a distance between metals through oxygen in a crystal plane {100} of calcium oxide having the rock-salt crystal structure in the third region **103** is 4.82 Å. Thus, the degree of a mismatch f between the crystal plane {100} in the second region **102** and the crystal plane {100} in the third region **103** is 0.08.

In this manner, the degree of a mismatch between the first region **101** and the second region **102** and the degree of a mismatch between the second region **102** and the third region **103** are sufficiently small; thus, the first region **101**, the second region **102**, and the third region **103** can be topotaxy.

If the crystal plane (1-1-4) in the first region **101** and the crystal plane {100} in the third region **103** are in contact with each other, the degree of a mismatch f is 0.18; thus, it is difficult to perform the heteroepitaxial growth. That is, the second region **102** is provided, whereby the heteroepitaxial growth from the first region to the third region can be performed. Thus, the second region **102** and the third region **103** can serve as a coating layer having a stable bond with the first region **101**.

<Boundaries Between Regions>

As described above, the first region **101**, the second region **102**, and the third region **103** have different compositions. The element contained in each region has a concentration gradient in some cases. For example, the second transition metal in the second region **102** may have a concentration gradient. In addition, the third region **103** may have a concentration gradient of a representative element because a representative element preferably segregates in the third region **103** as described later. Thus, the boundaries between the regions are not clear in some cases.

The difference of compositions of the first region **101**, the second region **102**, and the third region **103** can be observed using a TEM image, a STEM image, fast Fourier transform (FFT) analysis, energy dispersive X-ray spectrometry (EDX), an analysis in the depth direction by time-of-flight secondary ion mass spectrometry (ToF-SIMS), X-ray photoelectron spectroscopy (XPS), Auger electron spectroscopy, thermal desorption spectroscopy (TDS), or the like.

For example, in the TEM image and the STEM image, difference of constituent elements is observed as difference of brightness; thus, difference of constituent elements of the first region **101**, the second region **102**, and the third region **103** can be observed. Furthermore, also in plane analysis of EDX (e.g., element mapping), it can be observed that the first region **101**, the second region **102**, and the third region **103** contain different elements.

By line analysis of EDX and analysis in the depth direction using ToF-SIMS, a peak of concentration of each element contained in the first region **101**, the second region **102**, and the third region **103** can be detected.

However, clear boundaries between the first region **101**, the second region **102**, and the third region **103** are not necessarily observed by the analyses.

In this specification and the like, the third region **103** that is present in a superficial portion of the positive electrode active material **100** refers to a region from the surface of the positive electrode active material **100** to a region where a concentration of a representative element such as magnesium which is detected by analysis in the depth direction is ⅕ of a peak. As the analysis in the depth direction, the line analysis of EDX, analysis in the depth direction using ToF-SIMS, or the like, which is described above, can be used.

Furthermore, a peak of a concentration of a representative element is preferably present in a region from the surface of the positive electrode active material **100** to a depth of 3 nm toward the center, further preferably to a depth of 1 nm, and still further preferably to a depth of 0.5 nm.

Although the depth at which the concentration of the representative element becomes ⅕ of the peak is different depending on the manufacturing method, in the case of a manufacturing method described later, the depth is approximately 2 nm to 5 nm from the surface of the positive electrode active material.

The third region **103** that is present inside the first region **101** in the vicinity of a grain boundary, a crystal defect, or the like also refers to a region where a concentration of a representative element which is detected by analysis in the depth direction is higher than or equal to ⅕ of a peak.

A distribution of fluorine in the positive electrode active material **100** preferably overlaps with a distribution of the representative element. Thus, fluorine also has a concentration gradient, and a peak of a concentration of fluorine is preferably present in a region from the surface of the positive electrode active material **100** to a depth of 3 nm toward the center, further preferably to a depth of 1 nm, and still further preferably to a depth of 0.5 nm.

In this specification and the like, the second region **102** that is present in a superficial portion of the positive electrode active material **100** refers to a region where a concentration of the second transition metal which is detected by analysis in the depth direction is higher than or equal to ½ of a peak. The second region **102** that is present inside the first region **101** in the vicinity of a grain boundary, a crystal defect, or the like also refers to a region where a concentration of the second transition metal which is detected by analysis in the depth direction is higher than or equal to ½ of a peak. As the analysis method, the line analysis of EDX, analysis in the depth direction using ToF-SIMS, or the like, which is described above, can be used.

Thus, the third region **103** and the second region **102** overlap in some cases. Note that the third region **103** is preferably present in a region closer to the surface of the positive electrode active material particle than the second region **102** is. In addition, the peak of the concentration of the representative element is preferably present in a region

closer to the surface of the positive electrode active material particle than the peak of the concentration of the second transition metal is.

The peak of the second transition metal is preferably present in a region from a depth of 0.2 nm or more to a depth of 10 nm or less from the surface of the positive electrode active material **100** toward the center, further preferably in a region from a depth of 0.5 nm or more to a depth of 3 nm or less.

The measurement range of the XPS is from the surface of the particle of the positive electrode active material **100** to a region at a depth of approximately 5 nm. Thus, a concentration of an element present at a depth of approximately 5 nm from the surface can be analyzed quantitatively. Thus, the concentration of elements in the third region **103** and the second region **102** present at a depth of approximately 5 nm from the surface can be analyzed quantitatively.

When the surface of the positive electrode active material **100** is subjected to the XPS analysis and the concentration of the first transition metal is defined as 1, a relative value of the concentration of the second transition metal is preferably greater than or equal to 0.05 and less than or equal to 0.4, further preferably greater than or equal to 0.1 and less than or equal to 0.3. In addition, a relative value of the concentration of the representative element is preferably greater than or equal to 0.4 and less than or equal to 1.5, further preferably greater than or equal to 0.45 and less than or equal to 1.00. Furthermore, a relative value of the concentration of fluorine is preferably greater than or equal to 0.05 and less than or equal to 1.5, further preferably greater than or equal to 0.3 and less than or equal to 1.00.

Note that, as described above, elements contained in the first region **101**, the second region **102**, and the third region **103** may each have a concentration gradient; thus, the first region **101** may contain the element in the second region **102** or the third region **103**, such as fluorine. Similarly, the third region **103** may contain the element in the first region **101** or the second region **102**. In addition, the first region **101**, the second region **102**, and the third region **103** may each contain another element such as carbon, sulfur, silicon, sodium, calcium, chlorine, or zirconium.

[Particle Diameter]

If the particle diameter of the positive electrode active material **100** is too large, diffusion of lithium is difficult, whereas if the particle diameter is too small, it is difficult to maintain a crystal structure described later. Thus, D50 (also referred to as a median diameter) is preferably 5 μm or more and 100 μm or less, and further preferably 10 μm or more and 70 μm or less. In the case where the coating film is formed on the surface of the positive electrode active material **100** by a spray dry apparatus in a later step, it is preferable that the nozzle diameter and the maximum particle diameter of the positive electrode active material **100** be substantially the same. When the particle diameter is less than 5 μm and a spray dry apparatus having a nozzle diameter of 20 μm is used, secondary particles are covered collectively, which leads to a decrease in coverage.

To increase the density of the positive electrode active material layer, it is effective to mix large particles (the longest portion is approximately 20 μm or more and 40 μm or less) and small particles (the longest portion is approximately 1 μm) and embed spaces between the large particles with the small particles. Thus, there may be two peaks of particle size distribution.

The particle size of the positive electrode active material is influenced not only by the particle sizes of starting materials but also by a ratio between lithium and the first transition metal (hereinafter expressed as a ratio of Li to the first transition metal) which are contained in the starting material.

In the case where the particle size of the starting material is small, the grain growth needs to be performed at the time of baking so that the grain size of the positive electrode active material is in the above-described preferred range.

To promote the grain growth at the time of baking, it is effective to make the ratio of Li to the first transition metal of the starting material larger than 1, that is, to make the amount of lithium a little larger. For example, when the ratio of Li to the first transition metal is approximately 1.06, a positive electrode active material in which D50 is larger than or equal to 15 μm is easily obtained. Note that, as described later, lithium may be lost to the outside of a system in the formation process of the positive electrode active material; thus, the ratio between lithium and the first transition metal of the obtained positive electrode active material does not agree with the ratio between lithium and the first transition metal of the starting material in some cases.

However, if the amount of lithium is too large to make the particle size be in the preferred range, the capacity retention rate of a secondary battery containing the positive electrode active material might be decreased.

Then, the present inventors found that with the second region **102** containing the second transition metal in the superficial portion, the particle size can be in the preferred range by control of the ratio of Li to the first transition metal and a positive electrode active material having high capacity retention rate can be formed.

In the positive electrode active material of one embodiment of the present invention including a region containing the second transition metal in the superficial portion, the ratio of Li to the first transition metal in the starting material is preferably greater than or equal to 1.00 and less than or equal to 1.07, further preferably greater than or equal to 1.03 and less than or equal to 1.06.

[Formation of Second Region]

The second region **102** can be formed by coating particles of the composite oxide of lithium and the first transition metal with a material containing the second transition metal.

As the coating method of the material containing the second transition metal, a liquid phase method such as a sol-gel method, a solid phase method, a sputtering method, an evaporation method, a chemical vapor deposition (CVD) method, a pulsed laser deposition (PLD) method, or the like can be used. In this embodiment, the case where the sol-gel method which can be performed with a uniform coverage under an atmospheric pressure is used is described.

<Sol-Gel Method>

A method for forming a material containing the second transition metal using a sol-gel method is described with reference to FIGS. **4A-1**, **4A-2**, **4A-3**, **4B**, **4C**, **4D-1**, and **4D-2**.

First, an alkoxide of the second transition metal is dissolved in alcohol.

FIG. **4A-1** shows a general formula of the alkoxide of the second transition metal. In the formula of FIG. **4A-1**, M2 indicates the alkoxide of the second transition metal. R represents an alkyl group having 1 to 18 carbon atoms or a substituted or unsubstituted aryl group having 6 to 13 carbon atoms. Although FIG. **4A-1** shows the general formula in which the second transition metal has a valence of 4, one embodiment of the present invention is not limited thereto. The second transition metal may have a valence of 2, a valence of 3, a valence of 5, a valence of 6, or a valence of

7. In this case, the alkoxide of the second transition metal includes an alkoxy group corresponding to the valence of the second transition metal.

FIG. **4**A-**2** shows a general formula of the titanium alkoxide used when titanium is used as the second transition metal. R in FIG. **4**A-**2** represents an alkyl group having 1 to 18 carbon atoms or a substituted or unsubstituted aryl group having 6 to 13 carbon atoms.

As the titanium alkoxide, tetramethoxytitanium, tetraethoxytitanium, tetra-n-propoxytitanium, tetra-i-propoxytitanium (also referred to as tetraisopropyl orthotitanate, titanium (IV) isopropoxide, titanium tetraisopropoxide (IV), TTIP, and the like), tetra-n-butoxytitanium, tetra-i-butoxytitanium, tetra-sec-butoxytitanium, tetra-t-butoxytitanium, or the like can be used.

FIG. **4**A-**3** shows a chemical formula of titanium (IV) isopropoxide (TTIP) described in a formation method below, which is a kind of titanium alkoxide.

As a solvent in which the alkoxide of the second transition metal is dissolved, an alcohol such as methanol, ethanol, propanol, 2-propanol, butanol, or 2-butanol is preferably used.

Next, particles of composite oxide of lithium, a transition metal, magnesium, and fluorine are mixed into the alcohol solution of the alkoxide of the second transition metal and stirred in an atmosphere containing water vapor.

When the solution is put in an atmosphere containing H_2O, hydrolysis of water and an alkoxide of the second transition metal occurs as in FIG. **4**B. Then, as in FIG. **4**C, dehydration condensation occurs between the products of FIG. **4**B. When the hydrolysis of FIG. **4**B and the condensation reaction of FIG. **4**C occur repeatedly, a sol of an oxide of the second transition metal is generated. This reaction also occurs on a particle **110** of the composite oxide as in FIGS. **4**D-**1** and **4**D-**2**, and a layer containing the second transition metal is formed on the surface of the particle **110**.

After that, the particle **110** is collected, and the alcohol is vaporized. The details of the formation method are described later.

Note that in this embodiment, an example in which the particles of the composite oxide of lithium, the first transition metal, the representative element, and fluorine are coated with the material containing the second transition metal before the particles are applied to a positive electrode current collector is described; however, one embodiment of the present invention is not limited thereto. After the positive electrode active material layer including the particles of the composite oxide of lithium, the first transition metal, the representative element, and fluorine is formed on the positive electrode current collector, the positive electrode current collector and the positive electrode active material layer may be both soaked into an alkoxide solution of the second transition metal to be coated with the material containing the second transition metal.

[Segregation of Third Region]

The third region **103** can be formed by a sputtering method, a solid phase method, a liquid phase method such as a sol-gel method, or the like. However, the present inventors found that when a source of a representative element such as magnesium and a source of fluorine are mixed with a material of the first region **101** and then the mixture is heated, the representative element is segregated on a superficial portion of the positive electrode active material particle to form the third region **103**. In addition, they found that with the third region **103** formed in this manner, the positive electrode active material **100** has excellent cycle characteristics.

In the case where the third region **103** is formed through the heating as described above, the heating is preferably performed after the particle of the composite oxide is coated with the material containing the second transition metal. This is because even after the particle is coated with the material containing the second transition metal, the representative element such as magnesium is unexpectedly segregated on the surface of the particle when the heating is performed.

Segregation models of the representative element are described with reference to FIGS. **5**A to **5**C and FIGS. **6**A to **6**D. It is probable that the segregation model of the representative element such as magnesium is slightly different in accordance with the ratio between lithium and the first transition metal contained in a starting material. Then, a segregation model in which the ratio of Li to the first transition metal in the starting material is less than 1.03, that is, the amount of lithium is small, is described with reference to FIGS. **5**A to **5**C. In addition, a segregation model in which the ratio of Li to the first transition metal in the starting material is greater than or equal to 1.03, that is, the amount of lithium is large, is described with reference to FIGS. **6**A to **6**D. In these segregation models in FIGS. **5**A to **5**C and FIGS. **6**A to **6**D, the first transition metal is cobalt, the second transition metal is titanium, and the representative element is magnesium.

FIG. **5**A illustrates a model diagram of the vicinity of the surface of the particle **110** of the composite oxide containing lithium, cobalt, magnesium, and fluorine, which is formed at a ratio of Li to Co in the starting material of less than 1.03. A region **111** in the drawings contains lithium, cobalt, magnesium, and fluorine, and lithium cobaltate ($LiCoO_2$) is a main component of the region **111**. Lithium cobaltate has a layered rock-salt structure.

It is generally known that, at the time of synthesizing particles of the composite oxide containing lithium, cobalt, magnesium, and fluorine, lithium partly moves outside a system (a particle on which lithium is formed). This is because lithium is volatilized at the time of baking, lithium is eluted to a solvent at the time of mixing the starting material, and the like. Thus, the ratio of Li to Co in the particle **110** of the composite oxide containing lithium, cobalt, magnesium, and fluorine becomes smaller than the ratio of Li to Co in the starting material in some cases.

When the ratio of Li to Co in the starting material is less than 1.03, on the surface of the particle **110**, lithium is released from the lithium cobaltate and cobalt oxide is easily generated. Thus, as illustrated in FIG. **5**A, the surface of the particle **110** of the composite oxide is covered with a cobalt oxide (CoO) layer **114** in some cases.

The cobalt oxide has a rock-salt crystal structure. Thus, in the particle **110** in FIG. **5**A, the cobalt oxide layer **114** having a rock-salt crystal structure is provided over and in contact with the region **111** containing lithium cobaltate having a layered rock-salt crystal structure in some cases.

The particle **110** is coated with a material containing titanium by a sol-gel method or the like. FIG. **5**B illustrates a state where the particle **110** is coated with a layer **112** containing titanium by a sol-gel method. At the stage of FIG. **5**B, the layer **112** containing titanium is a gel of titanium oxide; thus, the crystallinity is low.

Next, the particle **110** coated with the layer **112** containing titanium is heated. Although the details of the heating conditions are described later, for example, FIG. **5**C illustrates a state where the particle **110** is heated in an oxygen atmosphere at 800° C. for two hours to form the positive electrode active material **100**, which is one embodiment of

the present invention. By heating, titanium in the layer **112** containing titanium is diffused into the inside of the particle **110**. At the same time, magnesium and fluorine contained in the region **111** are segregated on the surface of the particle **110**.

As described above, on the surface of the particle **110**, cobalt oxide having a rock-salt structure is present. In addition, magnesium oxide also has a rock-salt crystal structure. Thus, it is probable that magnesium is more stable in the state of being present as magnesium oxide on the surface of the particle **110** as compared with the state of being present inside the particle **110**. That could be why magnesium is segregated on the surface of the particle **110** when the particle **110** is heated.

Moreover, it is considered that fluorine contained in the starting material promotes the segregation of magnesium.

Fluorine has higher electronegativity than oxygen. Thus, it is probable that even in a stable compound such as magnesium oxide, when fluorine is added, uneven charge distribution occurs and a bond between magnesium and oxygen is weakened. Furthermore, it is probable that fluorine is substituted for oxygen in the magnesium oxide, whereby magnesium easily moves around the substituted fluorine.

Moreover, this can also be described from a phenomenon in which a melting point of a mixture decreases. When magnesium oxide (melting point: 2852° C.) and lithium fluoride (melting point: 848° C.) are added at the same time, the melting point of the magnesium oxide is lowered. It is considered that the melting point is lowered, whereby magnesium easily moves at the time of heating, and the segregation of magnesium easily occurs.

Lastly, the third region **103** becomes a solid solution of cobalt oxide and magnesium oxide which has a rock-salt crystal structure. Furthermore, fluorine is probably substituted for part of oxygen contained in the cobalt oxide and the magnesium oxide.

Cobalt sites of lithium cobaltate are substituted for part of the diffused titanium and lithium titanate is substituted for another part of the diffused titanium. The second region **102** after the heating contains lithium titanate having a rock-salt crystal structure.

The first region **101** after the heating contains lithium cobaltate having a layered rock-salt crystal structure.

Next, the case where the ratio of Li to Co in the starting material is larger than or equal to 1.03 is described with reference to FIGS. **6**A to **6**D. FIG. **6**A illustrates a model diagram of the vicinity of the surface of the particle **120** of the composite oxide containing lithium, cobalt, magnesium, and fluorine, which is formed at a ratio of Li to Co in the starting material of greater than or equal to 1.03. A region **121** in the drawings contains lithium, cobalt, magnesium, and fluorine.

Since the particle **120** in FIG. **6**A contains a sufficient amount of lithium, even when lithium is released from the particle **120** at the time of baking the particle **120** of the composite oxide of lithium, cobalt, magnesium, and fluorine or the like, lithium is diffused from the inside of the particle **120** to the surface thereof to compensate; as a result, a cobalt oxide layer is not easily formed on the surface.

FIG. **6**B illustrates a state where the particle **120** in FIG. **6**A is coated with a layer **122** containing titanium by a sol-gel method. At the stage of FIG. **6**B, the layer **122** containing titanium is a gel of titanium oxide; thus, the crystallinity is low.

FIG. **6**C illustrates the state where the particle **120** coated with the layer **122** containing titanium in FIG. **6**B starts to be heated. By heating, titanium in the layer **122** containing titanium is diffused into the inside of the particle **110**. The diffused titanium is bonded with lithium contained in the region **121** to become lithium titanate, and a layer **125** containing the lithium titanate is formed.

Since lithium is bonded with titanium to form lithium titanate, the amount of lithium is relatively insufficient at the surface of the particle **120**. Thus, it is probable that, as illustrated in FIG. **6**C, a cobalt oxide layer **124** is temporarily formed on the surface of the particle **120**.

FIG. **6**D illustrates the state where the state of FIG. **6**C is sufficiently heated to form the positive electrode active material **100**, which is one embodiment of the present invention. It is considered that, since the cobalt oxide layer **124** having a rock-salt crystal structure is present on the surface, magnesium is more stable in the state of being present as magnesium oxide on the surface of the particle **120** as compared with the state of being present inside the particle **120**. As in the case of FIGS. **5**A to **5**C, fluorine promotes the segregation of magnesium.

Thus, as illustrated in FIG. **6**D, magnesium and fluorine contained in the region **121** are segregated on the surface to be the third region **103** with the cobalt oxide.

In this manner, the positive electrode active material **100**, which includes the third region **103** containing magnesium oxide and cobalt oxide, the second region **102** containing lithium titanate, and the first region **101** containing lithium cobaltate, is formed.

Note that in the case where the representative element is segregated by heating, when the composite oxide containing lithium and the first transition metal included in the first region **101** is a polycrystal or has crystal defects, the representative element can be segregated not only in the superficial portion but also in the vicinity of a grain boundary of the composite oxide containing lithium and the first transition metal or in the vicinity of crystal defects thereof. The representative element segregated in the vicinity of a grain boundary or in the vicinity of crystal defects can contribute to further improvement in stability of the crystal structure of the composite oxide containing lithium and the first transition metal included in the first region **101**.

When the composite oxide containing lithium and the first transition metal included in the first region **101** includes a crack portion, the representative element is also segregated in the crack portion by heating. In addition, not only the representative element but also the second transition metal can be segregated. The crack portion is in contact with the electrolyte solution like the surface of the particle. Thus, the representative element and the second transition metal are segregated in the crack portion, and the third region **103** and the second region **102** are generated, whereby a chemically stable material can be used for the region in contact with the electrolyte solution. As a result, a secondary battery having excellent cycle characteristics can be provided.

The ratio between a representative element (T) and fluorine (F) in a starting material is preferably in a range of $T:F=1:x$ ($1.5 \leq x \leq 4$) (atomic ratio) because the segregation of the representative element effectively occurs. Further preferably, the ratio between T and F is approximately 1:2 (atomic ratio).

Since the third region **103** formed by segregation is formed by epitaxial growth, orientations of crystals in the second region **102** and the third region **103** are partly and substantially aligned with each other in some cases. That is, the second region **102** and the third region **103** become topotaxy in some cases. When the orientations of crystals in

the second region **102** and the third region **103** are substantially aligned with each other, these regions can serve as a more favorable coating layer.

However, not all of the representative elements such as magnesium which is added as a starting material need not be segregated in the third region **103**. For example, the first region **101** may contain a small amount of representative element such as magnesium.

<Fourth Region **104**>

In addition, as illustrated in FIG. **1**C, the positive electrode active material **100** may include a fourth region **104** on the third region **103**. Furthermore, when the positive electrode active material **100** contains a defect such as a crack portion **106**, the fourth region **104** may be present to embed the defect such as the crack portion **106**.

The fourth region **104** contains some elements contained in the second region **102** and the third region **103**. For example, the fourth region **104** contains the second transition metal and the representative element.

The fourth region **104** may have a projection, a stripe shape, or a layered shape. The fourth region **104** is formed using the second transition metal and the representative element not contained in the second region **102** or the third region **103** of the second transition metals and the representative elements contained in the starting material and the like. That is, with the fourth region **104**, the amount of the second transition metal and the representative element contained in the second region **102** and the third region **103** can be kept in an appropriate range and the crystal structures of the second region **102** and the third region **103** can be stabilized in some cases. Moreover, with the fourth region **104**, the defect such as the crack portion **106** included in the positive electrode active material **100** can be repaired.

The presence of the fourth region **104** and the shape of the fourth region **104** can be observed by a scanning electron microscope (SEM) or the like. Elements contained in the fourth region **104** can be analyzed by SEM-EDX or the like.

[Method for Forming Positive Electrode Active Material]

Next, an example of a method for forming the positive electrode active material **100**, which is one embodiment of the present invention, is described.

<Step 11: Preparation of Starting Materials>

First, starting materials are prepared. From the starting materials prepared in this process, the first region **101** and the third region **103** are formed finally.

As materials of lithium and the first transition metal contained in the first region **101**, a source of lithium and a source of the first transition metal are prepared. In addition, as materials of the compound of the representative elements contained in the third region **103**, a source of the representative element is prepared.

In addition to these sources, a source of fluorine is preferably prepared. Fluorine used for the materials has an effect of segregating the representative elements contained in the third region **103** on the surface of the positive electrode active material **100** in a later step.

As the source of lithium, for example, lithium carbonate and lithium fluoride can be used. As the source of the first transition metal, for example, an oxide of the first transition metal can be used. As the source of the representative element, for example, an oxide of the representative element contained in the third region and fluoride of the representative element contained in the third region can be used.

As the source of fluorine, for example, lithium fluoride and fluoride of the representative element contained in the third region can be used. That is, lithium fluoride can be used as either the source of lithium or the source of fluorine.

The amount of fluorine contained in the source of fluorine is preferably 1.0 time to 4 times (atomic ratio), further preferably 1.5 times to 3 times (atomic ratio) the amount of representative element contained in the source of the representative element.

<Step 12: Mixing of Starting Materials>

Next, the source of lithium, the source of the first transition metal, and the source of the representative element are mixed. In addition, the source of fluorine is preferably added. For example, a ball mill and a bead mill can be used for the mixing.

<Step 13: First Heating>

Next, the materials mixed in Step 12 are heated. In this step, the heating is referred to as baking or first heating in some cases. The heating is preferably performed at higher than or equal to 800° C. and lower than or equal to 1100° C., further preferably at higher than or equal to 900° C. and lower than or equal to 1000° C. The heating time is preferably greater than or equal to 2 hours and less than or equal to 20 hours. The baking is preferably performed in a dried atmosphere such as dry air. In the dried atmosphere, for example, the dew point is preferably lower than or equal to −50° C., further preferably lower than or equal to −100° C. In this embodiment, the heating is performed at 1000° C. for 10 hours, the temperature rising rate is 200° C./h, and dry air whose dew point is −109° C. flows at 10 L/min After that, the heated materials are cooled to room temperature.

By the heating in Step 13, the composite oxide of lithium and the first transition metal having a layered rock-salt crystal structure can be synthesized. At this time, the representative element and fluorine contained in the starting materials form a solid solution in the composite oxide. However, some representative elements have been already segregated on the surface of the composite oxide in some cases.

In addition, as the starting materials, particles of the composite oxide containing lithium, cobalt, fluorine, and magnesium which are synthesized in advance may be used. In this case, Step 12 and Step 13 can be omitted. For example, lithium cobalt oxide particles (C-20F, produced by NIPPON CHEMICAL INDUSTRIAL CO., LTD.) can be used as one of the starting materials. The lithium cobalt oxide particle has a diameter of approximately 20 μm and contains fluorine, magnesium, calcium, sodium, silicon, sulfur, and phosphorus in a region which can be analyzed by XPS from the surface.

<Step 14: Coating with Second Transition Metal>

Next, the composite oxide of lithium and the first transition metal is cooled to room temperature. Then, the surface of the composite oxide particle of lithium and the first transition metal is coated with a material containing the second transition metal. In the formation method example, a sol-gel method is used.

First, the alkoxide of the second transition metal which is dissolved in alcohol and the composite oxide particles of lithium and the first transition metal are mixed.

For example, in the case where titanium is used as the second transition metal, TTIP can be used as the alkoxide of the second transition metal. As alcohol, isopropanol can be used, for example.

Next, the above mixed solution is stirred in an atmosphere containing water vapor. The stirring can be performed with a magnetic stirrer, for example. The stirring time is not limited as long as water and TTIP in an atmosphere cause hydrolysis and polycondensation reaction. For example, the stirring can be performed at 25° C. and a humidity of 90% RH (Relative Humidity) for 4 hours.

As described above, when water and TTIP in an atmosphere are reacted, a sol-gel reaction can proceed more slowly as compared with the case where liquid water is added. Alternatively, when titanium alkoxide and water are reacted at room temperature, a sol-gel reaction can proceed more slowly as compared with the case where heating is performed at a temperature higher than the boiling point of alcohol which is a solvent, for example. A sol-gel reaction proceeds slowly, whereby a high-quality coating layer containing titanium with a uniform thickness can be formed.

After the above process, precipitate is collected from the mixed solution. As the collection method, filtration, centrifugation, evaporation and drying, or the like can be used. In this embodiment, filtration is used. For the filtration, a paper filter is used, and the residue is washed by alcohol which is the same as the solvent in which titanium alkoxide is dissolved.

Then, the collected residue is dried. In this embodiment, vacuum drying is performed at 70° C. for one hour.

<Step 15: Second Heating>

Next, the composite oxide particle coated with the material containing the second transition metal, which is formed in Step 14, is heated. This step is referred to as second heating in some cases. In the heating, the retention time within a specified temperature range is preferably shorter than or equal to 50 hours, further preferably longer than or equal to 2 hours and shorter than or equal to 10 hours, still further preferably longer than or equal to 1 hour and shorter than or equal to 3 hours. If the heating time is too short, there is concern that the segregation of the representative elements does not occur; however, if the heating time is too long, there is concern that the favorable second region **102** is not formed because diffusion of the second transition metal proceeds too much.

The specified temperature is preferably higher than or equal to 500° C. and lower than or equal to 1200° C., further preferably higher than or equal to 800° C. and lower than or equal to 1000° C. If the specified temperature is too low, there is concern that the segregation of the representative elements and the second transition metal does not occur. However, if the specified temperature is too high, there is concern that the first transition metal in the composite oxide particle is reduced to decompose the composite oxide particle, that a layered structure of lithium and the first transition metal in the composite oxide particle cannot be kept, and the like.

In this embodiment, the specified temperature is 800° C. and kept for 2 hours, the temperature rising rate is 200° C./h, and the flow rate of dry air is 10 L/min.

By the heating in Step 15, the composite oxide of lithium and the first transition metal and the oxide of the second transition metal covering the composite oxide become topotaxy. In other words, the first region **101** and the second region **102** become topotaxy.

By the heating in Step 15, the representative elements which form a solid solution inside the composite oxide particle of lithium and the first transition metal are unevenly distributed on the surface to form a solid solution, that is, the representative elements are segregated, the compound of the representative elements is formed, and the third region **103** is formed. At this time, the compound of the representative elements is formed by heteroepitaxial growth from the second region **102**. That is, the second region **102** and the third region **103** become topotaxy.

Since the second region **102** and the third region **103** contain crystals whose orientations are substantially aligned with each other and have a stable bond with the first region **101**, when the positive electrode active material **100** is used for the secondary battery, a change of the crystal structure in the first region **101** which is caused by charging and discharging can be effectively suppressed. Even when lithium is released from the first region **101** due to charging, the superficial portion having a stable bond can suppress release of oxygen and the first transition metal such as cobalt from the first region **101**. Furthermore, a chemically stable material can be used for a region in contact with the electrolyte solution. Thus, a secondary battery having excellent cycle characteristics can be provided.

Note that the entire first region **101** and second region **102** does not need to become topotaxy as long as part of the first region **101** and second region **102** becomes topotaxy. Furthermore, the entire second region **102** and third region **103** does not need to become topotaxy as long as part of the second region **102** and third region **103** becomes topotaxy.

In the case where the compound of the representative elements contained in the third region contains oxygen, the heating in Step 15 is preferably performed in an atmosphere containing oxygen. Heating in an atmosphere containing oxygen promotes the formation of the third region **103**.

Furthermore, fluorine contained in the starting materials promotes the segregation of the representative elements.

In this manner, in the method for forming the positive electrode active material of one embodiment of the present invention, after the elements forming the second region **102** are coated, heating is performed to form the third region **103**, and two kinds of regions can be formed on the surface of the positive electrode active material **100**. That is, in general, two coating steps are necessary for providing two kinds of regions in a superficial portion; however, in the method for forming the positive electrode active material of one embodiment of the present invention, only one coating step (sol-gel process) is needed, which is a formation method with high productivity.

<Step 16: Cooling>

Next, the particles heated in Step 15 are cooled to room temperature. The time of decreasing temperature is preferably long because topotaxy is easily generated. For example, the time of decreasing temperature from retention temperature to room temperature is preferably the same as the time of increasing temperature or longer, specifically longer than or equal to 10 hours and shorter than or equal to 50 hours.

<Step 17: Collecting>

Next, the cooled particles are collected. Moreover, the particles are preferably made to pass through a sieve. Through the above process, the positive electrode active material **100** including the first region **101**, the second region **102**, and the third region **103** can be formed.

This embodiment can be implemented in appropriate combination with any of the other embodiments.

Embodiment 2

In this embodiment, examples of materials which can be used for a secondary battery containing the positive electrode active material **100** described in the above embodiment are described. In this embodiment, a secondary battery in which a positive electrode, a negative electrode, and an electrolyte solution are wrapped in an exterior body is described as an example.

[Positive Electrode]

The positive electrode includes a positive electrode active material layer and a positive electrode current collector.

<Positive Electrode Active Material Layer>

The positive electrode active material layer contains at least a positive electrode active material. The positive electrode active material layer may contain, in addition to the positive electrode active material, other materials such as a coating film of the active material surface, a conductive additive, and a binder.

As the positive electrode active material, the positive electrode active material **100** described in the above embodiment can be used. When the above-described positive electrode active material **100** is used, a secondary battery with high capacity and excellent cycle characteristics can be obtained.

Examples of the conductive additive include a carbon material, a metal material, and a conductive ceramic material. Alternatively, a fiber material may be used as the conductive additive. The content of the conductive additive with respect to the total amount of the active material layer is preferably greater than or equal to 1 wt % and less than or equal to 10 wt %, more preferably greater than or equal to 1 wt % and less than or equal to 5 wt %.

A network for electric conduction can be formed in the active material layer by the conductive additive. The conductive additive also allows maintaining of a path for electric conduction between the positive electrode active material particles. The addition of the conductive additive to the active material layer increases the electric conductivity of the active material layer.

Examples of the conductive additive include natural graphite, artificial graphite such as mesocarbon microbeads, and carbon fiber. Examples of carbon fiber include mesophase pitch-based carbon fiber, isotropic pitch-based carbon fiber, carbon nanofiber, and carbon nanotube. Carbon nanotube can be formed by, for example, a vapor deposition method. Other examples of the conductive additive include carbon materials such as carbon black (e.g., acetylene black (AB)), graphite (black lead) particles, graphene, and fullerene. Alternatively, metal powder or metal fibers of copper, nickel, aluminum, silver, gold, or the like, a conductive ceramic material, or the like can be used.

Alternatively, a graphene compound may be used as the conductive additive.

A graphene compound has excellent electrical characteristics of high conductivity and excellent physical properties of high flexibility and high mechanical strength. Furthermore, a graphene compound has a planar shape. A graphene compound enables low-resistance surface contact. Furthermore, a graphene compound has extremely high conductivity even with a small thickness in some cases and thus allows a conductive path to be formed in an active material layer efficiently even with a small amount. For this reason, it is preferable to use a graphene compound as the conductive additive because the area where the active material and the conductive additive are in contact with each other can be increased. It is preferable to form the graphene compound serving as a conductive additive as a coating film to cover the entire surface of the active material with a spray dry apparatus, in which case the electrical resistance may be reduced. Here, it is particularly preferable to use, for example, graphene, multilayer graphene, or RGO as a graphene compound. Note that RGO refers to a compound obtained by reducing graphene oxide (GO), for example.

In the case where an active material with a small particle diameter (e.g., 1 μm or less) is used, the specific surface area of the active material is large and thus more conductive paths for the active material particles are needed. Thus, the amount of conductive additive tends to increase and the supported amount of active material tends to decrease relatively. When the supported amount of active material decreases, the capacity of the secondary battery also decreases. In such a case, a graphene compound that can efficiently form a conductive path even in a small amount is particularly preferably used as the conductive additive because the supported amount of active material does not decrease.

A cross-sectional structure example of an active material layer **200** containing a graphene compound as a conductive additive is described below.

FIG. **7**A shows a longitudinal cross-sectional view of the active material layer **200**. The active material layer **200** includes positive electrode active material particles **100**, a graphene compound **201** serving as a conductive additive, and a binder (not illustrated). Here, graphene or multilayer graphene may be used as the graphene compound **201**, for example. The graphene compound **201** preferably has a sheet-like shape. The graphene compound **201** may have a sheet-like shape formed of a plurality of sheets of multilayer graphene and/or a plurality of sheets of graphene that partly overlap with each other.

The longitudinal cross section of the active material layer **200** in FIG. **7**B shows substantially uniform dispersion of the sheet-like graphene compounds **201** in the active material layer **200**. The graphene compounds **201** are schematically shown by thick lines in FIG. **7**B but are actually thin films each having a thickness corresponding to the thickness of a single layer or a multi-layer of carbon molecules. The plurality of graphene compounds **201** are formed in such a way as to partly coat or adhere to the surfaces of the plurality of positive electrode active material particles **100**, so that the graphene compounds **201** make surface contact with the positive electrode active material particles **100**.

Here, the plurality of graphene compounds are bonded to each other to form a net-like graphene compound sheet (hereinafter referred to as a graphene compound net or a graphene net). The graphene net covering the active material can function as a binder for bonding active materials. The amount of a binder can thus be reduced, or the binder does not have to be used. This can increase the proportion of the active material in the electrode volume or weight. That is to say, the capacity of the secondary battery can be increased.

Here, it is preferable to perform reduction after a layer to be the active material layer **200** is formed in such a manner that graphene oxide is used as the graphene compound **201** and mixed with an active material. When graphene oxide with extremely high dispersibility in a polar solvent is used for the formation of the graphene compounds **201**, the graphene compounds **201** can be substantially uniformly dispersed in the active material layer **200**. The solvent is removed by volatilization from a dispersion medium in which graphene oxide is uniformly dispersed, and the graphene oxide is reduced; hence, the graphene compounds **201** remaining in the active material layer **200** partly overlap with each other and are dispersed such that surface contact is made, thereby forming a three-dimensional conduction path. Note that graphene oxide can be reduced either by heat treatment or with the use of a reducing agent, for example.

Unlike a conductive additive in the form of particles, such as acetylene black, which makes point contact with an active material, the graphene compound **201** is capable of making low-resistance surface contact; accordingly, the electrical conduction between the positive electrode active material particles **100** and the graphene compounds **201** can be improved with a smaller amount of the graphene compound **201** than that of a normal conductive additive. This increases

the proportion of the positive electrode active material particles **100** in the active material layer **200**, resulting in increased discharge capacity of the secondary battery.

Alternatively, the graphene compound may cover the entire surface of the active material in advance with a spray dry apparatus. After that, at the time of forming the positive electrode active material layer, a graphene compound can be further added to make the conductive path between the active materials more favorable.

As the binder, a rubber material such as styrene-butadiene rubber (SBR), styrene-isoprene-styrene rubber, acrylonitrile-butadiene rubber, butadiene rubber, or ethylene-propylene-diene copolymer can be used, for example. Alternatively, fluororubber can be used as the binder.

For the binder, for example, water-soluble polymers are preferably used. As the water-soluble polymers, a polysaccharide and the like can be used. As the polysaccharide, a cellulose derivative such as carboxymethyl cellulose (CMC), methyl cellulose, ethyl cellulose, hydroxypropyl cellulose, diacetyl cellulose, or regenerated cellulose, starch, or the like can be used. It is more preferred that such water-soluble polymers be used in combination with any of the above rubber materials.

Alternatively, as the binder, a material such as polystyrene, poly(methyl acrylate), poly(methyl methacrylate) (PMMA), sodium polyacrylate, polyvinyl alcohol (PVA), polyethylene oxide (PEO), polypropylene oxide, polyimide, polyvinyl chloride, polytetrafluoroethylene, polyethylene, polypropylene, polyisobutylene, polyethylene terephthalate, nylon, polyvinylidene fluoride (PVdF), polyacrylonitrile (PAN), ethylene-propylene-diene polymer, polyvinyl acetate, or nitrocellulose is preferably used.

A plurality of the above materials may be used in combination for the binder.

For example, a material having a significant viscosity modifying effect and another material may be used in combination. For example, a rubber material or the like has high adhesion or high elasticity but may have difficulty in viscosity modification when mixed in a solvent. In such a case, a rubber material or the like is preferably mixed with a material having a significant viscosity modifying effect, for example. As a material having a significant viscosity modifying effect, for example, a water-soluble polymer is preferably used. An example of a water-soluble polymer having an especially significant viscosity modifying effect is the above-mentioned polysaccharide; for example, a cellulose derivative such as carboxymethyl cellulose (CMC), methyl cellulose, ethyl cellulose, hydroxypropyl cellulose, diacetyl cellulose, or regenerated cellulose, or starch can be used.

Note that a cellulose derivative such as carboxymethyl cellulose obtains a higher solubility when converted into a salt such as a sodium salt or an ammonium salt of carboxymethyl cellulose, and accordingly, easily exerts an effect as a viscosity modifier. The high solubility can also increase the dispersibility of an active material and other components in the formation of slurry for an electrode. In this specification, cellulose and a cellulose derivative used as a binder of an electrode include salts thereof.

The water-soluble polymers stabilize viscosity by being dissolved in water and allow stable dispersion of the active material and another material combined as a binder such as styrene-butadiene rubber in an aqueous solution. Furthermore, a water-soluble polymer is expected to be easily and stably adsorbed to an active material surface because it has a functional group. Many cellulose derivatives such as carboxymethyl cellulose have functional groups such as a hydroxyl group and a carboxyl group. Because of functional groups, polymers are expected to interact with each other and cover an active material surface in a large area.

In the case where the binder covering or being in contact with the active material surface forms a film, the film is expected to serve as a passivation film to suppress the decomposition of the electrolyte solution. Here, the passivation film refers to a film without electric conductivity or a film with extremely low electric conductivity, and can inhibit the decomposition of an electrolyte solution at a potential at which a battery reaction occurs in the case where the passivation film is formed on the active material surface, for example. It is preferred that the passivation film can conduct lithium ions while suppressing electric conduction.

<Positive Electrode Current Collector>

The positive electrode current collector can be formed using a material that has high conductivity, such as a metal like stainless steel, gold, platinum, aluminum, or titanium, or an alloy thereof. It is preferred that a material used for the positive electrode current collector not dissolve at the potential of the positive electrode. Alternatively, the positive electrode current collector can be formed using an aluminum alloy to which an element that improves heat resistance, such as silicon, titanium, neodymium, scandium, or molybdenum, is added. Still alternatively, a metal element that forms silicide by reacting with silicon can be used. Examples of the metal element that forms silicide by reacting with silicon include zirconium, titanium, hafnium, vanadium, niobium, tantalum, chromium, molybdenum, tungsten, cobalt, and nickel. The current collector can have any of various shapes including a foil-like shape, a plate-like shape (sheet-like shape), a net-like shape, a punching-metal shape, and an expanded-metal shape. The current collector preferably has a thickness of 5 μm to 30 μm.

[Negative Electrode]

The negative electrode includes a negative electrode active material layer and a negative electrode current collector. The negative electrode active material layer may contain a conductive additive and a binder.

<Negative Electrode Active Material>

As a negative electrode active material, for example, an alloy-based material or a carbon-based material can be used.

For the negative electrode active material, an element which enables charge-discharge reactions by an alloying reaction and a dealloying reaction with lithium can be used. For example, a material containing at least one of silicon, tin, gallium, aluminum, germanium, lead, antimony, bismuth, silver, zinc, cadmium, indium, and the like can be used. Such elements have higher capacity than carbon. In particular, silicon has a significantly high theoretical capacity of 4200 mAh/g. For this reason, silicon is preferably used as the negative electrode active material. Alternatively, a compound containing any of the above elements may be used. Examples of the compound include SiO, Mg_2Si, Mg_2Ge, SnO, SnO_2, Mg_2Sn, SnS_2, V_2Sn_3, $FeSn_2$, $CoSn_2$, Ni_3Sn_2, Cu_6Sn_5, Ag_3Sn, Ag_3Sb, Ni_2MnSb, $CeSb_3$, $LaSn_3$, $La_3Co_2Sn_7$, $CoSb_3$, InSb, and SbSn. Here, an element that enables charge-discharge reactions by an alloying reaction and a dealloying reaction with lithium, a compound containing the element, and the like may be referred to as an alloy-based material.

In this specification and the like, SiO refers, for example, to silicon monoxide. SiO can alternatively be expressed as SiO_x. Here, x preferably has an approximate value of 1. For example, x is preferably 0.2 or more and 1.5 or less, more preferably 0.3 or more and 1.2 or less.

As the carbon-based material, graphite, graphitizing carbon (soft carbon), non-graphitizing carbon (hard carbon), a carbon nanotube, graphene, carbon black, and the like can be used.

Examples of graphite include artificial graphite and natural graphite. Examples of artificial graphite include mesocarbon microbeads (MCMB), coke-based artificial graphite, and pitch-based artificial graphite. As artificial graphite, spherical graphite having a spherical shape can be used. For example, MCMB is preferably used because it may have a spherical shape. Moreover, MCMB may preferably be used because it can relatively easily have a small surface area. Examples of natural graphite include flake graphite and spherical natural graphite.

Graphite has a low potential substantially equal to that of a lithium metal (higher than or equal to 0.05 V and lower than or equal to 0.3 V vs. Li/Li^+) when lithium ions are intercalated into the graphite (while a lithium-graphite intercalation compound is formed). For this reason, a lithium-ion secondary battery can have a high operating voltage. In addition, graphite is preferred because of its advantages such as a relatively high capacity per unit volume, relatively small volume expansion, low cost, and higher level of safety than that of a lithium metal.

Alternatively, for the negative electrode active material, an oxide such as titanium dioxide (TiO_2), lithium titanium oxide ($Li_4Ti_5O_{12}$), lithium-graphite intercalation compound (Li_xC_6), niobium pentoxide (Nb_2O_5), tungsten oxide (WO_2), or molybdenum oxide (MoO_2) can be used.

Still alternatively, for the negative electrode active material, $Li_{3-x}M_xN$ (M=Co, Ni, or Cu) with a Li_3N structure, which is a nitride containing lithium and a transition metal, can be used. For example, $Li_{2.6}Co_{0.4}N_3$ is preferable because of high charge and discharge capacity (900 mAh/g and 1890 mAh/cm^3).

A nitride containing lithium and a transition metal is preferably used, in which case lithium ions are contained in the negative electrode active material and thus the negative electrode active material can be used in combination with a material for a positive electrode active material which does not contain lithium ions, such as V_2O_5 or Cr_3O_8. In the case of using a material containing lithium ions as a positive electrode active material, the nitride containing lithium and a transition metal can be used for the negative electrode active material by extracting the lithium ions contained in the positive electrode active material in advance.

Alternatively, a material which causes a conversion reaction can be used for the negative electrode active material; for example, a transition metal oxide which does not form an alloy with lithium, such as cobalt oxide (CoO), nickel oxide (NiO), and iron oxide (FeO), may be used. Other examples of the material which causes a conversion reaction include oxides such as Fe_2O_3, CuO, Cu_2O, RuO_2, and Cr_2O_3, sulfides such as $CoS_{0.89}$, NiS, and CuS, nitrides such as Zn_3N_2, Cu_3N, and Ge_3N_4, phosphides such as NiP_2, FeP_2, and CoP_3, and fluorides such as FeF_3 and BiF_3.

For the conductive additive and the binder that can be included in the negative electrode active material layer, materials similar to those of the conductive additive and the binder that can be included in the positive electrode active material layer can be used.

<Negative Electrode Current Collector>

For the negative electrode current collector, a material similar to that of the positive electrode current collector can be used. Note that a material which is not alloyed with a carrier ion such as lithium is preferably used for the negative electrode current collector.

[Electrolyte Solution]

The electrolyte solution contains a solvent and an electrolyte. As a solvent of the electrolyte solution, an aprotic organic solvent is preferably used. For example, one of ethylene carbonate (EC), propylene carbonate (PC), butylene carbonate, chloroethylene carbonate, vinylene carbonate, γ-butyrolactone, γ-valerolactone, dimethyl carbonate (DMC), diethyl carbonate (DEC), ethyl methyl carbonate (EMC), methyl formate, methyl acetate, ethyl acetate, methyl propionate, ethyl propionate, propyl propionate, methyl butyrate, 1,3-dioxane, 1,4-dioxane, dimethoxyethane (DME), dimethyl sulfoxide, diethyl ether, methyl diglyme, acetonitrile, benzonitrile, tetrahydrofuran, sulfolane, and sultone can be used, or two or more of these solvents can be used in an appropriate combination in an appropriate ratio.

Alternatively, when one or more kinds of ionic liquids (room temperature molten salts) which have features of non-flammability and non-volatility is used as a solvent of the electrolyte solution, a secondary battery can be prevented from exploding or catching fire even when the secondary battery internally shorts out or the internal temperature increases owing to overcharging or the like. An ionic liquid contains a cation and an anion. The ionic liquid contains an organic cation and an anion. Examples of the organic cation used for the electrolyte solution include aliphatic onium cations such as a quaternary ammonium cation, a tertiary sulfonium cation, and a quaternary phosphonium cation, and aromatic cations such as an imidazolium cation and a pyridinium cation. Examples of the anion used for the electrolyte solution include a monovalent amide-based anion, a monovalent methide-based anion, a fluorosulfonate anion, a perfluoroalkylsulfonate anion, a tetrafluoroborate anion, a perfluoroalkylborate anion, a hexafluorophosphate anion, and a perfluoroalkylphosphate anion.

As an electrolyte dissolved in the above-described solvent, one of lithium salts such as $LiPF_6$, $LiClO_4$, $LiAsF_6$, $LiBF_4$, $LiAlCl_4$, LiSCN, LiBr, LiI, Li_2SO_4, $Li_2B_{10}Cl_{10}$, $Li_2B_{12}Cl_{12}$, $LiCF_3SO_3$, $LiC_4F_9SO_3$, $LiC(CF_3SO_2)_3$, $LiC(C_2F_5SO_2)_3$, $LiN(CF_3SO_2)_2$, $LiN(C_4F_9SO_2)(CF_3SO_2)$, and $LiN(C_2F_5SO_2)_2$ can be used, or two or more of these lithium salts can be used in an appropriate combination in an appropriate ratio.

The electrolyte solution used for a secondary battery is preferably highly purified and contains a small amount of dust particles and elements other than the constituent elements of the electrolyte solution (hereinafter also simply referred to as impurities). Specifically, the weight ratio of impurities to the electrolyte solution is less than or equal to 1%, preferably less than or equal to 0.1%, and further preferably less than or equal to 0.01%.

Furthermore, an additive agent such as vinylene carbonate, propane sultone (PS), tert-butylbenzene (TBB), fluoroethylene carbonate (FEC), LiBOB, or a dinitrile compound such as succinonitrile or adiponitrile may be added to the electrolyte solution. The concentration of a material to be added with respect to the whole solvent is, for example, higher than or equal to 0.1 wt % and lower than or equal to 5 wt %.

Alternatively, a gelled electrolyte obtained in such a manner that a polymer is swelled with an electrolyte solution may be used.

When a polymer gel electrolyte is used, safety against liquid leakage and the like is improved. Furthermore, a secondary battery can be thinner and more lightweight.

As a polymer that undergoes gelation, a silicone gel, an acrylic gel, an acrylonitrile gel, a polyethylene oxide-based

gel, a polypropylene oxide-based gel, a fluorine-based polymer gel, or the like can be used.

Examples of the polymer include a polymer having a polyalkylene oxide structure, such as polyethylene oxide (PEO); PVDF; polyacrylonitrile; and a copolymer containing any of them. For example, PVDF-HFP, which is a copolymer of PVDF and hexafluoropropylene (HFP) can be used. The formed polymer may be porous.

Instead of the electrolyte solution, a solid electrolyte including an inorganic material such as a sulfide-based inorganic material or an oxide-based inorganic material, or a solid electrolyte including a high-molecular material such as a polyethylene oxide (PEO)-based high-molecular material may alternatively be used. When the solid electrolyte is used, a separator and a spacer are not necessary. Furthermore, since the battery can be entirely solidified, there is no possibility of liquid leakage to increase the safety of the battery dramatically.

[Separator]

The secondary battery preferably includes a separator. As the separator, for example, paper; nonwoven fabric; glass fiber; ceramics; or synthetic fiber using nylon (polyamide), vinylon (polyvinyl alcohol-based fiber), polyester, acrylic, polyolefin, or polyurethane can be used. The separator is preferably formed to have an envelope-like shape to wrap one of the positive electrode and the negative electrode.

The separator may have a multilayer structure. For example, an organic material film such as polypropylene or polyethylene can be coated with a ceramic-based material, a fluorine-based material, a polyamide-based material, a mixture thereof, or the like. Examples of the ceramic-based material include aluminum oxide particles and silicon oxide particles. Examples of the fluorine-based material include PVDF and a polytetrafluoroethylene. Examples of the polyamide-based material include nylon and aramid (meta-based aramid and para-based aramid).

Deterioration of the separator in charging and discharging at high voltage can be suppressed and thus the reliability of the secondary battery can be improved because oxidation resistance is improved when the separator is coated with the ceramic-based material. In addition, when the separator is coated with the fluorine-based material, the separator is easily brought into close contact with an electrode, resulting in high output characteristics. When the separator is coated with the polyamide-based material, in particular, aramid, the safety of the secondary battery is improved because heat resistance is improved.

For example, both surfaces of a polypropylene film may be coated with a mixed material of aluminum oxide and aramid. Alternatively, a surface of the polypropylene film in contact with the positive electrode may be coated with the mixed material of aluminum oxide and aramid, and a surface of the polypropylene film in contact with the negative electrode may be coated with the fluorine-based material.

With the use of a separator having a multilayer structure, the capacity of the secondary battery per volume can be increased because the safety of the secondary battery can be maintained even when the total thickness of the separator is small.

[Exterior Body]

For an exterior body included in the secondary battery, a metal material such as aluminum and a resin material can be used, for example. An exterior body in the form of a film can also be used. As the film, for example, a film having a three-layer structure in which a highly flexible metal thin film of aluminum, stainless steel, copper, nickel, or the like is provided over a film formed of a material such as polyethylene, polypropylene, polycarbonate, ionomer, or polyamide, and an insulating synthetic resin film of a polyamide-based resin, a polyester-based resin, or the like is provided as the outer surface of the exterior body over the metal thin film can be used.

[Charging and Discharging Methods]

The secondary battery can be charged and discharged in the following manner, for example.

«CC Charge»

First, CC charge, which is one of charging methods, is described. CC charge is a charging method in which a constant current is made to flow to a secondary battery in the whole charging period and charge is terminated when the voltage reaches a predetermined voltage. The secondary battery is assumed to be an equivalent circuit with internal resistance R and secondary battery capacitance C as illustrated in FIG. **8**A. In that case, a secondary battery voltage V_B is the sum of a voltage V_R applied to the internal resistance R and a voltage V_C applied to the secondary battery capacitance C.

While the CC charge is performed, a switch is on as illustrated in FIG. **8**A, so that a constant current I flows to the secondary battery. During the period, the current I is constant; thus, according to the Ohm's law (V_R=R×I), the voltage V_R applied to the internal resistance R is also constant. In contrast, the voltage V_C applied to the secondary battery capacitance C increases over time. Accordingly, the secondary battery voltage V_B increases over time.

When the secondary battery voltage V_B reaches a predetermined voltage, e.g., 4.3 V, the charge is terminated. On termination of the CC charge, the switch is turned off as illustrated in FIG. **8**B, and the current I becomes 0. Thus, the voltage V_R applied to the internal resistance R becomes 0 V. Consequently, the secondary battery voltage V_B is decreased by the lost voltage drop in the internal resistance R.

FIG. **8**C shows an example of the secondary battery voltage V_B and charging current during a period in which the CC charge is performed and after the CC charge is terminated. The secondary battery voltage V_B increases while the CC charge is performed, and slightly decreases after the CC charge is terminated.

«CCCV Charge»

Next, CCCV charge, which is a charging method different from the above-described method, is described. CCCV charge is a charging method in which CC charge is performed until the voltage reaches a predetermined voltage and then constant voltage (CV) charge is performed until the amount of current flow becomes small, specifically, a termination current value.

While the CC charge is performed, a switch of a constant current power source is on and a switch of a constant voltage power source is off as illustrated in FIG. **9**A, so that the constant current I flows to the secondary battery. During the period, the current I is constant; thus, according to the Ohm's law (V_R=R×I), the voltage V_R applied to the internal resistance R is also constant. In contrast, the voltage V_C applied to the secondary battery capacitance C increases over time. Accordingly, the secondary battery voltage V_B increases over time.

When the secondary battery voltage V_B reaches a predetermined voltage, e.g., 4.3 V, switching is performed from the CC charge to the CV charge. While the CV charge is performed, the switch of the constant voltage power source is on and the switch of the constant current power source is off as illustrated in FIG. **9**B; thus, the secondary battery voltage V_B is constant. In contrast, the voltage V_C applied to the secondary battery capacitance C increases over time.

Since $V_B=V_R+V_C$ is satisfied, the voltage V_R applied to the internal resistance R decreases over time. As the voltage V_R applied to the internal resistance R decreases, the current I flowing to the secondary battery also decreases according to the Ohm's law ($V_R=R\times I$).

When the current I flowing to the secondary battery becomes a predetermined current, e.g., approximately 0.01 C, charge is terminated. On termination of the CCCV charge, all the switches are turned off as illustrated in FIG. **9**C, so that the current I becomes 0. Thus, the voltage V_R applied to the internal resistance R becomes 0 V. However, the voltage V_R applied to the internal resistance R becomes sufficiently small by the CV charge; thus, even when a voltage drop no longer occurs in the internal resistance R, the secondary battery voltage V_B hardly decreases.

FIG. **9**D shows an example of the secondary battery voltage V_B and charging current while the CCCV charge is performed and after the CCCV charge is terminated. Even after the CCCV charge is terminated, the secondary battery voltage V_B hardly decreases.

«CC Discharge»

Next, CC discharge, which is one of discharging methods, is described. CC discharge is a discharging method in which a constant current is made to flow from the secondary battery in the whole discharging period, and discharge is terminated when the secondary battery voltage V_B reaches a predetermined voltage, e.g., 2.5 V.

FIG. **10** shows an example of the secondary battery voltage V_B and discharging current while the CC discharge is performed. As discharge proceeds, the secondary battery voltage V_B decreases.

Next, a discharge rate and a charge rate will be described. The discharge rate refers to the relative ratio of discharging current to battery capacity and is expressed in a unit C. A current of approximately 1 C in a battery with a rated capacity X (Ah) is XA. The case where discharge is performed at a current of 2X A is rephrased as follows: discharge is performed at 2 C. The case where discharge is performed at a current of X/5 A is rephrased as follows: discharge is performed at 0.2 C. Similarly, the case where charging is performed at a current of 2X A is rephrased as follows: charging is performed at 2 C, and the case where charging is performed at a current of X/5 A is rephrased as follows: charging is performed at 0.2 C.

Embodiment 3

In this embodiment, examples of a shape of a secondary battery containing the positive electrode active material **100** described in the above embodiment are described. For the materials used for the secondary battery described in this embodiment, the description of the above embodiment can be referred to.

[Coin-Type Secondary Battery]

First, an example of a coin-type secondary battery is described. FIG. **11**A is an external view of a coin-type (single-layer flat type) secondary battery, and FIG. **11**B is a cross-sectional view thereof.

In a coin-type secondary battery **300**, a positive electrode can **301** doubling as a positive electrode terminal and a negative electrode can **302** doubling as a negative electrode terminal are insulated from each other and sealed by a gasket **303** made of polypropylene or the like. A positive electrode **304** includes a positive electrode current collector **305** and a positive electrode active material layer **306** provided in contact with the positive electrode current collector **305**. A negative electrode **307** includes a negative electrode current collector **308** and a negative electrode active material layer **309** provided in contact with the negative electrode current collector **308**.

Note that only one surface of each of the positive electrode **304** and the negative electrode **307** used for the coin-type secondary battery **300** is provided with an active material layer.

For the positive electrode can **301** and the negative electrode can **302**, a metal having a corrosion-resistant property to an electrolyte solution, such as nickel, aluminum, or titanium, an alloy of such a metal, or an alloy of such a metal and another metal (e.g., stainless steel) can be used. Alternatively, the positive electrode can **301** and the negative electrode can **302** are preferably covered with nickel, aluminum, or the like in order to prevent corrosion due to the electrolyte solution. The positive electrode can **301** and the negative electrode can **302** are electrically connected to the positive electrode **304** and the negative electrode **307**, respectively.

The negative electrode **307**, the positive electrode **304**, and the separator **310** are immersed in the electrolyte solution. Then, as illustrated in FIG. **11**B, the positive electrode **304**, the separator **310**, the negative electrode **307**, and the negative electrode can **302** are stacked in this order with the positive electrode can **301** positioned at the bottom, and the positive electrode can **301** and the negative electrode can **302** are subjected to pressure bonding with the gasket **303** located therebetween. In such a manner, the coin-type secondary battery **300** can be manufactured.

When the positive electrode active material described in the above embodiment is used in the positive electrode **304**, the coin-type secondary battery **300** with high capacity and excellent cycle characteristics can be obtained.

Here, a current flow in charging a secondary battery is described with reference to FIG. **11**C. When a secondary battery using lithium is regarded as a closed circuit, lithium ions transfer and a current flows in the same direction. Note that in the secondary battery using lithium, an anode and a cathode change places in charge and discharge, and an oxidation reaction and a reduction reaction occur on the corresponding sides; hence, an electrode with a high reaction potential is called a positive electrode and an electrode with a low reaction potential is called a negative electrode. For this reason, in this specification, the positive electrode is referred to as a "positive electrode" or a "plus electrode" and the negative electrode is referred to as a "negative electrode" or a "minus electrode" in all the cases where charge is performed, discharge is performed, a reverse pulse current is supplied, and a charging current is supplied. The use of the terms "anode" and "cathode" related to an oxidation reaction and a reduction reaction might cause confusion because the anode and the cathode change places at the time of charging and discharging. Thus, the terms "anode" and "cathode" are not used in this specification. If the term "anode" or "cathode" is used, it should be mentioned that the anode or the cathode is which of the one at the time of charging or the one at the time of discharging and corresponds to which of a positive (plus) electrode or a negative (minus) electrode.

Two terminals in FIG. **11**C are connected to a charger, and the coin-type secondary battery **300** is charged. As the charge of the coin-type secondary battery **300** proceeds, a potential difference between electrodes increases.

[Cylindrical Secondary Battery]

Next, an example of a cylindrical secondary battery will be described with reference to FIGS. **12**A to **12**D. A cylindrical secondary battery **600** includes, as illustrated in FIG. **12**A, a positive electrode cap (battery lid) **601** on the top

surface and a battery can (outer can) **602** on the side and bottom surfaces. The positive electrode cap and the battery can (outer can) **602** are insulated from each other by a gasket (insulating packing) **610**.

FIG. **12**B is a schematic cross-sectional view of the cylindrical secondary battery. Inside the battery can **602** having a hollow cylindrical shape, a battery element in which a strip-like positive electrode **604** and a strip-like negative electrode **606** are wound with a strip-like separator **605** located therebetween is provided. Although not illustrated, the battery element is wound around a center pin. One end of the battery can **602** is close and the other end thereof is open. For the battery can **602**, a metal having a corrosion-resistant property to an electrolyte solution, such as nickel, aluminum, or titanium, an alloy of such a metal, or an alloy of such a metal and another metal (e.g., stainless steel) can be used. Alternatively, the battery can **602** is preferably covered with nickel, aluminum, or the like in order to prevent corrosion due to the electrolyte solution. Inside the battery can **602**, the battery element in which the positive electrode, the negative electrode, and the separator are wound is provided between a pair of insulating plates **608** and **609** that face each other. Furthermore, a nonaqueous electrolyte solution (not illustrated) is injected inside the battery can **602** provided with the battery element. As the nonaqueous electrolyte solution, a nonaqueous electrolyte solution that is similar to that of the coin-type secondary battery can be used.

Since the positive electrode and the negative electrode of the cylindrical secondary battery are wound, active materials are preferably formed on both sides of the current collectors. A positive electrode terminal (positive electrode current collecting lead) **603** is connected to the positive electrode **604**, and a negative electrode terminal (negative electrode current collecting lead) **607** is connected to the negative electrode **606**. Both the positive electrode terminal **603** and the negative electrode terminal **607** can be formed using a metal material such as aluminum. The positive electrode terminal **603** and the negative electrode terminal **607** are resistance-welded to a safety valve mechanism **612** and the bottom of the battery can **602**, respectively. The safety valve mechanism **612** is electrically connected to the positive electrode cap **601** through a positive temperature coefficient (PTC) element **611**. The safety valve mechanism **612** cuts off electrical connection between the positive electrode cap **601** and the positive electrode **604** when the internal pressure of the battery exceeds a predetermined threshold value. The PTC element **611**, which serves as a thermally sensitive resistor whose resistance increases as temperature rises, limits the amount of current by increasing the resistance, in order to prevent abnormal heat generation. Barium titanate ($BaTiO_3$)-based semiconductor ceramic can be used for the PTC element.

Alternatively, as illustrated in FIG. **12**C, a plurality of cylindrical secondary batteries **600** may be sandwiched between a conductive plate **613** and a conductive plate **614** to form a module **615**. The plurality of cylindrical secondary batteries **600** may be connected in parallel, connected in series, or connected in series after being connected in parallel. With the module **615** including the plurality of cylindrical secondary batteries **600**, large electric power can be extracted.

FIG. **12**D is a top view of the module **615**. The conductive plate **613** is shown by a dotted line for clarity of the drawing. As illustrated in FIG. **12**D, the module **615** may include a wiring **616** which electrically connects the plurality of cylindrical secondary batteries **600** to each other. It is possible to provide the conductive plate **613** over the wiring **616** to overlap with each other. In addition, a temperature control device **617** may be provided between the plurality of cylindrical secondary batteries **600**. When the cylindrical secondary batteries **600** are overheated, the temperature control device **617** can cool them, and when the cylindrical secondary batteries **600** are cooled too much, the temperature control device **617** can heat them. Thus, the performance of the module **615** is not easily influenced by the outside air temperature.

When the positive electrode active material described in the above embodiment is used in the positive electrode **604**, the cylindrical secondary battery **600** with high capacity and excellent cycle characteristics can be obtained.

[Structural Examples of Secondary Battery]

Other structural examples of secondary batteries will be described with reference to FIGS. **13**A and **13**B, FIGS. **14**A-**1**, **14**A-**2**, **14**B-**1**, and **14**B-**2**, FIGS. **15**A and **15**B, and FIG. **16**.

FIGS. **13**A and **13**B are external views of a secondary battery. The secondary battery includes a circuit board **900** and a secondary battery **913**. A label **910** is attached to the secondary battery **913**. As shown in FIG. **13**B, the secondary battery further includes a terminal **951**, a terminal **952**, an antenna **914**, and an antenna **915**.

The circuit board **900** includes terminals **911** and a circuit **912**. The terminals **911** are connected to the terminals **951** and **952**, the antennas **914** and **915**, and the circuit **912**. Note that a plurality of terminals **911** serving as a control signal input terminal, a power supply terminal, and the like may be provided.

The circuit **912** may be provided on the rear surface of the circuit board **900**. The shape of each of the antennas **914** and **915** is not limited to a coil shape and may be a linear shape or a plate shape. Furthermore, a planar antenna, an aperture antenna, a traveling-wave antenna, an EH antenna, a magnetic-field antenna, a dielectric antenna, or the like may be used. Alternatively, the antenna **914** or the antenna **915** may be a flat-plate conductor. The flat-plate conductor can serve as one of conductors for electric field coupling. That is, the antenna **914** or the antenna **915** can serve as one of two conductors of a capacitor. Thus, electric power can be transmitted and received not only by an electromagnetic field or a magnetic field but also by an electric field.

The line width of the antenna **914** is preferably larger than that of the antenna **915**. This makes it possible to increase the amount of electric power received by the antenna **914**.

The secondary battery includes a layer **916** between the secondary battery **913** and the antennas **914** and **915**. The layer **916** has a function of blocking an electromagnetic field from the secondary battery **913**, for example. As the layer **916**, for example, a magnetic body can be used.

Note that the structure of the secondary battery is not limited to that shown in FIGS. **13**A and **13**B.

For example, as shown in FIGS. **14**A-**1** and **14**A-**2**, two opposite surfaces of the secondary battery **913** in FIGS. **13**A and **13**B may be provided with respective antennas. FIG. **14**A-**1** is an external view showing one side of the opposite surfaces, and FIG. **14**A-**2** is an external view showing the other side of the opposite surfaces. For portions similar to those in FIGS. **13**A and **13**B, a description of the secondary battery illustrated in FIGS. **13**A and **13**B can be referred to as appropriate.

As illustrated in FIG. **14**A-**1**, the antenna **914** is provided on one of the opposite surfaces of the secondary battery **913** with the layer **916** located therebetween, and as illustrated in FIG. **14**A-**2**, an antenna **918** is provided on the other of the

opposite surfaces of the secondary battery **913** with a layer **917** located therebetween. The layer **917** has a function of blocking an electromagnetic field from the secondary battery **913**, for example. As the layer **917**, for example, a magnetic body can be used.

With the above structure, both of the antennas **914** and **918** can be increased in size. The antenna **918** has a function of communicating data with an external device, for example. An antenna with a shape that can be applied to the antenna **914**, for example, can be used as the antenna **918**. As a system for communication using the antenna **918** between the secondary battery and another device, a response method that can be used between the secondary battery and another device, such as NFC, can be employed.

Alternatively, as illustrated in FIG. **14**B-**1**, the secondary battery **913** in FIGS. **13**A and **13**B may be provided with a display device **920**. The display device **920** is electrically connected to the terminal **911**. It is possible that the label **910** is not provided in a portion where the display device **920** is provided. For portions similar to those in FIGS. **13**A and **13**B, a description of the secondary battery illustrated in FIGS. **13**A and **13**B can be referred to as appropriate.

The display device **920** can display, for example, an image showing whether charge is being carried out, an image showing the amount of stored power, or the like. As the display device **920**, electronic paper, a liquid crystal display device, an electroluminescent (EL) display device, or the like can be used. For example, the use of electronic paper can reduce power consumption of the display device **920**.

Alternatively, as illustrated in FIG. **14**B-**2**, the secondary battery **913** illustrated in FIGS. **13**A and **13**B may be provided with a sensor **921**. The sensor **921** is electrically connected to the terminal **911** via a terminal **922**. For portions similar to those in FIGS. **13**A and **13**B, a description of the secondary battery illustrated in FIGS. **13**A and **13**B can be referred to as appropriate.

The sensor **921** has a function of measuring, for example, displacement, position, speed, acceleration, angular velocity, rotational frequency, distance, light, liquid, magnetism, temperature, chemical substance, sound, time, hardness, electric field, electric current, voltage, electric power, radiation, flow rate, humidity, gradient, oscillation, odor, or infrared rays. With the sensor **921**, for example, data on an environment (e.g., temperature) where the secondary battery is placed can be determined and stored in a memory inside the circuit **912**.

Furthermore, structural examples of the secondary battery **913** will be described with reference to FIGS. **15**A and **15**B and FIG. **16**.

The secondary battery **913** illustrated in FIG. **15**A includes a wound body **950** provided with the terminals **951** and **952** inside a housing **930**. The wound body **950** is soaked in an electrolyte solution inside the housing **930**. The terminal **952** is in contact with the housing **930**. An insulator or the like inhibits contact between the terminal **951** and the housing **930**. Note that in FIG. **15**A, the housing **930** divided into two pieces is illustrated for convenience; however, in the actual structure, the wound body **950** is covered with the housing **930** and the terminals **951** and **952** extend to the outside of the housing **930**. For the housing **930**, a metal material (such as aluminum) or a resin material can be used.

Note that as illustrated in FIG. **15**B, the housing **930** in FIG. **15**A may be formed using a plurality of materials. For example, in the secondary battery **913** in FIG. **15**B, a housing **930***a* and a housing **930***b* are bonded to each other, and the wound body **950** is provided in a region surrounded by the housing **930***a* and the housing **930***b*.

For the housing **930***a*, an insulating material such as an organic resin can be used. In particular, when a material such as an organic resin is used for the side on which an antenna is formed, blocking of an electric field from the secondary battery **913** can be inhibited. When an electric field is not significantly blocked by the housing **930***a*, an antenna such as the antennas **914** and **915** may be provided inside the housing **930***a*. For the housing **930***b*, a metal material can be used, for example.

FIG. **16** illustrates the structure of the wound body **950**. The wound body **950** includes a negative electrode **931**, a positive electrode **932**, and separators **933**. The wound body **950** is obtained by winding a sheet of a stack in which the negative electrode **931** overlaps with the positive electrode **932** with the separator **933** provided therebetween. Note that a plurality of stacks each including the negative electrode **931**, the positive electrode **932**, and the separator **933** may be stacked.

The negative electrode **931** is connected to the terminal **911** in FIGS. **13**A and **13**B via one of the terminals **951** and **952**. The positive electrode **932** is connected to the terminal **911** in FIGS. **13**A and **13**B via the other of the terminals **951** and **952**.

When the positive electrode active material described in the above embodiment is used in the positive electrode **932**, the secondary battery **913** with high capacity and excellent cycle characteristics can be obtained.

[Laminated Secondary Battery]

Next, an example of a laminated secondary battery will be described with reference to FIGS. **17**A to **17**C, FIGS. **18**A and **18**B, FIG. **19**, FIG. **20**, FIGS. **21**A to **21**C, FIGS. **22**A, **22**B**1**, **22**B**2**, **22**C, and **22**D, and FIGS. **23**A and **23**B. When the laminated secondary battery has flexibility and is used in an electronic device at least part of which is flexible, the secondary battery can be bent as the electronic device is bent.

A laminated secondary battery **980** is described with reference to FIGS. **17**A to **17**C. The laminated secondary battery **980** includes a wound body **993** illustrated in FIG. **17**A. The wound body **993** includes a negative electrode **994**, a positive electrode **995**, and a separator **996**. The wound body **993** is, like the wound body **950** illustrated in FIG. **16**, obtained by winding a sheet of a stack in which the negative electrode **994** overlaps with the positive electrode **995** with the separator **996** therebetween.

Note that the number of stacks each including the negative electrode **994**, the positive electrode **995**, and the separator **996** may be determined as appropriate depending on capacity and an element volume which are required. The negative electrode **994** is connected to a negative electrode current collector (not illustrated) via one of a lead electrode **997** and a lead electrode **998**. The positive electrode **995** is connected to a positive electrode current collector (not illustrated) via the other of the lead electrode **997** and the lead electrode **998**.

As illustrated in FIG. **17**B, the wound body **993** is packed in a space formed by bonding a film **981** and a film **982** having a depressed portion that serve as exterior bodies by thermocompression bonding or the like, whereby the laminated secondary battery **980** can be formed as illustrated in FIG. **17**C. The wound body **993** includes the lead electrode **997** and the lead electrode **998**, and is soaked in an electrolyte solution inside a space surrounded by the film **981** and the film **982** having a depressed portion.

For the film **981** and the film **982** having a depressed portion, a metal material such as aluminum or a resin material can be used, for example With the use of a resin

material for the film **981** and the film **982** having a depressed portion, the film **981** and the film **982** having a depressed portion can be changed in their forms when external force is applied; thus, a flexible secondary battery can be fabricated.

Although FIGS. **17**B and **17**C illustrate an example where a space is formed by two films, the wound body **993** may be placed in a space formed by bending one film.

When the positive electrode active material described in the above embodiment is used in the positive electrode **995**, the laminated secondary battery **980** with high capacity and excellent cycle characteristics can be obtained.

In FIGS. **17**A to **17**C, an example in which the laminated secondary battery **980** includes a wound body in a space formed by films serving as exterior bodies is described; however, as illustrated in FIGS. **18**A and **18**B, a secondary battery may include a plurality of strip-shaped positive electrodes, a plurality of strip-shaped separators, and a plurality of strip-shaped negative electrodes in a space formed by films serving as exterior bodies, for example.

A laminated secondary battery **500** illustrated in FIG. **18**A includes a positive electrode **503** including a positive electrode current collector **501** and a positive electrode active material layer **502**, a negative electrode **506** including a negative electrode current collector **504** and a negative electrode active material layer **505**, a separator **507**, an electrolyte solution **508**, and an exterior body **509**. The separator **507** is provided between the positive electrode **503** and the negative electrode **506** in the exterior body **509**. The exterior body **509** is filled with the electrolyte solution **508**. The electrolyte solution described in Embodiment 2 can be used for the electrolyte solution **508**.

In the laminated secondary battery **500** illustrated in FIG. **18**A, the positive electrode current collector **501** and the negative electrode current collector **504** also serve as terminals for an electrical contact with an external portion. For this reason, the positive electrode current collector **501** and the negative electrode current collector **504** may be arranged so as to be partly exposed to the outside of the exterior body **509**. Alternatively, a lead electrode and the positive electrode current collector **501** or the negative electrode current collector **504** may be bonded to each other by ultrasonic welding, and instead of the positive electrode current collector **501** and the negative electrode current collector **504**, the lead electrode may be exposed to the outside of the exterior body **509**.

As the exterior body **509** of the laminated secondary battery **500**, for example, a laminate film having a three-layer structure can be employed in which a highly flexible metal thin film of aluminum, stainless steel, copper, nickel, or the like is provided over a film formed of a material such as polyethylene, polypropylene, polycarbonate, ionomer, or polyamide, and an insulating synthetic resin film of a polyamide-based resin, a polyester-based resin, or the like is provided over the metal thin film as the outer surface of the exterior body.

FIG. **18**B illustrates an example of a cross-sectional structure of the laminated secondary battery **500**. Although FIG. **18**A illustrates an example including only two current collectors for simplicity, an actual battery includes a plurality of electrode layers.

The example in FIG. **18**B includes 16 electrode layers. The laminated secondary battery **500** has flexibility even though including 16 electrode layers. FIG. **18**B illustrates a structure including 8 layers of negative electrode current collectors **504** and 8 layers of positive electrode current collectors **501**, i.e., 16 layers in total. Note that FIG. **18**B illustrates a cross section of the lead portion of the negative electrode, and the 8 negative electrode current collectors **504** are bonded to each other by ultrasonic welding. It is needless to say that the number of electrode layers is not limited to 16, and may be more than 16 or less than 16. With a large number of electrode layers, the secondary battery can have high capacity. In contrast, with a small number of electrode layers, the secondary battery can have small thickness and high flexibility.

FIGS. **19** and **20** each illustrate an example of the external view of the laminated secondary battery **500**. In FIGS. **19** and **20**, the positive electrode **503**, the negative electrode **506**, the separator **507**, the exterior body **509**, a positive electrode lead electrode **510**, and a negative electrode lead electrode **511** are included.

FIG. **21**A illustrates external views of the positive electrode **503** and the negative electrode **506**. The positive electrode **503** includes the positive electrode current collector **501**, and the positive electrode active material layer **502** is formed on a surface of the positive electrode current collector **501**. The positive electrode **503** also includes a region where the positive electrode current collector **501** is partly exposed (hereinafter referred to as a tab region). The negative electrode **506** includes the negative electrode current collector **504**, and the negative electrode active material layer **505** is formed on a surface of the negative electrode current collector **504**. The negative electrode **506** also includes a region where the negative electrode current collector **504** is partly exposed, that is, a tab region. The areas and the shapes of the tab regions included in the positive electrode and the negative electrode are not limited to those illustrated in FIG. **21**A.

[Method for Manufacturing Laminated Secondary Battery]

Here, an example of a method for manufacturing the laminated secondary battery whose external view is illustrated in FIG. **19** will be described with reference to FIGS. **21**B and **21**C.

First, the negative electrode **506**, the separator **507**, and the positive electrode **503** are stacked. FIG. **21**B illustrates a stack including the negative electrode **506**, the separator **507**, and the positive electrode **503**. The secondary battery described here as an example includes 5 negative electrodes and 4 positive electrodes. Next, the tab regions of the positive electrodes **503** are bonded to each other, and the tab region of the positive electrode on the outermost surface and the positive electrode lead electrode **510** are bonded to each other. The bonding can be performed by ultrasonic welding, for example. In a similar manner, the tab regions of the negative electrodes **506** are bonded to each other, and the negative electrode lead electrode **511** is bonded to the tab region of the negative electrode on the outermost surface.

After that, the negative electrode **506**, the separator **507**, and the positive electrode **503** are placed over the exterior body **509**.

Subsequently, the exterior body **509** is folded along a dashed line as illustrated in FIG. **21**C. Then, the outer edge of the exterior body **509** is bonded. The bonding can be performed by thermocompression bonding, for example. At this time, a part (or one side) of the exterior body **509** is left unbonded (to provide an inlet) so that the electrolyte solution **508** can be introduced later.

Next, the electrolyte solution **508** is introduced into the exterior body **509** from the inlet of the exterior body **509**. The electrolyte solution **508** is preferably introduced in a reduced pressure atmosphere or in an inert gas atmosphere. Lastly, the inlet is bonded. In the above manner, the laminated secondary battery **500** can be manufactured.

When the positive electrode active material described in the above embodiment is used in the positive electrode **503**, the laminated secondary battery **500** with high capacity and excellent cycle characteristics can be obtained.

[Bendable Secondary Battery]

Next, an example of a bendable secondary battery is described with reference to FIGS. **22**A, **22**B**1**, **22**B**2**, **22**C and **22**D and FIGS. **23**A and **23**B.

FIG. **22**A is a schematic top view of a bendable secondary battery **50**. FIGS. **22**B**1**, **22**B**2**, and **22**C are schematic cross-sectional views taken along cutting line C**1**-C**2**, cutting line C**3**-C**4**, and cutting line A**1**-A**2**, respectively, in FIG. **22**A. The battery **50** includes an exterior body **51** and a positive electrode **11***a*, and a negative electrode **11***b* held in the exterior body **51**. A lead **12***a* electrically connected to the positive electrode **11***a* and a lead **12***b* electrically connected to the negative electrode **11***b* are extended to the outside of the exterior body **51**. In addition to the positive electrode **11***a* and the negative electrode **11***b*, an electrolyte solution (not illustrated) is enclosed in a region surrounded by the exterior body **51**.

FIGS. **23**A and **23**B illustrate the positive electrode **11***a* and the negative electrode **11***b* included in the battery **50**. FIG. **23**A is a perspective view illustrating the stacking order of the positive electrode **11***a*, the negative electrode **11***b*, and the separator **14**. FIG. **23**B is a perspective view illustrating the lead **12***a* and the lead **12***b* in addition to the positive electrode **11***a* and the negative electrode **11***b*.

As illustrated in FIG. **23**A, the battery **50** includes a plurality of strip-shaped positive electrodes **11***a*, a plurality of strip-shaped negative electrodes **11***b*, and a plurality of separators **14**. The positive electrode **11***a* and the negative electrode **11***b* each include a projected tab portion and a portion other than the tab. A positive electrode active material layer is formed on one surface of the positive electrode **11***a* other than the tab portion, and a negative electrode active material layer is formed on one surface of the negative electrode **11***b* other than the tab portion.

The positive electrodes **11***a* and the negative electrodes **11***b* are stacked so that surfaces of the positive electrodes **11***a* on each of which the positive electrode active material layer is not formed are in contact with each other and that surfaces of the negative electrodes **11***b* on each of which the negative electrode active material layer is not formed are in contact with each other.

Furthermore, the separator **14** is provided between the surface of the positive electrode **11***a* on which the positive electrode active material is formed and the surface of the negative electrode **11***b* on which the negative electrode active material is formed. In FIG. **23**A, the separator **14** is shown by a dotted line for easy viewing.

In addition, as illustrated in FIG. **23**B, the plurality of positive electrodes **11***a* are electrically connected to the lead **12***a* in a bonding portion **15***a*. The plurality of negative electrodes **11***b* are electrically connected to the lead **12***b* in a bonding portion **15***b*.

Next, the exterior body **51** is described with reference to FIGS. **22**B**1**, **22**B**2**, **22**C, and **22**D.

The exterior body **51** has a film-like shape and is folded in half with the positive electrodes **11***a* and the negative electrodes **11***b* between facing portions of the exterior body **51**. The exterior body **51** includes a folded portion **61**, a pair of seal portions **62**, and a seal portion **63**. The pair of seal portions **62** is provided with the positive electrodes **11***a* and the negative electrodes **11***b* positioned therebetween and thus can also be referred to as side seals. The seal portion **63** has portions overlapping with the lead **12***a* and the lead **12***b* and can also be referred to as a top seal.

Part of the exterior body **51** that overlaps with the positive electrodes **11***a* and the negative electrodes **11***b* preferably has a wave shape in which crest lines **71** and trough lines **72** are alternately arranged. The seal portions **62** and the seal portion **63** of the exterior body **51** are preferably flat.

FIG. **22**B**1** shows a cross section cut along the part overlapping with the crest line **71**. FIG. **22**B**2** shows a cross section cut along the part overlapping with the trough line **72**. FIGS. **22**B**1** and **22**B**2** correspond to cross sections of the battery **50**, the positive electrodes **11***a*, and the negative electrodes **11***b* in the width direction.

The distance between an end portion of the negative electrode **11***b* in the width direction and the seal portion **62** is referred to as a distance La. When the battery **50** changes in shape, for example, is bent, the positive electrode **11***a* and the negative electrode **11***b* change in shape such that the positions thereof are shifted from each other in the length direction as described later. At the time, if the distance La is too short, the exterior body **51** and the positive electrode **11***a* and the negative electrode **11***b* are rubbed hard against each other, so that the exterior body **51** is damaged in some cases. In particular, when a metal film of the exterior body **51** is exposed, there is concern that the metal film is corroded by the electrolyte solution. Thus, the distance La is preferably set as long as possible. However, if the distance La is too long, the volume of the battery **50** is increased.

The distance La between the end portion of the negative electrode **11***b* and the seal portion **62** is preferably increased as the total thickness of the stacked positive electrodes **11***a* and negative electrodes **11***b* is increased.

Specifically, when the total thickness of the stacked positive electrodes **11***a* and negative electrodes **11***b* and the separators **14** (not illustrated in FIGS. **22**B**1**, **22**B**2**, **22**C, or **22**D) is referred to as a thickness t, the distance La is preferably 0.8 times or more and 3.0 times or less, further preferably 0.9 times or more and 2.5 times or less, still further preferably 1.0 times or more and 2.0 times or less as large as the thickness t. When the distance La is in the above-described range, a compact battery which is highly reliable for bending can be obtained.

Furthermore, when a distance between the pair of seal portions **62** is referred to as a distance Lb, it is preferable that the distance Lb be sufficiently longer than a width Wb of the negative electrode **11***b*. In this case, even when the positive electrode **11***a* and the negative electrode **11***b* come into contact with the exterior body **51** by change in the shape of the battery **50** such as repeated bending, the position of part of the positive electrode **11***a* and the negative electrode **11***b* can be shifted in the width direction; thus, the positive and negative electrodes **11***a* and **11***b* and the exterior body **51** can be effectively prevented from being rubbed against each other.

For example, the difference between the distance Lb (i.e., the distance between the pair of seal portions **62**) and the width Wb of the negative electrode **11***b* is preferably 1.6 times or more and 6.0 times or less, further preferably 1.8 times or more and 5.0 times or less, still further preferably 2.0 times or more and 4.0 times or less as large as the total thickness t of the positive electrode **11***a* and the negative electrode **11***b*.

In other words, the distance Lb, the width Wb, and the thickness t preferably satisfy the relation of the following Formula 2.

[Formula 2]

$$\frac{Lb - Wb}{2t} \geq a \quad \text{(Formula 2)}$$

In the formula, a is 0.8 or more and 3.0 or less, preferably 0.9 or more and 2.5 or less, further preferably 1.0 or more and 2.0 or less.

FIG. **22**C illustrates a cross section including the lead **12***a* and corresponds to a cross section of the battery **50**, the positive electrode **11***a*, and the negative electrode **11***b* in the length direction. As illustrated in FIG. **22**C, a space **73** is preferably provided between end portions of the positive electrode **11***a* and the negative electrode **11***b* in the length direction and the exterior body **51** in the folded portion **61**.

FIG. **22**D is a schematic cross-sectional view of the battery **50** in a state of being bent. FIG. **22**D corresponds to a cross section along cutting line B**1**-B**2** in FIG. **22**A.

When the battery **50** is bent, a part of the exterior body **51** positioned on the outer side in bending is unbent and the other part positioned on the inner side changes its shape as it shrinks. More specifically, the part of the exterior body **51** positioned on the outer side in bending changes its shape such that the wave amplitude becomes smaller and the length of the wave period becomes larger. In contrast, the part of the exterior body **51** positioned on the inner side in bending changes its shape such that the wave amplitude becomes larger and the length of the wave period becomes smaller. When the exterior body **51** changes its shape in this manner, stress applied to the exterior body **51** due to bending is relieved, so that a material itself that forms the exterior body **51** does not need to expand and contract. As a result, the battery **50** can be bent with weak force without damage to the exterior body **51**.

Furthermore, as illustrated in FIG. **22**D, when the battery **50** is bent, the positions of the positive electrode **11***a* and the negative electrode **11***b* are shifted relatively. At this time, ends of the stacked positive electrodes **11***a* and negative electrodes **11***b* on the seal portion **63** side are fixed by the fixing member **17**. Thus, the plurality of positive electrodes **11***a* and the plurality of negative electrodes **11***b* are more shifted at a position closer to the folded portion **61**. Therefore, stress applied to the positive electrode **11***a* and the negative electrode **11***b* is relieved, and the positive electrode **11***a* and the negative electrode **11***b* themselves do not need to expand and contract. As a result, the battery **50** can be bent without damage to the positive electrode **11***a* and the negative electrode **11***b*.

Furthermore, the space **73** is provided between the end portions of the positive and negative electrodes **11***a* and **11***b* and the exterior body **51**, whereby the relative positions of the positive electrode **11***a* and the negative electrode **11***b* can be shifted while the end portions of the positive electrode **11***a* and the negative electrode **11***b* located on an inner side when the battery **50** is bent do not contact the exterior body **51**.

In the battery **50** illustrated in FIGS. **22**A, **22**B**1**, **22**B**2**, **22**C and **22**D and FIGS. **23**A and **23**B, the exterior body, the positive electrode **11***a*, and the negative electrode **11***b* are less likely to be damaged and the battery characteristics are less likely to deteriorate even when the battery **50** is repeatedly bent and unbent. When the positive electrode active material described in the above embodiment is used for the positive electrode **11***a* included in the battery **50**, a battery with more excellent cycle characteristics can be obtained.

Embodiment 4

In this embodiment, examples of electronic devices including the secondary battery of one embodiment of the present invention are described.

First, FIGS. **24**A to **24**G show examples of electronic devices including the bendable secondary battery described in Embodiment 3. Examples of an electronic device including a flexible secondary battery include television sets (also referred to as televisions or television receivers), monitors of computers or the like, digital cameras or digital video cameras, digital photo frames, mobile phones (also referred to as cellular phones or mobile phone devices), portable game machines, portable information terminals, audio reproducing devices, and large game machines such as pachinko machines.

In addition, a flexible secondary battery can be incorporated along a curved inside/outside wall surface of a house or a building or a curved interior/exterior surface of an automobile.

FIG. **24**A illustrates an example of a mobile phone. A mobile phone **7400** is provided with a display portion **7402** incorporated in a housing **7401**, an operation button **7403**, an external connection port **7404**, a speaker **7405**, a microphone **7406**, and the like. Note that the mobile phone **7400** includes a secondary battery **7407**. When the secondary battery of one embodiment of the present invention is used as the secondary battery **7407**, a lightweight mobile phone with a long lifetime can be provided.

FIG. **24**B illustrates the mobile phone **7400** that is bent. When the whole mobile phone **7400** is curved by external force, the secondary battery **7407** included in the mobile phone **7400** is also curved. FIG. **24**C illustrates the curved secondary battery **7407**. The secondary battery **7407** is a thin storage battery. The secondary battery **7407** is curved and fixed. Note that the secondary battery **7407** includes a lead electrode **7408** electrically connected to a current collector **7409**. The current collector **7409** is, for example, copper foil, and partly alloyed with gallium; thus, adhesion between the current collector **7409** and an active material layer in contact with the current collector **7409** is improved and the secondary battery **7407** can have high reliability even in a state of being bent.

FIG. **24**D illustrates an example of a bangle display device. A portable display device **7100** includes a housing **7101**, a display portion **7102**, an operation button **7103**, and a secondary battery **7104**. FIG. **24**E illustrates the bent secondary battery **7104**. When the curved secondary battery **7104** is on a user's arm, the housing changes its form and the curvature of a part or the whole of the secondary battery **7104** is changed. Note that the radius of curvature of a curve at a point refers to the radius of the circular arc that best approximates the curve at that point. The reciprocal of the radius of curvature is curvature. Specifically, part or the whole of the housing or the main surface of the secondary battery **7104** is changed in the range of radius of curvature from 40 mm to 150 mm. When the radius of curvature at the main surface of the secondary battery **7104** is greater than or equal to 40 mm and less than or equal to 150 mm, the reliability can be kept high. When the secondary battery of one embodiment of the present invention is used as the secondary battery **7104**, a lightweight portable display device with a long lifetime can be provided.

FIG. **24**F illustrates an example of a watch-type portable information terminal. A portable information terminal **7200** includes a housing **7201**, a display portion **7202**, a band **7203**, a buckle **7204**, an operation button **7205**, an input output terminal **7206**, and the like.

The portable information terminal **7200** is capable of executing a variety of applications such as mobile phone calls, e-mailing, viewing and editing texts, music reproduction, Internet communication, and a computer game.

The display surface of the display portion **7202** is curved, and images can be displayed on the curved display surface. In addition, the display portion **7202** includes a touch sensor, and operation can be performed by touching the screen with a finger, a stylus, or the like. For example, by touching an icon **7207** displayed on the display portion **7202**, application can be started.

With the operation button **7205**, a variety of functions such as time setting, power on/off, on/off of wireless communication, setting and cancellation of a silent mode, and setting and cancellation of a power saving mode can be performed. For example, the functions of the operation button **7205** can be set freely by setting the operation system incorporated in the portable information terminal **7200**.

The portable information terminal **7200** can employ near field communication that is a communication method based on an existing communication standard. For example, mutual communication between the portable information terminal **7200** and a headset capable of wireless communication can be performed, and thus hands-free calling is possible.

Moreover, the portable information terminal **7200** includes the input output terminal **7206**, and data can be directly transmitted to and received from another information terminal via a connector. In addition, charging via the input output terminal **7206** is possible. Note that the charging operation may be performed by wireless power feeding without using the input output terminal **7206**.

The display portion **7202** of the portable information terminal **7200** includes the secondary battery of one embodiment of the present invention. When the secondary battery of one embodiment of the present invention is used, a lightweight portable information terminal with a long lifetime can be provided. For example, the secondary battery **7104** illustrated in FIG. **24**E that is in the state of being curved can be provided in the housing **7201**. Alternatively, the secondary battery **7104** illustrated in FIG. **24**E can be provided in the band **7203** such that it can be curved.

A portable information terminal **7200** preferably includes a sensor. As the sensor, for example a human body sensor such as a fingerprint sensor, a pulse sensor, or a temperature sensor, a touch sensor, a pressure sensitive sensor, an acceleration sensor, or the like is preferably mounted.

FIG. **24**G illustrates an example of an armband display device. A display device **7300** includes a display portion **7304** and the secondary battery of one embodiment of the present invention. The display device **7300** can include a touch sensor in the display portion **7304** and can serve as a portable information terminal.

The display surface of the display portion **7304** is bent, and images can be displayed on the bent display surface. A display state of the display device **7300** can be changed by, for example, near field communication, which is a communication method based on an existing communication standard.

The display device **7300** includes an input output terminal, and data can be directly transmitted to and received from another information terminal via a connector. In addition, charging via the input output terminal is possible. Note that the charging operation may be performed by wireless power feeding without using the input output terminal.

When the secondary battery of one embodiment of the present invention is used as the secondary battery included in the display device **7300**, a lightweight display device with a long lifetime can be provided.

In addition, FIG. **24**H, FIGS. **25**A to **25**C, and FIG. **26** show examples of electronic devices including the secondary battery with excellent cycle characteristics described in the above embodiment.

When the secondary battery of one embodiment of the present invention is used as a secondary battery of a daily electronic device, a lightweight product with a long lifetime can be provided. As the daily electronic devices, an electric toothbrush, an electric shaver, electric beauty equipment, and the like are given. As secondary batteries of these products, in consideration of handling ease for users, small and lightweight stick type secondary batteries with high capacity are desired.

FIG. **24**H is a perspective view of a device which is called a vaporizer. In FIG. **24**H, a vaporizer **7500** includes an atomizer **7501** including a heating element, a secondary battery **7504** supplying power to the atomizer, and a cartridge **7502** including a liquid supply bottle, a sensor, and the like. To improve safety, a protection circuit which prevents overcharge and overdischarge of the secondary battery **7504** may be electrically connected to the secondary battery **7504**. The secondary battery **7504** in FIG. **24**H includes an output terminal for connecting to a charger. When the vaporizer **7500** is held by a user, the secondary battery **7504** becomes a tip portion; thus, it is preferable that the secondary battery **7504** have a short total length and be lightweight. With the secondary battery of one embodiment of the present invention which has high capacity and excellent cycle characteristics, the small and lightweight vaporizer **7500** which can be used for a long time for a long period can be provided.

Next, FIGS. **25**A and **25**B illustrate an example of a foldable tablet terminal A tablet terminal **9600** illustrated in FIGS. **25**A and **25**B includes a housing **9630***a*, a housing **9630***b*, a movable portion **9640** connecting the housings **9630***a* and **9630***b*, a display portion **9631** including a display portion **9631***a* and a display portion **9631***b*, a display mode changing switch **9626**, a power switch **9627**, a power saving mode changing switch **9625**, a fastener **9629**, and an operation switch **9628**. A flexible panel is used for the display portion **9631**, whereby a tablet terminal with a larger display portion can be provided. FIG. **25**A illustrates the tablet terminal **9600** that is opened, and FIG. **25**B illustrates the tablet terminal **9600** that is closed.

The tablet terminal **9600** includes a power storage unit **9635** inside the housings **9630***a* and **9630***b*. The power storage unit **9635** is provided across the housings **9630***a* and **9630***b*, passing through the movable portion **9640**.

Part of the display portion **9631***a* can be a touch panel region and data can be input when a displayed operation key is touched. Although a structure in which a half region in the display portion **9631***a* has only a display function and the other half region has a touch panel function is shown as an example, the display portion **9631***a* is not limited to the structure. The whole region in the display portion **9631***a* may have a touch panel function. For example, the display portion **9631***a* can display keyboard buttons in the whole region to be a touch panel, and the display portion **9631***b* can be used as a display screen.

Like the display portion **9631***a*, part of the display portion **9631***b* can be a touch panel region. A switching button for

showing/hiding a keyboard of the touch panel is touched with a finger, a stylus, or the like, so that keyboard buttons can be displayed on the display portion **9631***b*.

Touch input can be performed in the touch panel region and the touch panel region at the same time.

The display mode switch **9626** can switch the display between a portrait mode and a landscape mode, and between monochrome display and color display, for example. The power saving mode changing switch **9625** can control display luminance in accordance with the amount of external light in use of the tablet terminal **9600**, which is measured with an optical sensor incorporated in the tablet terminal **9600**. Another detection device including a sensor for detecting inclination, such as a gyroscope sensor or an acceleration sensor, may be incorporated in the tablet terminal, in addition to the optical sensor.

Although the display portion **9631***a* and the display portion **9631***b* have the same area in FIG. **25**A, one embodiment of the present invention is not limited to this example. The display portion **9631***a* and the display portion **9631***b* may have different areas or different display quality. For example, one display panel may be capable of higher-definition display than the other display panel.

The tablet terminal is closed in FIG. **25**B. The tablet terminal includes the housing **9630**, a solar cell **9633**, and a charge and discharge control circuit **9634** including a DCDC converter **9636**. The power storage unit of one embodiment of the present invention is used as the power storage unit **9635**.

The tablet terminal **9600** can be folded such that the housings **9630***a* and **9630***b* overlap with each other when not in use. Thus, the display portions **9631***a* and **9631***b* can be protected, which increases the durability of the tablet terminal **9600**. With the power storage unit **9635** including the secondary battery of one embodiment of the present invention which has high capacity and excellent cycle characteristics, the tablet terminal **9600** which can be used for a long time for a long period can be provided.

The tablet terminal illustrated in FIGS. **25**A and **25**B can also have a function of displaying various kinds of data (e.g., a still image, a moving image, and a text image), a function of displaying a calendar, a date, or the time on the display portion, a touch-input function of operating or editing data displayed on the display portion by touch input, a function of controlling processing by various kinds of software (programs), and the like.

The solar cell **9633**, which is attached on the surface of the tablet terminal, supplies electric power to a touch panel, a display portion, an image signal processor, and the like. Note that the solar cell **9633** can be provided on one or both surfaces of the housing **9630** and the power storage unit **9635** can be charged efficiently. The use of a lithium-ion battery as the power storage unit **9635** brings an advantage such as reduction in size.

The structure and operation of the charge and discharge control circuit **9634** illustrated in FIG. **25**B will be described with reference to a block diagram in FIG. **25**C. The solar cell **9633**, the power storage unit **9635**, the DC-DC converter **9636**, a converter **9637**, switches SW**1** to SW**3**, and the display portion **9631** are illustrated in FIG. **25**C, and the power storage unit **9635**, the DC-DC converter **9636**, the converter **9637**, and the switches SW**1** to SW**3** correspond to the charge and discharge control circuit **9634** in FIG. **25**B.

First, an example of the operation in the case where power is generated by the solar cell **9633** using external light is described. The voltage of electric power generated by the solar cell is raised or lowered by the DCDC converter **9636** to a voltage for charging the power storage unit **9635**. When the power from the solar cell **9633** is used for the operation of the display portion **9631**, the switch SW**1** is turned on and the voltage of the power is raised or lowered by the converter **9637** to a voltage needed for operating the display portion **9631**. When display on the display portion **9631** is not performed, the switch SW**1** is turned off and the switch SW**2** is turned on, so that the power storage unit **9635** can be charged.

Note that the solar cell **9633** is described as an example of a power generation means; however, one embodiment of the present invention is not limited to this example. The power storage unit **9635** may be charged using another power generation means such as a piezoelectric element or a thermoelectric conversion element (Peltier element). For example, the power storage unit **9635** may be charged with a non-contact power transmission module that transmits and receives power wirelessly (without contact) to charge the battery or with a combination of other charging means.

FIG. **26** illustrates other examples of electronic devices. In FIG. **26**, a display device **8000** is an example of an electronic device including a secondary battery **8004** of one embodiment of the present invention. Specifically, the display device **8000** corresponds to a display device for TV broadcast reception and includes a housing **8001**, a display portion **8002**, speaker portions **8003**, the secondary battery **8004**, and the like. The secondary battery **8004** of one embodiment of the present invention is provided in the housing **8001**. The display device **8000** can receive electric power from a commercial power supply. Alternatively, the display device **8000** can use electric power stored in the secondary battery **8004**. Thus, the display device **8000** can operate with the use of the secondary battery **8004** of one embodiment of the present invention as an uninterruptible power supply even when electric power cannot be supplied from a commercial power supply due to power failure or the like.

A semiconductor display device such as a liquid crystal display device, a light-emitting device in which a light-emitting element such as an organic EL element is provided in each pixel, an electrophoretic display device, a digital micromirror device (DMD), a plasma display panel (PDP), or a field emission display (FED) can be used for the display portion **8002**.

Note that the display device includes, in its category, all of information display devices for personal computers, advertisement displays, and the like other than TV broadcast reception.

In FIG. **26**, an installation lighting device **8100** is an example of an electronic device using a secondary battery **8103** of one embodiment of the present invention. Specifically, the lighting device **8100** includes a housing **8101**, a light source **8102**, the secondary battery **8103**, and the like. Although FIG. **26** illustrates the case where the secondary battery **8103** is provided in a ceiling **8104** on which the housing **8101** and the light source **8102** are installed, the secondary battery **8103** may be provided in the housing **8101**. The lighting device **8100** can receive electric power from a commercial power supply. Alternatively, the lighting device **8100** can use electric power stored in the secondary battery **8103**. Thus, the lighting device **8100** can operate with the use of the secondary battery **8103** of one embodiment of the present invention as an uninterruptible power supply even when electric power cannot be supplied from a commercial power supply due to power failure or the like.

Note that although the installation lighting device **8100** provided in the ceiling **8104** is illustrated in FIG. **26** as an

example, the secondary battery of one embodiment of the present invention can be used as an installation lighting device provided in, for example, a wall **8105**, a floor **8106**, a window **8107**, or the like other than the ceiling **8104**. Alternatively, the secondary battery can be used in a tabletop lighting device or the like.

As the light source **8102**, an artificial light source which emits light artificially by using power can be used. Specifically, an incandescent lamp, a discharge lamp such as a fluorescent lamp, and a light-emitting element such as an LED or an organic EL element are given as examples of the artificial light source.

In FIG. **26**, an air conditioner including an indoor unit **8200** and an outdoor unit **8204** is an example of an electronic device including a secondary battery **8203** of one embodiment of the present invention. Specifically, the indoor unit **8200** includes a housing **8201**, an air outlet **8202**, the secondary battery **8203**, and the like. Although FIG. **26** illustrates the case where the secondary battery **8203** is provided in the indoor unit **8200**, the secondary battery **8203** may be provided in the outdoor unit **8204**. Alternatively, the secondary batteries **8203** may be provided in both the indoor unit **8200** and the outdoor unit **8204**. The air conditioner can receive electric power from a commercial power supply. Alternatively, the air conditioner can use electric power stored in the secondary battery **8203**. Particularly in the case where the secondary batteries **8203** are provided in both the indoor unit **8200** and the outdoor unit **8204**, the air conditioner can operate with the use of the secondary battery **8203** of one embodiment of the present invention as an uninterruptible power supply even when electric power cannot be supplied from a commercial power supply due to power failure or the like.

Note that although the split-type air conditioner including the indoor unit and the outdoor unit is illustrated in FIG. **26** as an example, the secondary battery of one embodiment of the present invention can be used in an air conditioner in which the functions of an indoor unit and an outdoor unit are integrated in one housing.

In FIG. **26**, an electric refrigerator-freezer **8300** is an example of an electronic device using a secondary battery **8304** of one embodiment of the present invention. Specifically, the electric refrigerator-freezer **8300** includes a housing **8301**, a refrigerator door **8302**, a freezer door **8303**, the secondary battery **8304**, and the like. The secondary battery **8304** is provided in the housing **8301** in FIG. **26**. The electric refrigerator-freezer **8300** can receive electric power from a commercial power supply. Alternatively, the electric refrigerator-freezer **8300** can use electric power stored in the secondary battery **8304**. Thus, the electric refrigerator-freezer **8300** can operate with the use of the secondary battery **8304** of one embodiment of the present invention as an uninterruptible power supply even when electric power cannot be supplied from a commercial power supply due to power failure or the like.

Note that among the electronic devices described above, a high-frequency heating apparatus such as a microwave oven and an electronic device such as an electric rice cooker require high power in a short time. The tripping of a circuit breaker of a commercial power source in use of electronic devices can be prevented by using the secondary battery of one embodiment of the present invention as an auxiliary power source for supplying power which cannot be supplied enough by a commercial power source.

In addition, in a time period when electronic devices are not used, particularly when the proportion of the amount of power which is actually used to the total amount of power which can be supplied from a commercial power source (such a proportion referred to as a usage rate of power) is low, power can be stored in the secondary battery, whereby the usage rate of power can be reduced in a time period when the electronic devices are used. For example, in the case of the electric refrigerator-freezer **8300**, power can be stored in the secondary battery **8304** in night time when the temperature is low and the refrigerator door **8302** and the freezer door **8303** are not often opened and closed. On the other hand, in daytime when the temperature is high and the refrigerator door **8302** and the freezer door **8303** are frequently opened and closed, the secondary battery **8304** is used as an auxiliary power source; thus, the usage rate of power in daytime can be reduced.

According to one embodiment of the present invention, the secondary battery can have excellent cycle characteristics and improve reliability. Furthermore, in accordance with one embodiment of the present invention, a secondary battery with high capacity can be obtained; thus, the secondary battery itself can be made more compact and lightweight as a result of improved characteristics of the secondary battery. Thus, the secondary battery of one embodiment of the present invention is used in the electronic device described in this embodiment, whereby a more lightweight electronic device with a longer lifetime can be obtained. This embodiment can be implemented in appropriate combination with any of the other embodiments.

Embodiment 5

In this embodiment, examples of vehicles including the secondary battery of one embodiment of the present invention are described.

The use of secondary batteries in vehicles enables production of next-generation clean energy vehicles such as hybrid electric vehicles (HEVs), electric vehicles (EVs), and plug-in hybrid electric vehicles (PHEVs).

FIGS. **27**A to **27**C each illustrate an example of a vehicle using the secondary battery of one embodiment of the present invention. An automobile **8400** illustrated in FIG. **27**A is an electric vehicle that runs on the power of an electric motor. Alternatively, the automobile **8400** is a hybrid electric vehicle capable of driving appropriately using either an electric motor or an engine. One embodiment of the present invention can provide a high-mileage vehicle. The automobile **8400** includes the secondary battery. As the secondary battery, the modules of the secondary batteries illustrated in FIGS. **12**C and **12**D may be arranged to be used in a floor portion in the automobile. Alternatively, a battery pack in which a plurality of secondary batteries each of which is illustrated in FIGS. **17**A to **17**C are combined may be placed in a floor portion in the automobile. The secondary battery is used not only for driving an electric motor **8406**, but also for supplying electric power to a light-emitting device such as a headlight **8401** or a room light (not illustrated).

The secondary battery can also supply electric power to a display device of a speedometer, a tachometer, or the like included in the automobile **8400**. Furthermore, the secondary battery can supply electric power to a semiconductor device included in the automobile **8400**, such as a navigation system.

FIG. **27**B illustrates an automobile **8500** including the secondary battery. The automobile **8500** can be charged when the secondary battery is supplied with electric power through external charging equipment by a plug-in system, a contactless power feeding system, or the like. In FIG. **27**B,

secondary batteries **8024** and **8025** included in the automobile **8500** is charged with the use of a ground-based charging apparatus **8021** through a cable **8022**. In charging, a given method such as CHAdeMO (registered trademark) or Combined Charging System may be employed as a charging method, the standard of a connector, or the like as appropriate. The ground-based charging apparatus **8021** may be a charging station provided in a commerce facility or a power source in a house. With the use of a plug-in technique, the secondary battery **8024** included in the automobile **8500** can be charged by being supplied with electric power from the outside, for example. The charging can be performed by converting AC electric power into DC electric power through a converter such as an AC-DC converter.

Furthermore, although not illustrated, the vehicle may include a power receiving device so that it can be charged by being supplied with electric power from an above-ground power transmitting device in a contactless manner. In the case of the contactless power feeding system, by fitting a power transmitting device in a road or an exterior wall, charging can be performed not only when the electric vehicle is stopped but also when driven. In addition, the contactless power feeding system may be utilized to perform transmission and reception of electric power between vehicles. A solar cell may be provided in the exterior of the automobile to charge the secondary battery when the automobile stops or moves. To supply electric power in such a contactless manner, an electromagnetic induction method or a magnetic resonance method can be used.

FIG. **27**C shows an example of a motorcycle using the secondary battery of one embodiment of the present invention. A motor scooter **8600** illustrated in FIG. **27**C includes a secondary battery **8602**, side mirrors **8601**, and indicators **8603**. The secondary battery **8602** can supply electric power to the indicators **8603**.

Furthermore, in the motor scooter **8600** illustrated in FIG. **27**C, the secondary battery **8602** can be held in a storage unit under seat **8604**. The secondary battery **8602** can be held in the storage unit under seat **8604** even with a small size. The secondary battery **8602** is detachable; thus, the secondary battery **8602** is carried indoors when it is charged, and is stored before the motorcycle is driven.

In accordance with one embodiment of the present invention, the secondary battery can have improved cycle characteristics and the capacity of the secondary battery can be increased. Thus, the secondary battery itself can be made more compact and lightweight. The compact and lightweight secondary battery contributes to a reduction in the weight of a vehicle, and thus increases the driving radius. Furthermore, the secondary battery included in the vehicle can be used as a power source for supplying electric power to products other than the vehicle. In such a case, the use of a commercial power source can be avoided at peak time of electric power demand, for example. If the use of a commercial power source can be avoided at peak time of electric power demand, the avoidance can contribute to energy saving and a reduction in carbon dioxide emissions. Moreover, if the cycle characteristics are excellent, the secondary battery can be used for a long period; thus, the use amount of rare metals such as cobalt can be reduced.

This embodiment can be implemented in appropriate combination with the other embodiments.

Example 1

In this example, the positive electrode active materials which are embodiments of the present invention are formed, and the observation results of the positive electrode active materials by STEM, the results of TEM images subjected to fast Fourier transform, and the analysis results obtained by energy dispersive X-ray spectroscopy (EDX) are described. In addition, the evaluation results of characteristics of secondary batteries containing the positive electrode active materials are described.

[Formation of Positive Electrode Active Material]

«Sample 01»

In this example, a positive electrode active material of Sample 01, which contains lithium cobaltate as a composite oxide of lithium and a first transition metal contained in a first region, lithium titanate as an oxide of a second transition metal contained in a second region, and magnesium oxide as an oxide of a representative element contained in a third region, was formed.

In this example, lithium cobalt oxide particles (C-20F, produced by NIPPON CHEMICAL INDUSTRIAL CO., LTD.) were used as a starting material. Thus, in this example, Step 12 and Step 13 described in Embodiment 1 were omitted. Note that the above-described lithium cobalt oxide particles each have a particle diameter of approximately 20 μm, and contain fluorine, magnesium, calcium, sodium, silicon, sulfur, and phosphorus in a region which can be analyzed by XPS.

Next, as Step 14, the lithium cobalt oxide particles containing magnesium and fluorine were coated with a material containing titanium by a sol-gel method. Specifically, TTIP was dissolved in isopropanol, and an isopropanol solution of TTIP was formed. Then, the lithium cobalt oxide particles were mixed into the solution so that TTIP to lithium cobalt oxide containing magnesium and fluorine was 0.01 ml/g.

The above mixed solution was stirred with a magnetic stirrer for four hours, at 25° C., and at a humidity of 90% RH. Through the process, water in an atmosphere and TTIP caused hydrolysis and polycondensation reaction, and a layer containing titanium was formed on the surface of the lithium cobalt oxide particle containing magnesium and fluorine.

The mixed solution which had been subjected to the above process was filtered to collect the residue. As a filter for filtration, Kiriyama filter paper (No. 4) was used.

The collected residue was dried in a vacuum at 70° C. for one hour.

Next, the lithium cobalt oxide particles coated with the material containing titanium was heated. With a muffle furnace, the heating was performed under the following conditions: the flow rate of dry air was 10 L/min; the temperature was 800° C. (the temperature rising rate was 200° C./h); and the retention time was two hours. The dew point of the dry air is preferably lower than or equal to −109° C.

Then, the heated particles were cooled to room temperature. The time of decreasing temperature from the retention temperature to room temperature was 10 hours to 15 hours. After that, crushing treatment was performed. In the crushing treatment, the particles were made to pass through a sieve. The sieve has an aperture width of 53 μm.

Lastly, the cooled particles were collected, and the positive electrode active material of Sample 01 was obtained.

«Sample 02»

Sample 02 was formed as a comparative example by heating lithium cobalt oxide particles containing magnesium and fluorine without being coated with a material containing titanium.

Lithium cobalt oxide particles produced by NIPPON CHEMICAL INDUSTRIAL CO., LTD. (product name: C-20F) were used as the lithium cobalt oxide particles containing magnesium and fluorine.

The lithium cobalt oxide particles containing magnesium and fluorine were heated. The heating was performed under the following conditions: the temperature was 800° C. (the temperature rising rate was 200° C./h); the retention time was two hours; and the flow rate of oxygen was 10 L/min.

The heated particles were cooled and made to pass through a sieve like Sample 01 to obtain a positive electrode active material of Sample 02.

It is probable that Sample 02 is a positive electrode active material which contains lithium cobalt oxide inside and includes a region containing magnesium in a superficial portion.

«Sample 03»

Sample 03 was formed as a comparative example in the following manner: a region containing titanium was formed in lithium cobalt oxide particles which do not contain magnesium by a sol-gel method and then the lithium cobalt oxide particles were heated.

Lithium cobalt oxide particles produced by NIPPON CHEMICAL INDUSTRIAL CO., LTD. (product name: C-10N) were used. In the lithium cobalt oxide particles, magnesium is not detected and fluorine is detected at approximately 1 atomic % by XPS.

A region containing titanium was formed by a sol-gel method in the lithium cobalt oxide particles, and the lithium cobalt oxide particles were dried, heated, cooled, and made to pass through a sieve, like Sample 01. The obtained lithium cobalt oxide particles were used as a positive electrode active material of Sample 03.

It is probable that Sample 03 is a positive electrode active material which contains lithium cobalt oxide inside and includes a region containing titanium in a superficial portion.

«Sample 04»

For Sample 04, as a comparative example, lithium cobalt oxide particles were used as it is without being heated.

Lithium cobalt oxide particles produced by NIPPON CHEMICAL INDUSTRIAL CO., LTD. (product name: C-10N) were used.

Sample 04 is a positive electrode active material which does not have a coating layer.

«Sample 05»

For Sample 05, as a comparative example, lithium cobalt oxide particles containing magnesium and fluorine were used as it is without being heated.

Lithium cobalt oxide particles produced by NIPPON CHEMICAL INDUSTRIAL CO., LTD. (product name: C-20F) were used as the lithium cobalt oxide particles containing magnesium and fluorine. That is, Sample 05 was used as the same as the starting material of Sample 01.

Table 1 shows the conditions of Sample 01 to Sample 05.

TABLE 1

	Conditions
Sample 01	$LiCoO_2$ + Mg + F, coated with a material containing Ti, heated
Sample 02	$LiCoO_2$ + Mg + F, heated
Sample 03	$LiCoO_2$, coated with a material containing Ti, heated
Sample 04	$LiCoO_2$, not heated
Sample 05	$LiCoO_2$ + Mg + F, not heated

[STEM]

The obtained positive electrode active material of Sample 01 was observed by an electron microscope (JEM-ARM200F, manufactured by JEOL Ltd.) under the condition where the acceleration voltage was 200 kV. FIG. **28** shows the obtained electron microscope image. As shown in FIG. **28**, the positive electrode active material probably includes three different regions: the first region **101**; the second region **102**; and the third region **103**. The third region **103** is observed as a region brighter than the first region **101** and the second region **102**. Furthermore, crystal orientations of the first region **101** and the second region **102** are partly aligned with each other, and crystal orientations of the second region **102** and the third region **103** are partly aligned with each other.

[STEM-FFT]

FIG. **29A1** shows a fast Fourier transform (FFT) image of a region **103**FFT in the STEM image of FIG. **28**. In FIG. **29A2**, a center point O of FIG. **29A1** is shown by a cross, and bright points A, B, and C are each surrounded by a circle. Similarly, FIG. **29B1** shows an FFT image of a region **102**FFT. In FIG. **29B2**, a center point O of FIG. **29B1** is shown by a cross, and bright points A, B, and C are each surrounded by a circle. In addition, FIG. **29C1** shows an FFT image of a region **101**FFT. In FIG. **29C2**, a center point O of FIG. **29C1** is shown by a cross, and bright points A, B, and C are each surrounded by a circle.

In FIG. **29A2**, a distance d between the bright point A and the center point O is 0.256 nm, a distance d between the bright point B and the center point O is 0.241 nm, and a distance d between the bright point C and the center point O is 0.209 nm. In addition, ∠COA is 121°, ∠COB is 52°, and ∠AOB is 69°. From these results, the region **103**FFT probably contains magnesium oxide (MgO, cubic crystal).

Similarly, in FIG. **29B2**, the distance d between the bright point A and the center point O is 0.238 nm, the distance d between the bright point B and the center point O is 0.225 nm, and the distance d between the bright point C and the center point O is 0.198 nm. In addition, ∠COA is 123°, ∠COB is 52°, and ∠AOB is 71°. From these results, the region **102**FFT probably contains lithium titanate ($LiTiO_2$, cubic crystal).

In FIG. **29C2**, the distance d between the bright point A and the center point O is 0.240 nm, the distance d between the bright point B and the center point O is 0.235 nm, and the distance d between the bright point C and the center point O is 0.196 nm. In addition, ∠COA is 126°, ∠COB is 52°, and ∠AOB is 74°. From these results, the region **101**FFT probably contains lithium cobaltate ($LiCoO_2$, rhombohedral).

[EDX]

FIGS. **30A1**, **30A2**, **30B1**, **30B2**, **30C1**, and **30C2** show a high-angle annular dark field scanning transmission electron microscopy (HAADF-STEM) image and element mapping images with EDX of the positive electrode active material of Sample 01. FIG. **30A1** shows a HAADF-STEM image, FIG. **30A2** shows a mapping image of oxygen atoms, FIG. **30B1** shows a mapping image of cobalt atoms, FIG. **30B2** shows a mapping image of fluorine atoms, FIG. **30C1** shows a mapping image of titanium atoms, and FIG. **30C2** shows a mapping image of magnesium atoms. Note that in EDX element mapping images in FIGS. **30A2**, **30B1**, **30B2**, **30C1**, and **30C2** and FIGS. **31A2**, **31B1**, **31B2**, **31C1**, and **31C2**, a region where the number of elements is less than or equal to a lower limit of the detection is indicated in white, and as the number of elements is increased, the white region becomes black.

As shown in FIGS. **30**A**2** and **30**B**1**, it is found that the oxygen atoms and the cobalt atoms are distributed in the whole of the positive electrode active material particle. In contrast, as shown in FIGS. **30**B**2**, **30**C**1**, and **30**C**2**, it is found that the fluorine atoms, the titanium atoms, and the magnesium atoms are unevenly distributed in a region close to the surface of the positive electrode active material.

Next, FIGS. **31**A**1**, **31**A**2**, **31**B**1**, **31**B**2**, **31**C**1**, and **31**C**2** show a HAADF-STEM image and element mapping images with EDX of the positive electrode active material of Sample 05, which is a comparative example FIG. **31**A**1** shows a HAADF-STEM image, FIG. **31**A**2** shows a mapping image of oxygen atoms, FIG. **31**B**1** shows a mapping image of cobalt atoms, FIG. **31**B**2** shows a mapping image of fluorine atoms, FIG. **31**C**1** shows a mapping image of titanium atoms, and FIG. **31**C**2** shows a mapping image of magnesium atoms.

As shown in FIGS. **31**B**2** and **31**C**2**, it is found that, even in Sample 05 which is not heated, a certain amount of magnesium and fluorine is unevenly distributed in the vicinity of the surface.

[EDX Line Analysis]

FIG. **32** shows results of line analysis with TEM-EDX performed on a cross section of the vicinity of the surface of the positive electrode active material of Sample 01. FIG. **32** is a graph showing data detected on a line connecting the outside of the positive electrode active material of Sample 01 to the inside of the positive electrode active material, and a distance of 0 nm indicates the outside of the positive electrode active material and a distance of 14 nm indicates the inside of the particle. With EDX, the analysis region tends to be large, so that elements not only at a center of an electron beam irradiation region but also in a region around the center may be detected.

As shown in FIG. **32**, it is found that there are peaks of magnesium and titanium in the vicinity of the surface of the positive electrode active material of Sample 01, the distribution of magnesium is closer to the surface than the distribution of titanium is. It is also found that the peak of magnesium is closer to the surface than the peak of titanium is. In addition, it is probable that cobalt and oxygen are present from the outermost surface of the positive electrode active material particle.

As shown in FIG. **32**, fluorine is hardly detected. This is probably because fluorine, which is a light element, is difficult to detect with EDX.

From the above STEM images, FFT images, element mapping images with EDX, and EDX line analysis, it is found that Sample 01 is a positive electrode active material of one embodiment of the present invention, which includes the first region containing lithium cobaltate, the second region containing lithium, titanium, cobalt, and oxygen, and the third region containing magnesium and oxygen. It is found that, in Sample 01, part of the second region and part of the third region overlap.

In the graph of FIG. **32**, the amount of detected oxygen is stable at a distance of 4 nm or more. Thus, in this example, the average value O_{ave} of the amount of detected oxygen in the stable region is obtained, and a distance x of the measurement point at which the measurement value closest to 0.5 O_{ave}, the value of 50% of the average value O_{ave}, is obtained is assumed to be the surface of the positive electrode active material particle.

In this example, the average value O_{ave} of the amount of detected oxygen in a range from a distance of 4 nm to a distance of 14 nm is 674.2. The x axis of the measurement point at which the measurement value closest to 337.1, which is 50% of 674.2, is obtained indicates a distance of 1.71 nm. Thus, in this example, a distance of 1.71 nm in the graph of FIG. **32** is assumed to be the surface of the positive electrode active material particle.

When the surface of the positive electrode active material particle is set at a distance of 1.71 nm in FIG. **32**, the peak of magnesium and the peak of titanium are present at 0.72 nm and 1.00 nm, respectively, from the surface of the positive electrode active material particle.

The concentration of magnesium is higher than or equal to ⅕ of the peak from the surface of the positive electrode active material particle to a distance of 4.42 nm, that is, to a region at 2.71 nm from the surface. The measurement value of magnesium is less than ⅕ of the peak at a distance of 4.57 nm or more, that is, at a depth of 2.86 nm or more from the surface of the positive electrode active material particle. Thus, it is found that in Sample 01, a region from the surface to a depth of 2.71 nm is the third region.

Furthermore, the concentration of titanium is higher than or equal to ½ of the peak from a distance of 2.14 nm to a distance of 3.42 nm. Thus, it is found that a region from a depth of 0.43 nm to a depth of 1.71 nm from the surface of the positive electrode active material particle is the second region.

Next, evaluation results of charge and discharge characteristics of secondary batteries which are fabricated using the positive electrode active materials of Sample 01 to Sample 05 formed in the above manner are described.

[Fabrication of Secondary Batteries]

CR2032 coin-type secondary batteries (with a diameter of 20 mm and a height of 3.2 mm) were fabricated using the positive electrode active materials of Sample 01 to Sample 05 formed in the above manner.

A positive electrode formed by applying slurry in which a positive electrode active material (LCO), acetylene black (AB), and polyvinylidene fluoride (PVDF) were mixed at a weight ratio of 95:2.5:2.5 to a current collector was used.

A lithium metal was used for the counter electrode.

As an electrolyte contained in an electrolyte solution, 1 mol/L lithium hexafluorophosphate ($LiPF_6$) was used, and as the electrolyte solution, a solution in which ethylene carbonate (EC) and diethyl carbonate (DEC) at a volume ratio of 3:7 and vinylene carbonate (VC) at a 2 weight % were mixed was used.

A positive electrode can and a negative electrode can were formed of stainless steel (SUS).

[Evaluation of Charge And Discharge Characteristics]

Next, charge and discharge characteristics of the secondary batteries of Sample 01 and Sample 05 formed in the above manner were evaluated. The measurement temperature was 25° C. Twenty cycles of charging and discharging were performed at 4.6 V (CCCV, 0.5 C, a cutoff current of 0.01 C) and 2.5 V (CC, 0.5 C), respectively. Here, 1C was set to 137 mA/g, which was a current value per weight of the positive electrode active material.

FIG. **33** is a graph showing charge and discharge characteristics of the secondary battery using the positive electrode active material of Sample 01. FIG. **33** shows excellent charge and discharge characteristics with a wide plateau. In addition, results of 20 cycles of charging and discharging almost overlap, which means that the cycle characteristics are excellent.

FIG. **34** is a graph showing charge and discharge characteristics of the secondary battery of Sample 05, which is a comparative example. In the initial cycles, excellent charge and discharge characteristics are shown; however, as

indicated by arrows in FIG. **34**, charge capacity and discharge capacity decrease with an increase in cycles.

[Evaluation of Cycle Characteristics]

«Charging at 4.4 V»

The cycle characteristics of the secondary batteries of Sample 01 and Sample 05 charged at 4.4 V were evaluated. The measurement temperature was 25° C. The charging was performed at 4.4 V (CCCV, 0.5 C, a cutoff current of 0.01 C), and the discharging was performed at 2.5 V (CC, 0.5 C).

FIG. **35** is a graph showing the cycle characteristics of the secondary batteries charged at 4.4 V. In FIG. **35**, a solid line and a dotted line indicate secondary batteries containing the positive electrode active materials of Sample 01 and Sample 05, respectively. As shown in FIG. **35**, in the secondary battery containing Sample 01, an energy density retention rate is 99.5% even after 50 cycles of charging and discharging were performed, which shows extremely excellent cycle characteristics. In the secondary battery containing Sample 05, an energy density retention rate is 94.3% after 50 cycles were performed.

«Charging at 4.6 V»

The cycle characteristics of the secondary batteries of Sample 01 to Sample 04 charged at 4.6 V were evaluated. The measurement temperature was 25° C. The charging was performed to 4.6 V (CCCV, 0.5 C, a cutoff current of 0.01 C), and the discharging was performed to 2.5 V (CC, 0.5 C).

FIG. **36** is a graph showing the cycle characteristics charged at 4.6 V. As shown in FIG. **36**, in the secondary battery containing Sample 01, which is the positive electrode active material of one embodiment of the present invention, an energy density retention rate is 94.1% even after 50 cycles of charging and discharging were performed at a high voltage of 4.6 V, which shows extremely excellent cycle characteristics. On the other hand, the secondary batteries containing the positive electrode active materials of Sample 02, Sample 03, and Sample 04, which are comparative examples, are inferior to that of Sample 01, and in Sample 04, for example, energy density retention rate is 33.2% after 50 cycles were performed.

As described above, it is found that the positive electrode active material with the structure of one embodiment of the present invention can achieve an advantageous effect when charging and discharging is performed at a voltage higher than 4.4 V.

Example 2

In this example, the positive electrode active materials which are embodiments of the present invention are formed, and results of analysis which is different from that in Example 1 are described. In addition, evaluation results of characteristics of secondary batteries containing the positive electrode active materials under conditions different from those in Example 1 are described.

In this example, a positive electrode active material which contains lithium cobaltate as a composite oxide of lithium and a first transition metal contained in a first region, lithium titanate as an oxide of a second transition metal contained in a second region, and magnesium oxide as an oxide of a representative element contained in a third region, was formed.

[Formation of Positive Electrode Active Material and Fabrication of Secondary Battery]

«Sample 06 and Sample 07»

In this example, lithium cobalt oxide particles (C-20F, produced by NIPPON CHEMICAL INDUSTRIAL CO., LTD.) were used as a starting material.

Next, as Step 14, the lithium cobalt oxide particles were coated with titanium oxide by a sol-gel method and dried. Step 14 was performed in a manner similar to that in Example 1 except that mixture was performed so that TTIP to lithium cobalt oxide was 0.004 ml/g. The lithium cobalt oxide particles which are coated with the titanium oxide and are not heated yet are referred to as Sample 06.

Next, Sample 06, which is the lithium cobalt oxide particles coated with the titanium oxide, was heated. With a muffle furnace, the heating was performed at 800° C. in an oxygen atmosphere under the following conditions: the retention time was two hours; and the flow rate of oxygen was 10 L/min.

Then, as in Example 1, the particles were cooled and collected to obtain the positive electrode active material. The heated positive electrode active material is referred to as Sample 07.

[TEM-EDX]

Sample 06 and Sample 07, in particular, cracks generated in the particles and the vicinity of the cracks were subjected to analysis with TEM-EDX.

First, results of TEM-EDX plane analysis of titanium are shown in FIGS. **37**A, **37**B**1**, **37**B**2**, **37**C**1**, **37**C**2**, **37**D**1**, **37**D**2**, **37**E**1**, and **37**E**2** and FIGS. **38**A, **38**B**1**, **38**B**2**, **38**C**1**, **38**C**2**, **38**D**1**, **38**D**2**, **38**E**1**, and **38**E**2**.

FIGS. **37**A, **37**B**1**, **37**B**2**, **37**C**1**, **37**C**2**, **37**D**1**, **37**D**2**, **37**E**1**, and **37**E**2** show TEM-EDX analysis results of Sample 06 before heating. FIG. **37**A is a cross-sectional TEM image showing the surfaces of the particles and the crack portions. FIG. **37**B**1** and FIG. **37**B**2** show a HAADF-STEM image and a Ti mapping image of a region including the surface of the particle that is denoted by a circle marked with "1" in FIG. **37**A, respectively. Similarly, FIG. **37**C**1** and FIG. **37**C**2** show a HAADF-STEM image and a Ti mapping image of a region at a depth of approximately 20 nm from the surface in the crack portion that is denoted by a circle marked with "2" in FIG. **37**A, respectively. FIG. **37**D**1** and FIG. **37**D**2** show a HAADF-STEM image and a Ti mapping image of a region at a depth of approximately 500 nm from the surface in the crack portion that is denoted by a circle marked with "3" in FIG. **37**A, respectively. FIG. **37**E**1** and FIG. **37**E**2** show a HAADF-STEM image and a Ti mapping image of a region at a depth of approximately 1000 nm from the surface in the crack portion that is denoted by a circle marked with "4" in FIG. **37**A, respectively. Note that in EDX element mapping images in FIGS. **37**A, **37**B**1**, **37**B**2**, **37**C**1**, **37**C**2**, **37**D**1**, **37**D**2**, **37**E**1**, and **37**E**2**, FIGS. **38**A, **38**B**1**, **38**B**2**, **38**C**1**, **38**C**2**, **38**D**1**, **38**D**2**, **38**E**1**, and **38**E**2**, FIGS. **39**A, **39**B**1**, **39**B**2**, **39**C**1**, **39**C**2**, **39**D**1**, **39**D**2**, **39**E**1**, and **39**E**2**, and FIGS. **40**A, **40**B**1**, **40**B**2**, **40**C**1**, **40**C**2**, **40**D**1**, **40**D**2**, **40**E**1**, and **40**E**2**, a region where the number of elements is less than or equal to a lower limit of the detection is indicated in white, and as the number of elements is increased, the white region becomes black.

FIGS. **38**A, **38**B**1**, **38**B**2**, **38**C**1**, **38**C**2**, **38**D**1**, **38**D**2**, **38**E**1**, and **38**E**2** show TEM-EDX analysis results of Sample 07 after heating. FIG. **38**A is a cross-sectional TEM image showing the surfaces of the particles and the crack portions. FIG. **38**B**1** and FIG. **38**B**2** show a HAADF-STEM image and a Ti mapping image of a region including the surface of the particle that is denoted by a circle marked with "1" in FIG. **38**A, respectively. Similarly, FIG. **38**C**1** and FIG. **38**C**2** show a HAADF-STEM image and a Ti mapping image of a region at a depth of approximately 20 nm from the surface in the crack portion that is denoted by a circle marked with "2" in FIG. **38**A, respectively. FIG. **38**D**1** and FIG. **38**D**2** show a HAADF-STEM image and a Ti mapping image of a

region at a depth of approximately 500 nm from the surface in the crack portion that is denoted by a circle marked with "3" in FIG. **38**A, respectively. FIG. **38**E**1** and FIG. **38**E**2** show a HAADF-STEM image and a Ti mapping image of a region at a depth of approximately 1000 nm from the surface in the crack portion that is denoted by a circle marked with "4" in FIG. **38**A, respectively.

As shown in FIGS. **37**A, **37**B**1**, **37**B**2**, **37**C**1**, **37**C**2**, **37**D**1**, **37**D**2**, **37**E**1**, and **37**E**2** and FIGS. **38**A, **38**B**1**, **38**B**2**, **38**C**1**, **38**C**2**, **38**D**1**, **38**D**2**, **38**E**1**, and **38**E**2**, in Sample 06 before heating, segregation of titanium on the surfaces of the particles is observed; however, no segregation is observed in the crack portion. In contrast, in Sample 07 after heating, segregation of titanium is observed both on the surfaces of the particles and in the crack portion. That is, it is found that titanium is segregated at the surface of the crack portion by heating.

Next, results of TEM-EDX plane analysis of magnesium are shown in FIGS. **39**A, **39**B**1**, **39**B**2**, **39**C**1**, **39**C**2**, **39**D**1**, **39**D**2**, **39**E**1**, and **39**E**2**, and FIGS. **40**A, **40**B**1**, **40**B**2**, **40**C**1**, **40**C**2**, **40**D**1**, **40**D**2**, **40**E**1**, and **40**E**2**.

FIG. **39**A is a cross-sectional TEM image of Sample 06, which is the same as FIG. **37**A. FIGS. **39**B**1**, **39**C**1**, **39**D**1**, and **39**E**1** are HAADF-STEM images, which are the same as FIGS. **37**B**1**, **37**C**1**, **37**D**1**, and **37**E**1**. FIG. **39**B**2** shows a Mg mapping image of a region which is the same as FIG. **39**B**1**. FIG. **39**C**2** shows a Mg mapping image of a region which is the same as FIG. **39**C**1**. FIG. **39**D**2** shows a Mg mapping image of a region which is the same as FIG. **39**D**1**. FIG. **39**E**2** shows a Mg mapping image of a region which is the same as FIG. **39**E**1**.

FIG. **40**A is a cross-sectional TEM image of Sample 07, which is the same as FIG. **38**A. FIGS. **40**B**1**, **40**C**1**, **40**D**1**, and **40**E**1** are HAADF-STEM images, which are the same as FIGS. **38**B**1**, **38**C**1**, **38**D**1**, and **38**E**1**. FIG. **40**B**2** shows a Mg mapping image of a region which is the same as FIG. **40**B**1**. FIG. **40**C**2** shows a Mg mapping image of a region which is the same as FIG. **40**C**1**. FIG. **40**D**2** shows a Mg mapping image of a region which is the same as FIG. **40**D**1**. FIG. **40**E**2** shows a Mg mapping image of a region which is the same as FIG. **40**E**1**.

As shown in FIGS. **39**A, **39**B**1**, **39**B**2**, **39**C**1**, **39**C**2**, **39**D**1**, **39**D**2**, **39**E**1**, and **39**E**2**, and FIGS. **40**A, **40**B**1**, **40**B**2**, **40**C**1**, **40**C**2**, **40**D**1**, **40**D**2**, **40**E**1**, and **40**E**2**, in Sample 06 before heating, segregation of magnesium is not observed on the surfaces of the particles or in the crack portion. In contrast, in Sample 07 after heating, segregation of magnesium is observed both on the surfaces of the particles and in the crack portion.

Next, to quantify titanium and magnesium, EDX point analysis was performed on the regions indicated by circles marked with 1 to 6 in FIG. **37**A and the regions indicated by circles marked with 1 to 6 in FIG. **38**A. In each region, two points were measured.

FIGS. **41**A and **41**B show results of EDX point analysis in an atomic ratio of titanium to cobalt. FIG. **41**A shows results of Sample 06 before heating. Detection points 1 to 6 in FIG. **41**A correspond to the regions indicated by circles marked with 1 to 6 in FIG. **37**A. FIG. **41**B shows results of Sample 07 after heating. Detection points 1 to 6 in FIG. **41**B correspond to the regions indicated by circles marked with 1 to 6 in FIG. **38**A.

As shown in FIGS. **41**A and **41**B, in the crack portion of Sample 06, Ti/Co is less than or equal to 0.01 in each measurement point; in contrast, in the crack portion of Sample 07, the amount of titanium is increased in many points, and there are measurement points where Ti/Co is greater than or equal to 0.05. Furthermore, Ti/Co on the surfaces of the particles of Sample 07 is between 0.10 and 0.18.

Next, FIGS. **42**A and **42**B show results of EDX point analysis in an atomic ratio of magnesium to cobalt. The detection points are the same as those in FIGS. **41**A and **41**B.

As shown in FIGS. **42**A and **42**B, in Sample 06, Mg/Co is less than or equal to 0.03 both on the surfaces of the particles and in the crack portion; in contrast, in Sample 07, there are many points where the amount of magnesium is increased both on the surfaces of the particles and in the crack portion. Furthermore, Mg/Co on the surfaces of the particles is between 0.15 and 0.50, and that in the crack portion is between 0 and 0.22.

Next, CR2032 coin-type secondary batteries were fabricated using the positive electrode active material of Sample 07 after heating. A positive electrode formed by applying slurry in which a positive electrode active material (LCO) of Sample 02, AB, and polyvinylidene fluoride (PVDF) were mixed at a weight ratio of 95:3:2 to a positive electrode current collector was used. As the positive electrode current collector, 20-μm-thick aluminum foil was used. The amount of positive electrode active material layer containing the positive electrode active material, AB, and PVDF was 7.6 mg/cm^2.

A lithium metal was used for the counter electrode.

An electrolyte solution formed in such a manner that 1 mol/L $LiPF_6$ was dissolved in a solution in which ethylene carbonate (EC) and diethyl carbonate (DEC) were mixed at a volume ratio of 3:7, and vinylene carbonate (VC) was added to the solution at a 2 wt % was used.

[Initial Characteristics, Rate Characteristics]

Initial characteristics and rate characteristics of the secondary battery using the positive electrode active material of Sample 07 formed in the above manner were measured.

In the measurement of the initial characteristics, charging was performed at CCCV, 0.2 C, 4.6 V, and a cutoff current of 0.05 C, and discharging was performed at CC, 0.2 C, and a cutoff voltage of 3.0 V. Here, 1C was set to 160 mA/g, which was a current value per weight of the positive electrode active material. The measurement temperature was 25° C. Table 2 shows measurement results of initial characteristics.

TABLE 2

Initial charge capacity [mAh/g]	Initial discharge capacity [mAh/g]	Initial charge and discharge efficiency [%]
221.2	217.5	98.3

The rate characteristics were measured after the initial characteristics were measured. The measurement was performed by changing a discharge rate in the following order: 0.2 C charge/0.2 C discharge; 0.2 C charge/0.5 C discharge; 0.2 C charge/1.0 C discharge; 0.2 C charge/2.0 C discharge; 0.2 C charge/3.0 C discharge; 0.2 C charge/4.0 C discharge; and 0.2 C charge/5.0 C discharge. Note that the conditions other than the discharge rate are the same as those of the measurement of the initial characteristics. The measurement temperature was 25° C.

Table 3 shows the measurement results of the initial characteristics and the rate characteristics. In addition, FIG. **43** shows discharge curves of the rates.

TABLE 3

Rate [C]	Discharge capacity [mAh/g]	Discharge capacity retention rate [%]
0.2	218.2	100.0
0.5	215.8	98.9
1.0	213.1	97.7
2.0	207.9	95.3
3.0	204.0	93.5
4.0	198.8	91.1
5.0	184.3	84.5

[Temperature Characteristics]

Next, a cell was fabricated under conditions similar to those of a cell for evaluating the rate characteristics except that the amount of positive electrode active material layer was 8.2 mg/cm^2, and the temperature characteristics were measured. Charging was performed at 25° C., CCCV, 0.2 C, 4.6 V, and a cutoff current of 0.05 C. Discharging was performed at 25° C., 0° C., −10° C., −20° C., and 45° C. in this order, CC, 0.2 C, and a cutoff voltage of 3.0 V. FIG. **44** shows measurement results of temperature characteristics.

[Cycle Characteristics]

Next, a cell was fabricated under conditions similar to those of the cell for measuring the temperature characteristics, and the cycle characteristics were measured. In the measurement of the cycle characteristics, charging was performed at CCCV, 1.0 C, 4.55 V, and a cutoff current of 0.05 C, and discharging was performed at CC, 1.0 C, and a cutoff voltage of 3.0 V. The measurement temperature of the cycle characteristics was 45° C. and 100 cycles were measured. The discharge capacity retention rate after 100 cycles was 86%. FIG. **45** is a graph showing the discharge capacity retention rate of the measured cycle characteristics.

From the measurement results, the specific surface area of the positive electrode active material of Sample 07 was 0.13 m^2/g.

Furthermore, from the measurement results of particle size distribution of the positive electrode active material of Sample 07, the average particle diameter was 21.5 μm, 10% D was 13.1 μm, 50% D was 22.0 μm, and 90% D was 34.4 μm.

The tap density of the positive electrode active material of Sample 07 is 2.21 g/cm^3. The tap density was measured with MULTI TESTER MT-1000 (manufactured by SEISHIN ENTERPRISE Co., Ltd.).

As described above, it is found that the positive electrode active material of Sample 07 which is one embodiment of the present invention shows excellent initial charge and discharge capacity, rate characteristics, and cycle characteristics. In particular, the initial charge and discharge capacity is high, which is 98% or higher; thus, it is probable that a side reaction is inhibited. In addition, even at a high discharge rate of 2 C, an excellent capacity of 96.1% is shown using 0.2 C as a reference.

Example 3

In this example, a positive electrode active material including a region containing titanium and magnesium in a superficial portion was formed by changing the ratio of Li to the first transition metal of starting materials, and evaluation results of characteristics are shown.

[Formation of Positive Electrode Active Material]

In this example, positive electrode active materials of Samples 11 to 17, Samples 21 to 28, and Samples 31 to 40 in which cobalt was used as the first transition metal were prepared. Formation methods and conditions of these samples are as follows.

«Samples 11 to 17»

First, a source of lithium, a source of cobalt, a source of magnesium, and a source of fluorine, which are to be starting materials, were individually weighed. In this example, lithium carbonate, cobalt oxide, magnesium oxide, and lithium fluoride were used as the source of lithium, the source of cobalt, the source of magnesium, and the source of fluorine, respectively.

At that time, the starting materials of Sample 11 were weighed so that the ratio of Li to Co was 1.00. The starting materials of Sample 12 were weighed so that the ratio of Li to Co was 1.03. The starting materials of Sample 13 were weighed so that the ratio of Li to Co was 1.05. The starting materials of Sample 14 were weighed so that the ratio of Li to Co was 1.06. The starting materials of Sample 15 were weighed so that the ratio of Li to Co was 1.07. The starting materials of Sample 16 were weighed so that the ratio of Li to Co was 1.08. The starting materials of Sample 17 were weighed so that the ratio of Li to Co was 1.13.

In addition, the starting materials of each of Samples 11 to 17 were weighed so that, when the number of atoms of cobalt contained in the starting materials was set to 1, the number of atoms of magnesium was 0.01 and the number of atoms of fluorine was 0.02.

Next, the weighed starting materials were separately mixed with a ball mill for each sample.

Then, the mixed starting materials were baked. The baking was performed at 1000° C. for 10 hours under the following conditions: the temperature rising rate was 200° C./h; and the flow rate of dry air was 10 L/min.

Through the above process, particles of a composite oxide containing lithium, cobalt, fluorine, and magnesium were synthesized.

Next, TTIP was added to 2-propanol so that the amount of TTIP per weight of the positive electrode active material was 0.01 ml/g and then mixing was performed, so that a 2-propanol solution of tetra-i-propoxy titanium was formed.

To the 2-propanol solution of TTIP, the particles of a composite oxide containing lithium, cobalt, fluorine, and magnesium were added and then mixing was performed.

The above-described mixed solution was stirred with a magnetic stirrer for four hours, at 25° C., and at a humidity of 90% RH. Through the process, water in an atmosphere and TTIP caused hydrolysis and polycondensation reaction, and a layer containing titanium was formed on the surface of the lithium cobalt oxide particle containing magnesium and fluorine.

The mixed solution which had been subjected to the above process was filtered to collect the residue. As a filter for filtration, Kiriyama filter paper (No. 4) was used.

The collected residue was dried in a vacuum at 70° C. for one hour.

The dried particles were heated. The heating was performed in an oxygen atmosphere under the following conditions: the temperature was 800° C. (the temperature rising rate was 200° C./h); and the retention time was two hours.

The heated particles were cooled and subjected to crushing treatment. In the crushing treatment, the particles were made to pass through a sieve. The sieve has an aperture width of 53 μm.

The particles which were subjected to crushing treatment were used as the positive electrode active materials of Samples 11 to 17.

«Samples 21 to 27»

The starting materials of Samples 21 to 27 were the same as those of Samples 11 to 16. At that time, the starting materials of Sample 21 were weighed so that the ratio of Li to Co was 1.00. The starting materials of Sample 22 were weighed so that the ratio of Li to Co was 1.03. The starting materials of Sample 23 were weighed so that the ratio of Li to Co was 1.05. The starting materials of Sample 24 were weighed so that the ratio of Li to Co was 1.06. The starting materials of Sample 25 were weighed so that the ratio of Li to Co was 1.07. The starting materials of Sample 26 were weighed so that the ratio of Li to Co was 1.08. The starting materials of Sample 27 were weighed so that the ratio of Li to Co was 1.13.

Samples 21 to 27 were formed in manners similar to those of Samples 11 to 17 except that the concentration of TTIP in the 2-propanol solution was adjusted so that the amount of TTIP per weight of the positive electrode active material was 0.02 ml/g.

«Sample 28»

The ratio of Li to Co of the starting materials and the amount of TTIP of Sample 28 were the same as the ratio of Li to Co of the starting materials and the amount of TTIP of Sample 23. That is, in Sample 28, the starting materials were weighed so that the ratio of Li to Co was 1.05, and the amount of TTIP per weight of the positive electrode active material was 0.02 ml/g.

Note that in Sample 28, after the starting materials were mixed, baking was performed at 950° C.

Sample 28 was formed in a manner similar to that of Sample 23 except for the baking temperature.

It is probable that Samples 11 to 17 and Samples 21 to 28 are each a positive electrode active material which contains lithium cobaltate inside and includes a region containing titanium and magnesium in a superficial portion.

«Samples 31 to 40»

Samples 31 to 40 were formed as comparative examples, each of which did not include a region containing titanium.

The starting materials of Sample 31 were weighed so that the ratio of Li to Co was 1.00.

The starting materials of Sample 32 were weighed so that the ratio of Li to Co was 1.01. The starting materials of Sample 33 were weighed so that the ratio of Li to Co was 1.02. The starting materials of Sample 34 were weighed so that the ratio of Li to Co was 1.03. The starting materials of Sample 35 were weighed so that the ratio of Li to Co was 1.035. The starting materials of Sample 36 were weighed so that the ratio of Li to Co was 1.04. The starting materials of Sample 37 were weighed so that the ratio of Li to Co was 1.051. The starting materials of Sample 38 were weighed so that the ratio of Li to Co was 1.061. The starting materials of Sample 39 were weighed so that the ratio of Li to Co was 1.081. The starting materials of Sample 40 were weighed so that the ratio of Li to Co was 1.130.

In addition, the starting materials of each of Samples 31 to 40 were weighed so that, when the number of atoms of cobalt contained in the starting materials was set to 1, the number of atoms of magnesium was 0.01 and the number of atoms of fluorine was 0.02.

Next, the weighed starting materials were separately mixed with a ball mill for each sample.

Then, the mixed starting materials were baked. The baking was performed at 1000° C. for 10 hours under the following conditions: the temperature rising rate was 200° C./h; and the flow rate of dry air was 10 L/min.

Through the above process, particles of a composite oxide containing lithium, cobalt, fluorine, and magnesium were synthesized.

The synthesized particles were cooled and then heated. The heating was performed in an oxygen atmosphere under the following conditions: the temperature was 800° C. (the temperature rising rate was 200° C./h); and the retention time was two hours.

The heated particles were cooled and subjected to crushing treatment. In the crushing treatment, the particles were made to pass through a sieve. The sieve has an aperture width of 53 μm.

The particles which were subjected to crushing treatment were used as the positive electrode active materials of Samples 31 to 40.

Table 4 shows the formation conditions of Samples 11 to 17, Samples 21 to 28, and Samples 31 to 40.

TABLE 4

	Li/Co	TTIP	Baking temperature
Sample 11	1.00	0.01 ml/g	1000° C.
Sample 12	1.03		
Sample 13	1.05		
Sample 14	1.06		
Sample 15	1.07		
Sample 16	1.08		
Sample 17	1.13		
Sample 21	1.00	0.02 ml/g	1000° C.
Sample 22	1.03		
Sample 23	1.05		
Sample 24	1.06		
Sample 25	1.07		
Sample 26	1.08		
Sample 27	1.13		
Sample 28	1.05	0.02 ml/g	950° C.
Sample 31	1.00	—	1000° C.
Sample 32	1.01		
Sample 33	1.02		
Sample 34	1.03		
Sample 35	1.035		
Sample 36	1.04		
Sample 37	1.051		
Sample 38	1.061		
Sample 39	1.081		
Sample 40	1.130		

[XPS]

The positive electrode active materials of Samples 11 to 17, Samples 21 to 28, and Samples 31 to 40 were subjected to an XPS analysis. Table 5 shows results of the XPS analysis of Samples 11 to 17, Table 6 shows results of the XPS analysis of Samples 21 to 28, and Table 7 shows results of the XPS analysis of Samples 31 to 40. Tables 5 to 7 show a relative value of the concentration of each element under the condition where the concentration of cobalt is 1.

TABLE 5

	Relative value under condition where concentration of Co is 1											
	Li/Co	Li	Co	O	C	F	Mg	Ti	Si	Ca	Na	S
Sample 11	1.00	0.82	1.00	2.87	0.25	0.37	0.57	0.15	0.00	0.04	0.27	0.01
Sample 12	1.03	0.69	1.00	2.84	0.93	0.63	0.63	0.14	0.00	0.05	0.04	0.00
Sample 13	1.05	0.96	1.00	3.22	0.66	0.47	0.61	0.14	0.00	0.03	0.09	0.03
Sample 14	1.06	1.04	1.00	3.13	0.34	0.77	0.77	0.15	0.00	0.05	0.34	0.04
Sample 15	1.07	0.84	1.00	3.42	0.58	0.60	0.23	0.18	0.00	0.08	0.27	0.00
Sample 16	1.08	1.08	1.00	3.10	0.66	0.59	0.04	0.16	0.00	0.03	0.16	0.02
Sample 17	1.13	1.29	1.00	3.70	0.83	0.87	0.00	0.19	0.00	0.04	0.20	0.02

TABLE 6

	Relative value under condition where concentration of Co is 1											
	Li/Co	Li	Co	O	C	F	Mg	Ti	Si	Ca	Na	S
Sample 21	1.00	1.08	1.00	3.23	0.47	0.45	0.49	0.20	0.00	0.06	0.35	0.01
Sample 22	1.03	0.73	1.00	3.05	1.06	0.70	0.59	0.17	0.00	0.03	0.09	0.00
Sample 23	1.05	1.19	1.00	3.40	0.73	0.48	0.58	0.23	0.00	0.05	0.10	0.04
Sample 24	1.06	1.10	1.00	3.44	0.33	0.92	0.91	0.25	0.00	0.05	0.30	0.04
Sample 25	1.07	1.05	1.00	4.26	0.74	0.20	0.25	0.29	0.00	0.07	0.30	0.02
Sample 26	1.08	1.12	1.00	3.32	0.74	0.52	0.14	0.21	0.00	0.05	0.15	0.00
Sample 27	1.13	1.49	1.00	3.80	0.60	0.41	0.00	0.12	0.00	0.00	0.16	0.02
Sample 28	1.05	0.99	1.00	3.11	0.72	0.86	0.56	0.18	0.00	0.05	0.12	0.02

TABLE 7

	Relative value under condition where concentration of Co is 1								
	Li/Co	Li	Co	O	C	F	Mg	Ca	Na
Sample 31	1.00	0.51	1.00	2.45	0.69	0.08	0.27	0.03	0.08
Sample 32	1.01	0.67	1.00	2.65	0.77	0.08	0.28	0.03	0.08
Sample 33	1.02	0.53	1.00	2.51	0.66	0.09	0.27	0.02	0.06
Sample 34	1.03	0.79	1.00	2.93	0.92	0.09	0.35	0.04	0.14
Sample 35	1.04	0.65	1.00	2.33	0.48	0.11	0.32	0.03	0.11
Sample 36	1.04	0.69	1.00	2.73	0.56	0.11	0.38	0.05	0.16
Sample 37	1.05	0.67	1.00	3.04	0.64	0.09	0.35	0.04	0.21
Sample 38	1.06	0.83	1.00	2.65	1.03	0.29	0.10	0.05	0.11
Sample 39	1.08	0.80	1.00	2.79	1.04	0.26	0.03	0.08	0.10
Sample 40	1.13	0.77	1.00	2.72	0.22	0.99	0.00	0.01	0.26

FIGS. **46**A and **46**B are graphs in which the relative value of magnesium and the relative value of titanium are extracted from the analysis results of Tables 5 to 7. FIG. **46**A is a graph showing the ratio of Li to Co and the relative value of magnesium. FIG. **46**B is a graph showing the ratio of Li to Co and the relative value of titanium.

From the analysis results of Samples 31 to 40 in FIG. **46**A, it is found that, in the case where a coating layer containing titanium is not included, the concentration of magnesium is high in samples where the ratio of Li to Co is greater than or equal to 1.00 and less than or equal to 1.05. This is probably because magnesium contained in the starting materials is segregated in a range where the element concentration can be detected by XPS by heating. In contrast, in samples where the ratio of Li to Co is greater than or equal to 1.06, the concentration of magnesium is low; thus, it is probable that the segregation of magnesium does not easily occur when the amount of lithium is too large.

From the analysis results of Samples 11 to 16 and Samples 21 to 26 in FIG. **46**A, it is found that the concentration of magnesium in a range where the element concentration can be detected by XPS is higher in the case where a region containing titanium is included in a superficial portion than in the case where the region containing titanium is not included.

Moreover, in the case where the ratio of Li to Co is 1.06, in samples where the region containing titanium is not included, the concentration of magnesium in a range where the element concentration can be detected by XPS is low; in contrast, in samples where the region containing titanium is included, the concentration of magnesium in a range where the element concentration can be detected by XPS is high. That is, when the region containing titanium is formed in the superficial portion, magnesium is sufficiently segregated even in the case where the ratio of Li to Co is high.

Note that even if the region containing titanium is included, the concentration of magnesium is lower in the case where the ratio of Li to Co is 1.07 than in the case where the ratio of Li to Co is 1.06. Furthermore, it is probable that, in the case where the ratio of Li to Co is greater than or equal to 1.08, the segregation of magnesium does not easily occur even if the region containing titanium is included.

[Evaluation of Cycle Characteristics]

«Energy Density Retention Rate»

Next, cycle characteristics were evaluated in a manner similar to that of Example 1 using positive electrode active materials of Samples 11 to 14, Sample 16, Samples 21 to 24, and Sample 26.

The shape of the secondary battery, the materials and the mixture ratios of the positive electrode active material, the conductive additive, and the binder in the positive electrode, the counter electrode, the electrolyte solution, the exterior body, the conditions of the cycle characteristics test, and the like are the same as those in Example 1.

FIG. **47**A is a graph showing the energy density retention rates and the number of charge and discharge cycles at the time of charging at 4.6 V of secondary batteries using the positive electrode active materials of Samples 11 to 14 and Sample 16 which were formed so that the amount of TTIP per weight of the positive electrode active material was 0.01 ml/g. FIG. **47**B is a graph showing the energy density retention rates and the number of charge and discharge cycles at the time of charging at 4.6 V of secondary batteries using the positive electrode active materials of Samples 21 to 24 and Sample 26 which were formed so that the amount of TTIP per weight of the positive electrode active material was 0.02 ml/g.

As shown in FIG. **47**A, in the case where TTIP is 0.01 ml/g, Samples 11 to 14, that is, the positive electrode active materials in which the ratio of Li to Co is greater than or equal to 1.00 and less than or equal to 1.06 have excellent cycle characteristics. In particular, Samples 11 and 12, that is, the positive electrode active materials in which the ratio of Li to Co is greater than or equal to 1.00 and less than or equal to 1.03 have extremely excellent cycle characteristics. In contrast, in Sample 16 in which the ratio of Li to Co is 1.08, the energy density retention rate decreases at a relatively early stage.

As shown in FIG. **47**B, in the case where TTIP is 0.02 ml/g, Samples 21 to 24, that is, the positive electrode active materials in which the ratio of Li to Co is greater than or equal to 1.00 and less than or equal to 1.06 have excellent cycle characteristics. In particular, Samples 23 and 24, that is, the positive electrode active materials in which the ratio of Li to Co is greater than or equal to 1.05 and less than or equal to 1.06 have extremely excellent cycle characteristics.

FIG. **48** is a graph showing comparison between Sample 11 having the most excellent cycle characteristics in Samples 11 to 15 and Sample 23 having the most excellent cycle characteristics in Samples 21 to 25.

As shown in FIG. **48**, both Sample 11 and Sample 23 have excellent cycle characteristics; however, Sample 23 in which TTIP is 0.02 ml/g has more excellent cycle characteristics.

«Discharge Capacity Retention Rate»

Next, FIG. **49** shows evaluation results of a discharge capacity retention rate, which is one of the cycle characteristics of each of Samples 21 to 26 and Sample 28.

The shape of the secondary battery, the material and the mixture ratio of the positive electrode active material, the conductive additive, and the binder in the positive electrode, the counter electrode, the electrolyte solution, the exterior body, the conditions of the cycle characteristics test, and the like of Samples 21 to 26 are the same as those in Example 1.

The secondary battery using Sample 28 was formed in a manner similar to those of the secondary batteries using Samples 21 to 26 except that PVDF was used as a binder and the positive electrode active material (LCO), AB, and PVDF were mixed such that the weight ratio of LCO to AB and PVDF was 95:3:2, and evaluated.

As shown in FIG. **49**, Samples 21 to 24 and Sample 28 have excellent cycle characteristics. In particular, Sample 28 has extremely excellent cycle characteristics. In Sample 28, the discharge capacity retention rate after 50 cycles was higher than or equal to 85%.

In contrast, in Sample 25 and Sample 26 in which the ratios of Li to Co are 1.07 and 1.08, respectively, the discharge capacity retention rates decrease at a relatively early stage.

From the above results, it is found that in the case where TTIP per weight of the positive electrode active material is 0.02 ml/g, the ratio of Li to Co preferably has a range of greater than or equal to 1.00 and less than 1.07. Moreover, it is found that a sample in which the ratio of Li to Co has a range of greater than or equal to 1.05 and less than or equal to 1.06 has extremely excellent cycle characteristics.

FIGS. **50**A to **50**C show charge and discharge curves of the secondary batteries using Sample 28, which has extremely excellent cycle characteristics in FIG. **49**, Sample 24, and Sample 25, in which the degradation occurs at a relatively early stage.

FIG. **50**A, FIG. **50**B, and FIG. **50**C show charge and discharge curves of the secondary batteries using Sample 28, Sample 24, and Sample 25, respectively. Each of the figures shows overlap of results of 50 cycles of charge and discharge. As indicated by an arrow in each figure, the charge and discharge capacity decreases from the first cycle to the fiftieth cycle.

As shown in FIGS. **50**A and **50**B, Sample 28 and Sample 24, which are positive electrode active materials of one embodiment of the present invention, have high charge and discharge capacity and excellent charge and discharge characteristics. In addition, it is found that a decrease in charge and discharge capacity of each of Sample 28 and Sample 24 in FIGS. **50**A and **50**B is significantly suppressed as compared with Sample 25 in FIG. **50**C.

Example 4

In this example, SEM observation results and SEM-EDX analysis results of the positive electrode active material of Sample 24 formed in Example 2 are described.

Sample 24 was formed so that Li/Co was 1.06 and TTIP per weight of the positive electrode active material was 0.02 ml/g. FIG. **51**A shows a SEM image of Sample 24. FIGS. **51**B and **51**C each show an enlarged image of a part in FIG. **51**A.

As shown in FIGS. **51**A to **51**C, there are a large number of projected regions in a superficial portion of the positive electrode active material.

Next, FIGS. **52**A-**1**, **52**A-**2**, **52**B-**1**, **52**B-**2**, **52**C-**1**, and **52**C-**2** show analysis results of the positive electrode active material of Sample 24 using SEM-EDX. FIG. **52**A-**1** shows a SEM image of a superficial portion of the positive electrode active material, FIG. **52**A-**2** shows a mapping image of titanium, FIG. **52**B-**1** shows a mapping image of magnesium, FIG. **52**B-**2** shows a mapping image of oxygen, FIG. **52**C-**1** shows a mapping image of aluminum, and FIG. **52**C-**2** shows a mapping image of cobalt. Note that in EDX element mapping images in FIGS. **52**A-**2**, **52**B-**1**, **52**B-**2**, **52**C-**1**, and **52**C-**2**, a region where the number of elements is less than or equal to a lower limit of the detection is indicated in black, and as the number of elements is increased, the black region becomes white.

The same regions in FIGS. **52**A-**1**, **52**A-**2**, and **52**B-**1** are surrounded by dotted lines. When the regions surrounded by dotted lines are compared with each other, it is found that in the projected regions in the superficial portion of the positive electrode active material, titanium and magnesium are distributed.

Thus, it is found that Sample 24 is a positive electrode active material including the projected fourth region **104** containing titanium and magnesium over the third region **103**.

As shown in Example 2, Sample 24 is one of the samples which show extremely excellent cycle characteristics. Thus, it is found that, even if the fourth region is provided in the superficial portion or when the fourth region is provided, the positive electrode active material with excellent cycle characteristics can be obtained.

From the above results of Examples 1 to 3, it is found that when the region containing titanium is formed in the superficial portion, the positive electrode active material with excellent cycle characteristics can be obtained. In addition, it is found that, when the ratio of Li to Co is increased to increase the particle diameter of the positive electrode active material, the cycle characteristics might be degraded; however, the region containing titanium is formed in the superficial portion, whereby the range of the ratio of Li to Co in which excellent cycle characteristics is obtained can be widened. Furthermore, it is found that even when the fourth region containing titanium and magnesium is provided in the superficial portion of the positive electrode active material, excellent cycle characteristics is obtained.

Example 5

In this example, an example of a method for producing a positive electrode active material coated with graphene oxide is shown, and observation results of the positive electrode active material produced by the method with an electron microscope are described.

As shown in a process flow chart in FIG. **53**, a process for forming a coating film on a positive electrode active material includes the steps of: weighing graphene oxide (S**11**); mixing and stirring the graphene oxide and pure water (S**12**); controlling pH (S**13**); adding an active material (S**14**); completing a suspension (S**15**); spraying the suspension using a spray dry apparatus (S**16**); and collecting particles in a container (S**17**).

Note that in (S**12**), pure water is used as a dispersion medium; however, a dispersion medium is not particularly limited and ethanol or the like may be used. In addition, in (S**14**), the active material is a positive electrode active material.

FIG. **54** is a schematic view of a spray dry apparatus **280**. The spray dry apparatus **280** includes a chamber **281** and a nozzle **282**. A suspension **284** is supplied to the nozzle **282** through a tube **283**. The suspension **284** is supplied from the nozzle **282** to the chamber **281** in the form of mist and dried in the chamber **281**. The nozzle **282** may be heated with a heater **285**. Here, a region of the chamber **281** which is close to the nozzle **282**, for example, a region surrounded by dashed-two dotted line in FIG. **54**, is also heated with the heater **285**.

In the case of using a suspension containing a positive electrode active material and graphene oxide as the suspension **284**, powder of the positive electrode active material coated with the graphene oxide is collected in a collection container **286** through the chamber **281**.

The air in the chamber **281** may be suctioned by an aspirator or the like through a path indicated by an arrow **288**.

An example of conditions for forming the coating film is shown below.

First, a suspension was formed by dispersing graphene oxide into a solvent.

Although in pure water, graphene oxide is highly dispersible, pure water might react with an active material added later, so that Li might be dissolved or an active material might be damaged to change the surface structure. Thus, the graphene oxide was dispersed into a solution such that the ratio between ethanol and pure water was 4:6.

Stirring to disperse the graphene oxide into a solution was performed under the following conditions: a stirrer and an ultrasonic wave generator were used; a rotation rate was 750 rpm; and irradiation time with ultrasonic waves was 2 minutes.

Then, a LiOH aqueous solution was dropped to adjust pH to be pH7 (25° C.).

The positive electrode active materials (in this example, lithium cobalt oxide particles produced by NIPPON CHEMICAL INDUSTRIAL CO., LTD. (product name: C-20F)) were added, and stirring was performed using a stirrer and an ultrasonic wave generator under the following conditions: a rotation rate was 750 rpm; and irradiation time with ultrasonic waves was 1 minute. Through the above process, the suspension was prepared. The above lithium cobalt oxide particles produced by NIPPON CHEMICAL INDUSTRIAL CO., LTD. (product name: C-20F) contain at least fluorine, magnesium, calcium, sodium, silicon, sulfur, and phosphorus, and each have a diameter of approximately 20 μm.

Next, the suspension was sprayed uniformly with a spray nozzle (having a nozzle diameter of 20 μm) of the spray dry apparatus to obtain powder. The inlet temperature was 160° C. and the outlet temperature was 40° C. as the hot-air temperature of the spray dry apparatus, and the N_2 gas flow rate was 10 L/min.

FIG. **55** shows a cross-sectional TEM image of the obtained powder. In addition, FIG. **56** shows a SEM image of the obtained powder. When a positive electrode active material which was the same as the sprayed positive electrode active material (C-20F, produced by NIPPON CHEMICAL INDUSTRIAL CO., LTD.) was mixed with the graphene oxide with a planetary centrifugal mixer as a comparative example, coating was insufficient. FIG. **57** shows a SEM image of the comparative example.

It is found that, as compared with FIG. **57**, the coating film is uniformly formed on the surface of the powder in FIG. **56**.

FIGS. **58**A and **58**B illustrate a cross-sectional structure example of an active material layer **200** which is coated with graphene oxide with a spray dry apparatus and includes a graphene compound as a conductive additive.

FIG. **58**A is a longitudinal sectional view of the active material layer **200**. The active material layer **200** includes positive electrode active material particles **100** coated with graphene oxide, a graphene compound **201** as a conductive additive, and a binder (not illustrated). Here, graphene or multilayer graphene may be used as the graphene compound **201**, for example. The graphene compound **201** preferably has a sheet-like shape. The graphene compound **201** may have a sheet-like shape formed of a plurality of sheets of multilayer graphene and/or a plurality of sheets of graphene that partly overlap with each other.

In the longitudinal section of the active material layer **200**, as illustrated in FIG. **58**B, the positive electrode active

material **100** coated with a coating film **105** formed of graphene oxide is in contact with the graphene compound **201**. A plurality of graphene compounds **201** are formed in such a way as to be partly in contact with the positive electrode active material **100** coated with the coating film **105** and adhere to the coating film **105** of the adjacent positive electrode active material **100**, so that the graphene compounds **201** are in contact with each of the positive electrode active material **100**.

The graphene compound **201** and the coating film **105** are formed using carbon-based materials; thus, an excellent conductive path can be formed.

The coating film **105** is effective in protecting the crystal structure of the positive electrode active material **100** so as not to be in contact with the electrolyte solution and in forming the excellent conductive path.

REFERENCE NUMERALS

11*a*: positive electrode, **11***b*: negative electrode, **12***a*: lead, **12***b*: lead, **14**: separator, **15***a*: bonding portion, **15***b*: bonding portion, **17**: fixing member, **50**: secondary battery, **51**: exterior body, **61**: folded portion, **62**: seal portion, **63**: seal portion, **71**: crest line, **72**: trough line, **73**: space, **100**: positive electrode active material, **101**: first region, **101***p*: crystal plane, **102**: second region, **102***p*: crystal plane, **103**: third region, **103***p*: crystal plane, **104**: fourth region, **105**: coating film, **106**: crack portion, **110**: particle, **111**: region, **112**: layer containing titanium, **114**: cobalt oxide layer, **120**: particle, **121**: region, **122**: layer containing titanium, **124**: cobalt oxide layer, **125**: layer containing lithium titanate, **200**: active material layer, **201**: graphene compound, **280**: spray dry apparatus, **281**: chamber, **282**: nozzle, **283**: tube, **284**: suspension, **285**: heater, **286**: collection container, **288**: arrow, **300**: coin-type secondary battery, **301**: positive electrode can, **302**: negative electrode can, **303**: gasket, **304**: positive electrode, **305**: positive electrode current collector, **306**: positive electrode active material layer, **307**: negative electrode, **308**: negative electrode current collector, **309**: negative electrode active material layer, **310**: separator, **500**: laminated secondary battery, **501**: positive electrode current collector, **502**: positive electrode active material layer, **503**: positive electrode, **504**: negative electrode current collector, **505**: negative electrode active material layer, **506**: negative electrode, **507**: separator, **508**: electrolyte solution, **509**: exterior body, **510**: positive electrode lead electrode, **511**: negative electrode lead electrode, **600**: cylindrical secondary battery, **601**: positive electrode cap, **602**: battery can, **603**: positive electrode terminal, **604**: positive electrode, **605**: separator, **606**: negative electrode, **607**: negative electrode terminal, **608**: insulating plate, **609**: insulating plate, **611**: PTC element, **612**: safety valve mechanism, **613**: conductive plate, **614**: conductive plate, **615**: module, **616**: wiring, **617**: temperature control device, **900**: circuit board, **910**: label, **911**: terminal, **912**: circuit, **913**: secondary battery, **914**: antenna, **915**: antenna, **916**: layer, **917**: layer, **918**: antenna, **920**: display device, **921**: sensor, **922**: terminal, **930**: housing, **930***a*: housing, **930***b*: housing, **931**: negative electrode, **932**: positive electrode, **933**: separator, **950**: wound body, **951**: terminal, **952**: terminal, **980**: laminated secondary battery, **981**: film, **982**: film, **993**: wound body, **994**: negative electrode, **995**: positive electrode, **996**: separator, **997**: lead electrode, **998**: lead electrode, **7100**: portable display device, **7101**: housing, **7102**: display portion, **7103**: operation button, **7104**: secondary battery, **7200**: portable information terminal, **7201**: housing, **7202**: display portion, **7203**: band, **7204**: buckle, **7205**: operation button, **7206**: input output terminal, **7207**: icon, **7300**: display device, **7304**: display portion, **7400**: mobile phone, **7401**: housing, **7402**: display portion, **7403**: operation button, **7404**: external connection port, **7405**: speaker, **7406**: microphone, **7407**: secondary battery, **7408**: lead electrode, **7409**: current collector, **7500**: vaporizer, **7501**: atomizer, **7502**: cartridge, **7504**: secondary battery, **8000**: display device, **8001**: housing, **8002**: display portion, **8003**: speaker portion, **8004**: secondary battery, **8021**: ground-based charging apparatus, **8022**: cable, **8024**: secondary battery, **8100**: lighting device, **8101**: housing, **8102**: light source, **8103**: secondary battery, **8104**: ceiling, **8105**: wall, **8106**: floor, **8107**: window, **8200**: indoor unit, **8201**: housing, **8202**: air outlet, **8203**: secondary battery, **8204**: outdoor unit, **8300**: electric refrigerator-freezer, **8301**: housing, **8302**: refrigerator door, **8303**: freezer door, **8304**: secondary battery, **8400**: automobile, **8401**: headlight, **8406**: electric motor, **8500**: automobile, **8600**: motor scooter, **8601**: side mirror, **8602**: secondary battery, **8603**: indicator, **8604**: storage unit under seat, **9600**: tablet terminal, **9625**: power saving mode changing switch, **9626**: display mode changing switch, **9627**: power switch, **9628**: operation switch, **9629**: fastener, **9630**: housing, **9630***a*: housing, **9630***b*: housing, **9631**: display portion, **9631***a*: display portion, **9631***b*: display portion, **9633**: solar cell, **9634**: charge and discharge control circuit, **9635**: power storage unit, **9636**: DCDC converter, **9637**: converter, **9640**: movable portion.

This application is based on Japanese Patent Application Serial No. 2016-133997 filed with Japan Patent Office on Jul. 6, 2016, Japanese Patent Application Serial No. 2016-133143 filed with Japan Patent Office on Jul. 5, 2016, Japanese Patent Application Serial No. 2017-002831 filed with Japan Patent Office on Jan. 11, 2017, Japanese Patent Application Serial No. 2017-030693 filed with Japan Patent Office on Feb. 22, 2017, Japanese Patent Application Serial No. 2017-084321 filed with Japan Patent Office on Apr. 21, 2017, and Japanese Patent Application Serial No. 2017-119272 filed with Japan Patent Office on Jun. 19, 2017 the entire contents of which are hereby incorporated by reference.

The invention claimed is:

1. A lithium-ion secondary battery comprising

a positive electrode, the positive electrode comprising a positive electrode active material particle comprising lithium cobaltate,

wherein the positive electrode active material particle comprises a first region and a second region,

wherein the first region comprises a layered rock-salt crystal structure,

wherein the second region comprises a rock-salt crystal structure,

wherein the second region covers at least a first part of the first region,

wherein the positive electrode active material particle comprises titanium, magnesium, fluorine, and oxygen in the second region, and

wherein a crystal orientation of at least a second part of the first region and a crystal orientation of at least a part of the second region are substantially aligned with each other.

2. The lithium-ion secondary battery according to claim **1**,

wherein the titanium, the magnesium, the fluorine, and the oxygen are provided in a range from the surface of the positive electrode active material particle to a depth of 5 nm.

3. The lithium-ion secondary battery according to claim 1, wherein the positive electrode further comprises a conductive additive, and

wherein the conductive additive comprises carbon fiber, graphene or multilayer graphene.

4. The lithium-ion secondary battery according to claim 1, wherein a relative value of a concentration of the titanium is greater than or equal to 0.05 and less than or equal to 0.4 when the surface of the positive electrode active material particle is subjected to an XPS analysis and a concentration of cobalt is defined as 1.

5. The lithium-ion secondary battery according to claim 1, wherein a relative value of a concentration of the magnesium is greater than or equal to 0.4 and less than or equal to 1.5 when the surface of the positive electrode active material particle is subjected to an XPS analysis and a concentration of cobalt is defined as 1.

6. A lithium-ion secondary battery comprising a positive electrode, the positive electrode comprising a positive electrode active material particle comprising lithium cobaltate,

wherein the positive electrode active material particle comprises a first region and a second region,

wherein the first region comprises a layered rock-salt crystal structure,

wherein the second region comprises a rock-salt crystal structure,

wherein the positive electrode active material particle comprises titanium, magnesium, fluorine, and oxygen in the second region, wherein the second region extends from a surface of the positive electrode active material particle to an inside of the positive electrode active material particle where magnesium detected by a line analysis of energy dispersive X-ray spectroscopy (EDX) in a depth direction is ⅕ of a maximum peak of the magnesium in the line analysis, and

wherein a crystal orientation of at least a part of the first region and a crystal orientation of at least a part of the second region are substantially aligned with each other.

7. The lithium-ion secondary battery according to claim 6, wherein the titanium, the magnesium, the fluorine, and the oxygen are provided in a range from the surface of the positive electrode active material particle to a depth of 5 nm.

8. The lithium-ion secondary battery according to claim 6, wherein the positive electrode further comprises a conductive additive, and

wherein the conductive additive comprises carbon fiber, graphene or multilayer graphene.

9. The lithium-ion secondary battery according to claim 6, wherein a relative value of a concentration of the titanium is greater than or equal to 0.05 and less than or equal to 0.4 when the surface of the positive electrode active material particle is subjected to an XPS analysis and a concentration of cobalt is defined as 1.

10. The lithium-ion secondary battery according to claim 6,

wherein a relative value of a concentration of the magnesium is greater than or equal to 0.4 and less than or equal to 1.5 when the surface of the positive electrode active material particle is subjected to an XPS analysis and a concentration of cobalt is defined as 1.

* * * * *